REFERENCE ONLY

UNIVERSITY OF LONDON THESIS

Degree PhD Year 2006 Name of Author SLAVIK-SMITH, EC

COPYRIGHT

This is a thesis accepted for a Higher Degree of the University of London. It is an unpublished typescript and the copyright is held by the author. All persons consulting the thesis must read and abide by the Copyright Declaration below.

COPYRIGHT DECLARATION

I recognise that the copyright of the above-described thesis rests with the author and that no quotation from it or information derived from it may be published without the prior written consent of the author.

LOANS

Theses may not be lent to individuals, but the Senate House Library may lend a copy to approved libraries within the United Kingdom, for consultation solely on the premises of those libraries. Application should be made to: Inter-Library Loans, Senate House Library, Senate House, Malet Street, London WC1E 7HU.

REPRODUCTION

University of London theses may not be reproduced without explicit written permission from the Senate House Library. Enquiries should be addressed to the Theses Section of the Library. Regulations concerning reproduction vary according to the date of acceptance of the thesis and are listed below as guidelines.

A. Before 1962. Permission granted only upon the prior written consent of the author. (The Senate House Library will provide addresses where possible).

B. 1962 - 1974. In many cases the author has agreed to permit copying upon completion of a Copyright Declaration.

C. 1975 - 1988. Most theses may be copied upon completion of a Copyright Declaration.

D. 1989 onwards. Most theses may be copied.

This thesis comes within category D.

☑ This copy has been deposited in the Library of UCL

☐ This copy has been deposited in the Senate House Library, Senate House, Malet Street, London WC1E 7HU.

Ultrastructural and molecular characterisation of the neuronal nucleus

A thesis presented for the degree of

Doctor of Philosophy,
University of London

Elizabeth Slavik-Smith

Department of Anatomy and Developmental Biology,
University College London

2005

ProQuest LLC
789 East Eisenhower Parkway
P.O. Box 1346
Ann Arbor, MI 48106-1346

The real voyage of discovery consists not in seeking new landscapes but in having new eyes.

Marcel Proust

Abstract

Within the mammalian nucleus, many major cellular functions are performed including transcription, pre-mRNA splicing and ribosome assembly, all of which are important for successful gene expression, and, to achieve this, the nucleus has evolved as a highly organised, dynamic structure (Dundr and Misteli, 2001). In this study a complete ultrastructural and molecular investigation of the neuronal nucleus has been undertaken, characterising three subdomains in detail: speckles, the nucleolus, and the Cajal body.

It has recently been established that several human neurodegenerative diseases are associated with changes in the organisation of the neuronal nucleus, and this is believed to be the principle cause of cellular dysfunction and resulting clinical symptoms. Many of these diseases and their associated nuclear pathology have successfully been reproduced in transgenic mouse models.

In this study I have determined the detailed ultrastructural and molecular organisation of the nucleus of neurons within the striatum of the mouse brain and compared this to nuclei of striatal neurons in a transgenic mouse model of Huntington's disease and in a mutant mouse lacking the gene for the protein p80 coilin. In the HD mouse there is a dramatic reorganisation of the nucleus accompanied by the formation of a novel nuclear subdomain, the neuronal intranuclear inclusion (NII), which is associated with the movement of the Cajal body from the nucleolus to the NII. This occurs with a change in the molecular composition of the speckles and a major reorganisation in the structure of the nucleolus. In contrast, the p80 mutant mouse is characterised by major alterations in the distribution and molecular composition of the Cajal body. However, this is not similarly associated with dramatic changes in either the speckles or the nucleolus.

These studies clearly establish novel and important changes in the organisation of the neuronal nucleus associated with the formation of the NII in Huntington's disease.

Acknowledgements

There are many people that I would like to thank for their help over the past three years. In particular I would like to thank my supervisor, Stephen W. Davies. He has constantly supported me and his passion for research and science has been an inspiration. I would also like to thank current and former colleagues, all of who have offered support and friendship during my time in the lab. Mark Turmaine has always been willing to share his vast knowledge with regard to microscopy and help me when needed. Barbara Cozens was continually there to offer an extra pair of hands and lots of cups of tea! Lee-Jay Bannister was someone who always questioned my ideas and I will always be grateful to him for making me think. Rush Jolly has always been in a friendly face in the lab, willing to discuss any thoughts with and Aysha Raza has provided light relief in the form of numerous shoe-related conversations! . I wish Rush and Aysha the best of luck in getting their PhDs finished and continuing in whatever they wish to do.

My thanks also go to Gillian Bates and her group for the supply of R6/2 mice. I would also like to show gratitude to Angus I. Lamond (Dundee, UK) and A. Gregory Matera (Case Western, Cleveland, USA) for allowing me to visit their laboratories and discuss my findings, and, to Angus I. Lamond for providing several antibodies and to A. Gregory Matera for allowing me to analyse his knock-out mice.

I am also grateful to the BBSRC who provided financial support throughout this project.

Contents

Figures, Table and Graphs

Introduction

Materials & Methods

Results

List of Abbreviations

BLM	Bloom's syndrome
CAG	DNA sequence coding for *glutamine*
CB	Cajal body
CBP	CRE (cyclic-AMP response element) binding protein
CPSF	cleavage and polyadenylation specificity factor
CRS	Closed- reticulate structure
CstF64	64 kDa cleavage stimulation factor
CT	Christmas tree
CTD	C terminal domain
DAB	3,3"diaminobenzidine
DFC	dense fibrillar component
DNIs	dystrophic neurite inclusions
DM1 (2)	myotonic dystrophy type 1 (type 2)
DMPK	dystrophia myotonica-protein kinase
DNIs	dystrophic neurite inclusions
DRB	5,6-dichloro-1-beta-d-ribofuranosylbenzimidazole
DRPLA	dentatorubral and pallidoluysian atrophy
EAF1	ELL-Associated Factor 1
ELL	eleven-nineteen lysine-rich leukemia protein
EP	entopeduncular nucleus
EM	electron microscopy
EWS	Ewing's sarcoma
FC	fibrillar centre
FITC	Fluorescein (FITC)-conjugated
FLIP	fluorescence loss in photobleaching
FMR(P)	fragile X mental retardation (protein)
FRAP	fluorescence recovery after photobleaching
GC	granular component
GFP	green fluorescent protein
GPe	globus pallidus external segment
GPi	globus pallidus internal segment
HD	Huntington's disease
Hdh	Huntington's disease homologue
hnRNP	heterogeneous nuclear ribonucleoprotein
HSP	heat-shock protein
htt	huntingtin
IGCs	interchromatin granule clusters
IT15	Interesting transcript 15 – the HD gene
kb	kilobases
kDa	kiloDaltons
LM	light microscopy
MB**	muscleblind protein
MEF	mouse embryonic fibroblasts
MJD	Machado-Joseph disease
MLL	myeloid-lymphoid leukemia protein
NIIs	neuronal intranuclear inclusion
NLS	nuclear localisation signal
NoLS	nucleolar localisation signal
NORs	nucleolar organising regions

OPMD	Oculopharyngeal muscular dystrophy
ORS	Open-reticulate structure
p80 KO	p80 coilin knock
PAB2	poly(A)-binding protein 2
PAP	Poly(A) polymerase
PFs	perichromatin fibrils
PGs	perichromatin granules
PLP	paraformaldehyde/lysine/periodate
PML	promyelocytic leukemia
PNC	perinucleolar cap
PQBP	polyglutamine (Q) tract binding protein-1
PSF	polypyrimidine tract binding protein (PTB)- associated splicing factor
PSP1	Paraspeckle Protein 1
PTB	polypyrimidine tract binding protein
PTF	proximal element sequence
RG	arginine and glycine domain
RNP	ribonucleoprotein particle
RP	Retinitis Pigmentosa
RRM	RNA-recognition motif
RS domain	arginine/serine rich domain
SBMA	Spinal and bulbar muscular atrophy
SCA	spinocerebellar ataxia
scaRNA	small Cajal-body-specific RNAs
SMA	spinal muscular atrophy
SMN	survival of motor neuron protein
SNPr	substantia nigra pars reticulata
snoRNP	small nucleolar ribonucleoprotein particle
snoRNA	small nucleolar RNA
snRNA	small nuclear RNA
snRNP	small nuclear ribonucleoprotein particle
SON	supraoptic nuclei
SR proteins	arginine/serine rich domain (RS domain) proteins
SS	segregating structure
TAFs	transcription activity factors
TBP	tata binding protein
TCS	Treacher Collins syndrome
TEM	transmission electron microscopy
TIF	transcription initiation factors
TMG	trimethylguanosine
Topo II	DNA topoisomerase II
TRITC	Rhodamine (TRITC)-conjugated
UBF	upstream binding factor
UTR	untranslated region
WRN	Werner's syndrome
YFP	yellow fluorescent protein
ZNF9	zinc finger protein 9

Introduction

CHAPTER 1

Introduction

The mammalian nucleus is a highly organised, dynamic structure within which many of the cell's major functions occur including transcription, pre-mRNA splicing and ribosome assembly, all of which are vital for successful gene expression (Dundr and Misteli, 2001). Individual chromosomes in the interphase nuclei occupy discrete domains, which are called chromosome territories (Hebert and Matera, 2000). Numerous, morphologically distinct, membraneless domains including Cajal Bodies, the nucleolus, PML domains and speckles occupy the interchromatin spaces and are shown in figure1.1. It has now been suggested that the individual domains have defined spatial relationships with each other and with the surrounding genomic DNA (Schul *et al.*, 1998a). Using immunofluorescence microscopy, many nuclear factors often show a punctate staining pattern and localise to distinct bodies.

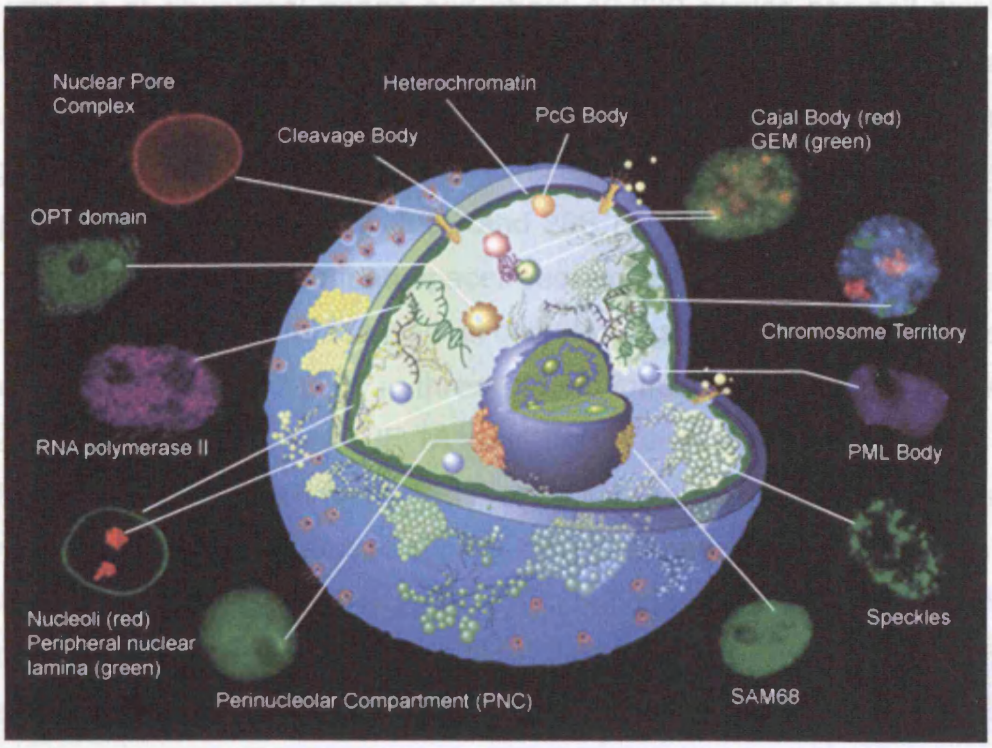

Figure 1.1
A schematic illustration summarising the various nuclear domains that constitute the mammalian cell nucleus (Adapted from Spector, 2003).

1.1 Nucleolus

The most prominent of all the subcompartments in the nucleus is the nucleolus and is one of the most extensively studied (Monneron and Bernhard, 1969; Dundr and Misteli, 2002). Most mammalian nuclei contain between one and four nucleoli. The main function of the nucleolus is the biogenesis of ribosomes (Shaw and Jordan, 1995), which involves transcribing rDNA, processing transcripts and assembling rRNA with ribosomal proteins. The average nucleolus of a mammalian cell can produce up to 10,000 ribosomes per minute (Huang, 2002).

1.1.1 Ribosomal Biogenesis

The nucleolus is assembled around repeats of ribosomal genes (rDNA) and they cluster at chromosomal loci called nucleolar organising regions (NORs) (Ghosh, 1976; Derenzini, 2000). Eukaryotic somatic cells can contain hundreds of ribosomal genes (Raska *et al.,* 2004). RNA polymerase I drives the transcription of ribosomal genes and about 40,000 copies per cell exist and synthesise pre-rRNA (Gerbi *et al.,* 2003). This many RNA polymerase I molecules are needed because as many as 50 polymerase molecules are thought to transcribe each rRNA gene simultaneously (Mosgoeller *et al.,* 2000). The pre-rRNA consists of 18S, 5.8S and 28S rRNA sequences together with internal and external transcribed spacer sequences. Upstream binding factor, (UBF), forms part of the transcriptional complex together with RNA polymerase I, Tata binding protein (TBP), three transcription activity factors (TAFs), transcription initiation factors, TIF-1A and TIF-1C, and other factors.

Mature ribosomal RNA biogenesis is a complicated process that is carried out by many factors; non-ribosomal proteins and ribonucleoproteins (RNPs) and small nucleolar RNAs (snoRNAs). RNA helicases and RNA chaperones mediate RNP folding and remodelling. 5S rRNA is synthesised in the nucleoplasm and then, together with ribosomal proteins that are synthesised in the cytoplasm, become recruited to the nucleolus and become integrated into pre-ribosomal particles (Tschochner and Hurt, 2003). With help from special adaptor molecules, the almost completed ribosomal subunits move to the cytoplasm.

1.1.2 Nucleolar Morphology

Nucleoli vary a great deal in appearance depending on the cell type. However, most nucleoli are composed of three morphologically distinct components: the fibrillar centres, the dense fibrillar component and the granular component (Shaw and Jordan, 1995) (figure 1.2). Different nucleolar proteins localise to the different regions of the nucleolus. There is a gradual transition from the fibrillar centres through the dense fibrillar component to the granular component. The fibrillar centres (FCs) are each found to accommodate four genes and a typical HeLa cell has about 30 FCs. Only approximately 120-150 of the total number of rDNA genes (approximately 540) are active in HeLa cells (Dundr and Misteli, 2001). FCs resemble NORs and are thought to be the interphasic counterparts of mitotic NORs (Goessens, 1984). Each gene has between 100-120 engaged RNA polymerase I molecules. The molecular organisation of an active ribosomal gene is a structure that resembles a Christmas tree and was first seen in spreads of amphibian oocytes (Raska, 2003). The dense fibrillar component (DFC) contains no rDNA but does contain an accumulation of elongating and full length primary transcripts together with fibrillarin and nuclear proteins involved in pre-mRNA cleavage. Cleavage events start in the DFC (GC). Late processing and rRNA assembly into ribosomal subunits occur in the (GC) (Carmo-Fonseca *et al.*, 2000).

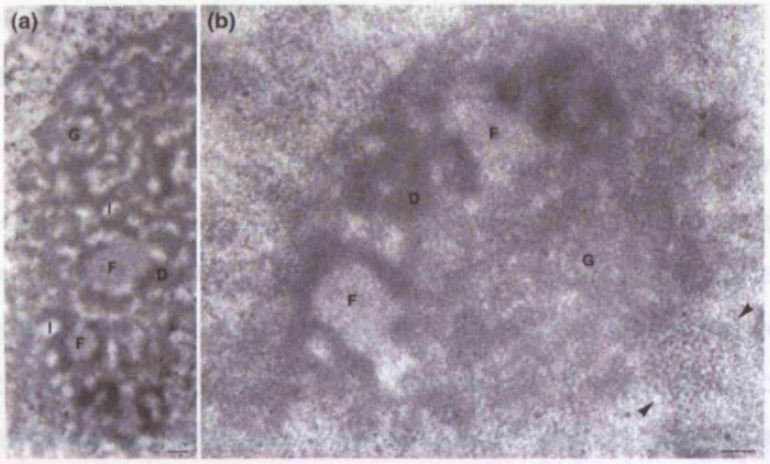

Figure 1.2
Ultrastructural characteristics of nucleoli from HeLa cells. (a) A reticulate nucleolus that is transcriptionally active. Fibrillar centres (F), dense fibrillar component (D) and granular component (G) can be seen. (b) This nucleolus has large FCs (F), surrounded by DCF (D). It is also possible to see a Cajal body (arrowheads). Scale bars = 200 nm (taken from Olson *et al.*, 2000).

1.1.3 Sites of rRNA Transcription

The site of actual pre-rRNA transcription is controversial. One study using electron microscopy to visualise the sites of labelled nucleotide incorporation in the nucleolus of HeLa cells (Koberna *et al.*, 2002) showed that the newly synthesised RNA was found in the DFC or bordering the DFC and FC but not in the FCs alone. Other studies support this notion (Hozak *et al.*, 1994; Cmarko *et al.*, 2000; Biggiogera *et al.*, 2001). However, results from other research groups contrast this idea. Mais and Scheer (2001), for example, visualised Br-U, UBF and RNA polymerase I in *Xenopus* oocytes surrounded by fibrillarin labelling. This suggests that transcription is occurring in the FCs and not the DFC. These contrasting findings have led to several possible models of the sites of rRNA transcription and these are illustrated in figure 1.3 (Huang, 2002).

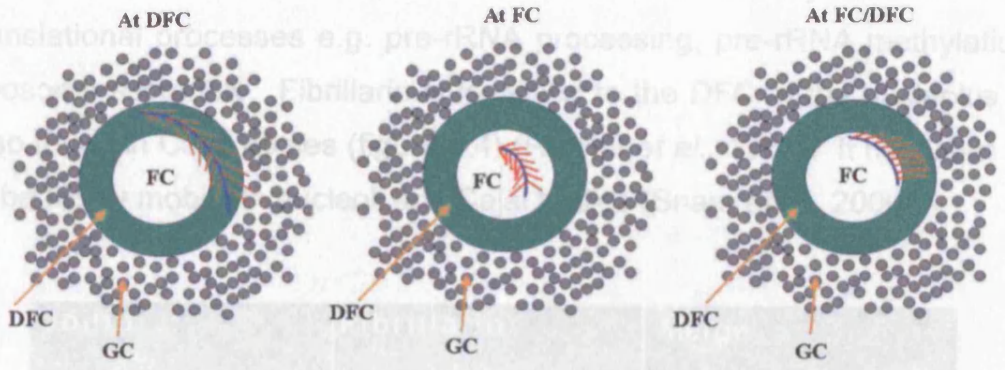

Figure 1.3
Schematic representation of the possible sites of rRNA transcription within the nucleolus (taken from Huang, 2002).

1.1.4 Proteins of the Nucleolus

It has been suggested that the nucleolus may have additional functions as well as those involved in ribosome subunit synthesis (Pederson, 1998; Scheer and Hock, 1999). Some of the proteins that constitute the nucleolus have also been shown to be engaged in a shuttling cycle between the nucleus and the cytoplasm and may play a key role in the transport of other proteins (Melese and Xue, 1995). Andersen *et al.* (2002) identified hundreds of protein components of the nucleolus using mass spectrometry. A complete list can be seen at:

www.dundee.ac.uk/lifesciences/lamonddatabase/flash.htm.

The list of proteins found to localise in the nucleolus highlight the fact that many biological processes and pathways function within the nucleolus; ribosome biogenesis, mRNA metabolism, translation, cell cycle regulation and signal recognition particles biogenesis. Experiments have shown that the nucleolus also appears to have other functions which include roles in nuclear export, modifying small RNAs, forming RNPs and controlling ageing (Olson *et al.*, 2000). Carmo-Fonseca *et al.* (2000) now suggests that molecular sequestration of proteins within the nucleolus is a mechanism to regulate cellular functions.

Fibrillarin

Fibrillarin is a component of the nucleolar U3 snoRNP complex that functions with other box C/D snoRNPs in site-specific 2'-O-methylation of pre-rRNA (Snaar *et al.*, 2000). Fibrillarin is also directly involved in post-translational processes e.g. pre-rRNA processing, pre-rRNA methylation and ribosome assembly. Fibrillarin is localised to the DFC of the nucleolus and is also found in Cajal bodies (figure 1.4) (Reimer *et al.*, 1987). It has been shown to be highly mobile in nucleoli and Cajal bodies (Snaar *et al.*, 2000).

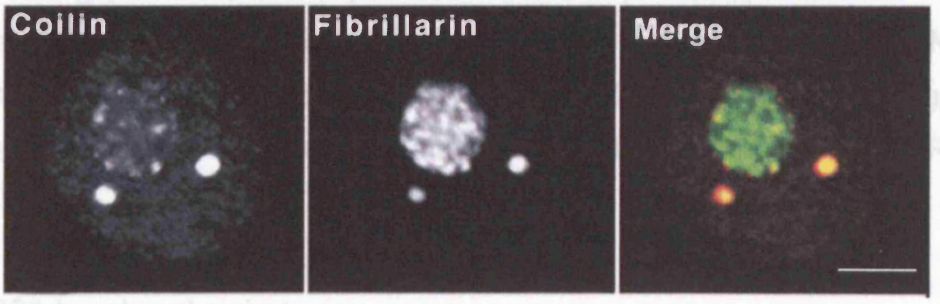

Figure 1.4
Confocal microscopy image showing trigeminal ganglion neurons double stained with p80 coilin and fibrillarin. Scale bar = 5 μm (taken from Pena *et al.*, 2001).

GAR1

GAR1 is found in the DFC of the nucleolus and is associated with a subset of snoRNAs (Girard *et al.*, 1994). GAR1 is believed to be involved in the processing of 35S primary transcripts of pre-rRNA and the synthesis of 18S rRNA (Shaw and Jordon, 1995).

Nopp140

Nopp140 interacts with largest subunit of RNA polymerase I and functions in the transcription of rRNA genes (Snaar *et al.*, 2000). It is found in a complex with NAP57 and also moves between cytoplasm and nucleolus, and between Cajal body and nucleolus. Nopp140 interacts with p80 coilin (Isaac *et al.*, 1998) and is found in Cajal bodies (Meier and Blobel, 1994) as well as the DFC of the nucleolus (Shaw and Jordon, 1995).

NAP57

NAP57 (Nopp140 -associated protein of 57 kDa) interacts with H/ACA snoRNPs and functions in pseudouridylation of rRNA (Snaar et a, 2000). It is found in the DFC of the nucleolus and exist in a complex with Nopp140. NAP57 is suggested to function in the chaperoning of ribosomal proteins and/or pre-ribosome assembly. NAP57 is also found in Cajal bodies (Meier and Blobel, 1994)

C23 (nucleolin)

C23 is found in the GC of the nucleolus and is involved in pre-rRNA processing (Sirri *et al.*, 2002). It is a nucleolar phosphoprotein that is involved in transcriptional control and also plays a role in the development of RNA in pre-ribosome formation (Shaw and Jordon, 1995). C23 has also been suggested to have a chaperone-like role in mediating interactions of proteins and rRNA (Xue and Melese, 1994).

B23 (nucleophosim)

B23 is found in the GC of the nucleolus and is involved in pre-rRNA processing (Sirri *et al.*, 2002). B23 is a highly conserved phosphoprotein protein and suggested to be play a role in the intermediate or later stages of ribosome biogenesis (Shaw and Jordon, 1995). It binds NLS sequences and is thought to shuttle between the nucleolus and the cytoplasm.

UBF

UBF (upstream binding factor) is found in the FCs and the DFC of the nucleolus (Shaw and Jordon, 1995). It is a transcription factor that forms part of RNA polymerase I transcription machinery (Hernandez-Verdun *et al.*, 2002).

RNA polymerase I

RNA polymerase I is found in FCs of the nucleolus. It forms part of the polymerase I transcription machinery (Hernandez-Verdun *et al.*, 2002) and is involved in transcribing only rDNA (Shaw and Jordon, 1995)

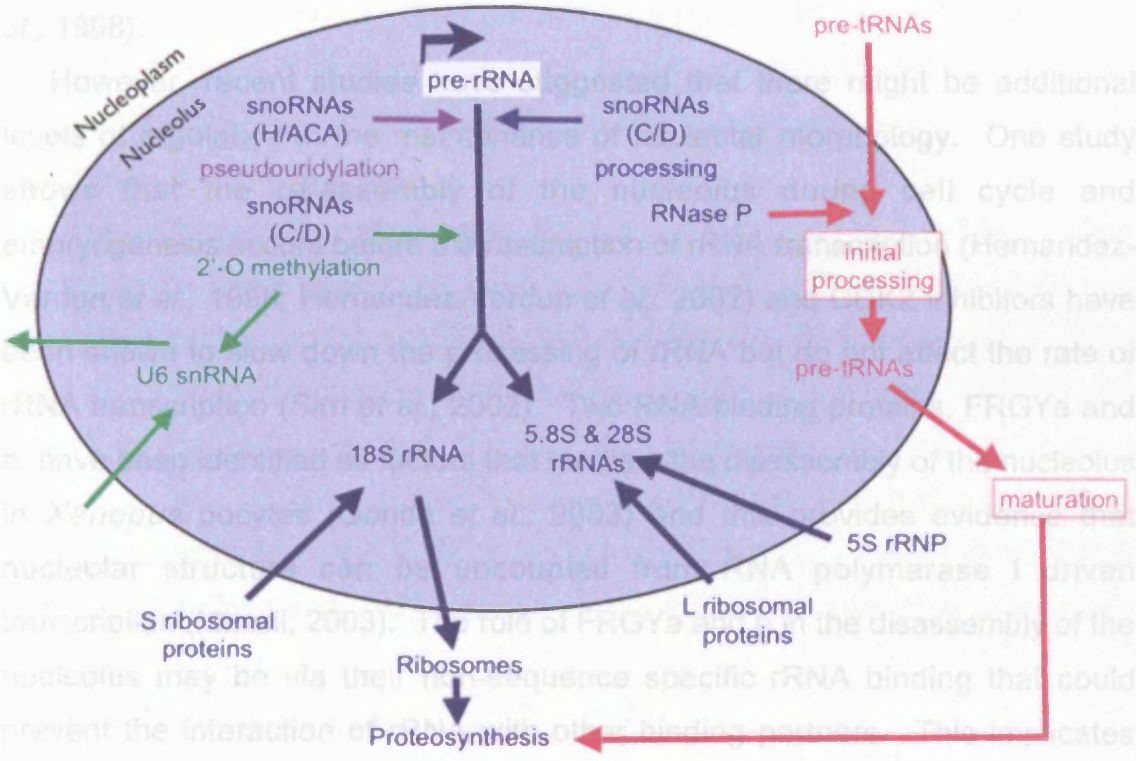

Figure 1.5
A schematic diagram showing the different functional pathways in the nucleolus. Pre-rRNAs are co-transcriptionally pseudouridinylated, 2'-O-methylated and cleaved. This is mediated by snoRNAs and rRNA is then assembled into large and small pre-ribosomal subunits. They are then exported to the cytoplasm. The nucleolus also functions in pre-tRNA maturation and modification of spliceosomal U6 snRNA (taken from Dundr and Misteli, 2001).

1.1.5 Nucleolar Dynamics

Fully active nucleoli are large with extensive intermingling of FCs, DFC and GC, whereas inactive nucleoli are often small and compact and the three morphological components frequently segregate (Shaw and Jordan, 1995). Despite the morphological differences, nucleoli are a permanent membrane-less structure seen in nearly all eukaryotic cells. Transcription driven by RNA polymerase I was originally suggested to be sufficient and necessary to organise and maintain this steady-state architecture (Weisenberger and Scheer, 1995). Several studies support this view and show that when rRNA transcription is inhibited with Actinomycin D, the nucleolus begins to segregate (Busch and Smetana, 1970; Granick, 1975). Also the introduction of ribosomal genes on minichromosomes results in the formation of 'mini-nucleoli' (Oakes *et al.,* 1998).

However, recent studies have suggested that there might be additional levels of regulation in the maintenance of nucleolar morphology. One study shows that the re-assembly of the nucleolus during cell cycle and embryogenesis occurs before the resumption of rRNA transcription (Hernandez-Verdun *et al.,* 1998; Hernandez-Verdun *et al.,* 2002) and CDK2 inhibitors have been shown to slow down the processing of rRNA but do not affect the rate of rRNA transcription (Sirri *et al.,* 2002). Two RNA-binding proteins, FRGYa and b, have been identified as factors that mediate the disassembly of the nucleolus in *Xenopus* oocytes (Gonda *et al.,* 2003) and this provides evidence that nucleolar structure can be uncoupled from RNA polymerase I driven transcription (Misteli, 2003). The role of FRGYa and b in the disassembly of the nucleolus may be via their non-sequence specific rRNA binding that could prevent the interaction of rRNA with other binding partners. This implicates rRNA itself in the maintenance of nucleolar morphology (Raska *et al.,* 2004).

All the research points towards a steady-state morphology for the nucleolus that is very dynamic and complicated. The maintenance of the nucleolar architecture involves an influx of components, transcription and RNA processing together with ribosome assembly and export (Snaar *et al.,* 1999; Misteli, 2001). There is evidence to suggest that no diffusion barrier exists between the nucleolus and the nucleoplasm (Melese and Xue, 1995) and there is a

continuous exchange of nucleolar components (Misteli, 2001). Therefore, the picture of a nucleolus must be a very dynamic image, with different molecules associating and disassociating at any given time. It is, however, an open system with the nucleolar structure being directly linked to its functional activity (Raska *et al.,* 2004).

1.1.6 The Nucleolus and Other Domains

Several sub-nuclear compartments are often associated with nucleoli including, the perinucleolar compartment (PNC) and the Cajal body (chapter 1.2.9). The PNC is an irregularly shaped structure ranging in size from 0.25 to 1 μm in diameter. It was first described by the localisation of hnRNP 1/PTB (polypyrimidine tract binding) protein (Ghetti *et al.,* 1992). Electron microscopy studies show that multiple, thick, electron-dense strands comprise the PNC, each 80-180 nm in diameter (Huang *et al.,* 1997). Huang (1998a) suggests that PNC are mainly seen in transformed cells and rarely seen in non-transformed primary cells in culture.

Several molecular components have been localised to the PNC. They include snRNAs transcribed by RNA polymerase III (Matera *et al.,* 1995) and three RNA binding proteins: PTB/hnRNP 1, CUG binding protein and KH-type splicing regulatory protein (KSRP) (Huang, 1998a). The presence of these factors in the PNC suggests that the PNC is involved in RNA metabolism (Huang *et al.,* 1998a). It has recently been shown that two small RNAs transcribed by RNA polymerase III are present in the PNC (Wang *et al.,* 2003) and that the presence of the PNC is dependent on continuous RNA polymerase III transcription.

1.2 The Cajal Body

Ramon Y Cajal (figure 1.6) first described the Cajal body in 1903 as a 'nucleolar accessory body' (reviewed by Gall, 2003). The small round structure was located within the nucleus and, together with the nucleolus, stained heavily when using silver staining techniques that Cajal had developed to stain neurons. The Cajal body did not attract much attention until it was first seen in non-neuronal cells many years later (Monneron and Bernhard, 1969) and termed the coiled body. It has more recently been suggested (Gall *et al.*, 2000) that this subdomain be renamed the Cajal body (CB).

Figure 1.6
Photograph of Ramon Y Cajal.

CBs are highly conserved in evolution (Bohmann *et al.*, 1995b) and are thought to play a role in snRNP transport and maturation (Sleeman and Lamond, 1999). CBs disassemble during mitosis and reforms during G1 phase after transcription is reinitiated (Andrade *et al.*, 1993; Ferreira *et al.*, 1994) and have been shown to be highly mobile structures that move throughout the nucleoplasm (Platani *et al.*, 2000) but are not found in cells of every tissue type.

1.2.1 Cajal Body Structure

Monneron and Bernhard used electron microscopy (EM) to investigate and describe the fine ultrastructure of mouse, rat and human nuclei. A "regressive EDTA method" was used to provide contrast between structures that contained RNA and those that do not. Many nuclei contained a spherical structure that was 0.3-0.5 μm in diameter and composed of what Monneron and Bernhard described as coiled threads. Similar images were seen in rat trigeminal neurons of 'nucleolar accessory body' (Hardin *et al.*, 1969) at EM. It was not until later that it was established that the coiled bodies described by Monneron and Bernhard, and, the accessory bodies seen in neurons, were in fact the same structure (Lafarga *et al.*, 1983). A combination of light and electron microscopy experiments showing the morphology and staining patterns of the

'coiled' body and 'accessory body' of Cajal in neurons revealed these structures were indeed the same nuclear body. Cajal bodies have now been reported in many different cell types and are seen with identical morphology in the nuclei of both plants and animal cells (Moreno Diaz de la Espina, 1980; Lamond and Carmo-Fonseca, 1993).

The ultrastructural appearance of the Cajal body is found to be a roughly spherical structure that is not bound by a membrane (Kinderman and LaVelle, 1976). The average diameter ranges from 0.1-1.0 μm depending on the cell type (Lamond and Carmo-Fonseca, 1993). CBs appear to be composed of coiled threads that have diameters of approximately 40-50 nm and are arranged as an accumulation of granules. The granules are embedded in low-density material (Lafarga *et al.,* 1983).

1.2.2 p80 coilin: the Cajal body marker protein

Human autoimmune sera was identified that stained Cajal bodies in cultured cells (Andrade *et al.,* 1991). From one of the sera, a cloned cDNA was isolated and found to encode a CB-protein. When run on a Western Blot, the protein was found to be 80 kDa in size and was named p80 coilin. Antibodies were affinity purified from the 80 kDa band and using immuno-electron microscopy the antigen was shown to localise predominantly to CBs (Raska *et al.,* 1991).

When p80 coilin was first sequenced it showed no clear homology to any other known protein motifs (Lamond and Carmo-Fonseca, 1993) until a similar protein was identified in the oocyte of *Xenopus* laevis (Tuma *et al.,* 1993). SPH-1, as the protein was called, was localised to the sphere organelles in the *Xenopus* oocytes. Sphere organelle were first seen as 'knobs' attached to lampbrush chromosomes from amphibian oocytes (Gall, 1954) and evidence now supports the notion that these are amphibian Cajal bodies (Gall *et al.,* 1995; Roth, 1995). It has since become evident that human p80 coilin and *Xenopus* SPH-1 are orthologous proteins (Bauer and Gall, 1997). The discovery of p80 coilin has also been used to show that Cajal bodies exist in plant cells (Beven *et al.,* 1995) and that they also contain U2B", U1, U2 and U6 snRNAs.

1.2.3 p80 coilin: structure

Full length p80 coilin is 576 amino acids in length and has a predicted mass of 62.6 kDa, but it runs on a SDS-PAGE at approximately 20 kDa greater (Chan *et al.*, 1994; Wu *et al.*, 1994). This discrepancy cannot be accounted for by post-translational modifications. p80 coilin does exhibit multiple phosphorylated serine residues in interphase nuclei and is hyperphosphorylated at mitosis (Carmo-Fonseca *et al.*, 1993). However, phosphorylation only has minor effects on the SDS-PAGE motility. The phosphorylation state of p80 coilin is probably more important for the proper localisation of p80 coilin and therefore Cajal body function (Hebert and Matera, 2000) (chapter 1.4).

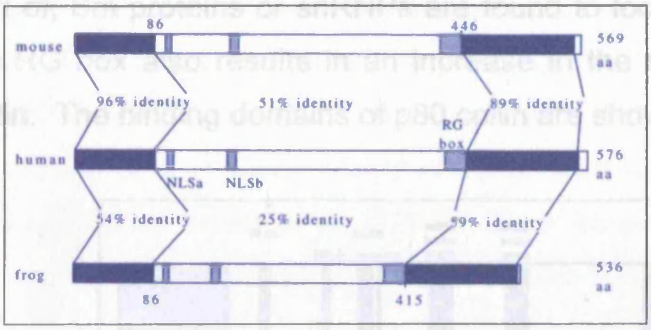

Figure 1.7
Schematic diagram showing the alignment of mouse, human and frog p80 coilin (taken from Tucker *et al.*, 2000).

The N-terminus and the C-terminus of amphibian and mammalian p80 coilin show more than 50% identical residues but only 33% of residues in the middle region and this is shown in figure 1.7. Therefore, the conserved protein motifs or domains are likely to be found in the highly homologous regions. When mouse and human sequences are aligned, together with the sequence from frog p80 coilin the homology can be clearly seen.

The first 100 amino acids of the N-terminus have several interesting properties. Deletion constructs of human p80 coilin revealed that the first 102 amino acids (18% of the molecule) targeted it to Cajal bodies within germinal vesicle of amphibians (Wu *et al.*, 1994). Bellini and Gall (1998) found that the same first 100 residues of the amino terminus of p80 coilin were both necessary and sufficient to bind single stranded nucleic acids and poly r(G) and poly (U) RNA homopolymers *in vitro*. The amino terminus has also been shown to interact with the nucleolar protein, Nopp140 (Isaac *et al.*, 1998).

The N-terminus also has a self-interacting domain and this has been shown to be necessary and sufficient to localise p80 coilin to Cajal bodies in HeLa cells (Hebert and Matera, 2000). However, hyperphosphorylation of p80 coilin was seen to cause a reduction in self-association. Two simple and bipartite nuclear localisation signals (NLSs) have also been identified in p80 coilin (Almeida *et al.*, 1998) together with a cryptic nucleolar localisation signal (NoSL) (Hebert and Matera, 2000).

Less is known about the C-terminus of p80 coilin but a stretch of arginine and glycine dipeptide residues, known as the RG box domain, has been located there and it has been shown by Hebert *et al.* (2001) that this motif binds to the survival of motor neurons protein, SMN, and is also essential for the proper CB formation. Without the RG motif no SMN or the macromolecular complex it is part of, Sm proteins or snRNPs are found to localise to CBs. The deletion of the RG box also results in an increase in the nucleoplasmic fraction of p80 coilin. The binding domains of p80 coilin are shown in figure 1.8.

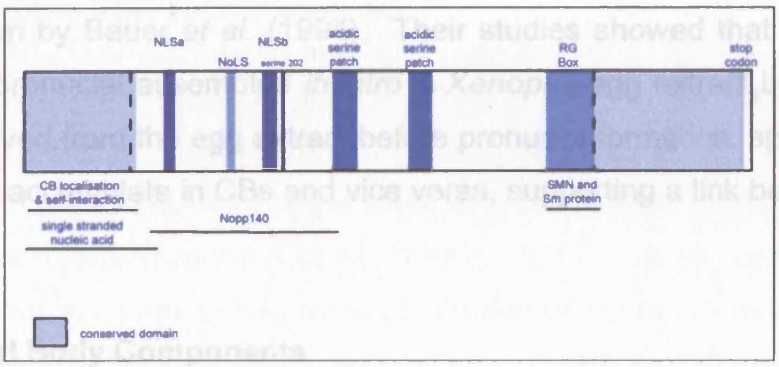

Figure 1.8
A diagram highlighting all the identified domains of p80 coilin.

1.2.4 p80 coilin: function

The actual function of p80 coilin is still unclear and it was thought that it was an important structural component of Cajal bodies. However, it has been shown that this is in fact not true as Bauer and Gall demonstrated that Cajal body-like structures could form in a nuclear extract that had been depleted of p80 coilin. Also, p80 coilin knock-out mice that have been created that lack 85% of the protein and are still viable and fertile (Tucker *et al.*, 2001). Exons 2

to 7 are deleted in the knockout mouse and using immunocytochemistry, 'residual' CBs can be identified that do not contain exon 1 of p80 coilin. These CBs fail to recruit snRNPs, Sm proteins and the SMN complex but the nucleolar proteins, fibrillarin and Nopp140, do accumulate in the 'residual' CBs (chapter 1.4.3). Thus, either the structural function of p80 coilin is not essential or another protein can take on its role in the nuclei lacking p80 coilin. It has also been shown that after microinjection of antibodies raised against p80 coilin in HeLa cells, CBs are seen to disappear (Almeida *et al.,* 1998), but no major cellular abnormalities were detected during this period. This suggests that whatever the function of p80 coilin, it can still be carried out by the nucleoplasmic pool.

Evidence has suggested a relationship between snRNPs and Cajal bodies since the discovery that snRNPs accumulate in CBs. A link between p80 coilin and snRNPs has also been shown with transient expression of p80 coilin mutants, some of which cause altered distribution of splicing snRNPs (Bohmann *et al.,* 1995a). Another connection between snRNPs and p80 coilin was shown by Bauer *et al.* (1994). Their studies showed that CBs could be found in pronuclei assembled *in vitro* in *Xenopus* egg extract, but if p80 coilin was removed from the egg extract before pronuclei formation, splicing snRNPs would not accumulate in CBs and vice versa, supporting a link between the two factors.

1.2.5 Cajal Body Components

Numerous molecular components have been detected in Cajal bodies and many of these molecules are involved in processing of all RNA types and transcription. Their identification was made easier with the identification of the CB marker, p80 coilin, as double-labelling experiments could be performed to discover additional CB components. As mentioned previously, splicing factors were among the first to be identified (Brasch and Ochs, 1992; Carmo-Fonseca *et al.,* 1992). Anti-Sm and anti-trimethylguanosine (TMG) staining showed both antigens localised to CBs as well as the well-known speckled pattern (Fakan *et al.,* 1984, Carmo-Fonseca *et al.,* 1991b). The presence of Sm and TMG in the CBs strongly supported the idea that snRNAs and snRNPs were also localised

in CBs. Since then all five of the major splicing snRNPs (U1, U2, U4, U5 and U6) have been localised to the Cajal body and all are subunits of the spliceosome (Carmo-Fonseca *et al.,* 1991a; Carmo-Fonseca *et al.,* 1991b; Huang and Spector *et al.,* 1992; Carmo-Fonseca *et al.,* 1992). However, the non-snRNP splicing factor, SC35, does not localise to CBs as immunoreactivity for anti-SC35 only reveals a speckled pattern of staining (Spector, 1991). Basal transcription factors TFIIF and TFIIH, Tata binding protein (TBP) and proximal element sequence-binding transcription factor (PTF) (Schul *et al.,* 1998b) as well as nucleolar components fibrillarin, Nopp140 and NAP57 have all been localised to CBs (Raska *et al.,* 1991; Meier and Blobel, 1992; Meier and Blobel, 1994). All of the CB components were also found elsewhere in the nucleus at equal or greater concentrations, and, even p80 coilin is not localised solely to the CBs, as it also exhibits a diffuse nucleoplasmic distribution. It has also been shown that there is heterogeneity among the components seen in different Cajal bodies within individual cells (Alliegro and Alliegro, 1998).

1.2.6 SMN: the SMA-determining gene

Survival of motor neuron protein (SMN) is the protein that is affected in spinal muscular atrophy (SMA). Detailed characterisation of the smallest deletions found in SMA patients allowed the identification and characterisation of the SMN gene (Lefebvre *et al.,* 1995). SMA is a recessive autosomal disorder that is characterised by degeneration of motor neurons in the spinal cord resulting in muscle weakness and often death in childhood and affects about 1 in 6000 births (Dubowitz, 1995; Lefebvre *et al.,* 1998; Meister *et al.,* 2002). Due to this, SMA is one of the leading hereditary causes of infant mortality.

The positional cloning strategy revealed that SMN gene is located on Chromosome 5 and exists in duplicate (Melki *et al.,* 1990; Burghes *et al.,* 1994). One copy is referred to as the telomeric copy, SMNt/SMN1, and one copy is called the centromeric copy, SMNc/SMN2. In 98% of SMA patients, SMN1 is lacking and SMN2 is a highly homologous copy (Lefebvre *et al.,* 1995). There are only 5 nucleotide differences between SMN1 and SMN2 (Lorson *et al.,* 1999) (figure 1.9). One of the differences is located in exon 7. It is a

translationally silent variant, but causes alternative splicing of exon 7 that is specific for SMN2 transcripts.

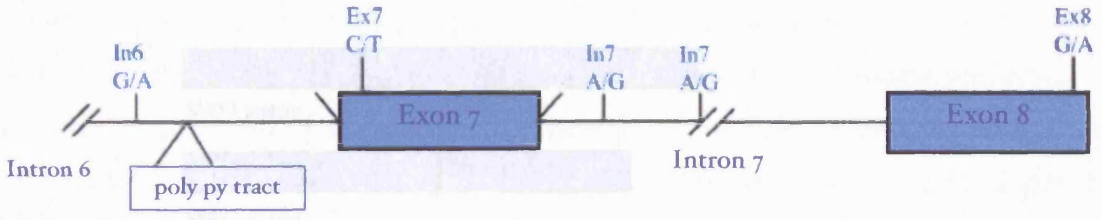

Figure 1.9
Schematic diagram showing the 5 nucleotide differences between SMN1 and SMN2 (taken from Lorson, 1999).

SMA patients show an increase in RNA transcripts lacking exon 7 compared to control individuals (Lorson *et al.*, 1999). The truncated transcripts represent the major form derived from SMN2. However, the presence of SMN2 gene in SMA patients and SMA mouse models is not sufficient to compensate for SMN1 defects (Monani *et al.*, 2000). In many cases of SMA, an increased number of SMN2 copies correlates with milder disease phenotypes, implying that SMN2 can sometimes be translated into a functional protein and could be a target as a modifying gene in SMA (Monani *et al.*, 2000).

The SMN gene encodes a protein that is 294 amino acids with a molecular weight of 38 kDa and shows no homology to any other proteins. It has 9 exons and they are numbered as shown in figure 1.10. In humans, SMN is a highly alternatively spliced protein (Jong *et al.*, 2000). Most SMN1 transcripts (90%) are full length but 10% are missing exon 5 or exon 7 and a small fraction are missing exon 3 or exon 3 and exon 7, whereas, only 20-30% of SMN2 transcripts are full length. The remaining transcripts have been shown to lack exon 3, exon 5 or exon 7 or a combination of all 3 exons. Murine SMN, on the other hand, is not alternatively spliced and shows 82% homology to human SMN at the amino acid level (Bergin *et al.*, 1997) but the mouse genome only has one copy.

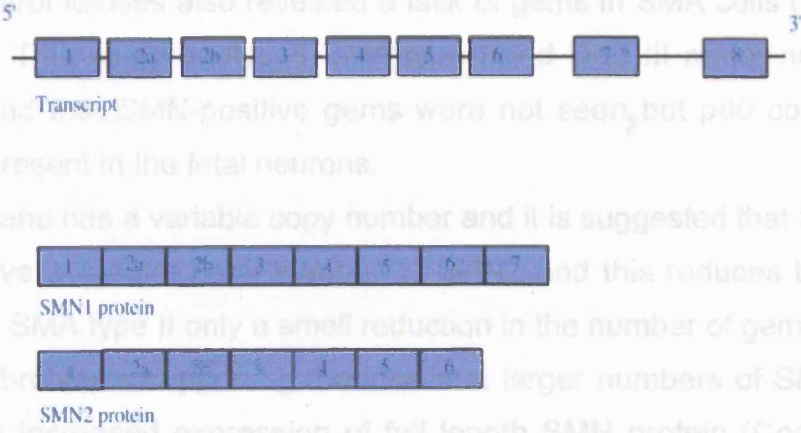

Figure 1.10
A diagram illustrating differential splicing of exon 7 in SMN1 and SMN2 transcripts.

In HeLa cells, SMN is found in both the cytoplasm and the nucleus (Liu and Dreyfuss, 1996). In some cell types, SMN localises in gems (chapter 1.2.10), but in many cell types, for example neurons, gems are not seen and SMN colocalises with p80 coilin in Cajal bodies (figure 1.11) (Carvalho *et al.*, 1999; Young *et al.*, 2000; Young *et al.*, 2001).

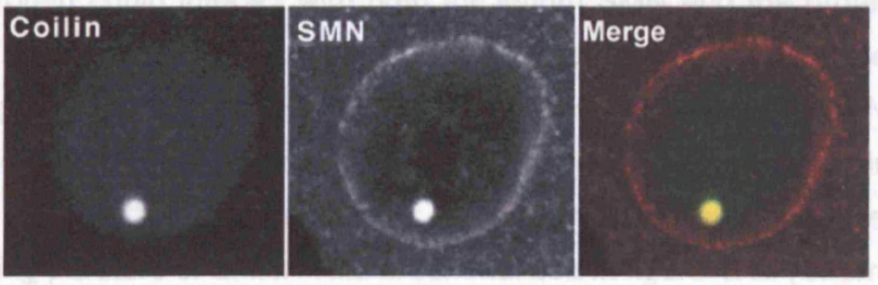

Figure 1.11
Double-immunolabelling of p80 coilin and SMN in neurons showing that p80 and SMN colocalise (taken from Pena *et al.*, 2001).

Immunocytochemical analysis of SMA patient fibroblasts shows a significant decrease in the number of gems in SMA type I (Coovert *et al.*, 1997) and a correlation between the number of gems and disease severity was reported. Immunofluorescence microscopy carried out on liver and spinal cord cells from

SMA or control fetuses also revealed a lack of gems in SMA cells (Lefebvre *et al.*, 1997). This study analysed SMA type I and type III motor neurons and demonstrated that SMN-positive gems were not seen, but p80 coilin-positive CBs were present in the fetal neurons.

SMN2 gene has a variable copy number and it is suggested that SMA type II patients have a greater copy number of SMN2 and this reduces the disease severity. In SMA type II only a small reduction in the number of gems was seen in patient fibroblasts supporting the idea that larger numbers of SMN2 genes can lead to increased expression of full length SMN protein (Coovert *et al.*, 1997). Therefore SMA type II patients have more SMN protein from the greater number of SMN2 genes and in sufficient amounts is able to assemble into gems. Frugier *et al.* (2000) also showed a reduction in the number of gems in nuclei from a mouse model of SMA that had a conditional deletion of murine SMN exon 7.

1.2.7 SMN Interacting Partners

When Liu and Dreyfuss (1996) screened a HeLa cDNA library using SMN as bait in the yeast two-hybrid system, SMN protein was found to interact with itself, fibrillarin and heterogeneous nuclear RNPs (hnRNPs). It was shown that SMN protein could interact with both full length SMN and the protein lacking exon 7 corresponding to the product of the alternatively spliced SMN2 transcript. Two novel proteins were also shown to interact with SMN. One of these novel proteins is Gemin2 (formerly known as SIP1 for SMN-interacting protein). Since then a large number of other proteins have been identified as interacting partners of SMN. This is summarised in figure 1.12 (Charroux *et al.*, 1999; Campbell *et al.*, 2000; Friesen and Dreyfuss, 2000; Jong *et al.*, 2000; Young *et al.*, 2000; Hebert *et al.*, 2001; Jones *et al.*, 2001; Matera and Hebert, 2001; Mourelatos *et al.*, 2001; Pellizzoni *et al.*, 2001b; Voss *et al.*, 2001; Wang and Dreyfuss, 2001).

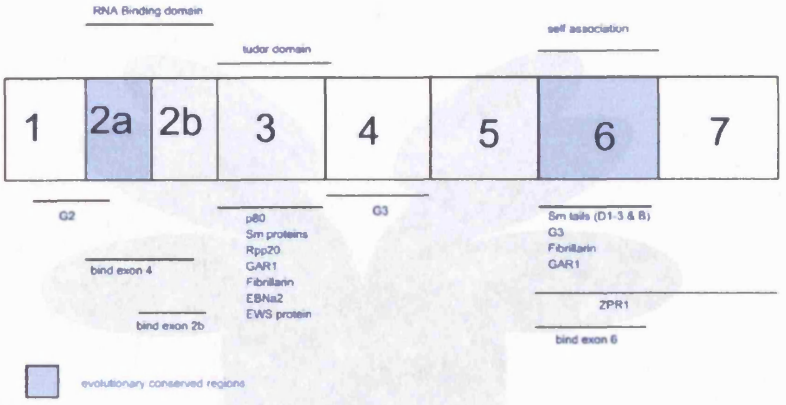

Figure 1.12
Diagram highlighting all the known binding domains of SMN protein.

1.2.8 SMN Complex

It has since been discovered that SMN protein is part of a macromolecular complex that has a molecular weight of 300 kDa with Gemin2 and up to five additional Gemin proteins (figure 1.13) (Campbell, *et al.*, 2000; Charroux *et al.*, 2000; Baccon *et al.*, 2002; Gubitz *et al.*, 2002; Pellizzoni *et al.*, 2002). In somatic cells, SMN and the Gemins colocalise in the cytoplasm and the nucleus (Charroux *et al.*, 1999). The cytoplasmic complex containing SMN and the other Gemins also contains Sm proteins that are components of the spliceosomal snRNPs (Liu *et al.*, 1997). Transfection studies with a deletion of the N-terminal of SMN (SMNΔN27) show that SMN has a critical role in the cytoplasmic association of snRNPs (Pellizzoni *et al.*, 1998). A reorganisation of snRNPs is seen when SMNΔN27 is overexpressed in the nucleus. Large CBs/gems are formed that contain mutated SMN, together with snRNPs and other nuclear proteins. The SMNΔN27 mutation also inhibits pre-mRNA splicing *in vitro* (Pellizzoni *et al.*, 1998) suggesting that SMN also plays a role in splicing. In the cytoplasm, SMN complex has a role in snRNA binding to Sm proteins and so it is implicated in the metabolism of snRNPs. The association of SMN and Gemin2 in the cytoplasm of *Xenopus* oocytes shows this. When antibodies directed against the SMN-Gemin2 complex were injected into oocytes the assembly of snRNP proteins and snRNAs were interfered with (Fischer *et al.*, 1997). A similar study has also been performed in HeLa cells and, in this case, pre-mRNA splicing was also inhibited (Meister *et al.*, 2000).

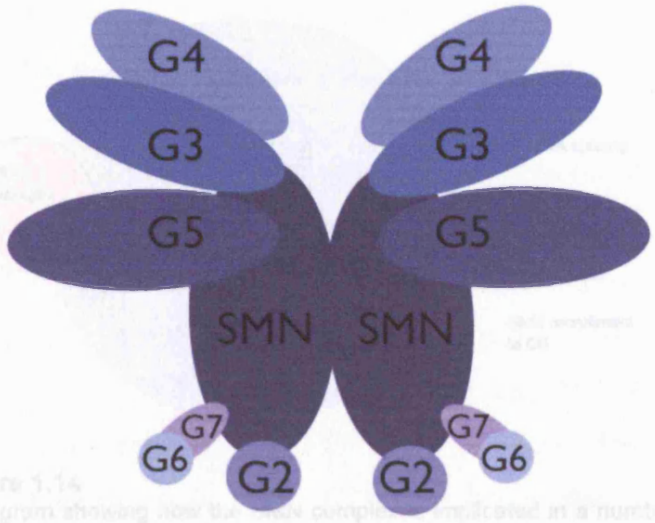

Figure 1.13
A schematic representation of the SMN complex (adapted from Charroux *et al.*, 2000).

The same study by Fischer *et al.* (1997) also showed that the SMN complex is thought to accompany the snRNPs into the nucleus to Cajal bodies. In CBs or gems, the SMN complex may have a role in the assembly of small nucleolar RNPs (snoRNPs) and metabolism for pre-rRNA splicing (Pellizzoni *et al.*, 2001a; Jones *et al.*, 2001; Whitehead *et al.*, 2002) due to the ability of SMN to interact with fibrillarin and GAR1 and their colocalisation in CBs. SMN may also play a role in the assembly of transcriptosomes which are large complexes containing RNA polymerase I, II or III, transcription factors and spliceosomes, for the coordinated synthesis and processing of mRNA and rRNA (Pellizzoni *et al.*, 2001b). The possible functions of the SMN complex are shown in figure 1.14. Any one of these interactions may be altered in SMA and therefore represent a defective pathway contributing to the pathology seen in SMA. An example of this has already been identified as SMA-causing mutations in the Tudor domain and SMN oligomerisation domain affect the binding of SMN to Sm proteins (Meister *et al.*, 2002) and implicates defects in spliceosomal snRNP assembly as part of the underlying the development of SMA (Carvalho *et al.*, 1999).

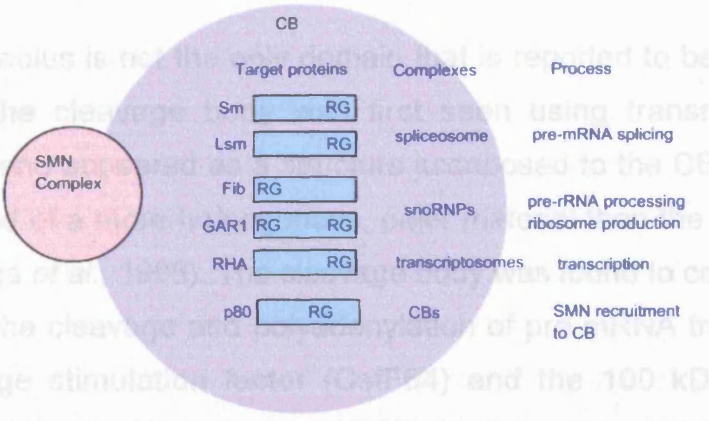

Figure 1.14
A diagram showing how the SMN complex is implicated in a number of cellular complexes. The SMN complex is suggested to mediate the assembly in Cajal bodies via its interactions with target proteins (taken from Terns and Terns, 2001).

1.2.9 Cajal Bodies and the Nucleolus

As first implicated by Cajal's original 'accessory' term for CBs, there appears to be an intimate relationship between the nucleolus and the Cajal body. A physical connection between the two structures can be seen using electron microscopy studies revealing fibres connecting CBs to the periphery of the nucleolus (Kinderman and LaVelle, 1976; Raska *et al.,* 1990). It is not only a spatial relationship that can be seen between these two subdomains, as there is also a molecular relationship as well. Cajal bodies contain several nucleolar proteins: fibrillarin, Nopp140, NAP57 and ribosomal protein S6 (Raska *et al.,* 1990; Raska *et al.,* 1991; Jimenez-Garcia *et al.,* 1994; Meier and Blobel, 1994). A number of these nucleolar factors have functions related to pre-rRNA processing. Fibrillarin is involved in pre-rRNA processing in yeast and is also associated with the C/D box snoRNAs that play a role in site-specific 2'-*O*-methylation and processing of rRNA (Weinstein and Steitz, 1999). Meier and Blobel have shown, using co-immunoprecipitation, that Nopp140 and NAP57 form a stoichiometric complex together in the nucleolus. It is suggested that they function in the chaperoning of ribosomal proteins and/or the assembly of pre-ribosomes. Phosphorylation is thought to regulate the interaction between the two compartments (Lyon *et al.,* 1997) and this will be discussed later (chapter 1.4).

1.2.10 Cajal Bodies and the Other Nuclear Domains

The nucleolus is not the only domain that is reported to be associated with the CB. The cleavage body was first seen using transmission electron microscopy and appeared as a structure juxtaposed to the CB. It was seen to be composed of a more homogenous, paler material than the CB (Schul *et al.*, 1996; Lafarga *et al.*, 1998). The cleavage body was found to contain two factors involved in the cleavage and polyadenylation of pre-mRNA transcripts: the 64 kDa cleavage stimulation factor (CstF64) and the 100 kDa cleavage and polyadenylation specificity factor (CPSF) (Schul *et al.*, 1996). Transcription factors, including TFIIE and TFIIF (RAP74) have also been localised to cleavage bodies in HeLa cells (Gall *et al.*, 1999).

Gems were first described on the basis of immunostaining with antibodies against the survival of motor neuron (SMN) protein (Liu and Dreyfuss, 1996). Gems have been frequently seen near or associated with CBs that have been identified using staining with an antibody to p80 coilin. It was later discovered that gems do not occur in every cell type and that the original HeLa cell line (PV) used by Dreyfuss was actually highly unusual in this regard. Recently a study of a variety of tissue types indicated that many adult mammalian cell types lack gems (Young *et al.*, 2000), and, SMN and other members of the SMN complex are seen to colocalise with p80 coilin at a single focus (Matera and Frey, 1998).

1.2.11 Cajal Body Function

Cajal bodies have been implicated in a number of key cellular processes mainly due to the components that have been shown to localise within them. This led to the idea that CBs were storage sites for many different factors but further evidence has identified a more dynamic role as several studies demonstrated that particular molecules are actually targeted to CBs. Three main areas of function for CBs have come to light: histone pre-mRNA 3'-end processing, pre-mRNA splicing and transcription.

1.2.12 Cajal bodies and Histone pre-mRNA 3'-end Processing

The function of Cajal bodies is still not known but it has been suggested that CBs play a role in histone pre-mRNA 3'-end processing. This is because CBs in amphibian oocytes were seen firmly attached to specific gene loci (Gall *et al.*, 1981) and *in situ* hybridisation showed that the sites of CB attachment were located at or very near to histone genes. The localisation of U7 snRNP to CBs supports the association between CBs and histone genes further as U7 snRNP cleaves the 3'-terminus of histone pre-mRNA (Frey and Matera, 1995). It is possible that the presence of U7 snRNP, in the attached CB, is a mechanism assuring its recruitment to the sites of histone pre-mRNA transcription. Frey and Matera (1995) also demonstrated the association of CBs with a subset of histone gene loci in HeLa cells. This was only seen for a small number of Cajal bodies as most CBs were found to be free in the nucleoplasm. However, the association between the Cajal body and gene loci does not have to be sustained for their expression (Shopland *et al.*, 2001).

The histone gene cluster is not the only gene cluster that is often seen to be associated with the Cajal body. It has also been shown that CBs can also be found juxtaposed to the snRNA genes (Jacobs *et al.*, 1999; Smith and Bentley Lawrence, 2000; Frey and Matera, 2001) as well as snoRNA host genes; the hsc70 gene hosting the U14 snoRNA, the S3 gene hosting the U15 snoRNA and the UHG gene hosting the U22 snoRNA (Schul *et al.*, 1999). These snoRNAs do not have their own genes but are encoded in the introns of other genes (the snoRNA hosting genes).

1.2.13 Cajal Bodies and Splicing or Processing of pre-mRNA

The presence of Sm epitope and the TMG cap together with the all the major and minor splicing snRNAs – U1, U2, U4, U5, U6, U11 and U12 – in CBs has led to speculation that CBs may function in splicing or in the general processing of pre-mRNA. However, as Cajal Bodies do not contain DNA and lack vital splicing factors such as SC35 or U2AF, nascent pre-mRNA or poly(A) mRNA (Matera, 1999), it is unlikely that they are actual sites of pre-mRNA transcription or splicing.

These reasons have lead researchers to focus on the idea that CBs may be involved in the biogenesis of snRNPs. It has been shown that nascent snRNPs do not accumulate in Cajal bodies, but maturing or mature snRNPs can be found in CBs in high concentrations. The first evidence to support this is pulse-chase experiments with titrated UTP that show a lag-time before CBs are labelled (Fakan and Bernhard, 1971). Secondly, pulses of Br-UTP revealed that CBs are separate from but adjacent to sites of transcription (Schul *et al.*, 1998b). Thirdly, the localisation of trimethylguanosine (TMG) cap and Sm protein epitopes to CBs shows that snRNPs concentrated within CBs are at least partially mature. This is because splicing snRNAs are synthesised in the nucleus but exported to the cytoplasm, where they are assembled into Sm particles, acquire the TMG cap and then return to the nucleus (Liu *et al.*, 1997). The presence of the Sm and TMG epitopes in CBs suggests that snRNAs have completed the cytoplasmic part of their life cycle.

This idea is further supported by the research of Dreyfuss and co-workers on SMN (Liu *et al.*, 1997). They showed that SMN is found in both the cytoplasm and the nucleus. In the nucleus, SMN is localised to CBs or gems and in the cytoplasm, it plays an important role in the cytoplasmic assembly of snRNPs (Fischer *et al.*, 1997). Antibodies directed against SMN and one of it binding partners, Gemin2, were shown to interfere with the proper assembly of Sm proteins and spliceosomal snRNAs when microinjected into HeLa cells. Mutational analysis of SMN in cultured cells has shown that over expression of an N-terminal deletion, called SMNΔN27, inhibits pre-mRNA splicing and causes a redistribution of splicing snRNPs into large CB-like structures (Pellizzoni *et al.*, 1998). This evidence suggests that SMN and its associated proteins may play a role within the nucleus that involves the recycling of splicing components and /or maintaining the active form of splicing machinery (Charroux *et al.*, 1999; Pellizzoni *et al.*, 1999).

Another connection between CBs and splicing was shown when amphibian oocytes where microinjected with radiolabelled U7 snRNA and the endogenous U7 snRNA within CBs was replaced by the injected constructs (Wu *et al.*, 1996). Narayanan *et al.* (1999) also used amphibian oocytes to demonstrate that microinjected fluorescently labelled C/D box small nucleolar RNAs (snoRNAs) associated with CBs transiently before accumulating in the nucleolus and

mutations to snoRNAs that remove the C/D box element (the nucleolar targeting region) resulted in the retention of the mutated snoRNAs in CBs.

When mammalian cells are microinjected with plasmids encoding the Sm proteins B, D1 and E, tagged with either green fluorescent protein (GFP) or yellow-shifted GFP (YFP) and then pulse expressed (Sleeman and Lamond, 1999), the newly synthesised fluorescently tagged snRNPs accumulate first in CBs, then the nucleolus and afterwards in speckles. This data suggests that transition of snRNPs through CBs and nucleoli is only part of their maturation pathway.

1.2.14 Cajal Bodies and Transcription

Recent studies have shown that CBs also contain the three eukaryotic RNA polymerases and other factors that function in transcription. From the data from these studies, Gall (2001) suggests Cajal bodies could be sites of transcription machinery assembly. It is thought that RNA polymerases associate with their respective transcriptional and processing factors in CBs, from where they are transported as pre-assembled complexes to the actual site of transcription. The first evidence to support this comes from staining of somatic CBs with a monoclonal antibody, 8WG16, which recognises the unphosphorylated C-terminal domain (CTD) of the large subunit of RNA polymerase II (Schul *et al.*, 1998b). This antibody also stains CBs in the *Xenopus* germinal vesicle (Gall *et al.*, 1999). A further two antibodies against RNA polymerase II also stain CBs: ARNA, an antibody that recognises an epitope outside the CTD, and, H14, an antibody that recognises the CTD when serine-5 is phosphorylated (Gall and Murphy, 1998). The H14 staining is quite surprising as the CTD becomes phosphorylated after RNA polymerase II has become bound to the chromatin template and before elongation. It therefore recognises an active form of RNA polymerase II. If germinal vesicles are exposed to 5,6-dichloro-1-beta-d-ribofuranosylbenzimidazole (DRB), an inhibitor of transcription, the H14 staining disappears over a period of time (two to three hours). The staining returns when the inhibitor is removed (Morgan *et al.*, 2000). DRB inhibits several protein kinases and prevents the phosphorylation of the CTD *in vitro* and *in vivo*. Gall speculated that this experiment shows that RNA polymerase II is

constantly entering and leaving CBs and in the presence of DRB, the phosphorylated form of RNA polymerase II leaves and is replaced with only the unphosphorylated form. A study demonstrating that newly synthesised RNA polymerase II subunits are targeted specifically to CBs supports the notion that RNA polymerase II moves through Cajal bodies (Morgan *et al.*, 2000). An epitope-tagged transcript of the RNA polymerase II subunit were injected into the cytoplasm of amphibian oocytes and within a few hours tagged RNA polymerase II protein was seen in CBs (Morgan *et al.*, 2000).

Nuclear proteins that are involved in transcription and the processing of RNA polymerase II transcripts have also been localised to or adjacent to CBs via immunostaining (figure 1.15). They include Tata binding protein (TBP), snRNA gene-specific transcription factor, PTF- and TFIIF (RAP74) (Schul *et al.*, 1998b) as well as TFIIH (Grande *et al.*, 1997).

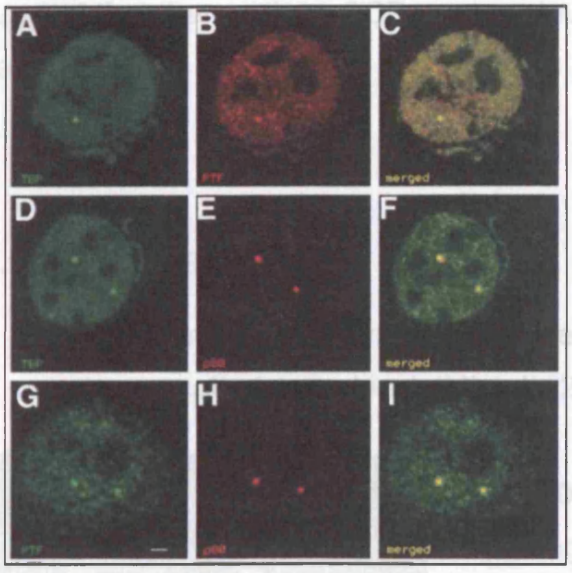

Figure 1.15
Immunostaining of Cajal bodies in HeLa cells demonstrating that TBP and PTF colocalise with p80 coilin (taken from Schul *et al.*, 1998b).

The evidence for RNA polymerase I and III is based only on immunostaining. Antibodies against two large subunits of RNA polymerase I have been localised to CBs in *Xenopus* germinal vesicles (Gall *et al.*, 1999). Two subunits of RNA polymerase III and one subunit shared by both RNA polymerase I and III have all been found to localise within oocyte CBs (Wang *et al.*, 1997). TFIIA, a transcription factor specific for 5S rRNA, has also been shown in oocyte CBs (Gall *et al.*, 1999).

Cajal bodies contain a variety of components that are involved in transcription and processing of all three types of RNA and include the three eukaryotic RNA polymerases. Even though many of these factors are found more abundantly elsewhere in the cell, targeting experiments have shown how many of them rapidly and specifically localise in CBs. These discoveries support the model of CB function as a site of preassembly of transcription machinery.

Pena *et al.* (2001) have shown that there is a relationship between transcription and the number of Cajal bodies and their relationship to the nucleolus. Mature trigeminal ganglion neurons (TGN) were studied and their cell body size, which is determined by transcriptional activity in diploid cells, was shown to correlate with the number of CBs seen per nucleus. There was a significant increase in CBs from small to large neurons. Large neurons also showed the highest percentage of nucleolar-associated CBs. These results suggest that the number of CBs per nucleus and CB localisation is transcription dependent.

1.3 Speckles

One nuclear compartment that occupies around 20% of the nuclear volume is commonly called 'speckles' (Misteli, 2000). Almost every essential pre-mRNA splicing factor is concentrated within the 20-40 domains called speckles or splicing factor compartments (Fu and Maniatis, 1990) as well as having a diffuse nucleoplasmic distribution (figure 1.16). Speckles were first described on the basis of their distinct morphology, long before the discovery of pre-mRNA splicing.

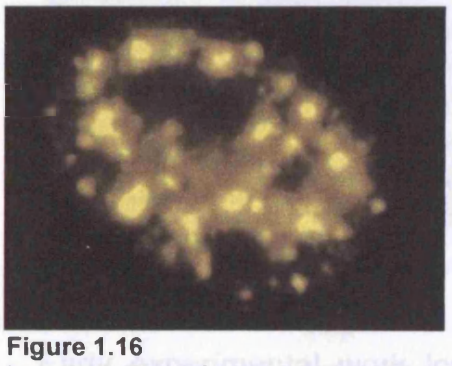

Figure 1.16
Immunostaining of speckles (from Misteli, 2000).

1.3.1 The Structure of Speckles

Using transmission electron microscopy (TEM), speckles are to be composed of two separate structures with differing ultrastructures (Puvion and Puvion-Dutilleul, 1996). The first, called interchromatin granule clusters (IGCs), have an apparent diameter of 0.8 to 1.8 μm and are composed of dense granules about 20-25 nm in diameter (Monneron and Bernhard, 1969) (figure 1.17). IGCs were first seen by Swift in 1959 and represent the major part of the speckle. They contain numerous factors that are involved in RNA synthesis and processing. The IGCs are interconnected by the second structure, the perichromatin fibrils (PFs) (Dundr and Misteli, 2001). The PFs are tiny fibres that are variable in diameter from 30 to 50 nm and are thought to represent nascent transcripts as they are rapidly labelled with [^{3}H]-uridine (Spector, 1993). Both structures can be seen by TEM without the need for antibody labelling and have also been visualised in living cells (Misteli and Spector, 1998). The IGCs and PFs compose a large latticework in the nucleus that can be seen to interact with the surface of the nucleolus and the nuclear envelope (Spector *et al.*, 1991).

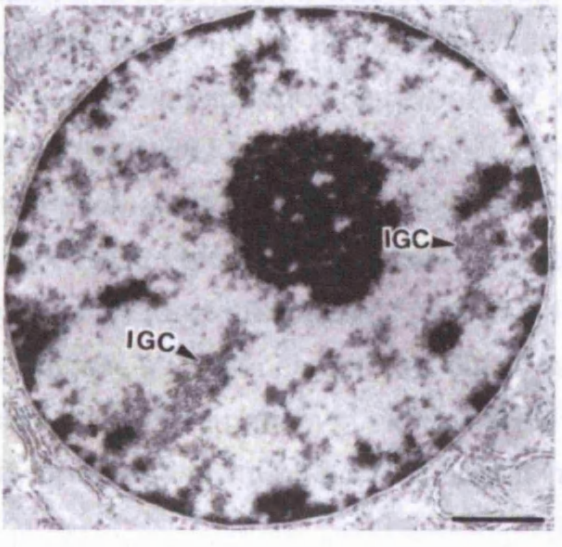

Figure 1.17
A transmission electron micrograph of mouse liver showing interchromatin granule clusters (IGCs). Scale bar = 1 μm (taken from Mintz *et al.*, 1999).

Early experimental work localised the small nuclear ribonucleoprotein particles (snRNPs) to speckles (Spector *et al.*, 1983) and led to the belief that speckles were involved in snRNP assembly. When the splicing factor SC35 was seen to colocalise with antibodies to snRNPs within speckles (Fu and Maniatis, 1990; Spector *et al.*, 1991), it provided the first evidence that speckles

also contained non-snRNP splicing components. An arginine/serine rich domain (RS domain) composed of approximately 120 amino acids at the C-terminal was discovered to be sufficient and essential to target proteins into the nucleus and specifically to speckles (Li and Bingham, 1991; Fu and Maniatis, 1992). Several splicing factors have this domain and they are termed the SR proteins. Studies have demonstrated that there are differences in the localisation pathways of different SR proteins (Caceres *et al.*, 1997; Dye and Patton, 2001). A second domain, the RNA-recognition motif (RRM) has been identified in SR proteins that either contains one or two RRMs. A single RRM requires a RS domain for proper localisation to speckles whereas SR proteins with two RRMs do not.

1.3.2 Transcription and Splicing

It was then suggested that these subdomains were more than just sites of snRNP assembly or storage and that speckles possibly corresponded to sites of spliceosomal assembly or splicing itself. More evidence was provided to support this idea when it was discovered that polyadenylated (poly(A)$^+$) RNA colocalised with snRNPs (Carter *et al.*, 1991).

The idea that speckles corresponded to sites of spliceosomal assembly or splicing itself was later to be proved incorrect when it was discovered that transcription and splicing occur together. Most RNA polymerase II transcripts are processed before being exported from the nucleus into the cytoplasm where they are translated into proteins (Spector, 1993). For the majority of transcripts, this processing includes splicing out of non-coding intron regions. Splicing occurs in an RNA-protein complex called a spliceosome that is composed of many proteins and snRNAs and is shown in figure 1.18.

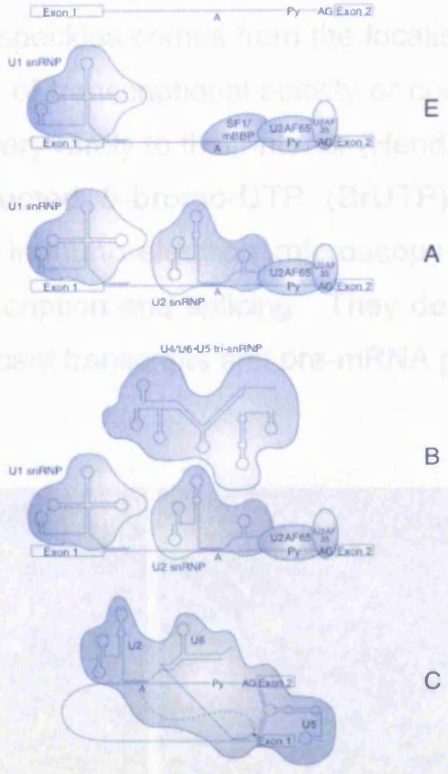

Figure 1.18
Diagram showing the spliceosome assembly pathway (taken from Graveley, 2000).

Experiments using adenovirus 2 as a model system to study the spatial relationship of transcription and splicing showed that after infection, RNA polymerase II, pre-mRNA splicing factors and hnRNP proteins were shuttled to sites of Ad2 RNA synthesis and all colocalised (Jimenez-Garcia and Spector, 1993).

Fluorescence microscopy data supports this idea and puts the position of genes at the periphery of or between speckles (Huang and Spector, 1996; Zeng *et al.*, 1997; Smith *et al.*, 1999) and that the association between nascent RNA and splicing factors is intron-dependent (figure 1.19). Nucleotide incorporation experiments and gene mapping studies showed that sites of active transcription can be found throughout the nuclear volume and that the majority of actively transcribing genes are found within the PFs and largely excluded from the IGCs (Misteli *et al.*, 1998).

Further evidence that suggests transcription and splicing generally occur at the periphery of speckles comes from the localisation of acetylated histones, a general indicator of transcriptional activity or competent DNA, to the periphery of speckles, but very rarely to their interior (Hendzel *et al.*, 1998). Cmarko *et al.* (1999) microinjected 5-bromo-UTP (BrUTP) into living cells and used postembedding immuno-electron microscopy to visualise various factors involved in transcription and splicing. They demonstrated that PFs were the major site of nascent transcripts and pre-mRNA processing.

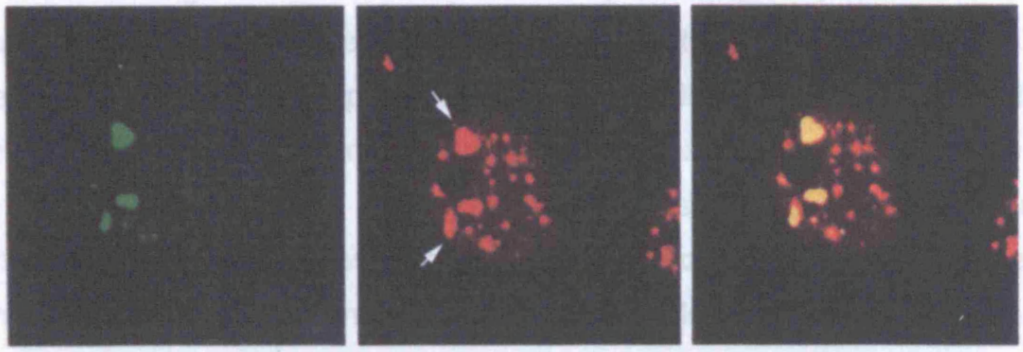

Figure 1.19
Immunostaining showing that transiently expressed RNA transcript containing introns are spatially associated with splicing factors. The RNAs are localised by FISH with biotinylated probes (green) and SC35 is detected using a monoclonal antibody (red) and colocalise to the same nuclear region (yellow) (taken from Huang and Spector, 1996).

The association of transcription sites with speckles does not simply reflect the amount of splicing factors bound to transcripts but it is suggested to be influenced in a locus specific manner. Neugebauer and Roth (1997) discovered that there was a gene specific accumulation of individual splicing factors at sites of transcription. They identified a single member of the SR family of proteins that can only be detected at ~20% of these sites.

However, a different study showed that the intranuclear position of transcriptionally active EVB genes, as well as nascent transcripts, revealed a random distribution with regard to speckles and therefore argued against the locus-specific organisation of mRNA genes and speckles (Melcak *et al.*, 2000). IGCs are therefore proposed as storage and/or assembly sites for pre-mRNA splicing factors and these splicing factors are recruited to sites of active transcription (Jimenez-Garcia and Spector, 1993).

Studies using time-lapse microscopy on living cells support this idea and it was seen that upon gene activation, pre-mRNA splicing factors are released from speckles and redistribute to sites of active transcription (Misteli and Spector, 1997).

The inhibition of transcription also causes a redistribution of splicing factors. When cells are treated with either Actinomycin-D or α-amanitin, inhibition of RNA polymerases is caused and splicing factors are seen to accumulate specifically in speckles and there is a subsequent enlargement of speckles (Carmo-Fonseca *et al.*, 1992; Zeng *et al.*, 1997) (chapter 1.4.4).

These findings have been summarized by Misteli (2000) and are shown in figure 1.20. The first image represents a transcriptionally active gene (red) that is associated with the periphery of a speckle (yellow). When transcription is inhibited, as in the second image, the gene is usually found some distance from the more rounded speckle. The last images shows that unspliced RNA (green) from highly expressed genes, or genes with numerous introns, may be released from sites of transcription and move towards speckles.

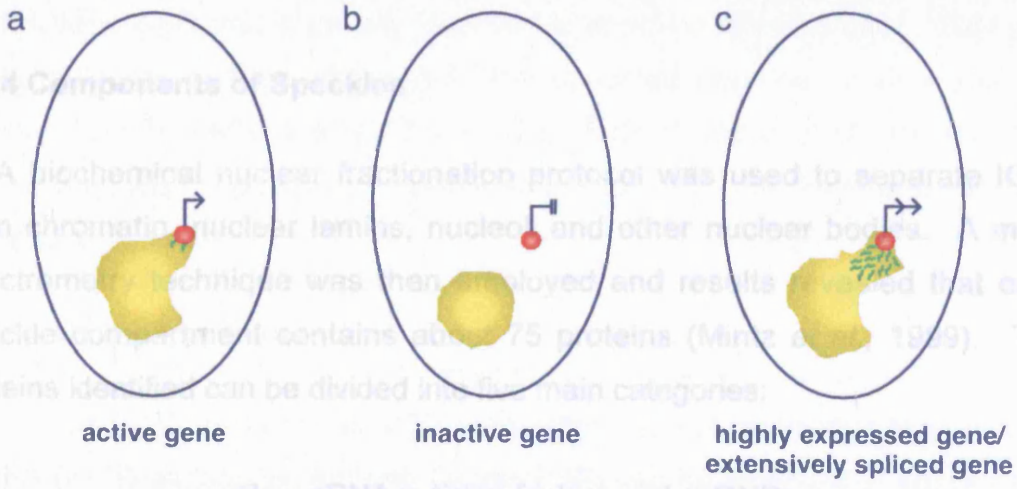

Figure 1.20
Diagram showing the relative positioning of transcription sites and speckles (taken from Misteli, 2000).

1.3.3 Screening and Trafficking

Speckles have also been suggested to play a functional role in pre-mRNA transcript screening and trafficking (Johnson *et al.*, 2000). In some cases of the disease, osteogenesis imperfecta, there is a mutation in the collagen type 1 gene, COL1A1, which results in a shift in the reading frame and the subsequent retention of intron 26 in the mutant RNA. The mutant transcripts do not accumulate at nuclear pores but can be seen to accumulate speckles. From these results, it is suggested that nuclear export of COL1A1 mRNA from the nucleus is a multi-step process (Johnson *et al.*, 2000). The first event is the movement of the mRNA from the gene into the adjacent speckle, which creates a RNA track on one side of the gene. The (normal) mRNA then moves into the nucleoplasm and, when it reaches the nuclear envelope, the mRNA translocates through the nuclear pore into the cytoplasm.

The results implicate speckles in the screening and entrapping of mutant COL1A1 RNA and imply that the correct splicing of pre-mRNA is not only needed for RNA maturation but also serves as a control step as the mutant mRNA is partially spliced but not exported.

1.3.4 Components of Speckles

A biochemical nuclear fractionation protocol was used to separate IGCs from chromatin, nuclear lamins, nucleoli and other nuclear bodies. A mass spectrometry technique was then employed and results revealed that each speckle compartment contains about 75 proteins (Mintz *et al.*, 1999). The proteins identified can be divided into five main categories:

i. Pre-mRNA splicing factors and snRNPs
ii. Transcription factors
iii. 3' processing factors
iv. SR protein kinases
v. Ribosomal proteins

1.3.5 Dynamics

Speckles are spatially dynamic with regard to movement and composition. The splicing factors within the IGCs are highly mobile and are constantly associating with and dissociating from the compartment (Misteli *et al.,* 1997). Although the overall position of the speckle is maintained (Eils *et al.,* 2000), each compartment undergoes continuous changes in shape, suggesting that there is a high degree of internal dynamics (Misteli, 2001). When the splicing factor, SF2/ ASF, was studied (Phair and Misteli, 2000) its residence time in speckles was not more than 45 seconds and at least 10,000 molecules of SF2/ASF are lost from the speckle per second per cell. This means that each speckle has a complete turnover of SF2/ASF within two minutes. The half-life of most splicing factors is fairly long and only 10-20% of any given splicing factor is engaged in the splicing reaction at any time *in vivo* (Misteli, 2000).

1.3.6 Speckles and RNA 3' Maturation

If RNA 3' processing is inhibited by treating cells with Ara-A, which does not affect RNA synthesis, a reversible disruption of the speckles can be seen. PABII is a poly(A) binding protein that is involved in the polyadenylation of pre-mRNA transcripts and is usually localised in speckles (Krause *et al.,* 1994) but when cells are treated with Ara-A, the speckles become smaller and still immunostain for PABII and SC35 and U2 snRNP B" (Schul *et al.,* 1998c). This points towards a structural relationship between speckles and RNA 3' maturation.

1.3.7 Role in Apoptosis

A study by Shav-Tel *et al.* (2001) indicates that polypyrimidine tract binding protein (PTB)-associated splicing factor (PSF) can be localised in speckles by using antibody B92 but this immunostaining disappears during apoptosis. In apoptotic cells, PSF redistributes from speckles into a globular nuclear structure and disassociates from PTB and binds to new binding partners, including U1-70k and SR proteins. It is suggested that the new functions acquired by PSF may be due to the protein's hyperphosphorylation. It has been reported that the

phosphorylated SR proteins are associated with the U1-snRNP complex during apoptosis (Utz *et al.*, 1998) and it is suggested that splicing factors can regulate apoptosis by regulating caspase activity.

1.3.8 Regulation via Phosphorylation

It was suggested that there must be signals generated in the nucleus that regulate the localisation of the factors to where they are temporally required for specific functions (Spector, 1993). With regard to splicing factors and speckles, it is believed to be a 2-step process that mainly involves the release of splicing factors from speckles, which is mediated by the RS domain found in many splicing proteins. The association of splicing factors with the target pre-mRNA follows this and is mediated by their RNA-recognition motif (RRM). It is the phosphorylation of the serine residues in the RS domain by SR protein kinases that displace the splicing factor from the speckle either individually or complexed to other components involved in RNA processing. The phosphorylation has the second effect of making the proteins "active" which leads to their incorporation into the spliceosome. It also allows the subsequent binding of the factors to the C-terminal domain of the large subunit of RNA polymerase II (Eils *et al.*, 2000). After the reaction, the dephosphorylation of the proteins by specific phosphatases allows them to return to the speckles. This is shown in figure 1.21.

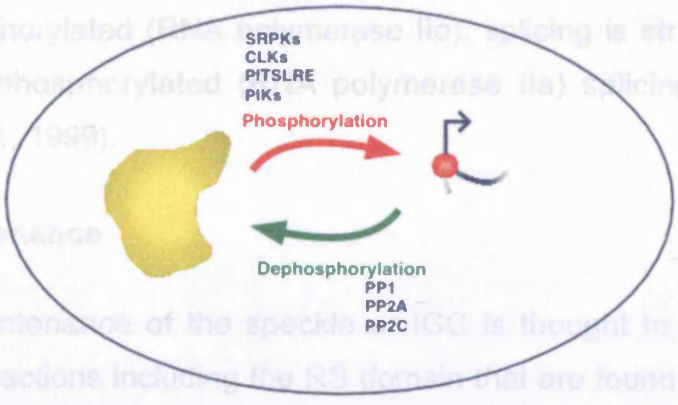

Figure 1.21
Diagram showing the mechanisms of splicing factor localisation by phosphorylation (taken from Misteli, 2000).

Evidence to support this suggestion was shown by the overexpression of different splicing factor specific protein kinases. This leads to the release of splicing factors from speckles and some the kinases have been located in the speckles (Gui *et al.,* 1994; Colwill *et al.,* 1996; Misteli, 2000). Time-lapse microscopy experiments in living cells have shown that the release of splicing proteins can be blocked in the presence of a kinase inhibitor (Misteli *et al.,* 1997). Other experiments have also shown that the accumulation of splicing factors in speckles upon inhibition of transcription requires serine-threonine protein phosphatase activity (Misteli and Spector, 1996). These experiments are discussed in chapter 1.4.4 and strongly support a control mechanism of splicing factor distribution by a cycle of phosphorylation and dephosphorylation and relocalisation of SR proteins can occur if there is an improper balance in the phosphorylation state. This phosphorylation could also modulate protein-protein interactions within the spliceosome itself, aiding the organisation of the spliceosome during splicing (Misteli, 1999).

Due to this finding it is believed that the IGCs are linked to the phosphorylation state of the SR proteins with dephosphorylated splicing factors favouring an association with speckles (Misteli and Spector, 1997) and, therefore, also the ability of the processing machinery to perform pre-mRNA splicing. It has also been shown if splicing factors cannot interact with the CTD of the large subunit of RNA polymerase II, they are not targeted to transcription sites and splicing is reduced (Misteli and Spector, 1999). The phosphorylation state of the CTD of RNA polymerase II also affects splicing: when hyperphosphorylated (RNA polymerase IIo), splicing is strongly activated but when hypophosphorylated (RNA polymerase IIa) splicing can be inhibited (Hirose *et al.,* 1999).

1.3.9 Maintenance

The maintenance of the speckle or IGC is thought to be due to protein-protein interactions including the RS domain that are found in the SR family of proteins (Sacco-Bubulya and Spector, 2002), rather than by an attachment to an IGC-specific framework. Upon overexpression of Clk/STY the stable population of poly(A)$^+$ RNA usually found in speckles is seen to redistribute and

becomes nucleoplasmic whereas the nascent transcripts remain at sites of transcription. It is therefore suggested that the stable population of poly(A) RNA may have a role in maintaining the organisation of splicing components in their nuclear domains and they could represent the core organising unit of the individual IGCs and the binding site for the pre-mRNA processing proteins.

Another motif thought to act as a protein-protein interaction sequence is the zinc finger motif (Dye and Patton, 2001). It has been shown to act as a subnuclear localisation domain and this raises the possibility that the zinc finger found in many splicing components might be involved in their localisation to speckles. Splicing proteins that have the zinc finger domain are SF1, U1-snRNP-specific protein C (U1C), SFa^{60}/SAP^{61}, SAP^{62}, $SF3a^{120}/SAP^{114}$, and hslu7. Another study showed splicing factors $SF3b^{155}/SAP^{155}$ did not contain a RS domain and was found to localise to speckles (Eilbracht and Schmidt-Zachmann, 2001). Mutation experiments revealed a threonine/proline-dipeptide domain (TP domain) that was required for the accumulation of $SF3b^{155}/SAP^{155}$ in speckles.

It has therefore been shown that speckles function in the storage and assembly of spliceosomal components with splicing factors moving towards active genes and pre-mRNA transcripts moving towards speckles. Figure 1.22 (Misteli, 2000) shows diagrammatically the potential functions of speckles; a) controlling the level of splicing factors in the nucleoplasm to optimise splicing; b) recycling splicing factors; c) controlling the relative ratios of multiple splicing factors in the nucleoplasm to regulate splice-site selection; d) site assembly of complexes involved in transcription and RNA processing to aid the coupling of transcription and RNA processing.

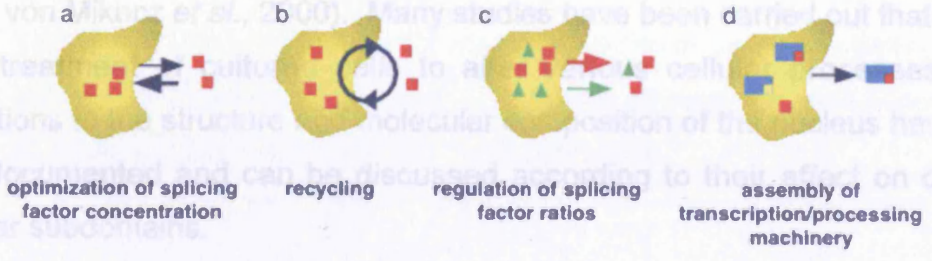

Figure 1.22
Diagram showing the possible functions of speckles (taken from Misteli, 2000).

The basic morphology of speckles at either light microscopy or TEM can indicate the transcriptional state of the cell. Cells with increased transcription show a decrease in the overall number and size of speckles whereas cells with reduced or no transcriptional activity have an increased number of speckles (Lamond and Earnshaw, 1998). Examining the different phosphorylation states of RNA polymerase II large subunit (LS) can also reveal the transcriptional activity of the cell. For example, hyperphosphorylation of RNA polymerase II LS CTD is a better indicator of the polymerase's tight association to speckles rather than its transcriptional activity as RNA polymerase II and splicing factors redistribute simultaneously according to the actual transcriptional activity of the nucleus (Bregman *et al.,* 1995; Kim *et al.,* 1997). This gives an image of a dynamic nucleus that reorganises its components through a mechanism of phosphorylation depending on the functional requirements of the cell.

1.4 Nuclear Architecture Meets Metabolic Activity

There appears to be a strong relationship between nuclear architecture and fundamental nuclear processes such as gene expression. The organisation of the nuclear subcompartments is thought to be a mechanism of bringing together molecules of related functions, thus improving the efficiency of cellular processes. The assembly of the substructures is a response to the metabolic requirements of the cell. Changes in the activity within the cell can cause alterations in the relative concentrations and distributions of different proteins in different nuclear structures (Carmo-Fonseca *et al.,* 1992; Lafarga *et al.,* 1994; Bregman *et al.,* 1995; Zeng *et al.,* 1997; Sleeman *et al.,* 1998; Pena *et al.,* 2001; von Mikecz *et al.,* 2000). Many studies have been carried out that involve drug treatment of cultured cells to alter various cellular processes. The alterations to the structure and molecular composition of the nucleus have been well documented and can be discussed according to their effect on different nuclear subdomains.

1.4.1 Alterations to the Nucleolus

Alterations in nucleolar morphology and size have been observed in response to changes in the transcriptional rate of the nucleolus. An example of this is osmotic stress, which causes cellular activation and induces the transient expression of immediate-early genes such as c-*fos* and c-*jun* that are transcription factors. Administration of hypertonic NaCl solution to rats by intraperitoneal injection results in osmotic stress and transcription of neurohormones is seen to increase in supraoptic nuclei (SON) neurons (Lafarga *et al.,* 1991). Nucleoli from dehydrated SON neurons have an increased diameter and, when viewed using an electron microscope, it is possible to see that there are large masses of granular component and small fibrillar centres (Lafarga *et al.,* 1991) (figure 1.23). It is suggested that the changes in size and arrangement are due to the osmotic induction of protein synthesis and the need for ribosomes. The changes in nucleolar structure are related to both RNA metabolism and protein synthesis. The increase in granular component may represent an increase in the processing of pre-rRNA and the decrease in the fibrillar centres may represent splitting of centres to make increase the number of transcription units. Therefore, the increase in transcription results in a change to the structure of the nucleolus.

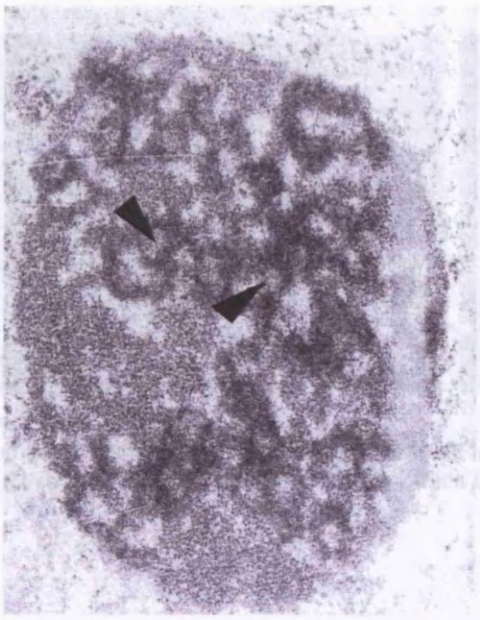

Figure 1.23
Nucleolus from an osmotically stimulated SON neuron. Large masses of GC can be seen with small FCs (arrowheads) (taken from Lafarga *et al.*, 1991). X29K

However, more recent studies have shown that the initial phase of osmotic stress actually results in transcription inhibition and this causes changes to the morphology of the nucleolus (Lafarga *et al.*, 1998; Berciano *et al.*, 2002). There is a partial segregation of the granular and dense fibrillar component and disruption to the fibrillar centres. This suggests that during a period of down regulation of transcription, the nucleolus undergoes morphological changes as well.

To support this idea, studies have shown that when all nuclear transcription is inhibited in many cell types with Actinomycin D, structural alterations to the nucleolus are seen. When cultured liver cells were treated with Actinomycin D, a progressive decrease in nucleolar size and a redistribution of nuclear components to form 'caps' was seen (Reynolds *et al.*, 1964) (figure 1.24). In HeLa cells, these caps have now been shown to immunolabel with a variety of different nuclear proteins: p80 coilin, fibrillarin, PSF, U1 snRNP (Carmo-Fonseca *et al.*, 1992). It has also been shown that the treatment of cells with Actinomycin D induces the redistribution of some nucleolar proteins. C23, B23 and the nucleolar RNA helicase, RH-II/Gu, all translocate from the nucleolus into the nucleoplasm after drug treatment (Perlaky *et al.*, 1997). Therefore, if transcription is inhibited the nucleolus becomes smaller, caps are formed and some nuclear proteins are seen to redistribute to different nuclear localisations.

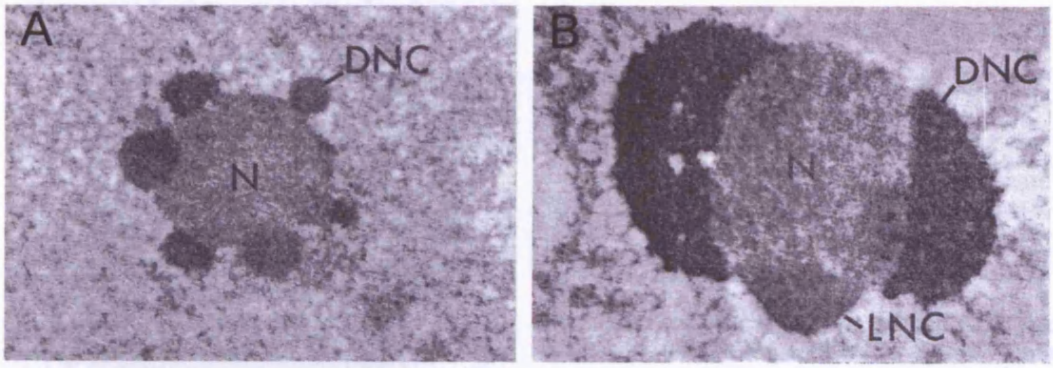

Figure 1.24
Nucleoli from Actinomycin D treated liver cells. It is possible to see two types of nucleolar caps; dense (DNC) or light (LNC) (taken from Reynolds *et al.*, 1964). X11K (A) and X20K (B)

Okadaic acid is a serine-threonine protein phosphatase inhibitor and prevents dephosphorylation. After HeLa cells were treated with okadaic acid, a decrease in the number of nucleoli per nucleus was seen and the remaining nucleoli became larger (Lyon *et al.*, 1997). There was also a change in the internal structure of the nucleolus. If dephosphorylation is inhibited there is a change in the number, size and morphology of nucleoli, suggesting that the phosphorylation of proteins plays an important role in controlling nucleolar organisation.

Cycloheximide not only inhibits protein synthesis but it also inhibits nucleolar rRNA synthesis (Gokal *et al.*, 1986). It does not however, affect extranucleolar synthesis of pre-mRNA (Lafarga *et al.*, 1994). SON neurons from rats treated with cycloheximide show changes to the organisation of the nucleolus (Lafarga *et al.*, 1994). There is also a decrease in the size of the nucleolus with the formation of larger and fewer fibrillar centres (figure 1.25). The fibrillar centres are often located eccentrically and not completely surrounded by the dense fibrillar component. These results support the concept that on-going nucleolar transcription is needed to maintain normal nucleolar assembly.

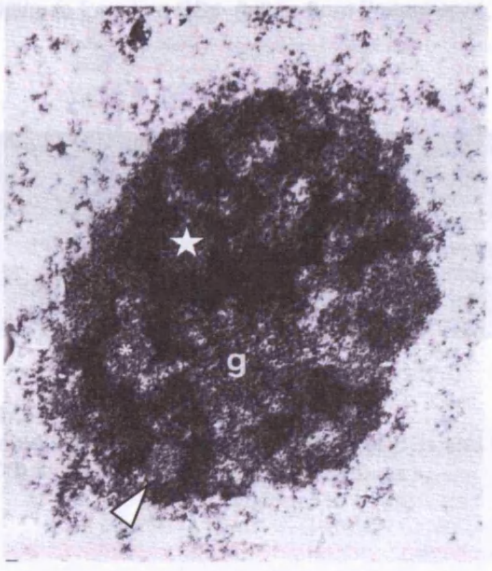

Figure 1.25
Nucleolus from cycloheximide treated SON neuron. It is possible to see large FCs (★) and FCs in direct contact with the nucleoplasm (arrowhead). GC=g (taken from Lafarga *et al.*, 1994). X23K

1.4.2 Alterations to Cajal Bodies

In HeLa cells that express p80 coilin fused to GFP, it has been shown that all Cajal bodies have the ability to move in every interphase nucleus (Platani *et al.*, 2000). These movements can be visualised over periods of one to two hours and involve a range of different movements; translocation through the nucleoplasm, joining together of individual CBs, separation of smaller bodies from larger ones, moving to and from the nucleolar periphery and within the nucleolus (figure 1.26). This shows that CBs are very mobile structures in the nucleus and can be catergorised into two different classes shown in table 1.1.

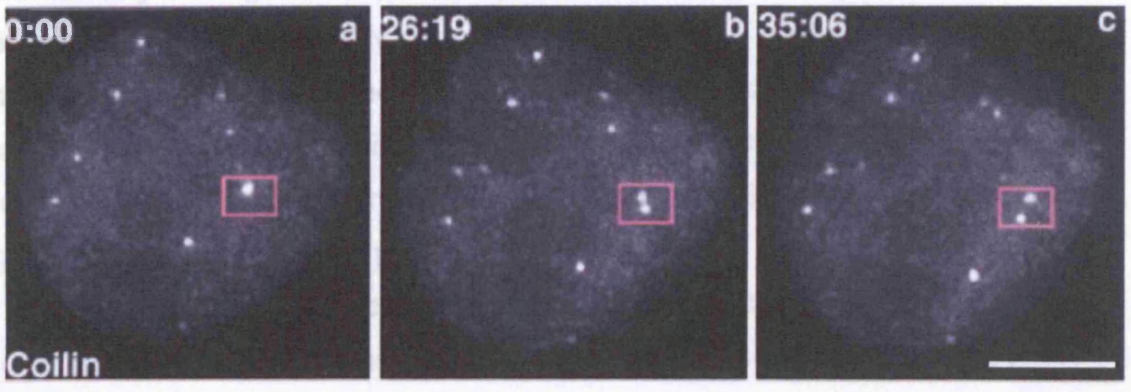

Figure 1.26

Images over a period of time showing the movements of Cajal bodies. The boxed area shows a CB splitting to form two CBs (taken from Platani *et al.*, 2000). Scale bar =1 μm.

Class	Size	Distance moved	Rate of movement	Type of movement
CB	≥ 0.4μm	small	slow	restricted
mini CB	≥ 0.2μm	large	fast	unrestricted

Table 1.1

A table summarising the two classes of CBs and the key features of each class (taken from Platani *et al.*, 2000).

The two classes of CBs vary in size, molecular composition and dynamic behaviour. The restricted movement of the larger CBs may reflect transcriptional association with specific gene loci (Platani *et al.*, 2000).

After osmotic stress, which causes cellular activation and an increase in the transcription of neurohormones in rat SON neurons, an increase in the number of Cajal bodies can be seen (Lafarga *et al.*, 1991). The formation of Cajal bodies may be closely related to the metabolic activity of the neuron, in particular, protein synthesis. There may be an increase in the number of CBs in response to an increase in transcription. When the initial phase of osmotic stress was examined more closely it was discovered that transcription is actually inhibited initially. A decrease in CBs was seen in this period and a peak of p80 coilin nucleolar cap formation was also observed (Lafarga *et al.*, 1998). The reverse is seen when this phase ends. The nucleolar caps appear to have the same ultrastructure as normal CBs suggesting that CBs are continually arising at the periphery of the nucleolus. When transcription is increased, the caps readily grow into mature CBs. Therefore, the increase in transcription means that there is an increase in the number of CBs per nucleus and a decrease in p80 coilin nucleolar caps. The decrease in transcription may represent a slowing down of the maturation of CBs so they become more prominent at the nucleolar periphery.

When all nuclear transcription is inhibited using Actinomycin D in HeLa cells, CBs are seen to disappear completely and the proteins that usually localise in CBs redistribute (Carmo-Fonseca *et al.*, 1992). p80 coilin forms a distinct nucleolar cap and snRNPs only accumulate in speckles. This is another example of CB formation being dependent on cellular activities, in particular transcription.

Heat shock also causes major changes in transcriptional activity as most RNA polymerase II transcription is inhibited with concomitant induction of specific "heat shock" genes. It may also affect pre-mRNA splicing (Carmo-Fonseca *et al.*, 1992). HeLa cells were heat shocked by a temperature shift from 37 °C to 45 °C for 15 minutes. Afterwards, the localisation of p80 coilin is unchanged and remains in CBs but snRNPs are no longer seen in CBs.

In rat SON neurons the fine ultrastructure of CBs can be altered by cycloheximide treatment (Lafarga et a, 1994). Protein and nucleolar rRNA synthesis are both inhibited by cycloheximide but it does not affect extranucleolar synthesis of pre-mRNA (Gokal *et al.*, 1986). After drug treatment alterations to CBs have been seen and include segregation of the

amorphous matrix, compactation of the coiled threads and formation of CB-derived dense bodies of a fibrillar nature (figure 1.27). This suggests that there is an association between the maintenance of normal CB ultrastructure and protein and rRNA synthesis.

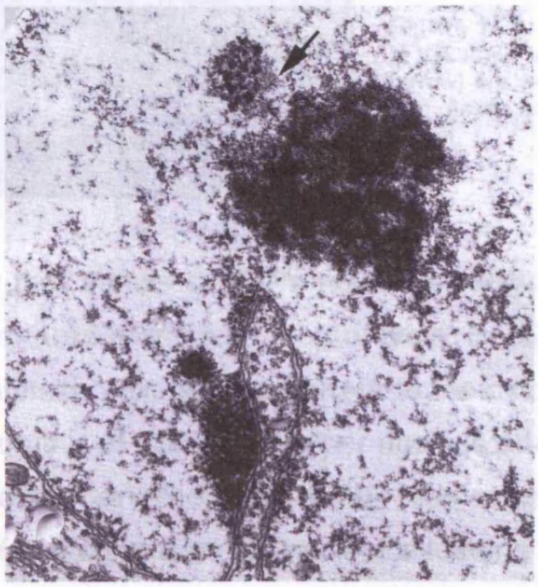

Figure 1.27
Electron micrograph of a CB showing a segregated portion of amorphous matrix (arrow) after cycloheximide treatment (taken from Lafarga *et al.*, 1994). X20K

If dephosphorylation is inhibited by the treatment of HeLa cells with the serine-threonine protein phosphatase inhibitor, okadaic acid, Cajal bodies appear inside the nucleolus and are found to stain positively for p80 coilin and snRNPs (figure 1.28) (Lyon *et al.*, 1997; Sleeman *et al.*, 1998). This suggests that the phosphorylation of certain CB proteins is important for the formation and localisation of CBs within the nucleus. Okadaic acid may disturb an existing equilibrium between the rate of snRNP entry and exit from the nucleolus. The overexpression of snRNPs has also been shown to trigger the *de novo* formation of CBs in cells that previously lacked them (Sleeman *et al.*, 2001) and this does not happen when p80 coilin is overexpressed. The results suggest that the formation of CBs may be linked to the level of snRNP expression.

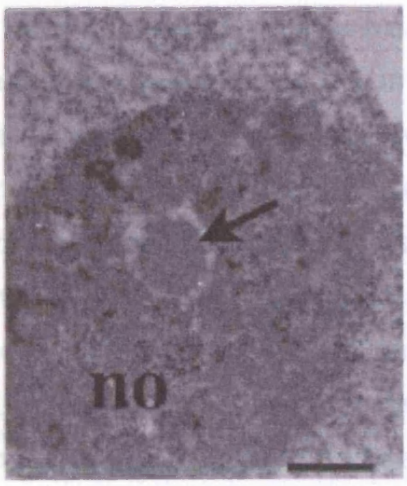

Figure 1.28
In Okadaic acid treated HeLa cells CBs (arrow) are seen in regions of the nucleolus (no) (taken from Lyon *et al.*, 1997). Scale bar =1 μm.

Another study that shows snRNPs no longer accumulating in the CBs of HeLa cell is after treatment with Leptomycin B (Carvalho *et al.*, 1999). Leptomycin B inhibits the export of U snRNA to the cytoplasm. There is also a decrease in the number of Cajal bodies per nucleus and a redistribution of p80 coilin to the nucleolus (Carvalho *et al.*, 1999). It is suggested that leptomycin B disrupts the flux of p80 coilin from the nucleolus leading to the disappearance of CBs. However, immunostaining of leptomycin B treated cells with antibodies against SMN or Gemin2 reveals that both proteins can still be seen in CBs but there is also increase in the number of gems (Carvalho *et al.*, 1999).

1.4.3 The p80 coilin Knock-out Mouse

The p80 coilin null mutant/knock-out (p80 KO) mouse is another example where alterations to Cajal bodies have been reported. p80 KO mice were generated that contained a deletion of exons 2 to exon 7 (85%) of the p80 coilin gene, which corresponds to the C-terminal 487 amino acids (Tucker *et al.*, 2001). The p80 KO mice showed reduced viability but were still fertile.

Tissue from the p80 KO mice or cells derived from mutant embryos displayed extranucleolar foci that contained fibrillarin and Nopp140. These foci were of similar size and shape to CBs and so termed 'residual' CBs. The 'residual' CBs did not contain splicing snRNPs or any proteins from the SMN complex (Tucker *et al.*, 2001). When sensory ganglion neurons from wild-type and knock-out animals were stained using the silver impregnation technique, in the knock-out mice only nucleoli showed a silver deposition, whereas, in the

wild-type mice both nucleoli and CBs were stained. When GFP-tagged mouse p80 coilin was transiently expressed in knock-out cells, this led to the formation of CBs that contained fibrillarin, Nopp140, snRNPs and SMN. These results suggest that full length p80 coilin is needed for the correct formation and maintenance of CBs and that the C-terminal of p80 coilin plays an important role in the recruitment of snRNPs and SMN complex to CBs.

Further studies using p80 KO mouse embryonic fibroblasts (MEF) revealed that the depletion of p80 coilin does not disrupt the processing of Sm snRNAs which is proposed to occur in CBs (Jady *et al.*, 2003). It was shown that Sm snRNAs colocalised in CB-sized nuclear foci with small Cajal-body-specific RNAs (scaRNAs), but not with fibrillarin or SMN. scaRNAs are Sm snRNA modification guide RNAs that play a role in the processing of snRNAs and localise within CBs (Jady *et al.*, 2003). These findings show that in p80 KO MEF cells, there are two different types of 'residual' CBs neither of which contain the SMN complex. These results also demonstrate that in the absence of full length p80 coilin, Sm snRNPs are able to colocalise in residual CBs with scaRNAs and that the internal modifications of Sm snRNAs are likely to occur in these foci.

As CBs are proposed to play a role in the biogenesis of small nucleolar RNPs (snoRNPs), the distribution of U3 snoRNP was investigated in the p80 KO MEF cells (Jady *et al.*, 2003). It was demonstrated that U3 snoRNP accumulates in the fibrillarin-positive 'residual' CBs. This finding suggests that the two different types of 'residual' CBs in the p80 KO cells carry out either the biogenesis of snRNPs or snoRNPs. The discovery of two different types of residual CBs, that accumulate either Sm snRNAs or snoRNAs, suggests that p80 coilin may play a role in coupling the biogenesis of Sm snRNPs and snoRNPs in one domain (Jady *et al.*, 2003).

1.4.4 Alterations to Speckles

The initial phase of osmotic stress is associated with a down-regulation of transcription in rat SON neurons and speckles are reported to become larger and fewer in number (figure 1.29) (Lafarga *et al.*, 1998). When transcription is activated, in the stress response phase, speckles are more numerous and

smaller in size. If all nuclear transcription is inhibited in HeLa cells using Actinomycin D or α-amanitin, speckles are also seen to decrease in number and become larger in size (Misteli *et al.*, 1997). The rounded up speckles contain U2, U4, U5 and U6 snRNPs as well as SC35 and hyperphosphorylated RNA polymerase II (Bregman *et al.*, 1995). Both studies show that when transcription is inhibited speckles become fewer and larger.

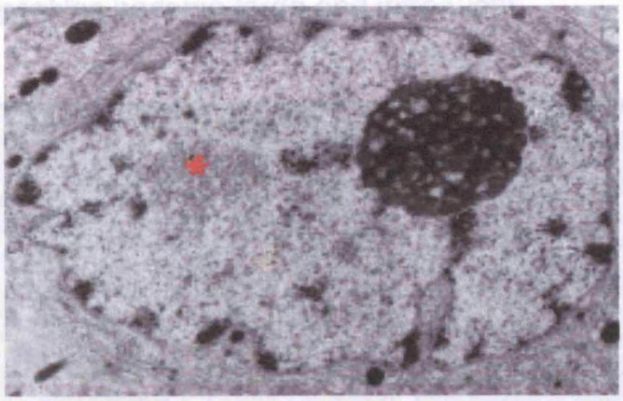

Figure 1.29
A nucleus from a SON neuron after the initial period of osmotic stress that has large speckles (red ★) (taken from Lafarga *et al.*, 1998). X9K

Heat shock causes major changes in transcriptional activity and most RNA polymerase II transcription is inhibited with concomitant induction of specific "heat shock" genes. It may also affect pre-mRNA splicing (Carmo-Fonseca *et al.*, 1992). HeLa cells that are heat shocked by a temperature raise from 37 ºC to 45 ºC for 15 minutes show a redistribution of snRNPs (figure 1.30). The splicing snRNPs no longer accumulate in speckles and a widespread rather than a diffuse nucleoplasmic staining pattern can be seen. A change in the transcriptional activity of a cell can cause alterations to the speckle staining pattern.

Figure 1.30
Heat shock affects the distribution of snRNPs. A widespread nucleoplasmic staining can be seen instead of the characteristic 'speckled' pattern (taken from Carmo-Fonseca *et al.*, 1992). Scale bar = 10 μm.

The inhibition of protein and rRNA synthesis by cycloheximide also depletes short half-life splicing factors (Berciano *et al.*, 2002) but has no affect on the extranucleolar synthesis of pre-mRNA (Gokal *et al.*, 1986). When rats were treated with cycloheximide, the characteristic speckle staining pattern was no longer seen in SON neurons. There is a redistribution of splicing factors to large and infrequent speckles and there is also a decrease in nucleoplasmic staining (figure 1.31). Therefore, if protein and rRNA synthesis is inhibited speckles become large and infrequent.

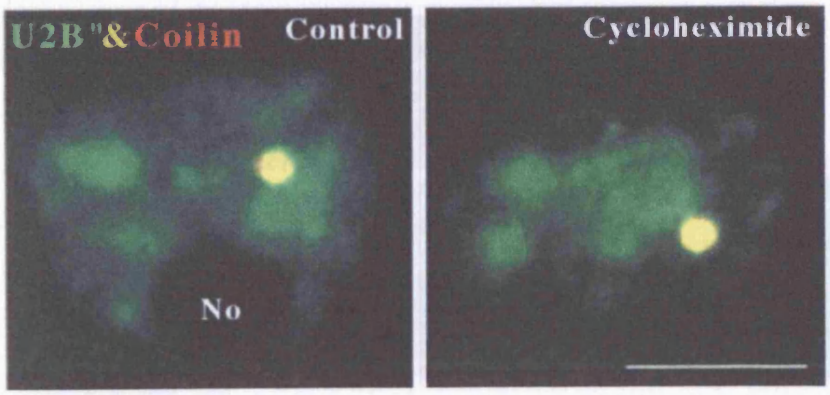

Figure 1.31
Cycloheximide treatment causes the redistribution of snRNPs in HeLa cells. Large, infrequent speckles are seen (Berciano *et al.*, 2002). Scale bar = 10 μm.

Okadaic acid is a serine-threonine protein phosphatase inhibitor and prevents protein dephosphorylation. After HeLa cells are treated with okadaic acid, the speckle staining pattern becomes more diffuse (figure 1.32) (Misteli *et al.*, 1997) suggesting that if dephosphorylation is prevented there is a gradual increase in the nucleoplasmic pool of splicing factors.

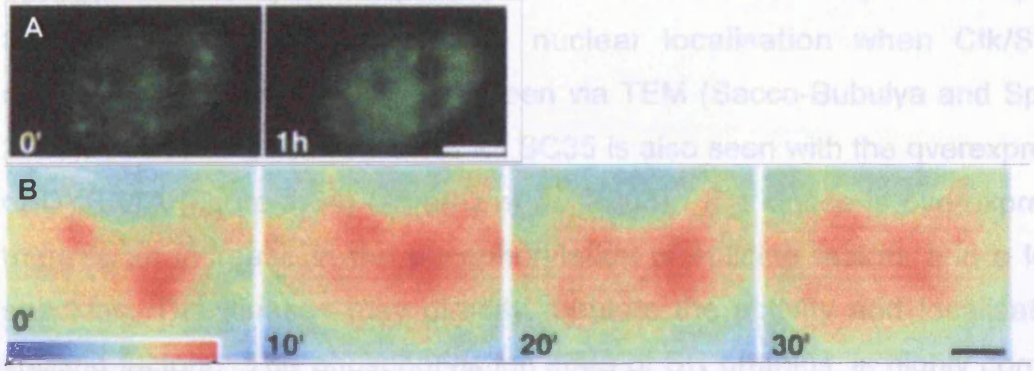

Figure 1.32
Okadaic acid causes a gradual increase in the nucleoplasmic pool of splicing factor, SF2/ASF (Misteli *et al.*, 1997). Scale bars: A = 5 μm; B = 720 nm.

It has also been shown that treatment of HeLa cells with staurospine, an inhibitor of protein kinases, causes a slight rounding up of some speckles (Misteli *et al.*, 1997). Staurospine was shown to prevent all the dynamic, peripheral movements in speckles. Therefore, preventing the phosphorylation of splicing factors causes speckles to become less dynamic (figure 1.33). The results from okadaic acid and staurospine treatment support the idea that the phosphorylation of SR protein splicing factors leads to their release from speckles.

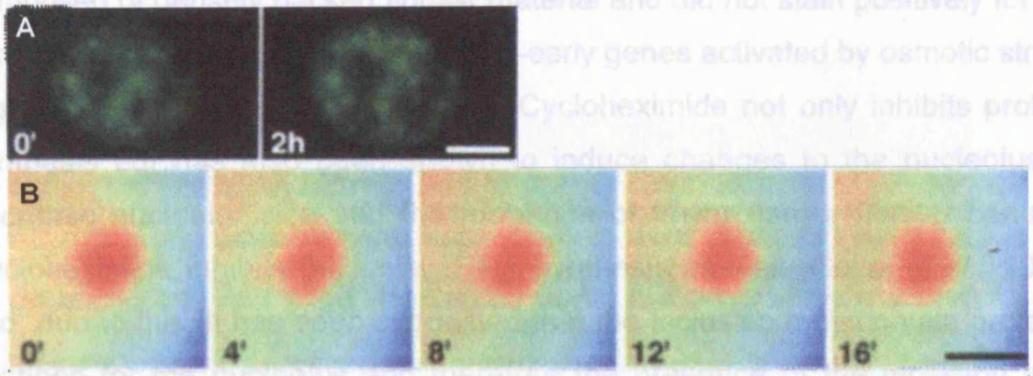

Figure 1.33
Staurospine treatment of HeLa cells prevents the dynamic, peripheral movements of speckles (Misteli *et al.*, 1997). Scale bars: A = 5 μm; b = 500 nm.

The overexpression of specific kinases has also been shown to disrupt the distribution and composition of speckles. The overexpression of kinases, Clk/STY and DYRK1A, both cause the disassembly of speckles (Colwill *et al.*, 1996; Sacco-Bubulya and Spector, 2002; Alvarez *et al.*, 2003). The SR protein, SC35, redistributes to a diffuse nuclear localisation when Clk/STY is overexpressed and IGCs are not seen via TEM (Sacco-Bubulya and Spector, 2002). A similar staining pattern for SC35 is also seen with the overexpression of DYRK1A (figure 1.34) (Alvarez *et al.*, 2003). If a kinase is overexpressed, there is an increase in the phosphorylation of splicing factors and a loss of speckles. The kinases may directly regulate the activity and localisation of splicing factors. The phosphorylation state of SR proteins is highly correlated with the structural organisation of one of the ultrastructural components of speckles, the IGCs. Phosphorylation of SR proteins may be a key event in their recruitment to transcription sites from speckles.

1.4.5 Formation of Aggregates

Many studies that used drug treatment to alter various cellular processes not only caused disruption of specific nuclear subdomains but also caused the formation of a nuclear aggregate or inclusion. In SON neurons, from rats that had been subjected to water deprivation and also had been treated with the protein synthesis inhibitor, cycloheximide, a dense body that was round in structure and ranges from 0.2 μm to 0.8 μm in diameter was seen using electron microscopy (Lafarga *et al.,* 1993). The nuclear inclusion was composed of densely packed fibrillar material and did not stain positively for *fos* immunoreactivity, one of the immediate-early genes activated by osmotic stress (figure 1.36A) (Lafarga *et al.,* 1993). Cycloheximide not only inhibits protein synthesis but has also been shown to induce changes to the nucleolus: a decrease nucleolar size and the formation of fewer, larger fibrillar centres. Cycloheximide inhibits nucleolar rRNA synthesis as well (Gokal *et al.,* 1986) and, due to this, it has been suggested that the inclusion may contain proteins destined for the nucleolus and therefore the presence of the inclusion may represent dysfunction of the nucleolus. However, no nucleolar proteins have been shown to localise to this inclusion to date.

The formation of a nuclear inclusion can also be seen when all nuclear transcription is inhibited using Actinomycin D in cultured liver cells (figure 1.36B) (Reynolds *et al.,* 1964). This again shows that if transcription is inhibited, a nuclear inclusion may form.

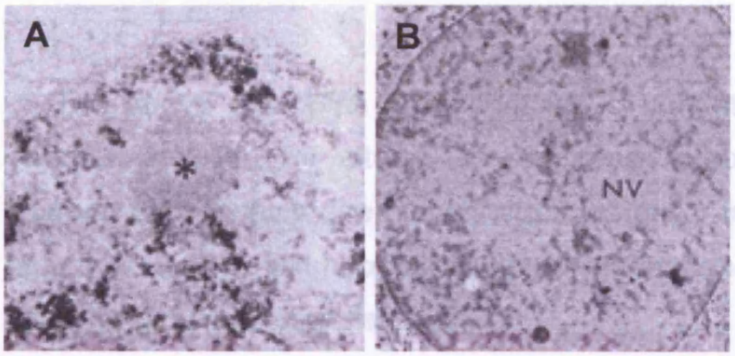

Figure 1.36
Inclusion formation in cells after cycloheximide treatment (A) or Actinomycin D treatment (B) (taken from Lafarga *et al.,* 1993; Reynolds *et al.,* 1964). X38K (A) and X5K (B)

Mutation analysis of survival of motor neuron (SMN) protein cause a number of alterations to the distribution of nuclear proteins. There is a dramatic relocalisation of many proteins to nuclear inclusions when SMNΔN27 is expressed. p80 coilin, snRNPs, fibrillarin, GAR1, U3 snoRNP, RNA polymerase IIa, RHA, TBP, PSF, CstF64 and CPSF160, but not RNA polymerase IIo, hnRNP or SC35 have been shown to localise in large CB/gems (figure 1.37) (Pellizzoni *et al.*, 1998; Pellizzoni *et al.*, 2001a; Pellizzoni *et al.*, 2001b). The SMNΔN27 mutation also inhibits splicing and the inclusion formation could be in response to this inhibition.

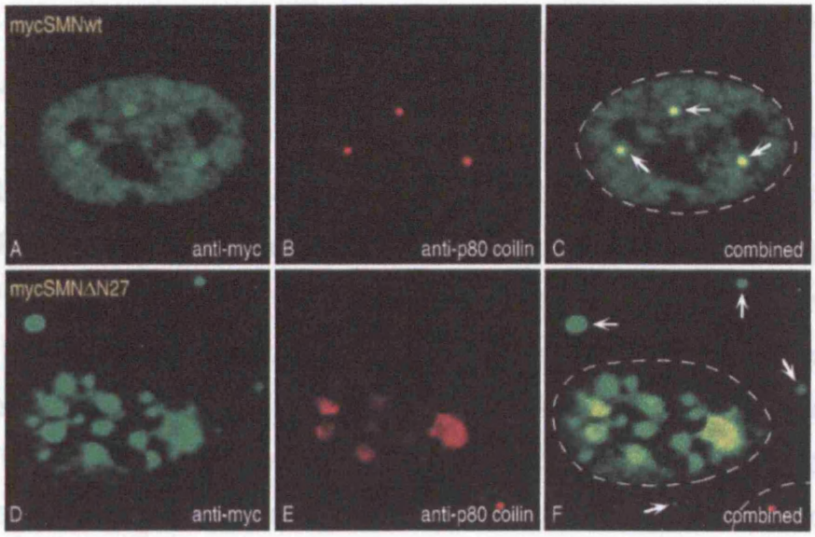

Figure 1.37
Expression of SMNΔN27 causes the redistribution of many nuclear factors to large nuclear inclusions that resemble large CBs/gems (Pellizzoni *et al.*, 1998).

The above examples show that the steady-state equilibrium of nuclear subdomains can be altered in response to experimental manipulation. Understanding why these nuclear changes occur in response to alterations in metabolic activity will hopefully help our understanding of the basic principles underlying nuclear organisation.

1.5 Nuclear Ultrastructure and Human Disease

Nuclear subcompartments have been implicated in a number of human diseases. PML (promyelocytic leukemia) bodies are absent in patients with promyelocytic leukemia (Hodges *et al.,* 1998) and the appearance of a perinucleolar cap (PNC) has been seen in transformed cells (Huang *et al.,* 1997). Changes in the nucleolus, Cajal body and speckles have also been associated with a variety of diseases.

1.5.1 The Nucleolus and Disease

Nucleolar proteins are also mutated in a number of diseases and one example is Treacher Collins syndrome (TCS) (Marsh *et al.,* 1998). TCS is a disorder of craniofacial development and is caused by a mutation in the TCS gene (TCOF1). Analysis of the TCOF1 gene in individuals affected by TCS revealed most mutations caused a premature stop codon. The protein encoded for by TCOF1 has been named treacle and is a nucleolar protein. Immunocytochemistry using an antibody generated against treacle showed that it localised to the nucleolus and the cytoplasm (Marsh *et al.,* 1998). The same group also demonstrated that in TCS, mutated treacle did not localise to the nucleolus. This was demonstrated by using the technique of *in vitro* site-directed mutagenesis to introduce mutations that are commonly found in individuals with TCS into the murine homologue of TCOF1. The mutated proteins were no longer seen to localise within the nucleolus and it is suggested that treacle plays a role in shuttling between the nucleolus and the cytoplasm.

Several proteins that localise to the nucleolus are involved in cancer including both the Werner's syndrome (WRN) and the Bloom's syndrome (BLM) gene products. Werner's syndrome is a rare autosomal recessive disorder that features premature aging and patients often die of cancer in the fourth or fifth decade (Marciniak *et al.,* 1998). Bloom's syndrome is a genetic disorder that is characterised by immunodeficiency, retarded growth and a predisposition to a wide variety of cancers (Wu *et al.,* 2000). BLM and WRN proteins are both part of the RecQ helicase family which are DNA helicases that affect genome stability (reviewed in Mohaghegh and Hickson, 2001). Cells derived from

patients affected by either disorder show increased genomic instability that manifests as an elevated frequency of homologous recombination events (Mohaghegh and Hickson, 2001). Both proteins have also been found in the nucleolus. Yankiwski *et al.* (2000) demonstrated that BLM localised to the nucleolus of human fibroblasts during S phase, however, in early G_1 phase BLM was absent from the nucleolus. WRN protein was also shown to be present in the nucleolus in a number of cell lines, including sarcomas and carcinomas (Marciniak *et al.,* 1998) and this localisation was not shown to be cell-cycle dependent.

Spinocerebellar ataxias (SCAs) are neurodegenerative disorders characterised by neuronal loss within the cerebellum and brainstem and part of the CAG triplet repeat diseases (chapter 1.7.1). SCA7 is caused by a CAG triplet repeat expansion in the coding region of ataxin-7 (David *et al.,* 1997). In COS-1 cells, wild-type ataxin-7 has been shown to have nuclear distribution and a portion of the protein is localised to the nucleolus (Kaytor *et al.,* 1999). This raises the possibility that the expansion of the polyglutamine tract in ataxin-7 seen in SCA7 may result in altered nucleolar function.

1.5.2 Cajal bodies/Gems and Disease

Spinal muscular atrophy (SMA) is caused by loss of function mutations in the SMN1 gene and results in the degeneration of motor neurons in the spinal cord (chapter 1.2.6). Defects in spliceosomal snRNP assembly may underlie the development of SMN (Carvalho et al., 1999) and, in SMA patients, a decrease in the number of gems is seen (Coovert *et al.*, 1997; Lefebvre *et al.*, 1997).

In tumour cells, a change in the localisation of Cajal bodies has been reported (Ochs *et al.,* 1994). When a number of different breast cancer cells were examined, several lines appeared to have Cajal bodies within the nucleolus as well as prominent nucleoplasmic CBs. CBs at both localisations stained positively for p80 coilin as well as fibrillarin and Sm proteins. Cajal bodies are also disrupted in a form of acute leukemia in which the Cajal body component, eleven-nineteen lysine-rich leukemia protein (ELL) is fused to myeloid-lymphoid leukemia protein (MLL) to form a chimeric fusion protein

(Polak et al., 2003). ELL is an RNA polymerase II transcription elongation protein that has been shown to localise in CBs with EAF1 (ELL-Associated Factor 1|) but in murine MLL-ELL leukemia cells neither p80 coilin or EAF1 are seen in CBs and immunocytochemistry with antibodies against either protein revealed a faint nucleoplasmic distribution (Polak *et al.,* 2003).

In a single study by Yamada *et al.* (2001) it as suggested that Cajal bodies can be seen juxtaposed to neuronal intranuclear inclusions (chapter 1.6.5) seen in neurons from individuals dentatorubral and pallidoluysian atrophy (DRPLA) and spinocerebellar ataxia 3 (SCA3), both of which are CAG triplet repeat diseases that result from polyglutamine expansions (chapter 1.7.1).

1.5.3 Speckles and Disease

Mutation in splicing factors can also give rise to specific human genetic diseases. Mutations in the U5 snRNP protein, precursor mRNA processing protein 8 (Prp8) (McKie *et al.,* 2001), and the U4/U6 snRNP proteins, Prp3 (Chakarova *et al.,* 2002) and Prp31 (Vithana *et al.,* 2001), all give rise to Retinitis Pigmentosa (RP). RP is characterised by progressive degeneration of the photoreceptors and this leads to blindness. The identification of mutations in three pre-mRNA splicing factor genes possibly highlights a mechanism of photoreceptor degeneration due to defects in pre-mRNA splicing (Chakarova *et al.,* 2002).

Oculopharyngeal muscular dystrophy (OPMD) is caused by a short expansion of the GCG triplet repeat encoding a polyalanine tract in the mRNA 3' processing and polyadenylation factor, poly(A)-binding protein 2 (PABP2). PABP2 has been shown to localise to speckles in C2 cells and research suggests that PABP2 plays a role in the expression of muscle-specific genes (Kim *et al.,* 2001). In OPMD, PABP2 is no longer seen to localise in speckles but accumulates in a neuronal intranuclear inclusion. The altered distribution of PABP2 may play a role in OPMD pathology.

The sequestration of splicing factors may contribute to the pathology of myotonic dystrophy (DM) (chapter 1.7.5). There are two types of DM; DM1 is caused by either a CTG-repeat expansion in the 3' untranslated region of the myotonic dystrophy protein kinase (DMPK) gene and DM2 is caused by a

CCTG tetranucleotide repeat expansion in intron 1 of the zinc finger protein 9 (ZNF9) gene (Fardaei *et al.*, 2002). The RNAs transcribed from these expanded loci accumulate in the nuclear foci, and RNA-binding proteins from the muscleblind protein family, such as MBNL, MBLL and MBXL, adhere to the transcripts and are suggested to be sequestered into the nuclear inclusion.This results in a trans-dominant dysregulation of pre-mRNA alternative splicing in muscle for several genes, including that of the insulin-receptor (Savkur *et al.*, 2004).

1.6 Huntington's Disease

Each of the fore mentioned nuclear subdomains (nucleolus, Cajal body and speckles) have been implicated in triplet repeat diseases. This family of diseases is characterized by an expanded CAG repeat tract and include nine such diseases: the spinocerebellar ataxias, (SCAs), dentatorubral and pallidoluysian atrophy (DRPLA) and spinal and bulbar muscular atrophy (SBMA) as well as Huntington's disease (HD). The most common CAG expansion disease is Huntington's disease and is associated with documented nuclear changes (Roizin *et al.*, 1979; DiFiglia *et al.*, 1997). HD is an autosomal dominantly inherited progressive neurodegenerative disease. Onset is usually in adult life, with a mean of around 40 years. The neuropathologic hallmark of the disease is neuronal loss and gliosis in the caudate nucleus and the putamen (the striatum) resulting in atrophy (figure 1.38). The medium-sized striatal neurons that contain gamma-aminobutyric acid and substance P, as neurotransmitters, are selectively depleted. Clinical symptoms include gradual involuntary movements, progressive dementia and psychiatric disturbances, especially mood disorder and personality changes (for a comprehensive review of the clinical profile of HD, see Harper, 1996).

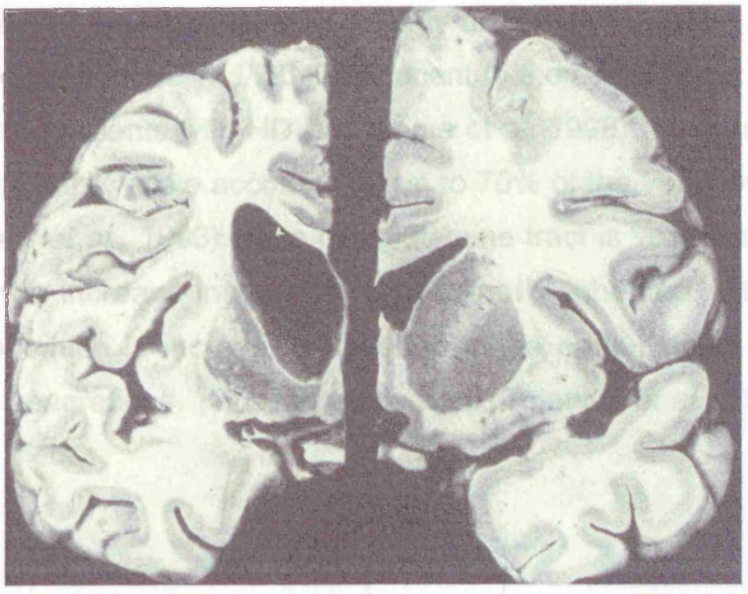

Figure 1.38
Photograph showing coronal brain sections. Severe atrophy in the brain of a patient with HD (left) compared with a control (right).

1.6.1 The Huntington's Disease Gene

The gene responsible for HD was identified in 1993 (Huntington's Disease Collaborative Research Group, 1993) and localised to human chromosome four. The affected gene, IT15 (Interesting Transcript 15), spans approximately 210 Kb within the 4p16.3 locus and has 67 exons. The mutation underlying HD is an expansion of a CAG/polyglutamine tract in the first exon. The CAG repeat length is highly polymorphic in the population (Kremer *et al.*, 1994). The CAG repeat size in the normal range is $(CAG)_6$ to $(CAG)_{39}$, whereas in the expanded range is $(CAG)_{35}$ to $(CAG)_{180}$ (Bates *et al.*, 1997). Individuals with repeat sizes between 35 and 39 do not always develop symptoms. Adult onset patients account for 90% cases and typically have expansions from 40-55 repeats, whereas juvenile onset cases only account for 10% of cases and are caused by expansions of greater than 70 repeats.

There is a well-established inverse correlation between CAG repeat length and age of onset (Stine *et al.*, 1993; Brinkman *et al.*, 1997) (figure 1.39). However, patients with identical repeat lengths can differ in their ages at onset and therefore genetic factors are likely to affect the age of onset, as can be seen by varying age of onset in family members with similar CAG sizes. It appears that there are a number of genetic modifiers, which can either, delay or

promote onset of the disease. One study discovered that the presence of a glutamic acid polymorphism, Δ2642, adjacent to the CAG repeat influenced the age at onset in patients with HD (Vuillaume et al. 1998). The number of CAG repeats in the upper allele accounts for up to 70% of the variation in the age of onset (Andrew *et al.*, 1993). The polyglutamine tract is very unstable and has been shown to increase in size when paternally inherited. HD also shows 'anticipation' which is increasing severity or the earlier onset of disease in subsequent generations (Gusella et al. 1993, Telenius *et al.*, 1993, Zuhlke et al. 1993).

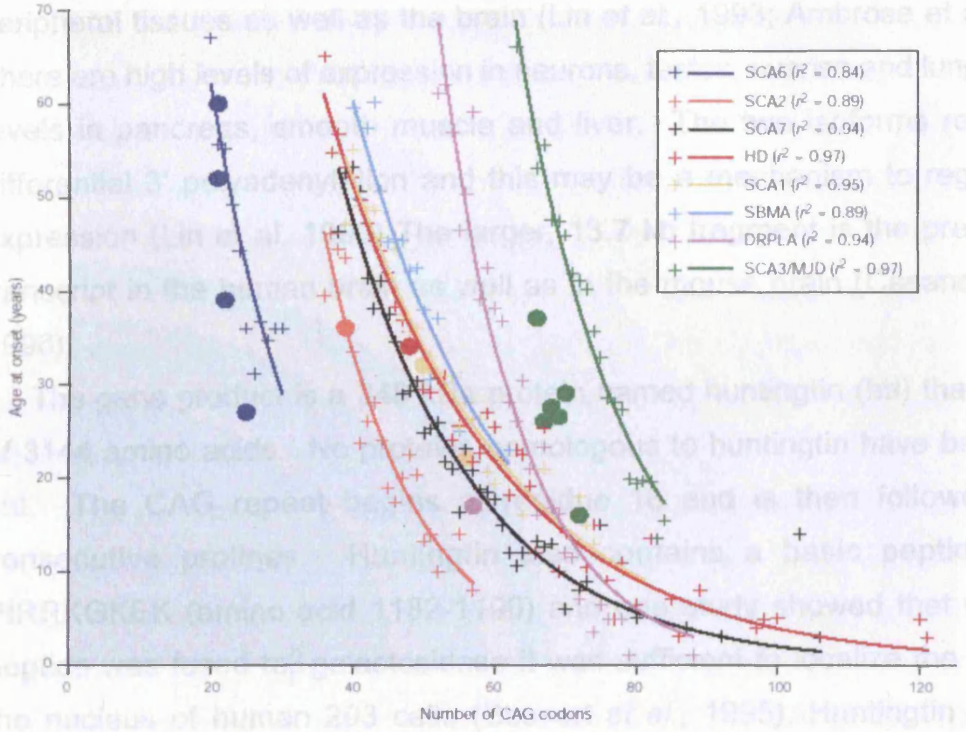

Figure 1.39
A graph showing the inverse correlation between CAG repeat length and age of onset for all the polyglutamine diseases (taken from Gusella and MacDonald, 2000).

A study recently showed that there are high levels of CAG repeat length variation in many tissues of a mouse model of HD (Kennedy and Shelbourne, 2000). The mice were generated by inserting 72-80 CAG repeats into the mouse HD gene and therefore full length mutant huntingtin was expressed. The mice demonstrate behavioural and pathological features that are indicative of early HD. Analysis of the repeat sizes of individual mutant alleles in tissues

derived from the mouse model demonstrated that the CAG mutation is unstable and prone to expansion in the striatum of these mice. The expansion was also shown to increase with age and some striatal cells from old HD mice contained mutations that had tripled in size. This suggests that repeat expansions can occur by a mechanism that is not based on replication.

1.6.2 Huntingtin mRNA and Protein

Northern blot and *in situ* hybridisation studies have shown that 10.3 and 13.6 kb transcripts are synthesised from the HD gene and are expressed in peripheral tissues as well as the brain (Lin *et al.,* 1993; Ambrose et al. 1994). There are high levels of expression in neurons, testes, ovaries and lung and low levels in pancreas, smooth muscle and liver. The two isoforms result from differential 3' polyadenylation and this may be a mechanism to regulate the expression (Lin et al. 1993) The larger, 13.7 kb fragment is the predominant transcript in the human brain as well as in the mouse brain (Casanova *et al.,* 1996).

The gene product is a 348 kDa protein named huntingtin (htt) that consists of 3144 amino acids. No proteins homologous to huntingtin have been found yet. The CAG repeat begins at residue 18 and is then followed by 29 consecutive prolines. Huntingtin also contains a basic peptide region PIRRKGKEK (amino acid 1182-1190) and one study showed that when this peptide was fused to β-galactosidase it was sufficient to localize the protein in the nucleus of human 293 cells (Bessert *et al.,* 1995). Huntingtin protein is ubiquitously expressed and seen in many tissue types. Despite this fact, the neuronal pathology of HD is selective and largely restricted to specific areas of the brain, the striatum and the cortex (Landwehrmeyer *et al.,* 1995).

Studies investigating the localisation of the huntingtin protein have also shown that it is expressed at higher levels in the brain (Strong *et al.,* 1993). The protein has been shown to have both cytoplasmic and nuclear localisations in cultured human and murine cells (De Rooij *et al.,* 1996; Hoogeveen *et al.,* 1993). Immunostaining by DiFiglia *et al.* (1995) of human and rat brain reveals huntingtin to be localized in neurons, particularly cell bodies and dendrites. Immuno-electron microscopy showed huntingtin to be in the matrix of the

cytoplasm and around the membranes of vesicles. It is therefore suggested that htt may have a function in vesicle trafficking (DiFiglia et al. 1995; Sapp et al. 1997; Velier et al. 1998).

A more recent study suggests that huntingtin is found in the nucleus of human cells. Kegel *et al.* (2000) investigated the distribution of huntingtin in normal and HD patient fibroblasts using a variety of different antibodies. The results showed full length wild-type huntingtin in the nucleus and that both normal and mutant huntingtin were present diffusely throughout the nucleoplasm as well as being associated with the nucleolus, speckles and PML bodies. The same study discovered that both mutant and normal huntingtin repressed transcription when targeted to DNA. These findings have led to the suggestion that huntingtin may function in the regulation of transcription and mutant huntingtin may disrupt this. Tao and Tartakoff (2001) have also shown a nuclear pool of an N-terminal 70 kDa huntingtin in the nucleus of HeLa cells. It has also been suggested that huntingtin plays a role in the normal function of some nuclear and perinuclear organelles and helps to maintain their morphology (Hilditch-Maguire *et al.,* 2000). The nuclear organelles are the nucleolus and the speckles and therefore implicate huntingtin in RNA biogenesis and trafficking.

The mouse, rat and pufferfish homologues of the huntingtin gene have been identified and cloned (Lin *et al.,* 1994; Schmitt *et al.,* 1995; Baxendale *et al.,* 1993). The human and mouse genes share 90% homology and the highest degree of sequence identity is within the first 5 exons where identical exon boundaries are seen but with different sized introns (Lin *et al.,* 1995). The pufferfish gene is also highly conserved and shares 69% homology to the human gene. The murine CAG repeat encodes only 7 glutamines and is interrupted by a CAA. The pufferfish glutamine repeat is only 4 CAGs long and is encoded for by 2 CAGs and 2 CAAs.

The function of normal huntingtin remains unclear. Several groups have generated *Hdh* (the mouse homologue of huntingtin) knockout mice and these mice have all been shown to be embryonic lethal (Nasir *et al.* 1995; Duyao *et al.* 1995). Heterozygous knockout has no distinguishable effect. Likewise, in humans the loss of one htt allele does not produce HD pathology. This information supports the hypothesis that HD is caused by a 'gain of function'

mutation. The condition known as Wolf-Hirschhorn syndrome also provides evidence to support this idea because in the disorder there is a loss of the telomeric region of chromosome four (including the HD gene), yet suffers show no related symptoms of HD (Gottfried et al. 1981).

1.6.3 Interacting Partners of Huntingtin

Huntingtin has been shown to interact with a large number of other proteins (Faber *et al.,* 1998; Jones, 1999; Steffan *et al.,* 2000; Dunah *et al.,* 2002; Harjes and Wanker, 2003; Holbert e al, 2003). It is possible that mutant htt interacts abnormally with cellular proteins. Interacting partners of huntingtin include:

Glyceraldehyde-3-phosphate dehyrogenase (GAPDH)
Calmodulin
Huntingtin-interacting protein 1 (HIP1)
Huntingtin-interacting protein 2 (HIP2)
Huntingtin-associated protein 1 (HAP1)
Huntingtin-associated protein 40 (HAP40)
WW domain proteins (HYPA, HYPB, HYPC)
Cystathionine –synthase
SH3-containing Grb-like protein 3 (SH3GL3)
Sp1
TAFII130
Cdc42-interacting protein 4 (CIP4)

The interactions of huntingtin can be altered by the increase in CAG repeats in mutant huntingtin. For example, the WW-domain proteins, HYPA, HYPB and HYPC, interact with the proline-rich region adjacent to the polyglutamine region of both wild-type and mutant huntingtin. This interaction is increased as the polyglutamine repeat increases (Faber *et al.* 1998). HYPA and HYPC are known to be involved in pre-mRNA splicing, whereas HYPB has been identified as a transcription factor (Passani *et al.* 2000; Rega *et al.,* 2001). It is therefore suggested that altered mRNA synthesis and processing may play a role in HD pathogenesis.

Using the yeast two-hybrid system, recent research found that full length huntingtin interacts with both Sp1 and TAFII130 (Dunah *et al.,* 2002). The

interaction of Sp1 is stronger when the CAG repeat is expanded but for TAFII130 the interaction is unaffected by the polyglutamine length. Sp1 is a transcription factor whose main function is recruitment of the general transcription factor, TFIID to DNA. TAFII130 forms part of a multi-subunit complex with TFIID, Tata binding protein (TBP) and many other TBP-associated factors (TAFs). This suggests that the CAG repeat expansion in htt may disrupt transcription through its interaction with transcription factors. It has also been shown that Sp1 binds more tightly with the soluble form of huntingtin than the aggregated form (Li *et al.,* 2002b) and this interaction may lead to the reduction in expression of Sp1-regulated genes.

One study showed that mutant htt exon 1 protein was able to interact with p53 and the co-activator CBP and co-repressor mSin3 *in vitro* (Steffan *et al.,* 2000). These three proteins are involved in p53-mediated transcriptional regulation and therefore the results also implicate transcriptional dysregulation in HD pathogenesis.

N-CoR represses transcription through the formation of a complex of repressor proteins including mSin3 and histone deacetylases. Boutell *et al.* (1999) showed that the N-terminus of huntingtin interacts with N-CoR but this interaction is CAG repeat length dependent. The same group also demonstrated that in HD the localisation of N-CoR and mSin3 is altered. In control brains, using immunohistochemistry, both N-CoR and mSin3A showed a nuclear and cytoplasmic distribution but in HD brains, the nuclear staining was no longer seen. mSin3A immunoreactivity also localized to approximately 5% of the total number of neuronal intranuclear inclusions (NIIs) when mSin3A immunoreactivity was compared to N-terminal huntingtin immunoreactivity (Jones, 1999). This again supports the idea that normal transcriptional activity may be distributed in HD.

1.6.4 Transgenic Mouse Model of HD

Following the discovery of the gene affected in HD, a transgenic mouse model of HD was created (Manigiarini *et al.,* 1996). The model was developed by expressing a construct of exon 1 of human huntingtin carrying a $(CAG)_{130}$ repeat expansion and 262 bp of intron 1 under the control of the human huntingtin promoter (Mangiarini *et al.,* 1996) (figure 1.40). This produces a protein that corresponds to approximately the first 90 amino acids of normal huntingtin (CAG_{21}) and represents about 3% of the wild-type protein (Sathasivam *et al.,* 1999). The HD transgenic mice were created by microinjection of the construct into single cell CDAxC57Bl/6 mouse embryos. Six lines were established and four contain different expanded CAG repeats of a size that is usually associated with the juvenile form of the disease: R6/0 $(CAG)_{142}$, R6/1 $(CAG)_{115}$, R6/2 $(CAG)_{145}$ and R6/5 $(CAG)_{135\text{-}156}$. Of these mice the R6/0 mRNA is not translated, whereas the R6/1, R6/2 and R6/5 all produce full length mRNA and protein expressed at differing levels. An additional two lines, HDex6 and HDex27 contained a normal sized repeat of $(CAG)_{18}$ as a control. The size of the repeat length was determined by PCR-amplification followed by sequence analysis (Mangiarini *et al.,* 1996).

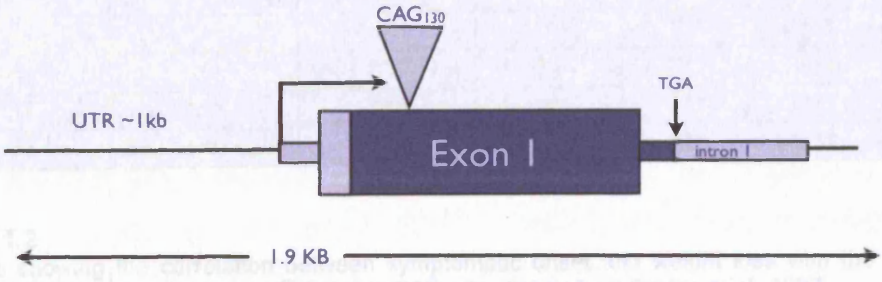

Figure 1.40
The construct of the R6/2 transgenic line (UTR = untranslated region, TGA = stop codon).

The R6/2 transgenic mouse line has been extensively studied and greatly helped in the understanding of the molecular pathology of HD. The R6/2 mouse model of HD is used exclusively in my studies. The R6/1 and R6/5 lines do develop a phenotype but the R6/2 is the most aggressive and the disease progression is in a number of weeks rather than months. The age of disease

onset is from 4 weeks and death usually occurs around 12 or 13 weeks of age (table 1.2). The cause of death is generally unknown. The mutation in these mice is not acting at the mRNA level as huntingtin protein can be detected upon western blot using N-terminal huntingtin antibodies (Davies *et al.*, 1997). These animals do develop behavioral problems similar to those seen in HD, including in-coordination, abnormal involuntary movements, seizures and weight loss. Despite this, these mice do not show specific neuronal cell loss in the striatum like human patients. However, this is consistent with the idea that it is neuronal dysfunction that is responsible for the symptoms of the disease, rather than neuronal death.

	Phenotype			Neuropathology		
Age in weeks	Brain weight loss	Body weight loss	Symptoms	Ubiquitin in nucleus	NII by EM	Nuclear indentation
2	-	-	-	-	-	-
3	-	-	-	-	-	-
3.5	-	-	-	-	-	-
4	-	-	-	-	+	-
4.5	-	-	-	-	+	-
5	+	-	-	-	+	-
6	++	-	-	+	++	-
7	+++	+	-	+	++	-
8	+++	+	-	+	++	+
9	+++	+	+	+	+++	+
10	+++	++	+	++	+++	+
11	+++	+++	++	+++	+++	+
12	+++	+++	++	+++	+++	++
13	+++	+++	+++	+++	+++	++

Table 1.2
A table showing the correlation between symptomatic onset and weight loss with the appearance of nuclear inclusions and nuclear indentation in R6/2 mice (taken from Davies *et al.*, 1997).

A variety of mouse models of Huntington's disease have now been created. Although the R6/2 transgenic mice are the most extensively studied, other mouse models have also been generated that express a mutant truncated HD gene or full length HD gene that has been added to the normal mouse genome which, already has two wild-type murine HD genes. Knock-in mouse models have been engineered as well and replicate the exact human mutation found in

HD patients as an abnormally long polyglutamine tract is inserted in the endogenous murine HD gene (for a comprehensive review of the mouse models of HD, see Menalled and Chesselet, 2002; Rubinsztein, 2002; Hickey and Chesselet, 2003).

1.6.5 The Neuronal Intranuclear Inclusion

Immunocytochemical studies of the R6/2 transgenic mouse brains showed that mutant huntingtin is also found in both the cytoplasm and the nucleus. Using antibodies raised against the N-terminal of huntingtin, Davies *et al.* (1997) revealed additional staining in the R6/2 mice compared to that seen in control mice. A 'densely stained circular inclusion' was seen within neuronal nuclei. Antibodies against ubiquitin also labeled the neuronal intranuclear inclusion (NII) (figure 1.41).

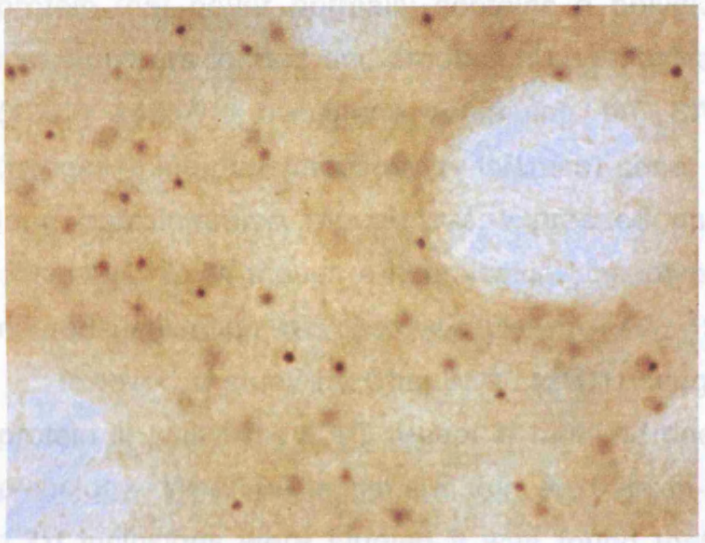

Figure 1.41
Light photomicrograph of R6/2 transgenic striatum at low power. NIIs labelled by anti-ubiquitin antibody are seen as immunoreactive foci.

NIIs show immunoreactivity for the N-terminus of htt but are not immunoreactive for antibodies to the C-terminus of htt. Immuno-electron microscopy studies revealed that these nuclear inclusions were not the nucleolus or Cajal body of the cell's nucleus (Davies *et al.,* 1997). The ultrastructural morphology of NIIs was originally described as a pale, granular and fibrous structure that was approximately 2 μm in diameter. Other nuclear changes seen using electron microscopy include a membrane invagination, an increase in nuclear pore density, lipofuscin accumulation, condensation of chromatin and neuronal shrinkage (Davies *et al.,* 1999). It has also been shown that NII appear before the onset of symptoms. NIIs have previously been described at EM in biopsies from human HD tissue (Roizin *et al.,* 1979) and human HD post-mortem tissue (DiFiglia *et al.* 1997; Becher *et al.* 1998; Gourfinkel-An *et al.,* 1998). In addition

to nuclear inclusions, inclusions within dystrophic neuronal processes have been seen in both HD post-mortem tissue and HD transgenic mice (DiFiglia *et al.* 1997; Bates *et al.*, 1998). The dystrophic neurite inclusions (DNIs) have also been shown to be immunoreactive for the N-terminus of huntingtin and ubiquitin.

The presence of NIIs has been shown in most of the CAG repeat disorders, including SCA1 (Skinner *et al.*, 1997) and MJD/SCA3 (Paulson *et al.*, 1997). It has also been shown that when CAG repeats are introduced into a gene for a protein that never normally contains a polyglutamine sequence, nuclear inclusions are formed and produce a neurological phenotype. Ordway *et al.* (1997) added a transgene containing 146 CAG repeats into the HRPT (hypoxanthine-phosphoribosyltransferase) gene. The protein containing the long polyglutamine repeat was expressed and nuclear inclusions were observed. Even though a neurological phenotype was seen, no evidence of neurodegeneration was observed (Ordway *et al.*, 1997).

However, a study by Chai *et al.* (2001) suggests that the context of the protein in which the CAG repeat is mutated does play an important role in pathology. When full length and truncated ataxin-3 (mutated in SCA3 (chapter 1.7)) inclusions were studied, it was found that nuclear factors, CBP and Mastermind-like-1 (MAML1) colocalised only to NII formed by full length ataxin-3, whereas the splicing factor SC35 colocalised only to NIIs formed by truncated fragment of ataxin-3. It is therefore suggested that the protein sequence surrounding the CAG repeat plays a role in which other proteins are recruited to NIIs.

Several studies indicated that it is the presence of the mutant protein in the nucleus that determines whether it forms aggregates or not. Saudou *et al.* (1998) showed that when mutant huntingtin was transfected into cultured striatal neurons and nuclear localisation was blocked, no NIIs were formed and neurodegeneration was not induced. When a construct in which the nuclear localisation signal of a different CAG triplet repeat disease protein, ataxin-1 (mutated in SCA1 (chapter 1.7)) was mutated and used to generate transgenic mice, these mice did not develop a disease either (Klement *et al.*, 1998). This also suggests that the nuclear localisation of the protein plays a crucial role in cellular toxicity.

1.6.6 Molecular Composition of NII

Subsequent analysis has also revealed many other components colocalise to the NII in mouse and cell culture as well as in human tissue. These include chaperones Hsc70, Hsp70, Hsp40, BiP & HDJ-2 and the 20S, 19S & 11S subunits of the 26S proteasome, SUMO-1, α-synuclein and transcription factors CBP, TBP, Sp1, TAFII130 and mSin3A (Huang *et al.,* 1998b; Boutell *et al.,* 1999; Davies *et al.,* 1999; Jones, 1999; Shimohata *et al.,* 2000a; Steffan *et al.,* 2000; Nucifora *et al.,* 2001; Suhr *et al.,* 2001; Waelter et al. 2001; Dunah *et al.,* 2002; Kim *et al.,* 2002; Li *et al.,* 2002b; Yu *et al.,* 2002). Some of these studies suggest that the proteins are sequestered into the NII and the normal localisation for the given protein is depleted. The consequence of the sequestration of these proteins into the NII may leave the molecule inactive and therefore disrupt normal cellular functions (Nucifora *et al.,* 2001; McCampbell and Fischbeck, 2001).

However, Yu *et al.* (2002) investigated the expression and localisation of the transcription factors CBP, TBP and Sp1 in transgenic mouse models of HD. All three proteins were shown to have a diffuse nucleoplasmic distribution that was similar to control brains as well being localised in the NII. Western blots were also used to show that CBP was not trapped in the NII. Together these results suggest that disruption to transcription in HD may be as a result of altered interactions of htt with transcription factors and not due to the irreversible sequestration of the proteins in NIIs.

Supporting this further is a recent study that demonstrated the dynamics of inclusions. HeLa or O23 cells were cotransfected with constructs encoding Htt-150Q together with 19Q-GF, TBP-GFP or Hsp70-YFP (Kim *et al.,* 2002) and the dynamic properties of the proteins were compared using fluorescence recovery after photobleaching (FRAP) or fluorescence loss in photobleaching (FLIP). The FRAP experiments revealed that TBP has a slower recovery time compared to Hsp70 and the results demonstrated that inclusions have different molecular interactions with different associated proteins. The FLIP analysis showed that Hsp70 could be released from the inclusion therefore suggesting that the surface of NIIs have the ability to bind and release molecules. The findings also imply that the molecules seen to colocalise with NIIs, using

immunohistochemistry, may not be sequestered irreversibly into the inclusions. Stenoien *et al.* (2002) also demonstrated the dynamic nature of NIIs using an expanded ataxin-1 construct in HeLa cells and FRAP analysis. The results demonstrated that two different types of inclusions existed; ones with rapid exchange of components with the nucleoplasmic pool and ones that have slow, varying exchange.

1.6.7 Mechanisms Underlying HD Pathology

The pathogenic mechanism of the mutant huntingtin has yet to be discovered. Various mechanisms have been suggested to account for the neurodegeneration in HD. These include defects in energy metabolism, oxidative stress and glutamate excitiotoxicity. The mechanism by which the CAG repeat expansion ultimately causes pathology, however, still remains unclear. One proposed pathway involves transcription. It is suggested that mutant huntingtin with an increase in CAG repeats may resemble a transcription factor because many other proteins containing high numbers of CAG repeats are themselves transcription factors (Cha, 2000). Cha proposes several different modes of action for mutant huntingtin in transcription dysregulation; (1) A 'gain of function' resulting from the increase in CAG repeat length leading to direct binding of mutant htt to DNA, disrupting normal transcription. (2) The binding of huntingtin to transcription factors resulting in an inactive complex that may repress transcription. (3) Huntingtin may bind to co-repressor proteins making them inactive and therefore increasing transcription of normally inactive genes. (4) Transcription factors may be sequestered by htt reducing their 'normal' levels within the cell.

1.6.8 Gene Expression Changes

A study using a combination of mircoarray and Northern analyses to assess the changes in mRNA levels showed that the expression levels of some genes were affected in R6/2 transgenic mice (Luthi-Carter *et al.*, 2000). These included increases and decreases in transcription. The data implicated dysregulation of mRNAs encoding neurotransmitter receptors and related second messenger systems as an early part of HD pathology. A further study

by the same group has gone to show that mRNAs changes can only be detected after four weeks of age that coincides with early pathology and early symptoms in the R6/2 mice (Luthi-Carter *et al.*, 2002b). It was also revealed that alterations in gene expression were not specific to the brain, but were also seen in skeletal muscle.

Research by the same group again has also shown gene expression changes are not limited to HD but can also been seen in another mouse model of a different polyglutamine disease, DRPLA (Luthi-Carter *et al.*, 2002a). Some of the gene expression changes seen were specific to the DRPLA mouse but several of the same changes were also seen in the HD mouse. This suggests that some altered gene expressions are caused by an expanded CAG repeat independently of the context of the protein it is located in, whereas, others are dependent on the protein context. It has also been shown that mice expressing a larger N-terminal mutant huntingtin fragment showed fewer gene expression changes compared to mice expressing a shorter htt fragment (Chan *et al.*, 2002). This data is suggested to also support the idea that htt protein context is important in the pathology of HD and can influence the CAG repeat-related alterations of mRNA expression.

1.6.9 Changes to Transcriptional Pathways

Several recent studies have suggested that altered interactions with transcription co-activators or co-repressors may cause the pathology of HD and include p53, CBP, Sp1, TAFII130, N-CoR and mSin3A (Steffan *et al.*, 2000; McCampbell *et al.*, 2000; Shimohata *et al.*, 2000b; Nucifora *et al.*, 2001; Dunah *et al.*, 2002; Jones *et al.*, 1999). The altered interactions have already been discussed (chapter 1.6.3) and all implicate transcriptional dysregulation in HD pathogenesis.

Steffan *et al.* (2001) have also shown that the N-terminus of huntingtin can interact and bind directly with CBP and P/CAF (p300/CBP-associated factor) not through their polyglutamine domain, but through their acetyltransferase domain. In free-cell assays, the presence of huntingtin exon1 protein with 51 CAG repeats lead to a decrease in activity of CBP, p300 and P/CAF, and, in cultured cells, the expression of huntingtin exon1 protein with 103 CAG repeats

caused a reduction in the level of acetylated histones H3 and H4. The decrease in histone acetylation was more distinct with larger polyglutamine repeats.

The decrease in histone acetylation is suggested to cause a decrease in gene expression and therefore it has been proposed that the use of a compound to inhibit cellular histone deacetylation could compensate for the loss of acetyltransferase activity. In a Drosophila model of HD, with both CAG_{93} or CAG_{48}, that was given histone deacetylase inhibitors in food, the flies lived longer and there was a decrease in the level of neurodegeneration seen (Steffan *et al.*, 2001). This is summarized in figure 1.42. Further studies have also demonstrated that histone deacetylase inhibitors can reduce cell loss in different models of polyglutamine diseases (McCampbell *et al.*, 2001; Hockly *et al.*, 2003; Ryu *et al.*, 2003). These findings also support the hypothesis that part of the pathology of HD may be caused by transcriptional dysfunction.

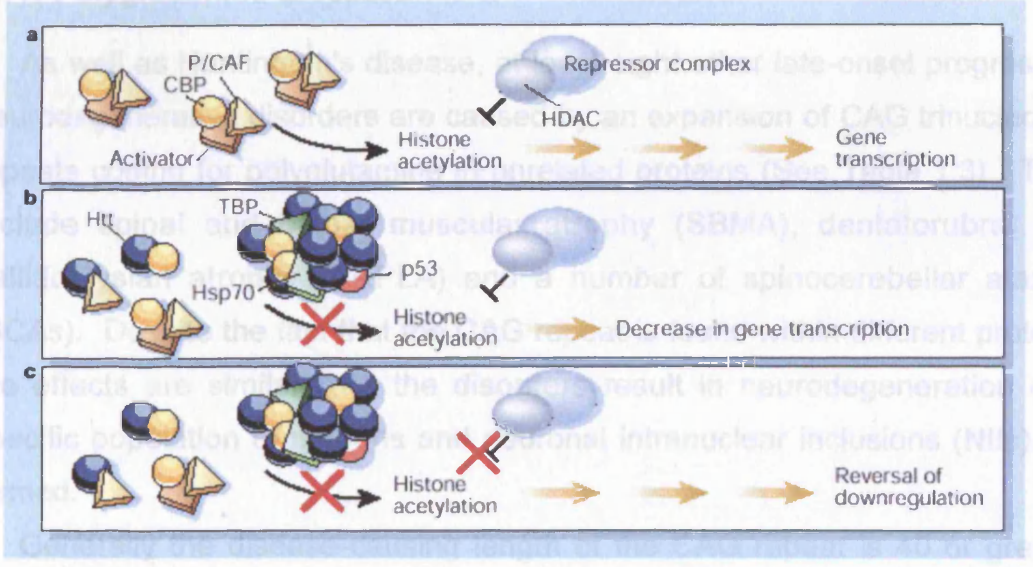

Figure 1.42
Diagram showing the potential mechanisms of Huntington's disease and gene expression (taken from Bates, 2001). (A) Complexes containing activator proteins and acetyltransferases turn on transcription whereas repressor complexes and histone deacetylases (HDACs) switch expression off. (B) Mutant huntingtin inhibits histone acetylation by blocking histone acetylases or sequestering them into inclusions (Steffan *et al.*, 2001), resulting in decreased transcription. (C) The balance between histone acetylation and deacetylation can be improved by molecules that inhibit histone deacetylation.

It is apparent HD and the polyglutamine diseases do have transcriptional changes but whether these are primary or secondary responses to the CAG expansion remains to be discovered. These experiments have led to possible therapeutic targets, in the form of histone deacetylase inhibitors and could potentially be used in patients.

1.7 Other Repeat Diseases

Triplet repeat diseases can be categorized into two subclasses based on the location of the repeat in the gene. In the first class the repeat is located in the coding sequence of the gene and this group of disorders is collectively referred to as the 'polyglutamine diseases'. The second class has the repeat in non-coding sequences of the gene and includes Fragile X and myotonic dystrophy.

1.7.1 Polyglutamine Diseases

As well as Huntington's disease, at least eight other late-onset progressive neurodegenerative disorders are caused by an expansion of CAG trinucleotide repeats coding for polyglutamine in unrelated proteins (See Table 1.3). They include spinal and bulbar muscular atrophy (SBMA), dentatorubral and pallidoluysian atrophy (DRPLA) and a number of spinocerebellar ataxias (SCAs). Despite the fact that the CAG repeat is found within different proteins the effects are similar. All the disorders result in neurodegeneration of a specific population of neurons and neuronal intranuclear inclusions (NIIs) are formed.

Generally the disease-causing length of the CAG repeat is 40 or greater whereas healthy individuals have CAG repeats with fewer residues. Larger CAG repeats result in an earlier age of onset and the disease severity also increases. Observations have shown that the polyglutamine repeat itself plays a central role in pathogenesis of these diseases and the presence of the CAG repeat expansion imparts a 'gain-of-function' to the protein.

The study of transgenic animal models and human post-mortem tissue for each of the triplet repeat diseases has lead to the identification of NIIs that stain positively for the expanded CAG repeat protein and ubiquitin (Davies *et al.*,

1997; Paulson *et al.*, 1997; Skinner *et al.*, 1997; Hayashi *et al.*, 1998; Holmberg *et al.*, 1998; Li *et al.*, 1998; Koyano *et al.*, 1999). Ultrastructurally all the NIIs appear to have the same morphology (figure 1.43). The only exception to this is SCA6 where studies have differing results; Ishikawa *et al.* (1999) first suggested that mutated ataxin-6 is only found in cytoplasmic inclusions in Purkinje cells that do not stain positively for ubiquitin. However, the same group, in 2001, then demonstrated that small inclusions could be identified using a monoclonal antibody 1C2 that recognises expanded polyglutamine tracts (Ishikawa *et al.*, 2001). It has also been shown that the NIIs recruit many proteins like those seen in HD and these include NEDD8, various chaperones, 26S proteasome complex, CBP, PML and PQBP-1 (polyglutamine (Q) tract binding protein-1) (Stenoien *et al.*, 1999; Chai *et al.*, 1999; Yamada *et al.*, 2001; Okazawa *et al.*, 2002).

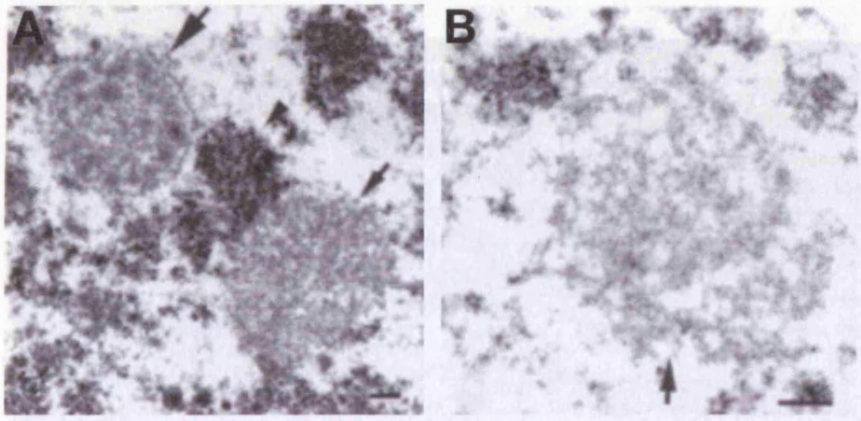

Figure 1.43 Electron micrographs of NIIs (arrows) in neurons from SCA3 brain (A) and DRPLA transgenic mouse brain (B). Scale bars = 0.2 (taken from Yamada *et al.*, 2001).

The spinocerebellar ataxias (SCAs) and dentatorubral and pallidoluysian atrophy (DRPLA) are dominantly inherited neurological disorders characterized by degeneration of the cerebellum, spinocerebellar tracts and brain stem neurons. The clinical features shared by the SCAs are ataxia, dysarthria and eventual bulbar dysfunction. The gene products in most of the SCAs are novel proteins of unknown function and the 2 exceptions are SCA6 and SCA17: SCA6 gene product is the -1A voltage-gated calcium channel (CACN1A1) (Zhuchenko *et al.*, 1997) and in SCA17 it is the transcription factor TBP that is mutated (Nakamura *et al.*, 2001). Ataxin-3 has been suggested to be a histone-binding protein that has the ability to repress transcription (Li *et al.*, 2002b).

Atrophin-1 has also been implicated in a role in transcriptional repression (Wood *et al.*, 2000). The normal subcellular localisation of the each protein varies.

Spinal and bulbar muscular atrophy (SBMA) is an X-linked, recessive neurodegenerative disease that typically causes progressive, symmetric wasting and weakness, initially of the proximal muscles of the hip and shoulder (Ringel *et al.*, 1978). Androgen insensitivity is also seen and frequently causes breast development in males. It was the first member of the polyglutamine diseases to be identified when it was discovered that exon 1 of the androgen receptor (AR) in SBMA patients had an expanded $(CAG)_n$ repeat. It was also the first member of the class in which the normal functions of the disease-causing protein was known (La Spada *et al.*, 1991). Immunocytochemistry has shown that the normal cellular distribution of the AR protein is not affected in SBMA but there is additional immunoreactivity in the form of NIIs (Li *et al.*, 1998).

Disease	Gene Product	Normal (CAG)n	Expanded (CAG)n	Protein localisation	Reference
HD	huntingtin	6-39	35-180	cytoplasmic and nuclear	Bates *et al.*, 1997
SCA1	ataxin-1	6-44	39-82	nuclear	Skinner *et al.*, 1997
SCA2	ataxin-2	17-31	36-63	cytoplasmic	Huynh *et al.*, 1999
SCA3	ataxin-3	12-41	62-84	cytoplasmic and nuclear	Tait *et al.*, 1998
SCA6	CACNA1A	4-18	21-33	cell membrane	Ishikawa *et al.*, 1999
SCA7	ataxin-7	4-35	37-306	nuclear	Cancel *et al.*, 2000
SCA17	TBP	29-42	47-55	nuclear	Nakamura *et al.*, 2001
DRPLA	atrophin-1	6-36	49-84	cytoplasmic	Knight *et al.*, 1997
SBMA	androgen receptor	10-36	40-62	cytoplasmic and nuclear	Li *et al.*, 1998

Table 1.3
A table summarising the features of diseases caused by expanded CAG tracts (adapted from Cummings and Zoghbi, 2000).

1.7.2 Non-Coding Repeat Expansion Disorders

The non-coding nucleotide repeat diseases are caused by a large and variable repeat expansion that is located in the non-coding part of the gene. They result in multiple tissue dysfunction or degeneration. The phenotype of each disease can also vary and this may be due to a marked degree of somatic heterogeneity. Individuals that have an intermediate sized expansion often show no clinical symptoms but transmission to the next generation leads to the larger mutations.

Disease	Gene	Protein	Repeat	Normal repeat	Expanded repeat	Disease mechanism	Reference
Fragile X syndrome	FMR1	FMRP	CGG	6-53	>230	loss of function	Fu *et al.*, 1991
Fragile XE syndrome	FMR2	FMRP-2	GCC	6-35	>200	loss of function	Knight *et al.*, 1993
Friedreich ataxia	X25	Frataxin	GAA	7-35	>100	loss of function	Campuzano *et al.*, 1996
Myotonic Dystrophy1	DMPK	DMPK	CTG	5-37	>50	loss of protein function, gain of mRNA function	Davies *et al.*, 1992
Myotonic Dystrophy2	ZNF9	ZNF9	CCTG	6-26	75-11,000	loss of protein function, gain of mRNA function	Liquori *et al.*, 2003
SCA8	SCA8	-	CTG	16-37	110-250	loss of function ?	Koob *et al.*, 1999
SCA12	SCA12	PPP2R2B	CAG	7-28	55-78	loss of function	Holmes *et al.*, 2001

Table 1.4
A table summarising the features of diseases caused by expansion of non-coding nucleotides (adapted from Cummings and Zoghbi, 2000).

Not all the repeat sequences are the same in this group of disorders (CGG, GCC, GAA, CTG, CCTG AND CAG) and the number of repeats can vary from 50 to over 10 thousand. The actual repeat sequence and its location with respect to the given gene are both important factors in the mechanism for each of the diseases. The pathological mechanism for each disease is different and is dependent upon either the loss of function of a particular protein or in some

disorders, the gain of function due to a toxic transcript. The main features of each of these disorders are summarised in table 1.4 and some will be discussed more fully.

1.7.3 Fragile X Syndrome

Fragile X syndrome is the most common form of inherited mental retardation. The gene mutated is FMR1 that is highly conserved and consists of 17 exons. Located at the 5'-untranslated region (5'-UTR) of the transcript is a CGG trinucleotide repeat (Hoogeveen *et al.,* 2002). The normal repeat length and content is highly polymorphic and ranges from 6 to 53. In Fragile X patients, the CGG is greatly expanded to over 230 repeats and the transcript becomes abnormally hypermethylated resulting in the silencing of the FMR1 gene (Jin and Warren, 2000). Fragile X is therefore caused by the loss of FMR1 gene product. Repeats of 60 to 230 are called premutations and normal transcripts and proteins levels are seen but are very unstable during transmission to offspring. This expansion can only occur by maternal transmission. Affected males have a more severe phenotype due to the X-linkage.

The protein encoded by FMR1 gene is fragile X mental retardation protein (FMRP) and it has been implicated in RNA binding and may play a role in translational control (Siomi *et al.,* 1993). The subcelluar localisation of FMRP shows that it has a cytoplasmic and nuclear distribution. An immuno-electron microscopy study (Willemsen *et al.,* 1996) demonstrated that FMRP is associated with the granular component of the nucleolus. FMRP has also been shown to be a nucleocytoplasmic shuttling protein that selectively binds to a subset of mRNAs, forms messenger ribonucleoprotein (mRNP) complexes and associates with translating ribosomes (Ceman *et al.,* 1999). The same investigation also showed that FMRP interacts with C23 (nucleolin) that is a nucleolar protein that forms part of the mRNP complexes. It is suggested that part of the molecular basis of Fragile X is the translational overexpression of selected mRNA due to the loss of FMRP (Warren, Neuroscience 2004).

1.7.4 Fragile X Premutation

Individuals with a premutation were originally believed to have no clinical symptoms but a number of investigations have shown some premutation carriers have tremor with ataxia, mild learning disabilities and emotional problems (Hagerman *et al.*, 2002). It has been shown that individuals with a premutation have increased FMR1 mRNA levels that can be up to 8 times higher than normal and slightly reduced FMRP protein levels (Kenneson *et al.*, 2001). It is suggested that there is impairment in the translation process and a compensatory induction of FMR1 mRNA synthesis. A recent study has shown that the expanded CGG tract in the 5'-UTR of FMR1 mRNA impedes the translation of FMRP in a length-dependent manner (Napierala *et al.*, 2005).

Post-mortem examination of the brains of elderly, symptomatic premutation carriers revealed the presence of intranuclear inclusions in neuronal and astrocytic nuclei of the cortex that stained positively for ubiquitin (Greco *et al.*, 2002). The inclusions were found in all cases examined and it is suggested that it is the increased mRNA levels that are important for the formation of the inclusion and play a role in the development of the clinical symptoms seen in premutation carriers.

A 'knock-in' CGG triplet repeat mouse has been generated carrying 98 repeats, which is in the premutation range (Willemsen et at, 2003). Immunohistochemical investigations in these mice have demonstrated the presence of inclusions in neurons as well (figure 1.44). Ubiquitin, 20S core of the proteasome and Hsp40 all colocalise in the inclusion but FMRP does not. When the presence of total DNA or RNA in the inclusions was investigated neither was found but the group does not rule out the possibility that FMR1 transcripts may be present but not detected to date.

A Drosophila model of fragile X premutation also forms inclusions that contain ubiquitin, parts of the proteasome and chaperones (Jin *et al.*, 2003). These results indicate that the ubiquitin/proteasome pathway is somehow involved (like in the polyglutamine diseases) but it is important to remember that the CGG repeat is not translated, it is only transcribed, and therefore it is not mutant protein that is being misfolded or targeted for degradation. The Drosophila model also demonstrates that the CGG expansion alone can cause

neurodegeneration and is therefore an example of RNA-mediated neurodegeneration.

Figure 1.44
Immunohistochemical localisation of ubiquitin (green) and ethidiumbromide staining total RNA (red) in a neuron from an expanded repeat mouse (72 weeks). Overlay of the two images demonstrates that ethidiumbromide staining does not localise to ubiquitin positive intranuclear inclusions. X700 (taken from Willemsen *et al.*, 2003).

1.7.5 Myotonic Dystrophy

Myotonic Dystrophy (DM) is the most common form of muscular dystrophy affecting adults. Myotonia, muscle weakness and progressive muscle wasting characterise the disease. Phenotypes are highly variable and anticipation is shown. Two different loci for DM have been identified. The most common form is DM1 that accounts for 98% of cases. DM1 is caused by a CTG trinucleotide expansion in the 3'-UTR of Myotonic Dystrophy Protein Kinase (DMPK). DM2 is caused by a tetranucleotide expansion (CCTG) in intron 1 of zinc finger protein 9 (ZNF9) (Liquori *et al.*, 2001). In DM1 and DM2 transcripts containing the expanded repeats form nuclear foci within DM cells. Despite the repeat expansion occurring in unrelated genes, the phenotypes seen in DM1 and DM2 are so similar that a common mechanism has been suggested. One suggestion is that the novel 'gain of function' is not related to the protein, but to the mRNA transcript. The foci seen in both DM1 and DM2 cells may sequester various other proteins in a similar mechanism that is suggested to be part of the problem in the polyglutamine diseases. It has been shown that proteins related to *Drosophila* muscleblind proteins colocalise with the foci (Fardaei *et al.*, 2002) (figure 1.45). The functional role of these proteins is not understood in mammalian cells but one study demonstrates that the muscleblind proteins regulate alternative splicing of specific pre-mRNAs (Ho *et al.*, 2004). Altered

insulin-receptor splicing has been shown in both DM1 and DM2 muscle (Savkur *et al.*, 2001; Savkur *et al.*, 2004). These findings suggest that an important feature of the RNA-mediated pathogenesis model for DM is the disrupted splicing of specific pre-mRNA targets.

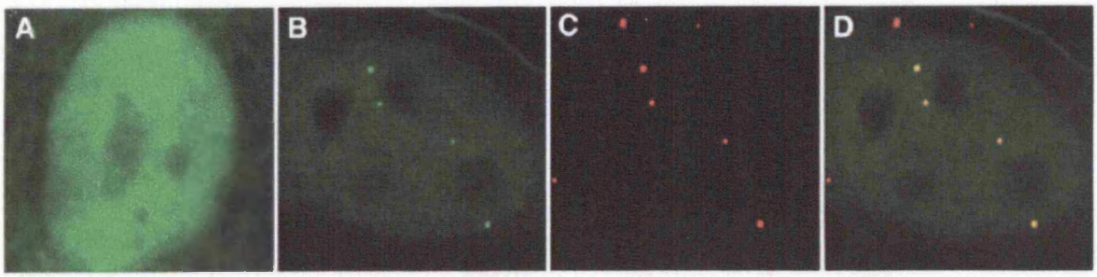

Figure 1.45
Transient expression of GFP-tagged muscleblind protein in control (A) and DM1 cells (B-D). In DM1 cells muscleblind protein is localised to nuclear foci (B). In DM1 cells DMPK expanded RNA transcripts are seen in nuclear foci as well (C). Merged images show that muscleblind and the transcripts colocalise (D) (taken from Fardaei *et al.*, 2002).

1.7.6 SCA8

SCA8 is another disease where the symptoms include a progressive ataxia with cerebellar atrophy and is caused by an expanded CTG repeat in the 3'-terminal exon (Koob *et al.*, 1999). The size of the CTG repeat that causes the disease ranges from 110 to 250, surprisingly, shorter or longer repeat lengths do not produce the disease. The SCA8 transcripts containing the CTG repeat are alternatively spliced and polyadenylated and are primarily expressed in brain tissue (Nemes *et al.*, 2000). The SCA8 transcript does not encode a protein, as no open reading frames (ORFs) are present. It is believed that the spliced transcripts do not function as mRNA but are organised as natural antisense transcripts that possibly regulate the expression of other genes.

When a genetic modifier screen was performed using SCA8(CTG)118 as the phenotype, mutations in four genes were found (Mutsuddi *et al.*, 2004). One of these genes was Muscleblind that is implicated in DM and implies that there are parallels between DM and SCA8. Differences between the phenotypes of these diseases may be explained by the different expression patterns of the their transcripts (Mosemiller *et al.*, 2003). The multi-systemic features of DM1 and DM2 are consistent with the broad expression of DMPK and ZNF9 transcripts, whereas, SCA8 transcripts are predominantly expressed

in the brain, which is the major site of pathology in SCA8.

Discovering the mechanism by which these untranslated repeat expansions cause neurodegenerative diseases is now important and it is possible that RNA may be uncovered as the cause of more diseases.

1.8 Aims and Objectives

The aim of this work is to investigate the morphology of three nuclear subdomains (the nucleolus, the Cajal body and the speckles) in the nuclei of neurons within the mouse striatum. A molecular characterisation of each of the subdomains will also be undertaken. The results of these studies will then be compared to a mouse model of Huntington's disease, the R6/2 transgenic mouse and a mutant mouse lacking the nuclear protein p80 coilin, the p80 coilin knock-out mouse.

It has been well documented that alterations to each of these subdomains occur in response to changes in cellular activities. Therefore, any differences seen in the organisation of the R6/2 nuclei or the p80 KO nuclei compared to that of the wild type nuclei, will help to gain a better understanding of the cellular pathways affected in these two mutant mice.

Materials & Methods

CHAPTER 2
Materials and Methods

2.1 Tissue Preparation

Animals were anesthetized with an overdose of sodium pentobarbitone (Sagatal, 100 mg/kg, intraperitoneally) and perfused through the left cardiac ventricle with 35 to 50 ml of a 2% paraformaldehyde/lysine/periodate (PLP) fixative in phosphate buffer (pH 7.4) or 4% paraformaldehyde with or without 0.1% gluteraldehyde. The brains were removed after decapitation and placed in the appropriate fresh fixative.

2.1.1 Tissue Preparation for Electron Microscopy

Brains for standard transmission electron microscopy (TEM) were placed in a fresh solution of 4% paraformaldehyde with 0.1% gluteraldehyde for a minimum of 24 hours at 4°C. Brains for immuno-electron microscopy were placed in either 2% PLP fixative in phosphate buffer (pH 7.4) or 4% paraformaldehyde with or without 0.1% gluteraldehyde for a minimum of 24 hours at 4 °C depending on which antibody was being used (table 2.1). After post-fixation, brains were bonded using superglue (cyanoacrylate) to the mounting block of a Vibratome Series 1000. The Vibratome reservoir was filled with 0.1 M phosphate buffer and coronal sections were cut of either 50 or 200 µm and collected into 'dimple tray' containing 0.1 M phosphate buffer.

2.1.2 Tissue Processing for Electron Microscopy

For standard TEM 200 µm thick sections were osmicated (60 mins 1% OsO4 in 0.1 M phosphate buffer at 4°C) and then *en-bloc* stained in a solution of 2% uranyl acetate (in 0.1 M sodium acetate) for 45 minutes at 4 °C. The sections were then dehydrated though a graded ethanol series (25%, 50%, 70%, 90%, 100% x4); and cleared in propylene oxide (100%x4). Sections were then incubated in a solution of 50% araldite resin in propylene oxide for 45 minutes and then left in pure araldite resin on a rotator overnight. The sections were

then placed between two sheets of Melanex (ICI) and put in an oven overnight at 60% to polymerise the araldite resin.

The striatum from the embedded sections were superglued onto resin blocks and the block face was polished until smooth. Using a Reichert Ultracut ultramicrotome semithin (1 µm) sections were cut with glass knives. The semithin sections were collected on glass slides, dried on a hot plate and counter-stained with toludine blue. These sections were then viewed under a light microscope to ensure the correct area of brain was being examined. Ultrathin sections (approximately 70 nm) were cut using a diamond knife and only sections that were silver-gold were collected on copper-mesh grids. When the sections had dried onto the grids, they were then counter-stained with lead citrate for approximately 4 minutes and viewed in a Jeol 1010 electron microscope.

2.1.3 Immunocytochemistry For Electron Microscopy

Vibratomed sections of brain (50 µm) were incubated free-floating in primary antibody that was diluted to the appropriate concentration in either primary antibody buffer or phosphate buffer, for 72 hours at 4 °C. Depending on which antibody was being used either 2% PLP or 4% paraformaldehyde fixed tissue was used (table 2.1). The sections were then washed in the correct buffer and incubated in either biotinylated or immunogold secondary antibodies.

Sections that were incubated with biotinylated secondary antibodies were then visualised using HRP-DAB reaction product (chapter 2.2.2) For immunogold, sections were incubated in immunogold secondary antibodies at a concentration of 1:200 in phosphate buffer overnight at 4 °C. Sections were then fixed in 0.1% gluteraldehyde for 10 minutes at room temperature. Sections were then silver-enhanced using Nanoprobes HQ Silver Enhancement Kit. This was carried out in the dark for approximately 5 minutes. Sections were then washed in acetate followed by phosphate buffers and processed for TEM.

The immunogold sections were osmicated in 1% osmium tetraoxide (in 0.1 M phosphate buffer) for only 7 minutes at °C as the silver enhancement reaction product can be removed by the osmium solution. Similarly, sections processed

with DAB are processed in 1% osmium tetraoxide for only 30 minutes at 4 °C. The sections were then washed and dehydrated as for standard TEM (chapter 2 1.2). Neither process involves *en-bloc* staining with uranyl acetate, although individual sections can be stained with lead citrate.

2.2 Tissue Processing

2.2.1 Tissue Preparation for Light Microscopy

Brains for light microscopy were placed in 2% PLP fixative in phosphate buffer (pH 7.4) for 4 to 6 hours before being transferred to a cryoprotectant solution of 30% sucrose in 0.1 M Tris (pH 7.4) for 48 hr at 4 °C. Brains that had been placed in 30% sucrose were mounted in Tissue-Tek OCT compound (Miles Laboratories), frozen with powdered solid CO_2, and sectioned in the coronal plane at 40 µm on a Leica SM2000R sledge microtome. Sections were collected using a paintbrush and then put serially in a 'dimple tray' filled with the correct buffer, and, stored at 4 °C until needed.

2.2.2 Immunocytochemistry For Light Microscopy

Sections were incubated free-floating in primary antibodies that were diluted to the appropriate concentration in primary antibody buffer (0.1 M Tris-HCL, 0.3% Triton and 0.02% sodium azide) or phosphate buffer at 4 °C for 72 hr. The sections were washed in the appropriate buffer prior to being processed with biotinylated secondary antibody for 2 hours at room temperature and at a concentration of 1:200. Sections were washed again before being transferred into an ABC solution (VectorLabs) for a further 2 hours at a concentration of 1:100 and at room temperature. The solution ABC consists of 10 µl avidin, 10 µl of biotinylated horseradish peroxidase and 980µl of buffer.

After washing in buffer, a solution of 3,3"diaminobenzidine (DAB) (containing 25 µg DAB, 33 µl hydrogen peroxide and 100 ml of buffer) was then used to localise the sites of peroxidase activity. Sections were examined under a light microscope periodically until an appropriate level of staining was seen. Sections were washed again and then mounted onto gelatinised slides.

The slide-mounted sections were allowed to air dry for at least 24 hours before finally being passed though an ascending ethanol series (70%, 80%, 90%, 95%, 100% x2) to dehydrate and cleared in two changes of Histoclear for 10 minutes. Slides were then coverslipped, using DPX as a mountant, which was allowed to harden before viewing.

2.2.3 Immunocytochemistry For Immunofluorescence

Sections for immunofluorescence were incubated free-floating in primary antibodies that were diluted to the appropriate concentration in primary antibody buffer (0.1 M Tris-HCL, 0.3% Triton and 0.02% sodium azide) or phosphate buffer at 4 °C for 72 hrs as with the other labelling protocols. If double-labelling was being performed, sections were incubated in a solution that contained both primary antibodies. However, each primary antibody must have been raised in a different host species, as this is the basis for differentiation between labels. After incubation in primary antibody/antibodies, the sections were washed in 0.1 M phosphate buffer and then incubated in secondary antibody/antibodies conjugated to a fluorophore diluted to a concentration 1:100 in 0.1 M phosphate buffer for two hours in the dark. If double-labelling was being carried out, the secondary antibodies must all be conjugated to different florophores e.g. FITC or TRITC, and, they must not be raised in the same species that was used to raise any of the primary antibodies. For these reasons, a series of secondary antibodies all raised in donkey and conjugated to a variety of fluorophores were used. The fluorophore-conjugated secondary antibodies are from Jackson Immunochemicals. Sections were then washed in 0.1 M phosphate buffer in the dark.

The sections were then labelled with pyronin Y or DAPI. For DAPI labelling, the sections were mounted on glass slides and, before the sections dried, the slides are coated with Vectashield DAPI mounting medium, which contains the nucleic acid-counterstaining fluorophore DAPI, coverslipped and sealed with a small rim of clear nail varnish.

Sections to be stained with pyronin Y were incubated for 2 minutes in a diluted pyronin Y solution (1:6000 dilution in phosphate buffer of a 10 mM stock from Sigma). The sections were then washed in buffer and mounted on glass

slides. To mount the coverslips, MOWIOL/Dabco, was used and this hardens so no nail varnish was needed. All slides were stored at4 °C in the dark until they were analysed using a Leica confocal microscope.

Antigen	Source	Code	Species	Dilution	Fixation	Solution
Fibrillarin	Pollard, Scripps Research Institute, La Jolla, USA	72B9	Mouse	1:1000	4%	1°mAb/PB
Fibrillarin	Pollard, Scripps Research Institute, La Jolla, USA	17C12	Mouse	1:1000	4%	1°mAb/PB
Fibrillarin	Abcam, Cambridge, UK	Ab5821	Rabbit	1:1000	4%	1°mAb/PB
Nopp140	U.T Meier, Albert Einstein College of Medicine, New York, USA	RF12	Rabbit	1:1000	4%	PB
GAR1	W. Filipowi, Friedrich Miescher Institut, Basel, Switzerland	-	Rabbit	1:1000	4%	1°mAb
C23	Santa Cruz, Autogen Bioclear, Wiltshire, UK	H-250	Rabbit	1:1000	4%	PB
B23	Abcam, Cambridge, UK	Ab15440	Rabbit	1:1000	-	-
Topo II	Santa Cruz, Autogen Bioclear, Wiltshire, UK	H-286	Rabbit	1:1000	PLP	1°mAb
UBF	Santa Cruz, Autogen Bioclear, Wiltshire, UK	H-300	Rabbit	1:1000	4%	1°mAb
RNA Pol I (RPAA194)	Santa Cruz, Autogen Bioclear, Wiltshire, UK	N-16	Goat	1:1000	PLP/4%	PB
Hsc70	Santa Cruz, Autogen Bioblear, Wiltshire, UK	K-19	Goat	1:1000	PLP/4%	1°mAb
p80 coilin	A.I. Lamond, University of Dundee, UK	204/10	Rabbit	1:1000	PLP/4%	1°mAb
SMN	BD Transduction Lab, Oxford, UK	610646	Mouse	1:1000	PLP/4%	1°mAb
SMN	G. Dreyfuss, University of Pennsylvania, USA	18163	Mouse	1:1000	PLP/4%	1°mAb
Gemin2	G. Dreyfuss, University of Pennsylvania, USA	2E17	Mouse	1:1000	PLP/4%	1°mAb
Gemin4	G. Dreyfuss, University of Pennsylvania, USA	17D10	Mouse	1:1000	PLP/4%	1°mAb
Gemin3/ DP103	BD Transduction Lab, Oxford, UK	612152	Mouse	1:1000	PLP/4%	1°mAb
U2"snRNP	EuroDiagnostica, Mansfield, UK	4G3	Mouse	1:1000	PLP/4%	1°mAb
EWS	Santa Cruz, Autogen Bioclear, Wiltshire, UK	N-18	Goat	1:1000	PLP	PB
PAP	Santa Cruz, Autogen Bioclear, Wiltshire, UK	V-18	Goat	1:1000	PLP	1°mAb
Profilin	Santa Cruz, Autogen Bioclear, Wiltshire, UK	N-20	Goat	1:1000	PLP	PB
CPSF-1	Santa Cruz, Autogen Bioclear, Wiltshire, UK	N-20	Goat	1:1000	PLP	PB
SC-35	Sigma, Dorset, UK	S4045	Mouse	1:1000	PLP/4%	1°mAb
HYPA	M.E. MacDonald, Massachusetts General Hospital, Boston, USA	AF-1	Rabbit	1:1000	PLP/4%	1°mAb
HYPC	M.E. MacDonald, Massachusetts General Hospital, Boston, USA	CF-1	Rabbit	1:1000	PLP/4%	1°mAb
TMG	Oncogene, Merck Biosciences, Nottingham, UK	-	Mouse	1:1000	PLP/4%	1°mAb
PSP1	A. Fox, University of Dundee, UK	-	Rabbit	1:1000	PLP/4%	1°mAb
Huntingtin	Santa Cruz, Autogen Bioclear, Wiltshire, UK	N-18	Goat	1:1000	PLP/4%	1°mAb

Table 2.1
A table showing the different antibodies used throughout this thesis. In the Fixation column, PLP =2% paraformaldehyde/lysine/periodate (PLP) fixative in phosphate buffer (pH 7.4) and 4% = 4% paraformaldehyde. In the Solution column, 1°mAb = primary antibody solution and PB = 0.1M phosphate buffer.

Results

CHAPTER 3

Results

3.1 Ultrastructure of Neuronal Nucleus

Most (90 to 98%) of striatal neurons have a smooth nuclear membrane (Kemp and Powell, 1971) and a predominantly dispersed configuration of chromatin with occasional small aggregates of condensed chromatin. This ultrastructure corresponds to a single type of neuron, the medium spiny projection cell. To ensure that the same cell type was being compared only non-indented nuclei were examined.

3.1.1 Ultrastructure of Neuronal Nucleolus

The structure of a typical mammalian nucleolus has been well documented (chapter 1.1.2 and figure 3.1) and it is suggested that the formation and maintenance of nucleolar morphology relies upon rRNA transcription and processing. To determine the ultrastructural features of neuronal nucleoli, I have analysed the nucleoli of striatal neurons in the normal 10-week-old mouse. Nuclei containing nucleoli were randomly sampled.

The nucleolus is easily identifiable in an ultrathin section under the transmission electron microscope (TEM). It is a spherical, electron-dense organelle that is located in the nucleus of the cell. From my analysis of striatal neurons, most cells are mononucleolated (88%) and occasionally binucleolated (12%). I did not see a nucleus that contained more than 2 nucleoli. The mean number of nucleoli per cell is 1.11+/-0.03.

After closely examining the ultrastructure of the striatal nucleoli, it is possible to distinguish two classes:

Type I) Closed-reticulate structure (CRS)

Type II) Open-reticulate structure (ORS)

CRS nucleoli were seen in 44% of the cells that were examined (graph

3.1A). These nucleoli have an ordered structure (figure 3.2A) but it is not possible to distinguish clearly the 3 components that constitute a 'classic' nucleolus: the fibrillar centres (FCs), the dense fibrillar component (DFC) and the granular component (GC). It is possible to see very small FCs, which are round, low-density fibrillar areas. The FCs are surrounded by what appears to be a dark, granular material, which constitutes the majority of the nucleolar volume. It is not possible to clearly differentiate the dense fibrillar component from the granular component. These nucleoli are spherical and the average diameter is 0.83+/-0.03 μm (graph 3.1B).

The CRS nucleoli occasionally have a perinucleolar cap structure (PNC). The PNC is generally smaller than the nucleolus and appears to be composed of a material that is less electron dense than the fibrillar-granular component of the nucleolus. There seems to be no actual connection between the PNC and the fibrillar-granular component of the nucleolus and in some nuclei, there even appears to be a small gap between the two structures.

The second class of nucleoli seen in striatal neurons, the ORS, does not have an evenly distributed morphology and was observed in 56% of nuclei examined (graph 3.1A). In a typical mammalian cell the FCs accounts for only 2% of the nucleolus (Shaw and Jordan, 1995), but these striatal nucleoli have one or two very large FCs, together with several small FCs (figure 3.2B). These FCs are not evenly distributed within the individual nucleoli. In some cases the FCs appear to be exposed to the nucleoplasm and not surrounded by the dense fibrillar component as characteristically observed in many cell types by many investigators. Like the CRS nucleoli, it is not possible to distinguish the dense fibrillar component from the granular component.

Some ORS nucleoli also have a PNC. It is smaller than the nucleolus and has the same appearance as that seen in CRS nucleoli. The ORS nucleoli are not as uniformly spherical as the CRS nucleoli and their average diameter is 0.90+/-0.03 μm (graph 3.1B).

In both classes some nucleoli are surrounded by what appears to be a halo of electron-dense particles. I believe this to be perichromatin granules (PG) and perichromatin fibrils (PFs) that have associated with condensed perinucleolar chromatin at the nucleolar periphery. The PGs and PFs can be seen to completely encircle the nucleolus or just part of it.

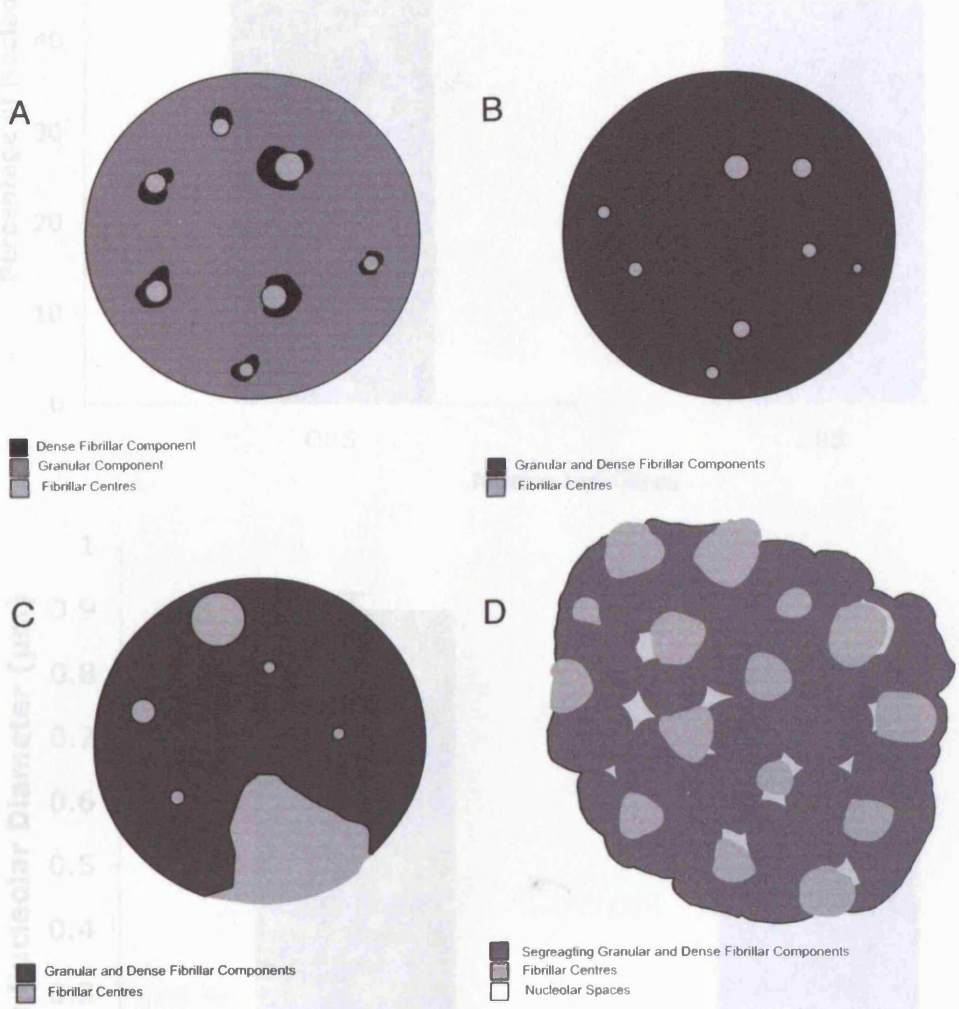

Figure 3.1
Schematic Diagrams Showing the Organisation of Nucleoli.

(A) A typical nucleolus from a mammalian nucleus. Small compact areas of DFCs surround the FCs and the GC accounts for the majority of the nucleolus.

(B) In striatal neurons of a 10-week-old mouse, nucleoli with small FCs surrounded by an entanglement of DFC and GC can be seen and have been classed as closed-reticulate structure (CRS) nucleoli.

(C) A second class of nucleoli can be seen in striatal neurons, the open-reticulate structure (ORS) nucleoli. These nucleoli have very large FCs that occupy a considerable volume of the nucleolus.

(D) In R6/2 transgenic mouse, a third class of nucleoli can be seen in the striatal neurons. The nucleoli in these cells is segregating and the FCs are medium sized and numerous. The entanglement of DFC and GC is forming small microspheres as well as areas of nucleoli that seem to be empty of any component.

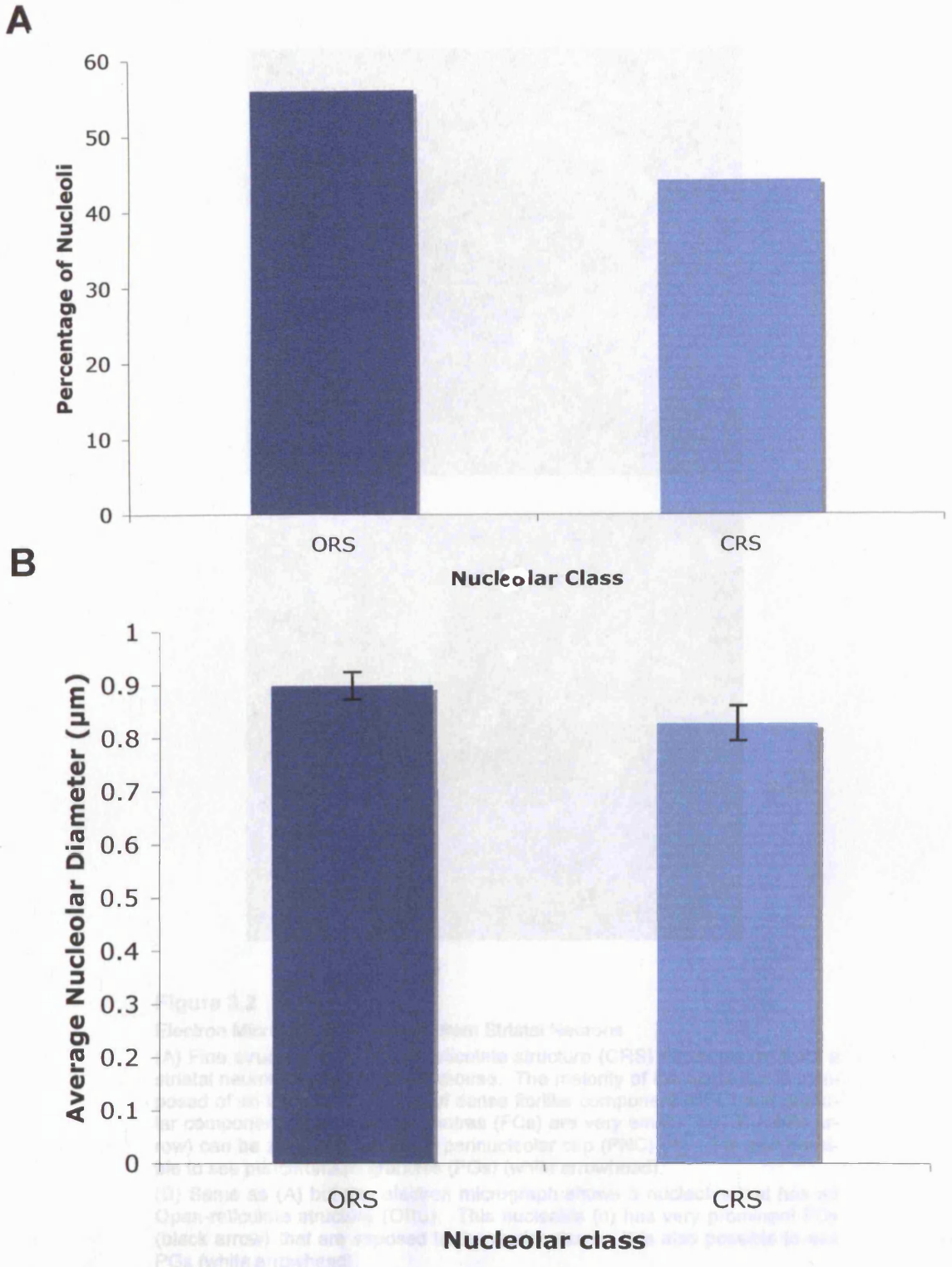

Graph 3.1

Analysis of the Class and Diameters of Nucleoli in Murine Striatal Nuclei

(A) A histogram showing the percentages of nucleoli that show an open-reticulate structure (ORS) or a closed-reticulate structure (CRS) in 10-week-old mice. A 95% confidence interval that the probability of ORS is between 46% and 65% and for CRS is between 35% and 54%.

(B) A histogram showing the average diameters of ORS or CRS nucleoli in 10-week-old mice. It is possible to see that ORS nucleoli have a slightly larger average diameter than the CRS nucleoli. Error bars are standard errors of mean.

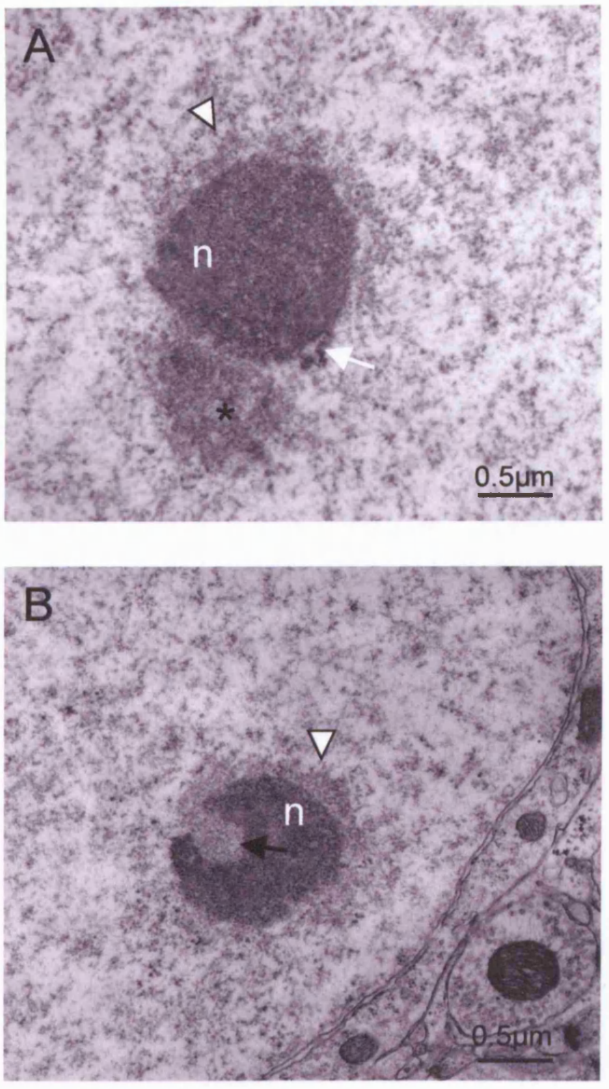

Figure 3.2

Electron Micrographs of Nucleoli from Striatal Neurons

(A) Fine structure of a Closed-reticulate structure (CRS) nucleolus (n) from a striatal neuron of a 10-week-old mouse. The majority of the nucleolus is composed of an intermingled mass of dense fibrillar component (DFC) and granular component (GC). Fibrillar centres (FCs) are very small. A CB (white arrow) can be seen and there is a perinucleolar cap (PNC) (*). It is also possible to see perichromatin granules (PGs) (white arrowhead).

(B) Same as (A) but this electron micrograph shows a nucleolus that has an Open-reticulate structure (ORS). This nucleolus (n) has very prominent FCs (black arrow) that are exposed to the nucleoplasm. It is also possible to see PGs (white arrowhead).

3.1.2 Ultrastructure of Neuronal Cajal Bodies

The Cajal body (CB), originally described by Cajal in 1903 in a variety of neurons, is a round-to-oval structure seen in the nucleus and it has been well documented (chapter 1.2.1 and Gall, 2003). I have analysed CBs in striatal neurons from the 10-week-old mouse to determine their organisation and their spatial relationship to other nuclear subdomains. Out of 100 nuclei observed at the TEM level, only 28% of nuclei had a clearly distinguishable CB. The CBs seen where situated in 2 different localisations within the nucleus: free in the nucleoplasm or associated with the nucleolus.

In all the striatal neurons examined, most CBs appeared to have a similar morphology and are identifiable as an oval to round structure composed of both granules and dense coiled threads embedded in a lower density matrix. 79% of CBs seem were nucleolar-associated and only 21% were free in the nucleoplasm (graph 3.2A). In a few neurons, CBs occurred that had a dense fibrillar structure that was very compact and had no amorphous matrix. From TEM analysis alone it is not possible to decide if these are indeed CBs or nuclear bodies (NB) of a different type.

The nucleolar-associated CBs have an average diameter of 0.23+/-0.02 μm (graph 3.2B) and protrude from the nucleolar periphery (figure 3.3A). In most cases the CB is found to be juxtaposed to the nucleolus but can easily be distinguished from the nucleolus as the electron dense strands and granules of the CB have a different morphology from either the GFC or the GC of the nucleolus. The less dense fibrillar matrix of the CB appears to be in direct contact with the nucleolus.

The free/nucleoplasmic CBs have an average diameter of 0.28+/0.03 μm (graph 3.2B) and do not appear to be associated with any other nuclear domain (figure 3.3B). Many CBs have tiny fibrils radiating into the nucleoplasm from the amorphous matrix.

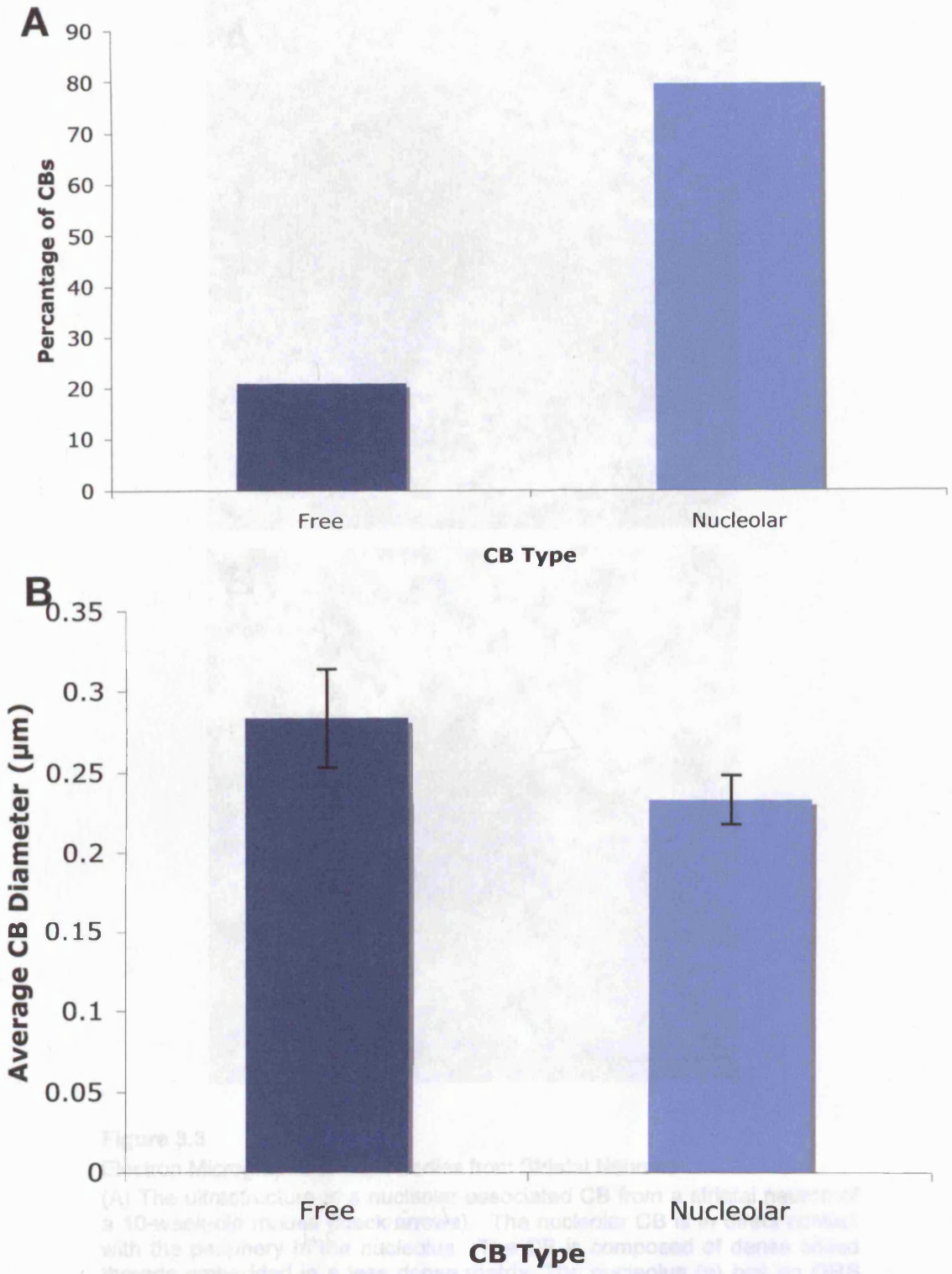

Graph 3.2

Analysis of Cajal Bodies in Murine Striatal Nuclei

(A) A histogram showing the percentages of CBs that are either free in the nucleoplasm or nucleolar-associated and found at the periphery of the nucleolus in 10-week-old mice. It is possible to see that most of the CBs in the striatal neurons are nucleolar-associated CBs. A 95% confidence interval that the probability of nucleolar CBs is between 70% and 86% and for free CBs is between 14% and 30%.

(B) A histogram showing the average diameters of free or nucleolar-associated CBs in 10-week-old mice. Free CBs appear to have larger average diameters compared to those of the nucleolar-associated CBs. Error bars are standard errors of mean.

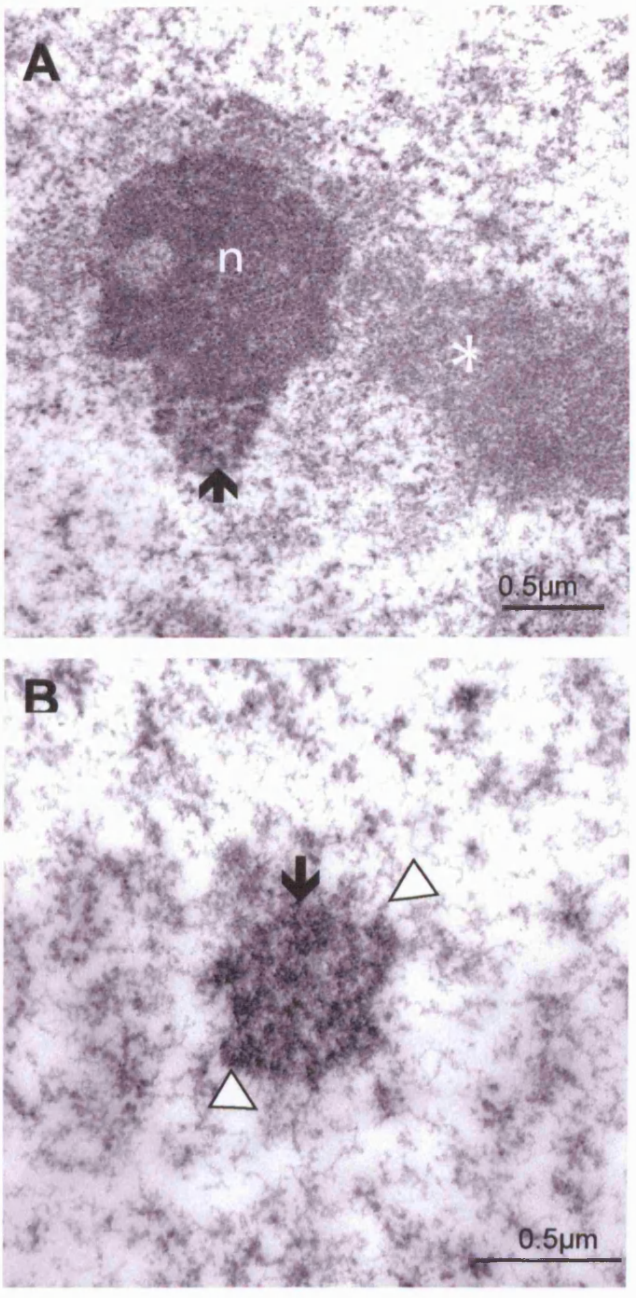

Figure 3.3

Electron Micrographs of Cajal Bodies from Striatal Neurons

(A) The ultrastructure of a nucleolar-associated CB from a striatal neuron of a 10-week-old mouse (black arrows). The nucleolar CB is in direct contact with the periphery of the nucleolus. The CB is composed of dense coiled threads embedded in a less dense matrix. The nucleolus (n) has an ORS morphology and a PNC (*).

(B) The fine structure of a free, nucleoplasmic CB (black arrows) from a striatal neuron of a 10-week-old mouse. This CB has the same morphology as the nucleolar CB, but does not appear to have a spatial relationship with any other nuclear domain. Note the small fibrils (white arrowheads) projecting from the CB periphery.

3.1.3 Ultrastructure of Neuronal Speckles

The nuclear subdomains that are known as speckles contain pre-messenger RNA (pre-mRNA) splicing factors and at the ultrastructural level are composed of interchromatin granule clusters (IGCs) and perichromatin fibrils (PFs) (chapter 1.3). I have investigated the morphology of the speckles and IGCs in the striatal neurons of the 10-week-old mouse. Although it is possible to distinguish IGCs from the chromatin in the nucleoplasm of the nucleus without antibodies (figure 3.4), it has been hard to quantify the shape and number per nuclei. Unlike the CB or nucleolus, the IGCs do not have a very obvious morphology and this makes quantifying them via electron microscopy difficult. Speckles are composed of numerous granules that are connected via thin fibrils, which are the PFs. Each nucleus contains a varying number of speckles, which have an irregular shape and differing diameter.

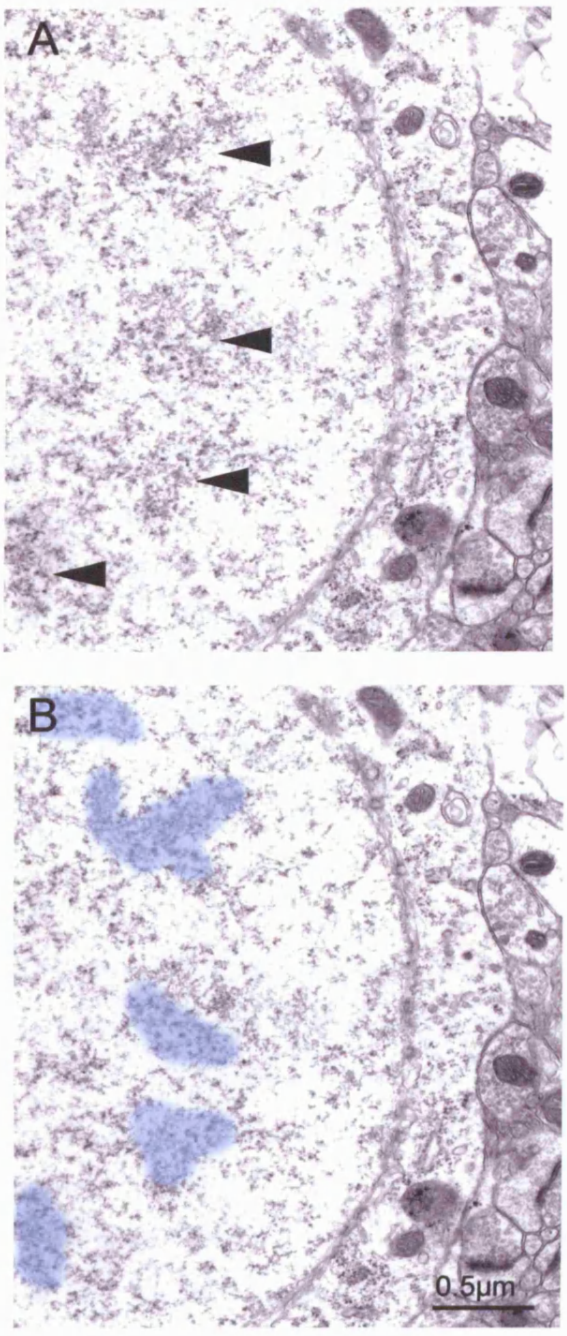

Figure 3.4

Electron micrographs of Speckles from Murine Striatal Neurons

(A) The fine structure of speckles (black arrowheads) in a striatal neuron from 10-week-old mouse. Perichromatin fibrils (PFs) and interchromatin granule clusters (IGCs) correspond to speckles at the ultrastructural level. IGCs represent the main part of speckles and comprise granules that appear to be connected with fibres.

(B) Same image as (A) but the IGCs have been highlighted in pale blue.

3.2 Molecular Composition of Neuronal Nucleus

Use of immunocytochemical methods have localised a large number of nuclear proteins to specific subcompartments of the cellular nucleus. However the vast majority of such studies have utilised human cells in culture with antibodies generated against the human protein sequence. Few studies have investigated nuclear localisation in murine cells and even fewer in murine neuronal cells. In these studies I have attempted to define the molecular organisation of the murine neuronal nucleus using antisera to a large number of neuronal proteins.

3.2.1 Molecular Composition of Neuronal Nucleolus

The molecular organisation of the nucleolus in striatal neurons can be examined using a variety of well-characterised antibodies and different nucleolar proteins have been shown to localise to the different structural components of the nucleolus: the fibrillar centres, the dense fibrillar and the granular components (figure 3.5). Using this as a guide, I analysed the distribution of a number of key nucleolar factors in murine striatal neurons.

Immunocytochemical identification of the dense fibrillar component of the nucleolus is most usually achieved with antibodies to the protein fibrillarin. One such antibody that has been used in many studies is a monoclonal antibody termed 72B9. Immunocytochemistry using a number of different fibrillarin antibodies localised fibrillarin to the nucleolus and to the nucleolar-associated and nucleoplasmic Cajal bodies (CBs) (figure 3.6B). The immunoreactivity for all the fibrillarin antibodies revealed an intense staining of one or more nucleoli per nucleus, which could be seen as a spherical structure located within the nucleus at low magnification (figure 3.6C). When the magnification was increased, many nucleoli appeared to stain uniformly and completely encompassed one to three small accessory Cajal bodies.

Two other nucleolar proteins that are suggested to be localised to the same region of the nucleolus (the dense fibrillar component) as fibrillarin are GAR1 and Nopp140. Immunocytochemistry for a GAR1 antibody revealed a similar staining pattern to that seen for fibrillarin; round structures located within the

nucleus and frequent accessory Cajal bodies (data not shown). Immunoreactivity for a Nopp140 antibody showed nucleoplasmic staining as well as nucleolar labelling (figure 3.6D). Very distinct and intense staining of nucleolar-associated Cajal bodies, which varied in number from one to three were seen. Antibodies to both proteins also occasionally labelled nucleoplasmic CBs.

C23 (nucleolin) is a nucleolar protein found in the granular component of the nucleolus, together with B23 (nucleophosim). Unfortunately, antibodies generated against B23 showed no staining of the nucleolus revealing only nucleoplasmic staining. However an antibody against C23 did show staining of the nucleolus together with nucleoplasmic labelling (figure 3.6E). The staining pattern for C23 revealed a rim of immunoreactivity at the periphery of the nucleolus and no CB staining.

Upstream binding factor (UBF) is another nucleolar protein and it has been used as a marker for fibrillar centres. Immunoreactivity for the UBF antibody revealed nucleolar staining but a different pattern was seen from that of other nucleolar proteins (figure 3.6A). At the light microscopy level, some nucleoli appear to stain as an accumulation of small foci. RNA polymerase I is also localised to fibrillar centres but when I used an antibody to this protein no staining of fibrillar centres was seen. Instead nucleoplasmic immunoreactivity was seen with infrequent, irregular nuclear foci that were very small (figure 3.6F).

DNA topoisomerase II (topo II) is an essential enzyme that mediates a variety of chromosome activities including transcription, recombination, and chromosome condensation and has been localised to the nucleolus using immunocytochemistry (Zini *et al.*, 1994). In the nuclei of striatal neurons in the mouse, an antibody against topo II revealed nucleoplasmic staining as well as labelling of the nucleolus (data not shown). The immunoreactivity appeared to be similar to that seen for C23 with a rim at the edge of the nucleolus but also included complete labelling of adjacent Cajal bodies.

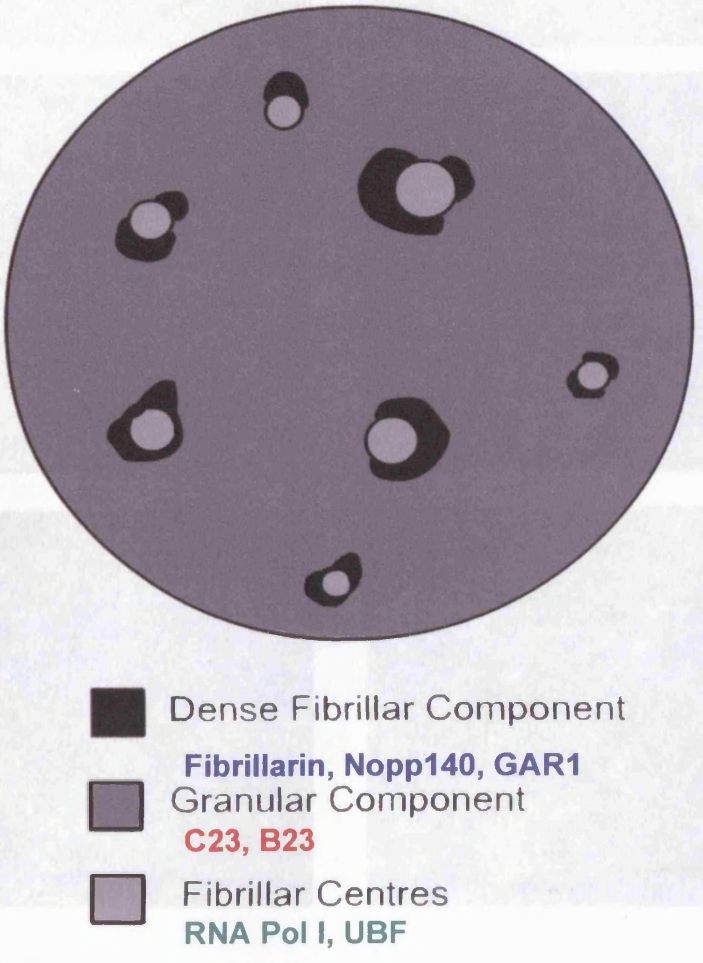

Figure 3.5
Schematic Diagram Showing the Molecular Organization of Nucleoli.
Different nucleolar proteins (coloured text) have been shown to localise to different structural regions of the nucleolus; dense fibrillar component (black), granular component (dark grey) and the fibrillar centres (grey).

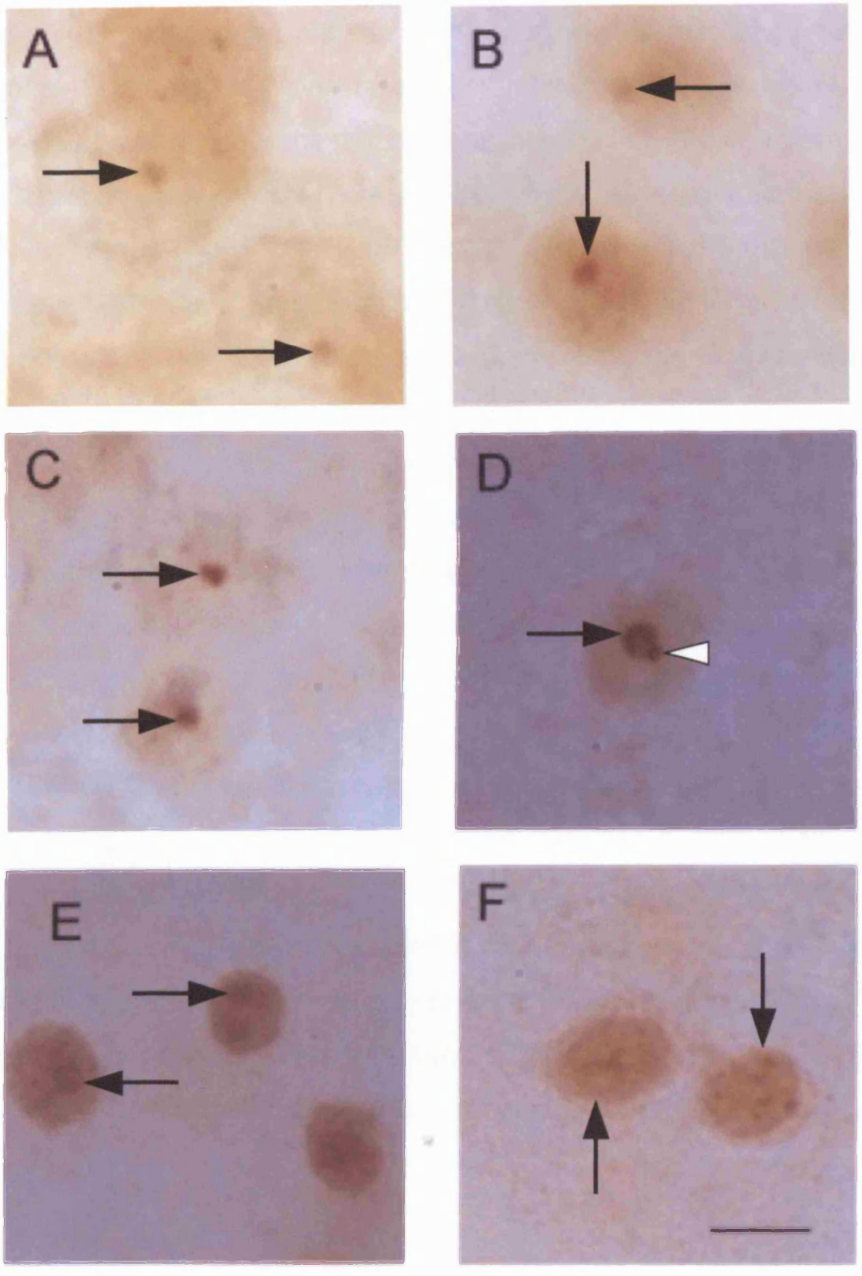

Figure 3.6
Molecular Composition of Nucleoli from Striatal Neurons
Photomicrographs showing immunoreactivity for a variety of nucleolar proteins in striatal neurons from 10-week-old mouse. The UBF (A), fibrillarin (B/C), Nopp140 (D), C23 (E), and RNA Polymerase I (F) immunoreactive nucleoli are indicated with arrows.
The UBF (A) immunoreactivity reveals a pale nucleoplasm with infrequent nucleolar staining. The nucleolar immunoreactivity appears as spherical foci in the nucleus (black arrows).
The fibrillarin (B) immunoreactivity using 17C12 antibody shows an intense nucleolar staining (black arrows) with diffuse nucleoplasmic stain. It is possible to see that some nuclei contain more than 1 nucleolus.
The fibrillarin (C) immunoreactivity using Abcam antibody also shows intense nucleolar staining (black arrows) and a diffuse nucleoplasmic stain.
The Nopp140 (D) immunoreactivity reveals a pale nucleoplasmic stain together with nucleolar staining (black arrow). The nucleolar staining appears as a spherical structure that has a pale centre and a more intense peripheral ring. It is also possible to distinguish nucleolar-associated CBs (white arrowhead).
The C23 (E) immunoreactivity shows nucleolar staining as a round nuclear foci (black arrows) which has an outer ring of more intense staining. Nucleoplasmic staining can also be seen and some nuclei have more RNA POL I (F) immunoreactivity shows nucleoplasmic staining with infrequent, irregular nuclear foci (black arrows). (A-F) Scale bar= 10 μm

From my ultrastructural analysis of the murine striatum, it appears that most striatal nuclei contain only one nucleolus. To confirm this result, 100 nuclei were analysed and the number of nucleoli seen using three different nucleolar markers were recorded. The average numbers were as follows for fibrillarin 1.21+/-0.04, Nopp140 1.21+/-0.04 and C23 1.21+/-0.04 (graph 3.3A). The antibody from Abcam against fibrillarin showed that 79% of nuclei contained one nucleolus and only 21% contained two nucleoli. Similar results were seen with Nopp140 and C23 (graph 3.3B).

I have further analysed the ultrastructural distribution of some of these proteins. Using pre-embedding immuno-electron microscopy with DAB, I was able to see that fibrillarin had a heterogeneous distribution over the nucleolus and was localised to the entanglement of dense fibrillar component and granular component of the nucleolus (figure 3.7A/B). Unfortunately none of the other nucleolar antibodies worked due to the fixation needed for the antibodies to work (table 2.1) and the fixation needed for immuno-EM.

In the course of my studies I looked at the distribution of the chaperone Hsc70 and, using light microscopy, the staining appeared to concentrate in a spherical structure in the striatal nuclei (data not shown). The immunoreactivity was not like that for fibrillarin as the staining was heterogeneous. When this was repeated for pre-embedding immuno-electron microscopy with DAB, it was clear that Hsc70 was localised to the nucleolus but only at the periphery (figure 3.7C/D).

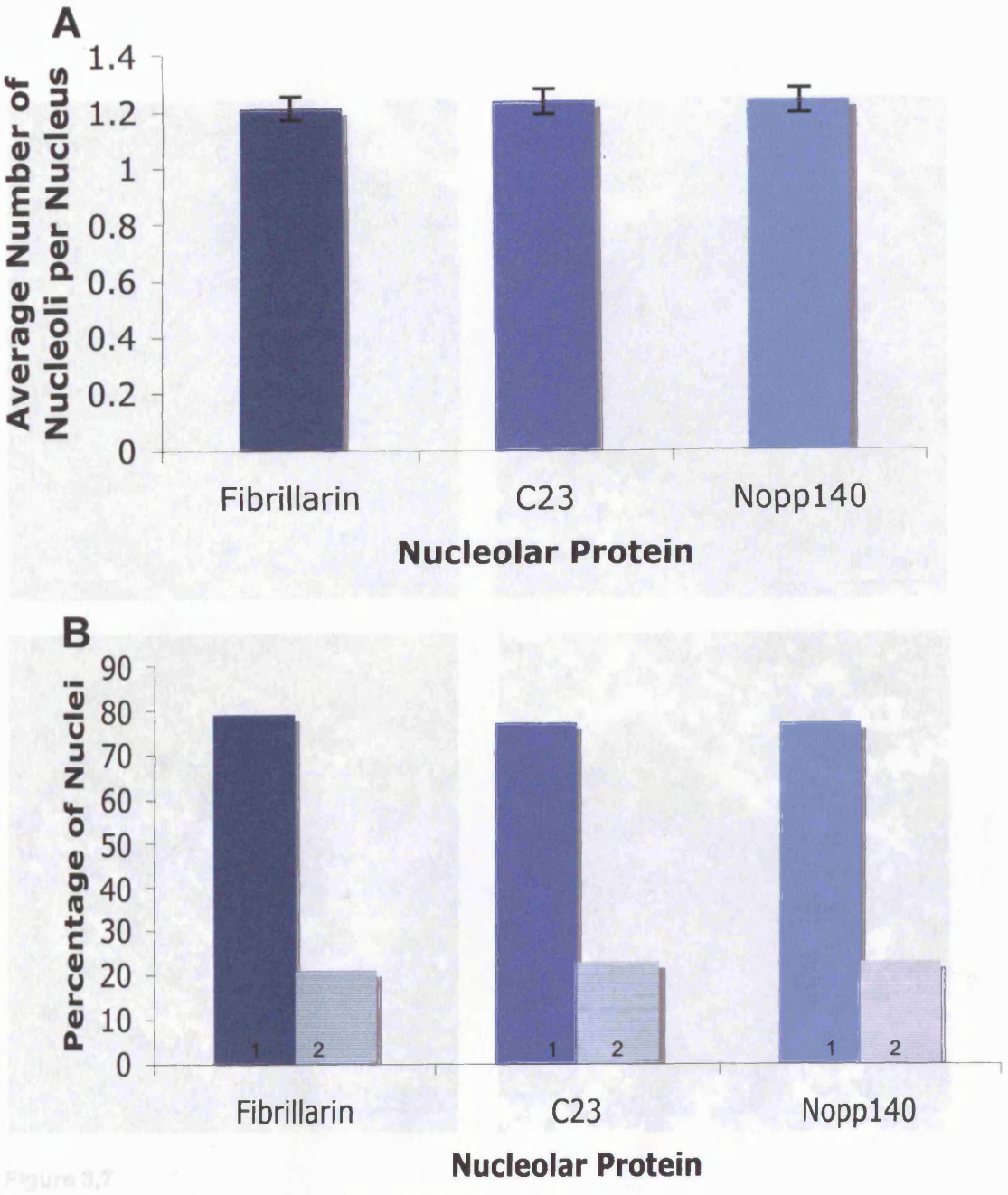

Graph 3.3

Analysis of the Molecular Composition of Nucleoli in Murine Striatal Nuclei

(A) A histogram showing the average number of nucleoli per nuclei when analysed with antibodies to three different nucleolar proteins in 10-week-old mouse. Error bars are standard errors of mean.

(B) A histogram showing the percentage of nuclei that contained either one or two nucleoli when quantified with antibodies to three different nucleolar proteins in 10-week-old mouse. Most nuclei when analysed with any of the three proteins have only one nucleolus

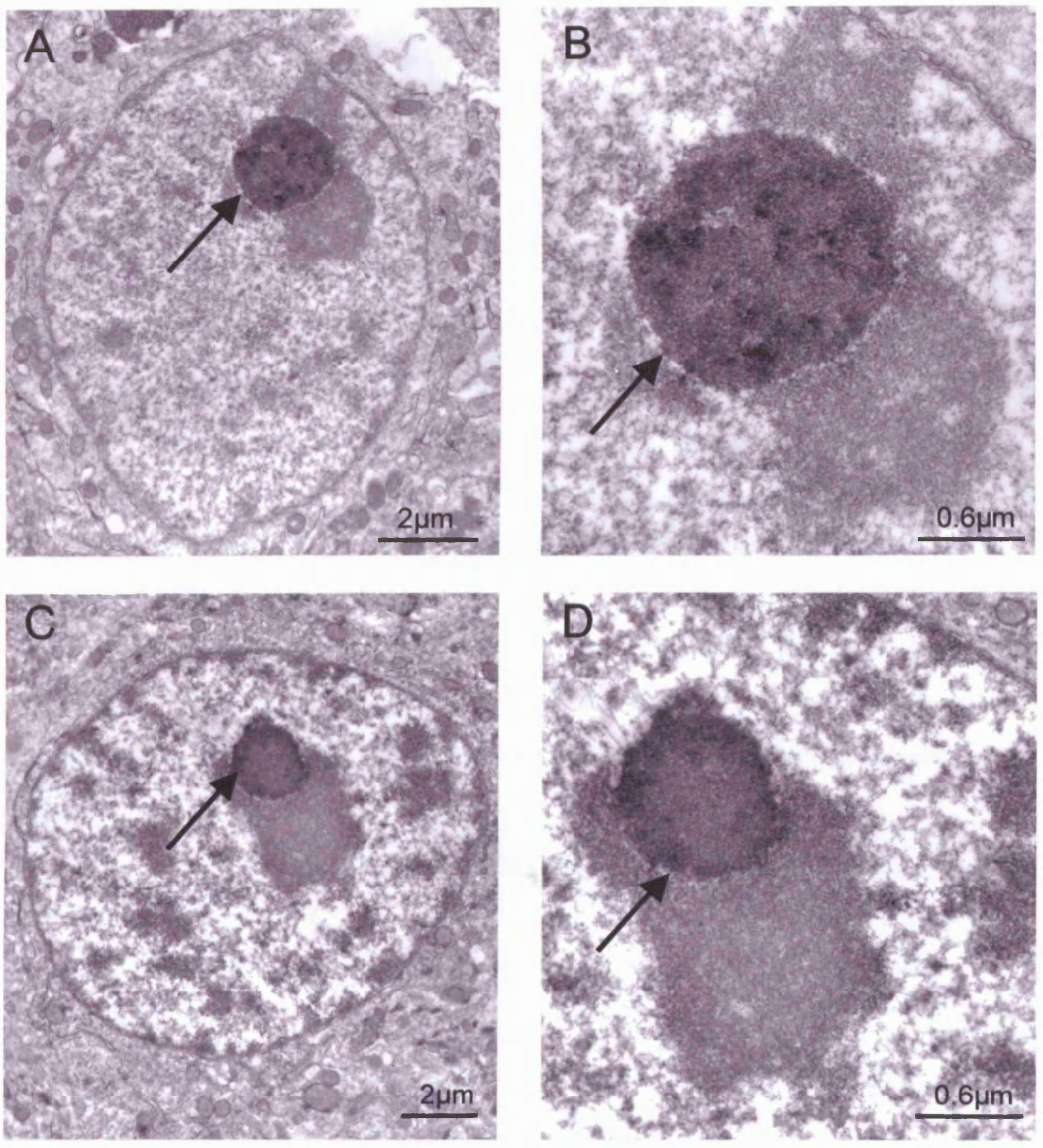

Figure 3.7

Molecular Composition of Nucleoli from Striatal Neurons

(A) and (B) Electron micrographs of fibrillarin immunoreactivity in striatal neurons from 10-week-old mouse. The immunoreactivity clearly shows that fibrillarin is localised to the entanglement of Dense Fibriilar Component and the Granular Component of the nucleolus (black arrows).

(C) and (D) Electron micrograph of Hsc70 immunoreactivity in striatal neurons from 10-week-old mouse. The staining reveals that Hsc70 is localised to periphery of the nucleolus (black arrows).

3.2.2 Molecular Composition of Neuronal Cajal Bodies

The functional role of the Cajal body (CB) has yet to be defined, but it has been suggested to play a role in snRNP biogenesis because of the functions of some of the proteins that have been shown to concentrate in CBs. I analysed the molecular composition of CBs in the murine striatum at different ages. Using immunocytochemistry I have defined CBs as a nucleoplasmic foci staining intensely with a given antibody.

p80 coilin is a nucleoplasmic-shuttling phosphoprotein that is known as the molecular marker of CBs (chapter 1.2.2) and immunocytochemistry using the 204/10 p80 coilin antibody (a gift from A.I Lamond, Dundee, UK) revealed CBs as well as a diffuse nucleoplasmic staining (figure 3.8A). Using light microscopy, the number of p80 coilin positive CBs ranged from 1 to 4 and, when 100 nuclei were analysed, the average number of per nuclei being 2.29 +/-0.1 at 4 weeks of age and 2.35 +/-0.09 at 12 weeks of age (table 3.1). The size of p80 coilin positive CB within nuclei varied and as the average diameter was generally less than 0.5 μm it was not possible to measure them using the light microscope. This staining pattern did not change from 4 weeks to 12 weeks.

snRNPs (small nuclear ribonucleoprotein particles) have previously been reported to accumulate in CBs as part of a maturation pathway and immunocytochemistry using an antibody generated against U2" snRNP labelled CBs (figure 3.8E). The average number of CBs that contained U2" snRNP was 0.88+/-0.06 at 4 weeks of age and at 12 weeks of age this number had not changed and remained at 0.88+/-0.06 (table 3.1).

Cajal body protein	4 weeks of age	10 weeks of age	12 weeks of age
p80 coilin	2.29+/-0.1	2.4+/-0.08	2.35+/-0.09
U2" snRNP	0.88+/-0.06	0.89+/-0.06	0.88+/-0.06

Table 3.1
A table showing the average number of CBs per nucleus for either p80 coilin or U2" snRNP at different ages.

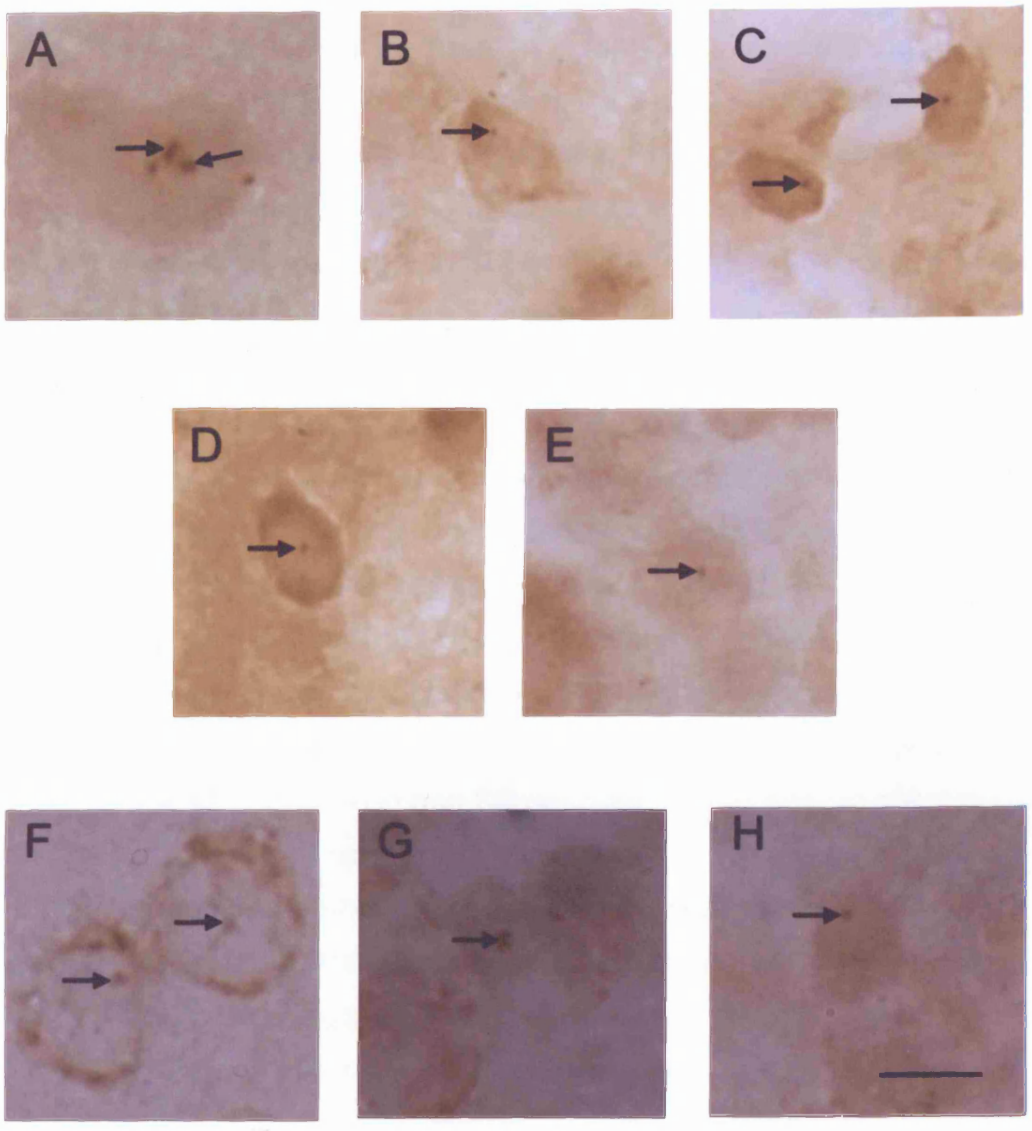

Figure 3.8
Light Microscopy Immunostaining of Cajal Bodies from Murine Striatal Nuclei.
Photomicrographs showing immunoreactivity for a variety of Cajal body proteins in nuclei of striatal neurons from 10-week-old mice. The p80 coilin (A), SMN (B), Gemin2 (C), Gemin4 (D), U2 snRNP (E), Gemin3 (F), PAP (G) and EWS (H) immunoreactive CBs are indicated by black arrows and a diffuse nucleoplasmic stain can also be seen. The p80 coilin (A) immunoreactivity shows that more than one CB can be seen using this CB marker whereas immunoreactivity for all the other CB proteins reveal only one CB per nucleus. Scale bar = 10 μm

SMN, the Survival of Motor Neuron protein, has been seen in CBs and gems depending on the cell type (chapter 1.2.6). In murine striatal neurons, immunoreactivity for an antibody against SMN was localised to nuclear foci as well as showing a diffuse nucleoplasmic and cytoplasmic staining pattern (figure 3.8B). Due to the number and size of these foci, I believe that they are CBs. Usually only one CB per nuclei was seen with the SMN antibody but occasionally nuclei did contain 2-3 CBs and the average number was 1.16 +/- 0.06 at 10 weeks of age (graph 3.4A). SMN can be found in the nucleus as part of a macromolecular complex, the SMN Complex, and Gemin2 to 7 have been shown to form part of this complex (chapter 1.2.8). Antibodies against Gemin2 and Gemin4 both showed a similar staining pattern: cytoplasmic, faint nucleoplasmic and bright CB (figure 3.8C/D). Gemin4 did not label the nucleolus although it is suggested that it has been detected there (Charroux *et al.*, 2000). The Gemins, like SMN, more frequently stained only one CB per nuclei with the average for Gemin2 being 1.09+/-0.06 at 10 weeks of age (graph 3.4A). Graph 3.4A shows that at 10 weeks of age in the murine striatum, the only Cajal body protein on average to be found in more than one CB per nucleus was p80 coilin. The other Cajal body proteins that I analysed generally were only found to localise in one CB per nucleus and this did not change from 4 weeks to 12 weeks of age.

Antibodies against other proteins that have been previously shown to localise in CBs were also used to see where they were distributed in murine striatal nuclei. Cleavage and polyadenylation specificity factor (CPSF) is involved in mRNA polyadenylation and plays a role in the splicing of single-intron pre-mRNAs. It has been suggested that it has a CB or gem localisation (Hofmann *et al.*, 2002). Profilin binds to and sequesters actin monomers and therefore is involved in the regulation of actin polymerisation. Although it is found in axonal and dendritic processes in the mouse brain, more recently it has been found in CBs (Giesemann *et al.*, 1999; Skare *et al.*, 2003). SmB is one of the core proteins that are found in all major snRNPs, which form the major component of the spliceosome. A diffuse distribution of CPSF, profilin and SmB immunoreactivity was observed in the nucleoplasm (data not shown). Gemin3 forms part of the SMN complex and interacts with SMN (Campbell *et al.*, 2000). Poly(A) polymerase (PAP) is involved in the polyadenylation of 3'

prime ends of mRNA (Schul *et al.*, 1996). Ewing's sarcoma (EWS) is a RNA-binding protein and it also interacts with SMN (Young *et al.*, 2003). Immunoreactivity for Gemin3, PAP and EWS appeared as darkly stained foci in the nucleus and the size of these foci are characteristic of Cajal bodies but they appeared infrequently (figure 3.8F-H).

I used pre-embedding immuno-electron microscopy with DAB for some of the antibodies against CB proteins to see if the structures seen at light microscopy correlated with the CBs seen ultrastructurally, and, to see if there was a difference in staining between the CB at different localisations. Using anti-p80 coilin it was possible to see staining associated with the nucleolus as infrequent nucleolar-associated CBs (figure 3.9A-B) or a very thin ring at the nucleolar periphery (figure 3.9C-D). This technique allowed the visualisation of on average only one CB per nuclei and as the immunocytochemistry performed at light microscopy showed nuclei contained 1-3 CBs, it was apparent that immuno-electron microscopy was not going to allow me to see all CBs, which proteins they contained, and, their relationships with other nuclear domains.

To tackle this problem, I used double labelling confocal microscopy. Pyronin Y labels RNA and as the nucleolus contains a high focal concentration of RNA it can be clearly distinguished in the nucleus, which contains a lower, more diffuse distribution of RNA. Pyronin Y can be seen in the red channel of the confocal microscope so it can be used in conjunction with the fluorescent secondary antibody FITC. I used Pyronin Y with either p80 coilin or SMN antibodies to see if the number of CBs was different depending on which CB marker was being used to visualise them and to ascertain if CBs in different localisation's (nucleolar-associated or free) have different molecular compositions (figure 3.10).

The confocal microscope allows entire nuclei to be visualised by carrying a Z-series scan. Although it was thought that many antibodies only penetrate the top one to two microns of tissue, from my confocal studies this was seen to be inaccurate. The average diameter of a murine striatal nucleus is approximately 10 μm and when a Z-series was completed antibody staining could be seen throughout the whole nucleus.

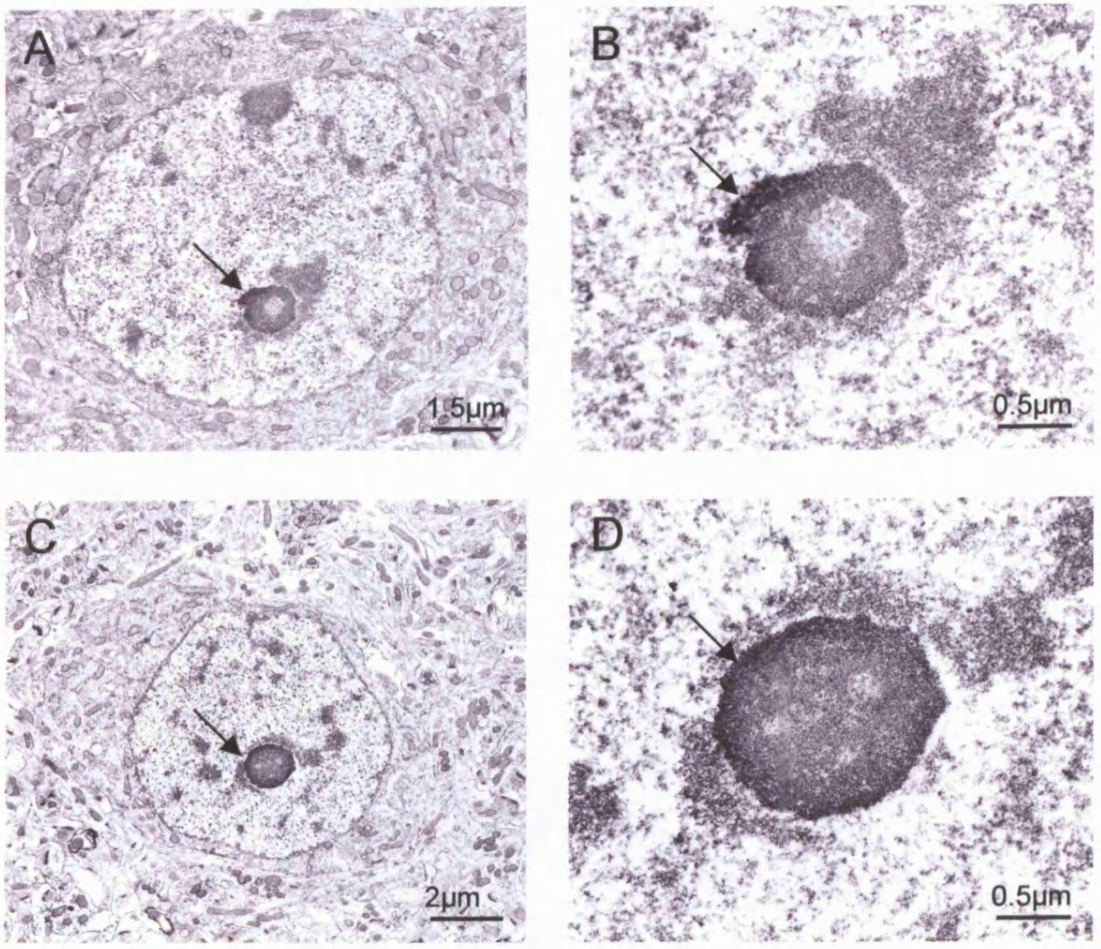

Figure 3.9

Molecular Composition of Cajal Bodies Murine Striatal Nuclei

Immuno-Electron Microscopy of Cajal bodies in 10-week-old mouse with antibodies to p80 coilin

(A and C) Low power electron micrographs of p80 coilin immunoreactivity (black arrows). (B and D) High power electron micrographs of p80 coilin immunoreactivity.

(A and B) A deposition of DAB reaction product labels a CB at the nucleolar periphery (black arrows).

(C and D) A deposition of DAB reaction product labels the periphery of the nucleolus with no visible Cajal bodies.

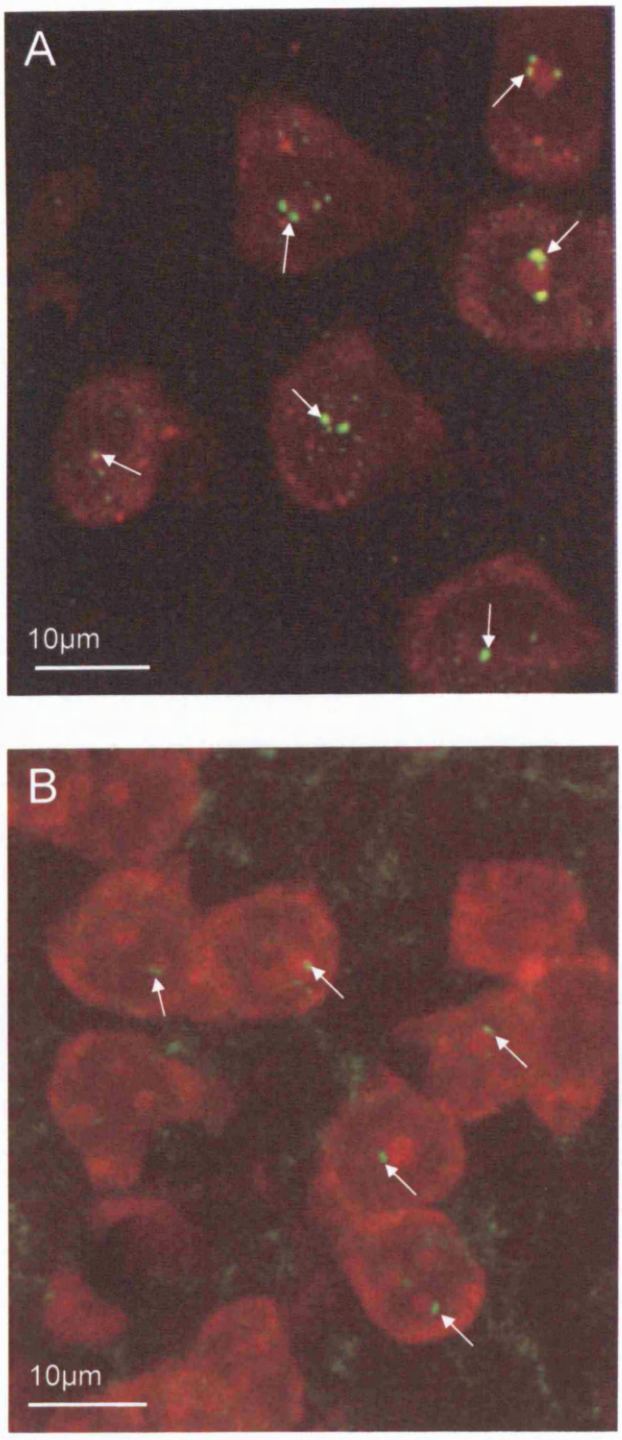

Figure 3.10
Localisation of Cajal Bodies in Murine Striatal Nuclei
Confocal Microscopy Immunofluorescence of Cajal bodies in 10-week-old mouse
(A) p80 coilin immunofluorescence (green) in conjunction pyronin Y staining (red) shows the distribution and different localisations of CBs in a Z-series stack. In most visible nuclei it is possible to see between two and four nucleolar-associated CBs (small white arrows) and the nucleolus can be seen as an accumulation of pyronin Y staining in the nucleus.
(B) SMN immunofluorescence (green) in conjunction pyronin Y staining (red) shows the distribution and different localisations of CBs in a Z-series stack. Most nuclei show one CB that is nucleolar-associated (white arrows).

Using the confocal microscope, I analysed 100 reconstructed nuclei, which contained CBs that were immunoreactive for either p80 coilin or SMN (figure 3.10A-B). Labelling with the 204.9 p80 coilin antibody coupled with a FITC labelled secondary antibody showed striatal nuclei contained between one to four CBs (table 3.2) and, like those seen using light microscopy, varied in size from approximately 0.1 μm to 0.3 μm in diameter (figure 3.10A). The average number of CBs per nucleus was 2.53+/-0.09 (graph 3.4B) and 47% of nuclei contained 2 CBs (table 3.2). When the p80 coilin antibody was substituted with SMN antibody only one to two CBs were seen per nucleus (table 3.2). 84% of nuclei contained only one SMN positive CB and the average number of CBs per nucleus was 1.16+/-0.04 (graph 3.4B).

Number of Cajal bodies	Percentage of Nuclei (%)	
	p80 coilin	SMN
1	35	84
2	47	16
3	16	0
4	2	0

Table 3.2
A table showing the percentage of nuclei that contained 1,2,3 or 4 CBs containing either p80 coilin or SMN. Chi-Square test for independence (X^2_s= 53.43; p<0.001).

The localisation of CBs was analysed in murine striatal nuclei using the same two CB protein antibodies and CBs were recorded as either nucleolar-associated or free in the nucleoplasm. Anti-p80 coilin fluorescence showed 89% of the total number of CBs were found to be nucleolar-associated and only 11% of CBs were free in the nucleoplasm (graph 3.4C). 99% CBs identified using SMN antibody were nucleolar-associated (graph 3.4C) and all of these CBs appeared to be similar in size whereas p80 coilin positive CBs varied in size. p80 coilin and SMN fluorescence staining also revealed that some nuclei contained both nucleolar-associated and free CBs. For p80 coilin CBs this occurred in 10% of the total number of nuclei analysed but for SMN CBs it was only seen in 1% of nuclei.

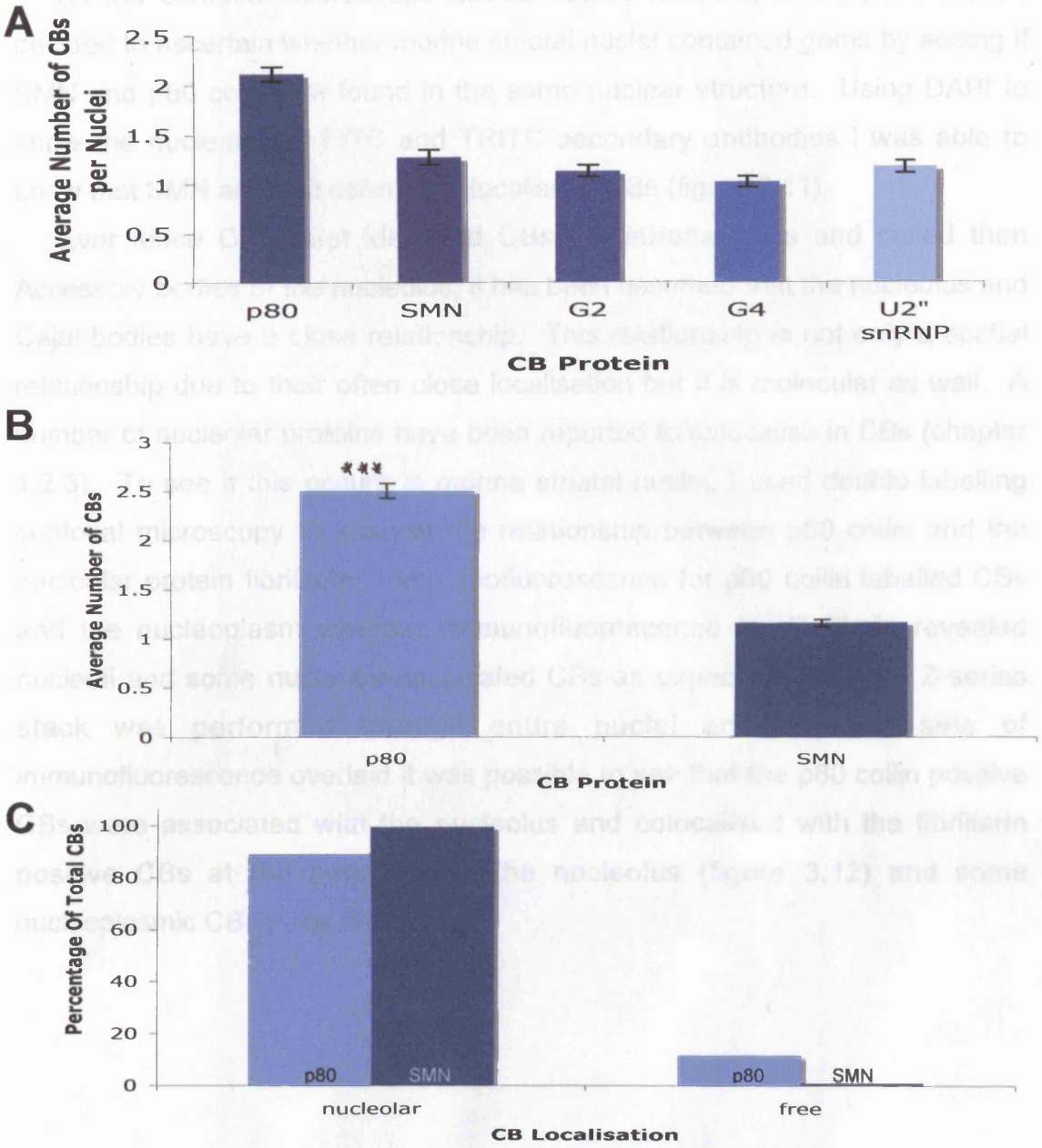

Graph 3.4

Analysis of the Molecular Composition of Cajal Bodies in Murine Striatal Nuclei

(A) A histogram showing the average number of CBs per nuclei when analysed with antibodies to different CB proteins using a light microscope in 10-week-old mouse. Apart from p80 coilin, all other CB proteins only reveal one CB per nucleus on average. Oneway ANOVA ($F = 47.63$; $p<0.001$). Error bars are standard errors of mean.

(B) A histogram showing the average number of CBs per nuclei when analysed with antibodies to either p80 coilin or SMN using a confocal microscope in 10-week-old mouse. A Z-series was performed and entire nuclei reconstructed and CBs counted. p80 coilin appears to be present in more CBs compared to SMN. Student's unpaired *t*-test ($t = 15.40$; ***$p<0.001$). Error bars are standard errors of mean.

(C) A histogram showing the percentage of CBs that are either free or nucleolar-associated seen using either antibodies to p80 coilin or SMN in 10-week-old mouse. Very few free SMN positive CBs were seen. Chi-Square test for independence ($X^2_s = 8.95$; $p<0.01$).

As the confocal microscope allows double labelling to be performed, I decided to ascertain whether murine striatal nuclei contained gems by seeing if SMN and p80 coilin are found in the same nuclear structure. Using DAPI to show the nucleus and FITC and TRITC secondary antibodies I was able to show that SMN and p80 coilin do colocalise in CBs (figure 3.11).

Ever since Cajal first identified CBs in neuronal cells and called then Accessory bodies of the nucleolus, it has been assumed that the nucleolus and Cajal bodies have a close relationship. This relationship is not only a spatial relationship due to their often close localisation but it is molecular as well. A number of nucleolar proteins have been reported to colocalise in CBs (chapter 1.2.5). To see if this occurs in murine striatal nuclei, I used double labelling confocal microscopy to analyse the relationship between p80 coilin and the nucleolar protein fibrillarin. Immunofluorescence for p80 coilin labelled CBs and the nucleoplasm whereas immunofluorescence for fibrillarin revealed nucleoli and some nucleolar-associated CBs as expected. When a Z-series stack was performed through entire nuclei and the two sets of immunofluorescence overlaid it was possible to see that the p80 coilin positive CBs were associated with the nucleolus and colocalised with the fibrillarin positive CBs at the periphery of the nucleolus (figure 3.12) and some nucleoplasmic CBs (data not shown).

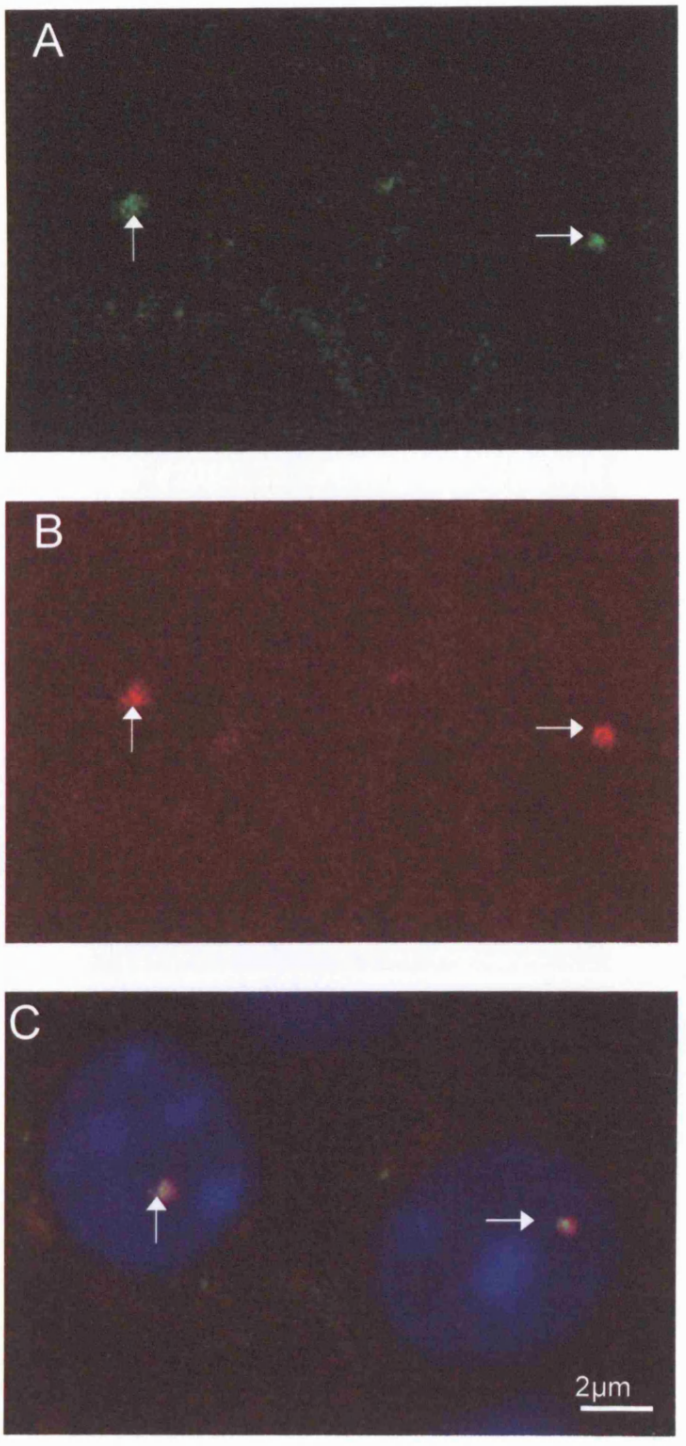

Figure 3.11
Molecular Composition of Cajal Bodies from Murine Striatal Nuclei

Confocal Microscopy Immunofluorescence of Cajal bodies

Triple labelling indirect immunofluorescence using antibodies to p80 coilin (A) and SMN (B) together with DAPI to show the nucleus (blue). The immunofluorescence for both proteins reveals one nuclear foci (white arrows) and when they are overlaid (C) it is possible to see that p80 coilin and SMN colocalise (yellow) in the same nuclear foci which is a CB (white arrow) but the colocalisation is not complete as some red is visible.

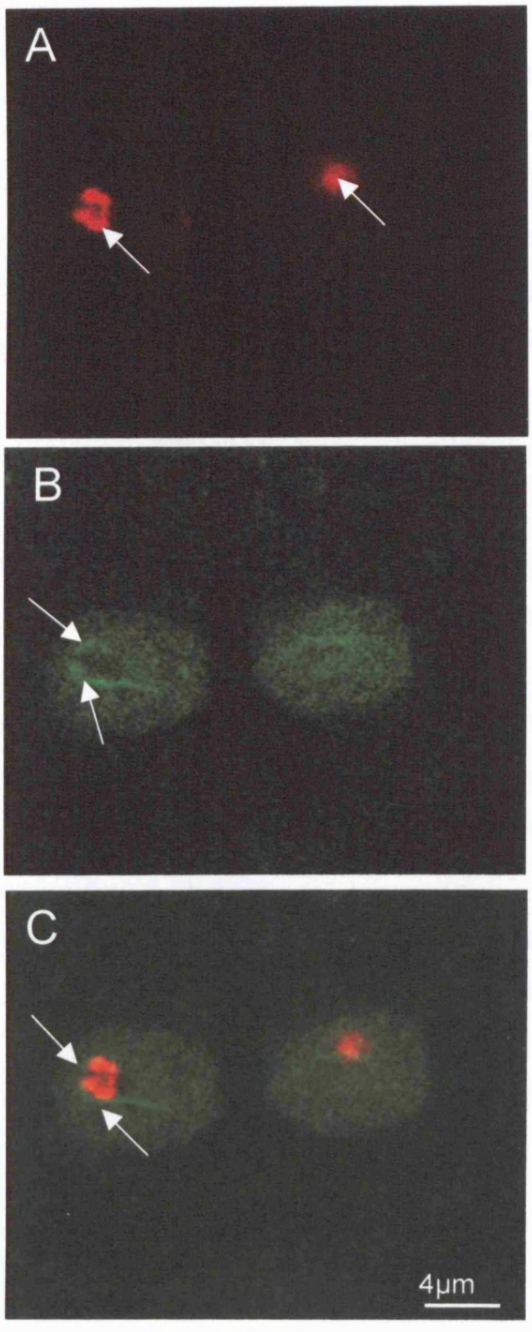

Figure 3.12
Confocal Microscopy Immunofluorescence of Cajal Bodies from Murine Striatal Nuclei
Double labelling indirect immunofluorescence using antibodies to fibrillarin (A) and p80 coilin (B).
(A) Fibrillarin immunofluorescence reveals specific, nucleolar staining that is indicated by white arrows. The immunofluorescence of fibrillarin is not solid throughout the nucleolus but appears to have an irregular, 'patchy' distribution.
(B) p80 coilin immunofluorescence reveals Cajal bodies (white arrows) and a nucleoplasmic distribution that excludes the nucleolus.
(C) The overlay of (A) and (B) shows that the CBs revealed, using a p80 coilin antibody, are nucleolar-associated CBs (white arrows) and that these CBs also contain fibrillarin (yellow).

3.2.3 Molecular Composition of the Neuronal Speckles

Many proteins that are involved in pre-messenger RNA splicing are found in speckles, I have analysed the molecular composition of speckles in striatal neurons of the mouse. A monoclonal anti-splicing factor SC35 antibody reacts with 2 non-snRNP splicing factors: SC35 and with the SC35-related factor SF2/ASF. Immunocytochemistry using this antibody labels SC35 as a speckled pattern in the nucleoplasm, excluding the nucleolus (figure 3.13A). The speckled distribution consists of numerous irregularly shaped nuclear foci that are all suggested to be interconnected. Two other proteins involved in pre-mRNA splicing, HYPA and HYPC also showed a similar speckled staining pattern (figure 3.13B). An antibody specific for 2,2,7-trimethylguanosine (m3G/TMG), which forms part of a complex with snRNPs, labels TMG as a speckled pattern occupying a portion of the nucleoplasm excluding the nucleolus (figure 3.13C).

A recently identified nuclear domain that is closely related to the speckle is the paraspeckle (Fox *et al.*, 2002) and a protein that has been shown to localise to paraspeckles is Paraspeckle Protein 1 (PSP1). To see if murine striatal nuclei have paraspeckles, double labelling immunofluorescence was performed using an antibody to PSP1 and an antibody against a protein that is localised to speckles, TMG (figure 3.14). Immunofluorescence for both antibodies showed a nuclear distribution but when the images were overlaid only a small area of co-localisation was seen and therefore striatal neuronal nuclei do contain paraspeckles.

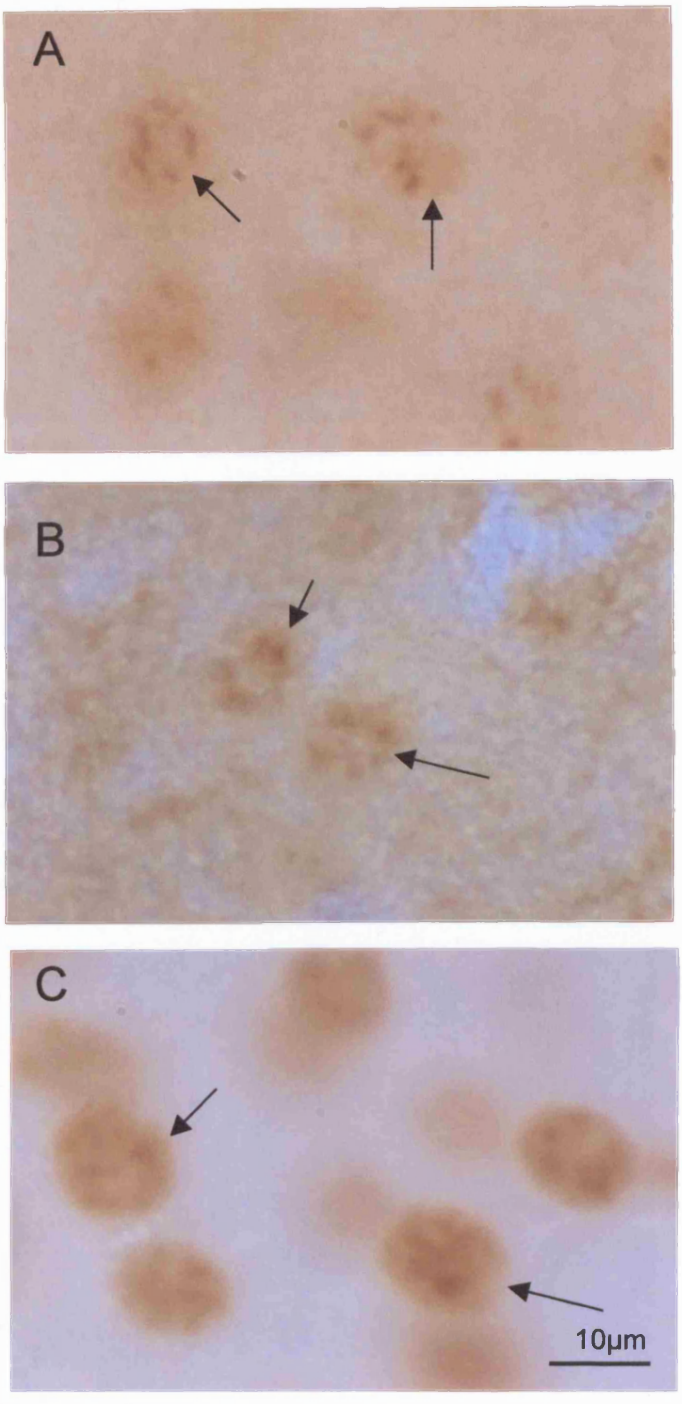

Figure 3.13
Light Microscopy Immunostaining of Speckles from Murine Striatal Nuclei

Photomicrographs showing immunoreactivity for a variety of speckle proteins in striatal neurons from 10-week-old mice. The SC35 (A), HYPA (B) and TMG (C) proteins localise in a speckled nuclear pattern and are also diffusely distributed throughout the nucleoplasm (black arrows).

3.3 Ultrastructure of R6/2 Neuronal Nucleus

In 10-week-old R6/2 transgenic mice, nuclei of striatal neurons have a round to oval shape and frequently have a prominent membrane invagination. They have a normal, dispersed distribution of chromatin with the occasional body of condensed chromatin.

3.3.1 Ultrastructure of R6/2 Neuronal Nucleolus

To study the effects of Huntington's disease (HD) on nucleolar morphology, I have analysed nucleoli of the striatal neurons in 10-week-old R6/2 transgenic mice. Nuclei containing nucleoli were randomly sampled.

From my analysis of R6/2 striatal neurons it is possible to determine that most cells are mononucleolated (87%) and occasionally binucleolated (13%). No nuclei contained more than 2 nucleoli. The mean number of nucleoli per cell is 1.13+/-0.03.

Using the previously described nucleolar classes/ultrastructures (chapter 3.1.2), it is possible to divide the R6/2 nucleoli into the same classes: closed-reticulate structure (CRS) and open-reticulate structure (ORS). However, there is also a third class that has not been reported in the wild type neuronal nucleus. I have termed this the segregating structure (SS) and it will be described below.

The CRS was seen in 37% of the cells that were examined (graph 3.5A), and it is defined as an ordered ultrastructure that reveals small fibrillar centres (FCs) surrounded by a dense material that consists of an entanglement of the dense fibrillar component (DFC) with the granular component (GC) (figure 3.15A). These nucleoli are spherical and have an average diameter of 0.84+/-0.04 μm (graph 3.5B).

The CRS nucleoli can have a perinucleolar cap (PNC) and it is an electron dense structure that lies adjacent to the nucleolus. It seems to be composed of matter that is similar in appearance to the FCs. It has an irregular shape and can be smaller or larger than the nucleolus itself. Perichromatin granules (PGs) and perichromatin fibrils (PFs) are also seen at the nucleolar periphery.

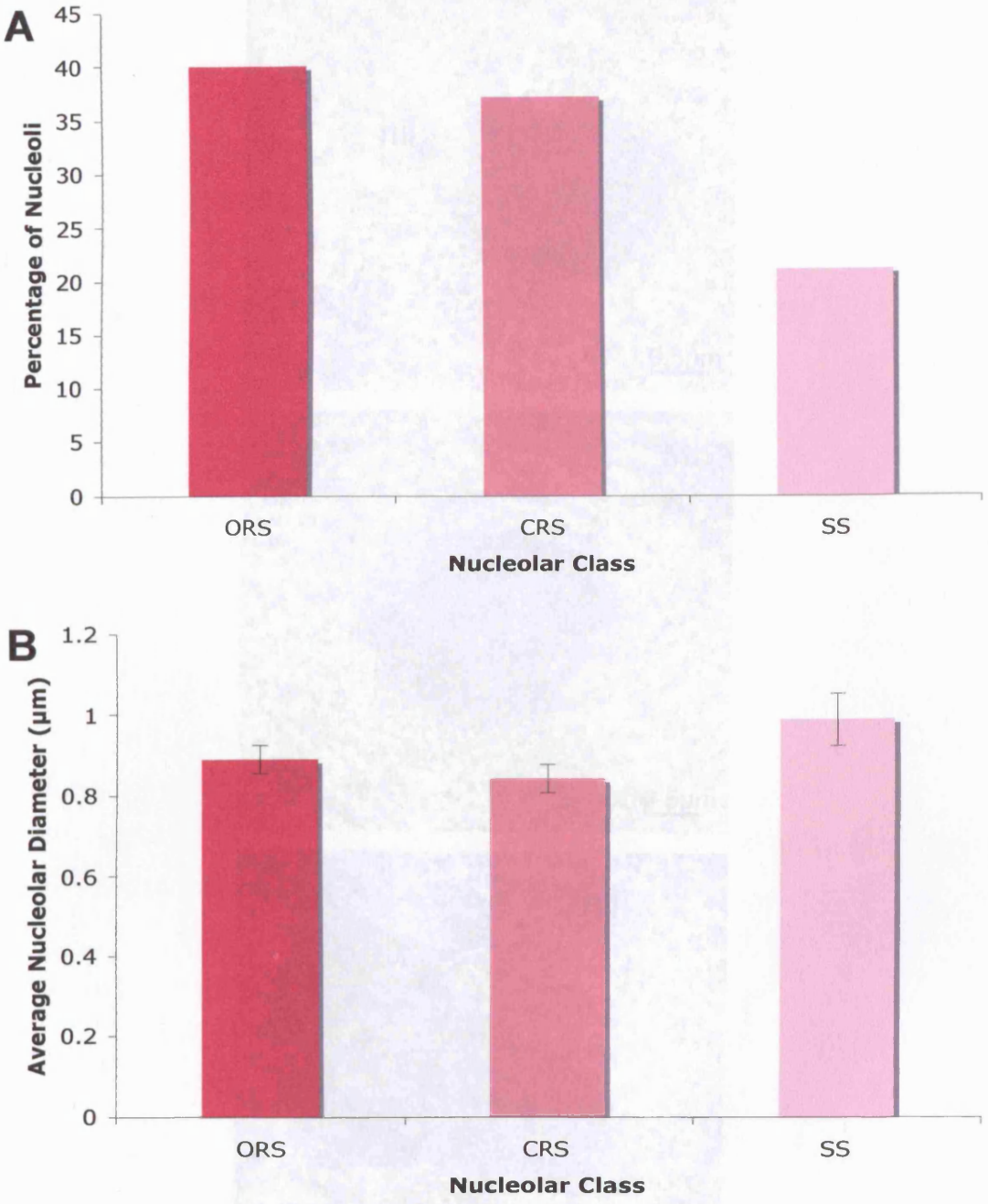

Graph 3.5

Analysis of the Class and Diameters of Nucleoli in R6/2 Striatal Nuclei

(A) A histogram showing the percentages of nucleoli that show an open-reticulate structure (ORS), a closed-reticulate structure (CRS) or a segregating structure (SS) in 10-week-old R6/2 transgenic mice. A 95% confidence interval that the probability of ORS is between 33% and 52%, for CRS is between 28% and 47%, and for SS is between 14% and 30%.

(B) A histogram showing the average diameters of ORS, CRS and SS nucleoli in 10-week-old R6/2 transgenic mice. It is possible to see that SS nucleoli have a slightly larger average diameter compared to the ORS and CRS nucleoli. Error bars are standard errors of mean.

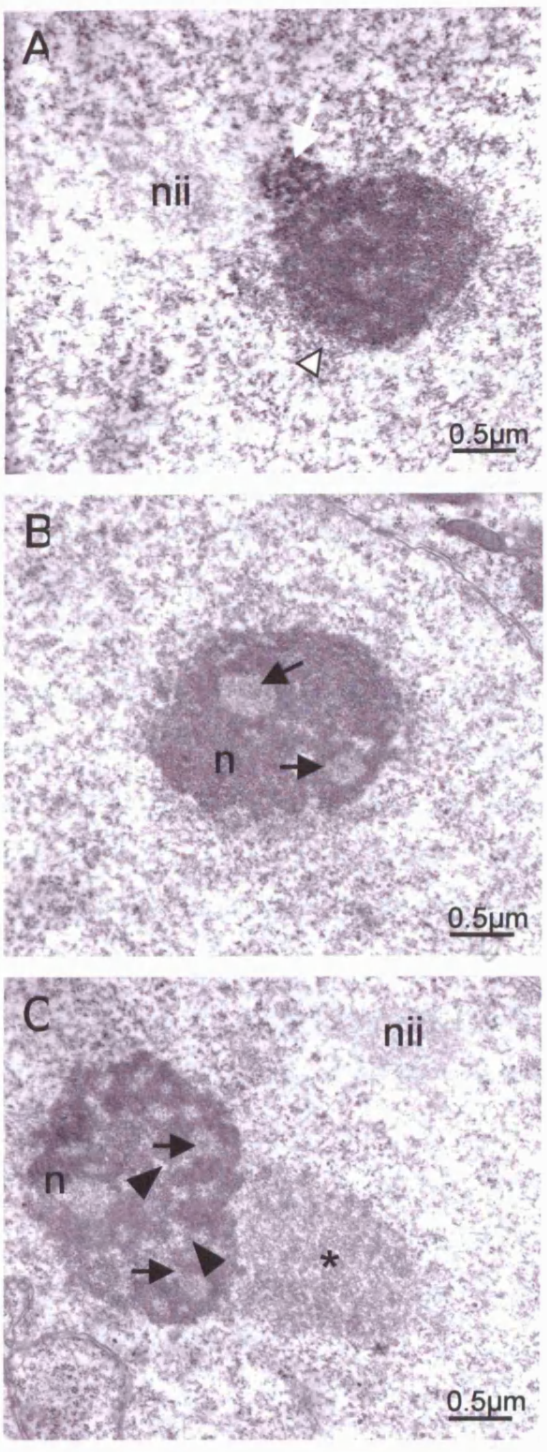

Figure 3.15

Electron micrographs of Nucleoli in R6/2 Striatal Nuclei

(A) The ultrastructure of a CRS nucleolus (n) from a striatal neuron of 10-week-old R6/2 transgenic mouse. This nucleolus has small FCs that are engulfed in a twisted mass of DFC and GC. There is a CB (white arrow) and a neuronal intranuclear inclusion (nii). It is also possible to see perichromatin granules (PGs) (white arrowhead).

(B) The ultrastructure of an ORS nucleolus (n) from a striatal neuron of 10-week-old R6/2 transgenic mouse. As in (B) large FCs are visible (black arrows) that are surrounded by the DFC/GC entanglement.

(C) The ultrastructure of a segregating structure (SS) nucleolus (n) from a striatal neuron of 10-week-old R6/2 transgenic mouse. The compact nucleolar morphology appears to be fragmenting. Medium sized FCs (black arrows) are seen and the DFC/GC seem to forming small microspheres that are segregating from each other. Due to this fragmenting intranucleoar vacuoles appear to be present (black arrowheads). A perinuceloar cap (PNC) (*) is also present together with a neuronal intranuclear inclusion (nii).

The ORS was seen in 42% of nuclei that were examined (graph 3.5A) and in this class of nucleoli, a very disordered ultrastructure can be seen (figure 3.15B). Some FCs of the ORS nucleoli are very large and can occupy a substantial portion of the nucleolar volume. Smaller FCs are seen too and both types of FCs are frequently located at the periphery of the nucleolus and not engulfed by the dense material that constitutes the rest of the ORS nucleolus. Similar to the CRS nucleoli this dense material seems to be composed of the DFC and the GC entangled together.

The ORS nucleoli can also have a PNC, PGs and PFs, all of which are similar to that described for the CRS nucleoli. The ORS nucleoli are not as spherical as the CRS nucleoli and the average diameter is 0.89+/-0.04 μm (graph 3.5B).

The third class of nucleolus, seen only in the R6/2 striatal neurons, is the segregating structure (SS). The SS nucleoli showed alterations in the organisation of nucleolar components that were not observed in either the CRS or the ORS nucleoli (figure 3.15C). A frequent change was the formation of numerous FCs that are larger than the FCs of the CRS but not as greater size as those in the ORS. The GC/DFC entanglement appears to be forming microspheres which are seen as particles surrounded by a clear halo. This causes the formation of intranucleolar vacuoles. The nucleolus appears to be segregating and fragmenting.

The SS nucleoli are seen in 21% of cells observed (graph 3.5A) and have an average diameter of 0.99+/-0.06 μm (graph 3.5B). These nucleoli have a very irregular shape and they can also have a PNC that resembles that of the CRS/ORS nucleoli as well as PGs and PFs.

3.3.2 Ultrastructure of R6/2 Neuronal Cajal Bodies

As part of the study on the effects of HD on the neuronal nuclear ultrastructure, I decided to examine the morphology and distribution of Cajal bodies in R6/2 transgenic mouse at 10 weeks of age. At the ultrastructural level only 28% of striatal neurons examined contained a distinct CB. The basic

morphology of the CBs in R6/2 nuclei was the same as that seen in the normal murine neuronal nuclei. Most CBs were of round to oval in shape and were composed of coiled strands of fibrillar material surrounded by a low-density amorphous matrix. Many CBs also had tiny fibrils radiating from their periphery into the nucleoplasm.

On examining the spatial relationship between the CBs in the R6/2 neurons and other nuclear domains a striking discovery was made. The CBs frequently occurred in association with the nucleolus (31%) or free in the nucleoplasm (23%) but most were seen in close proximity to the neuronal intranuclear inclusion (NII) (46%) (graph 3.6A). There were no morphological differences between the CBs in any localisation (figure 3.16). The average diameter of the nucleolar-associated, nucleoplasmic and NII-associated CBs were 0.24+/-0.03 μm, 0.28+/-0.03 μm and 0.36+/-0.02 μm respectively (graph 3.6B).

The nucleolar-associated CBs are seen to protrude from the nucleolar periphery and are in direct continuity with the nucleolus. In some cases the NII-associated CBs are seen to be in direct contact with the NII periphery or the tiny fibrils radiating from the CB are touching the NII. Infrequently, it was possible to see a CB in close proximity to the nucleolus and a NII.

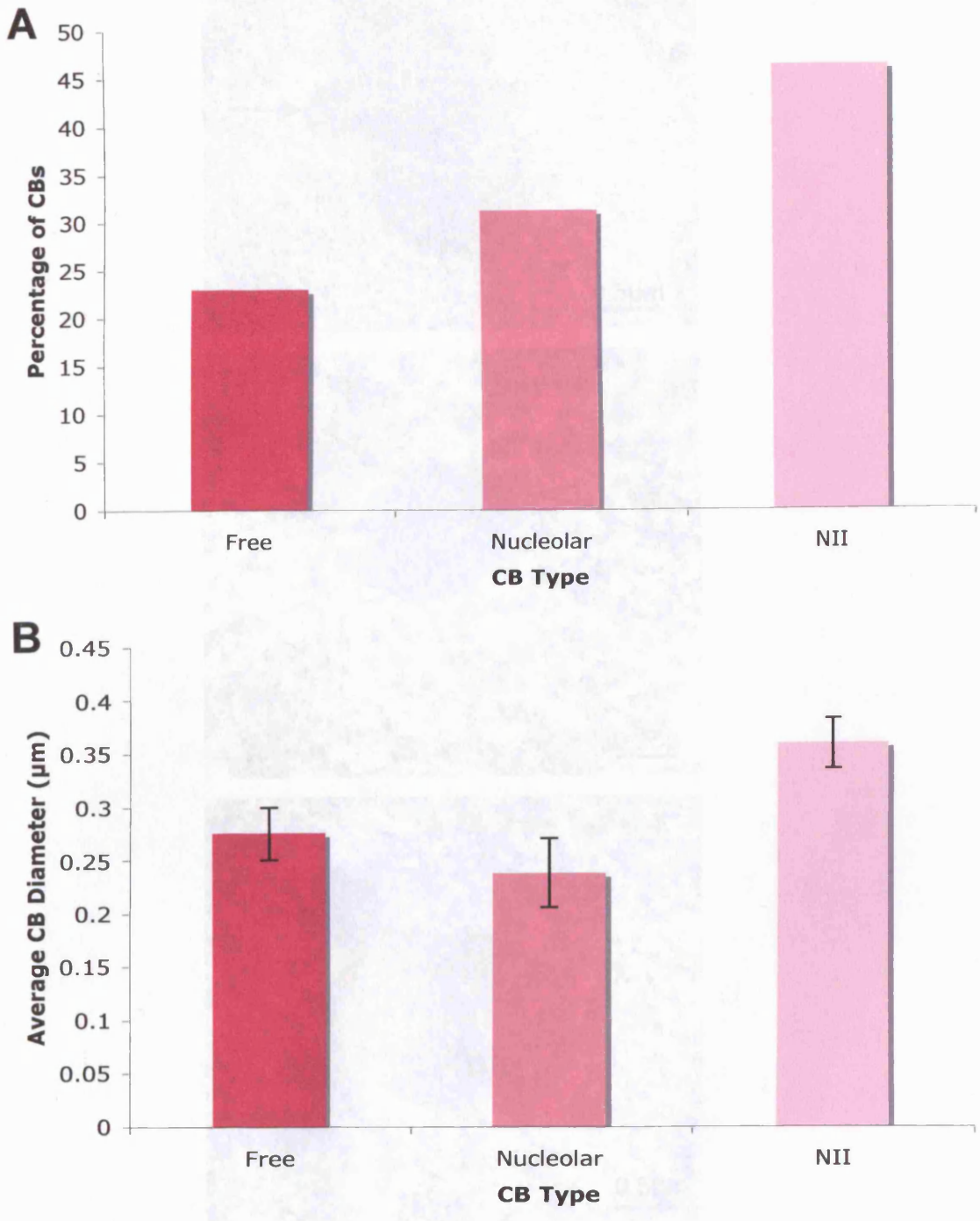

Graph 3.6

Analysis of Cajal Bodies in R6/2 Striatal Nuclei

(A) A histogram showing the percentages of CBs that are free in the nucleoplasm, nucleolar-associated or NII-associated in 10-week-old R6/2 transgenic mice. Nearly half the CBs are NII-associated in the R6/2 striatal neurons. A 95% confidence interval that the probability of nucleolar CBs is between 23% and 41%, for free CBs is between 16% and 32%, and for NII CBs is between 37% and 56%.

(B) A histogram showing the average diameters of free, nucleolar-associated or NII-associated CBs in 10-week-old R6/2 transgenic mice. The NII-associated CBs appear to have greater average diameters compared to those of the free or nucleolar-associated CBs. Oneway ANOVA ($F = 5.94$; $p<0.01$). Error bars are standard errors of mean.

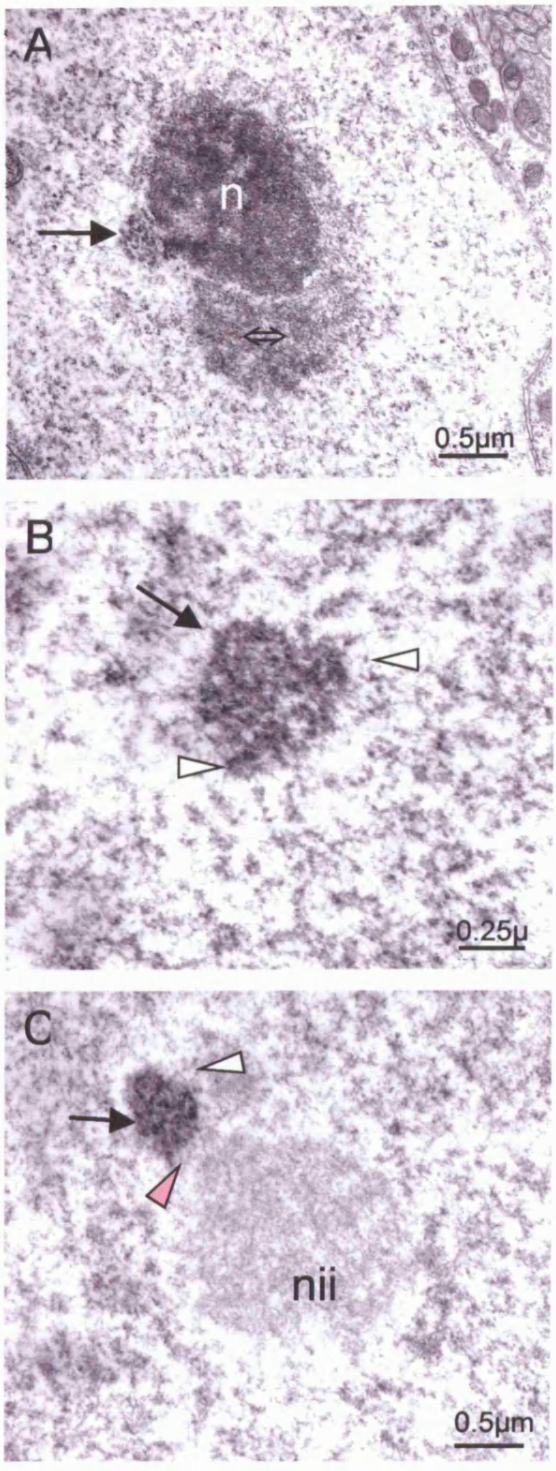

Figure 3.16
Electron micrographs of Cajal Bodies from R6/2 Striatal Neurons
(A) The ultrastructure of a nucleolar-associated CB (black arrow) from a striatal neuron from 10-week-old R6/2 transgenic mouse. The CB is in direct contact with the nucleolar periphery. The CB is composed of dense coiled threads embedded in a less dense matrix. The nucleolus (n) has a SS morphology and has a perinucleolar cap (PNC) (⇔).
(B) The fine structure of a free, nucleoplasmic CB (black arrow) in a striatal neuron from 10-week-old R6/2 transgenic mouse. The CB is composed of dense coiled threads that are embedded in an amorphous matrix. It is possible to see small fibres radiating from the edge of the CB (white arrowheads). The CB does not have any spatial relationship with other nuclear domains.
(C) The ultrastructure of a NII-associated CB (black arrow) from a striatal neuron from 10-week-old R6/2 transgenic mouse. The CB is in direct contact with a NII (nii) and has the characteristic CB morphology. Small radiating fibres can be seen around the CB (white arrowhead) together with fibres that appear to be connecting the CB to the NII (pink arrowhead).

3.3.3 Ultrastructure of R6/2 Neuronal Speckles

I have analysed the morphology of speckles in 10-week-old R6/2 transgenic mice. Speckles are the nuclear domains where pre-mRNA splicing factors are localised and are composed of interchromatin granule clusters (IGCs) and perichromatin fibrils (PFs) at the ultrastructural level. Due to the irregular shape of the IGCs, which constitute the major part of speckles, it has not been possible to quantify the speckles in the R6/2 transgenic mouse. It is possible to identify them and distinguish the numerous granules that are interconnected via thin fibrils, which are the PFs (figure 3.17).

3.3.4 Ultrastructure of R6/2 Neuronal NII

In 10-week-old R6/2 transgenic mice neuronal intranuclear inclusion (NII) can be seen in the nucleus of striatal neurons. NIIS are round structures that are easily distinguishable from the surrounding chromatin. They are pale in appearance and composed of fine granular material (figure 3.15A & 3.16C). Occasionally, NIIs may have fibrous elements, but these are relatively rare. NIIs are approximately 1.5 to 2 μm in diameter.

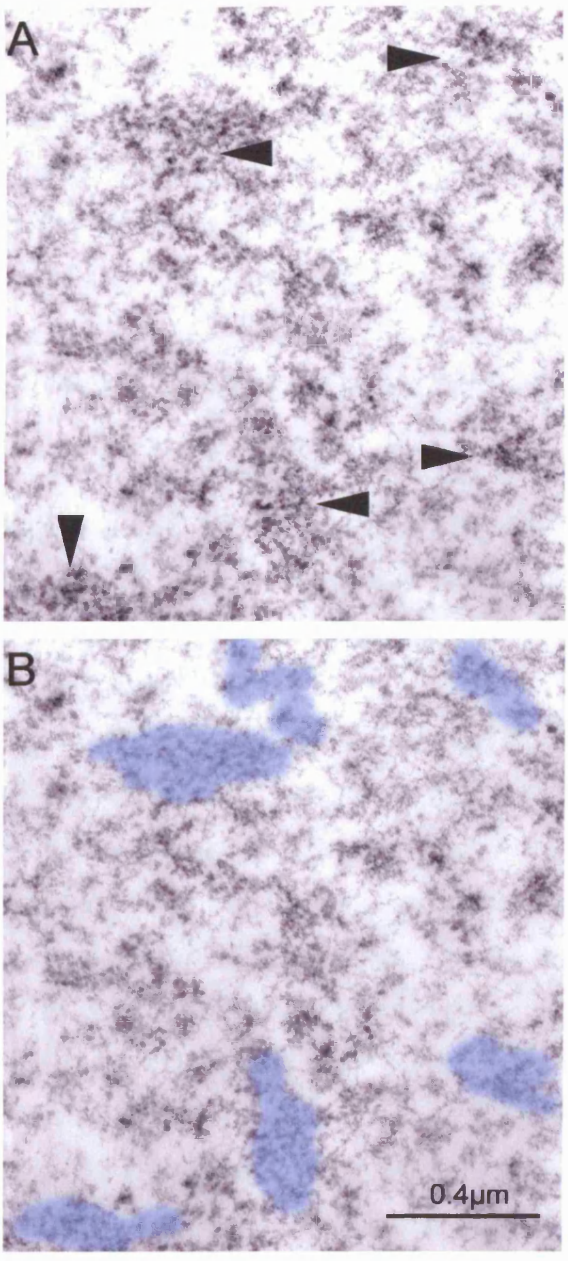

Figure 3.17
Electron micrographs of Speckles from R6/2 Striatal Neurons
(A) The fine structure of speckles (black arrowheads) in a striatal neuron from 10-week-old R6/2 transgenic mouse. The speckles are composed of perichromatin fibrils (PFs) and interchromatin granule clusters (IGCs). IGCs represent the main part of speckles and comprise of granules that appear to be connected with fibres.
(B) Same image as (A) but the IGCs have been highlighted in pale blue.

3.4 Molecular Composition of R6/2 Neuronal Nucleus

In these studies I have attempted to analyse the molecular organisation of the R6/2 transgenic mouse neuronal nucleus using the same antisera that was used to examine the murine neuronal nucleus. I wished to determine if there were any changes in the subnuclear localisation of proteins found within the nucleus due to HD.

3.4.1 Molecular Composition of R6/2 Neuronal Nucleolus

As described previously the nucleolus has been shown to contain three structurally distinct regions: the fibrillar centres, the dense fibrillar and the granular components (figure 3.5). To see if any changes occur in the distribution of nucleolar proteins in HD, a number of nucleolar markers were examined using immunocytochemistry.

Fibrillarin is one nucleolar protein that is used as a marker of the dense fibrillar component of the nucleolus. In the nuclei of R6/2 striatal neurons fibrillarin immunoreactivity was localised to the nucleolus (figure 3.18A). No nucleoplasmic staining was seen but intense, spherical nucleoli were visible together with nucleolar-associated Cajal bodies. It was also possible to see free Cajal bodies labelled with fibrillarin immunoreactivity.

The nucleolar protein, Nopp140, has been reported to be localised in the dense fibrillar component of the nucleolus and in the R6/2 striatal nuclei, an antibody against Nopp140 revealed nucleoplasmic and nucleolar staining (figure 3.18C). At high magnification this nucleolar immunoreactivity could be seen as a ring at the nucleolar periphery with a pale centre. Nucleolar-associated Cajal bodies could be seen as very distinct structures adjoining the nucleolus while free Cajal bodies were also visible.

C23 (nucleolin) is another nucleolar protein and it is usually located in the granular component. An antibody against C23 showed pale nucleoplasmic immunoreactivity and nucleolar staining (figure 3.18B). At high magnification, staining of the nucleolus appears to be only a subtle ring at the nucleolar periphery and infrequent free CBs. B23 (nucleophosim) is also reported to localise to the granular component of the nucleolus but when I used an antibody

to this protein no immunoreactivity could be seen in the R6/2 transgenic mouse.

A nucleolar protein that is used as a marker for fibrillar centres is upstream binding factor (UBF). Unfortunately the UBF antibody revealed no staining in the R6/2 transgenic mouse. RNA polymerase I is also localised to fibrillar centres and when I used an antibody against this protein a heterogeneous nucleoplasmic staining was seen (figure 3.18E).

An essential enzyme that mediates a variety of chromosome activities is DNA topoisomerase II (topo II) and it has been shown to localise in the nucleolus (Zini *et al.*, 1994). In the nuclei of R6/2 striatal neurons, an antibody against topo II shows nucleoplasmic labelling as well as staining the nucleolus (figure 3.18D). The immunoreactivity is a rim at the edge of the nucleolus and adjoining nucleolar-associated Cajal bodies. No free Cajal bodies were seen.

I analysed 100 nuclei to establish the average number of nucleoli per nuclei. In R6/2 striatal nuclei the average numbers seen were as follows fibrillarin 1.14+/-0.04, Nopp140 1.20+/-0.04 and C23 1.27+/-0.04 (graph 3.7A). The antibody from Abcam against fibrillarin showed that 86% of nuclei contained one nucleolus and only 14% contained two nucleoli. Similar results were seen with Nopp140 and C23 (graph 3.7B).

As I had discovered that the chaperone Hsc70 was localised to the nucleolar periphery in nuclei of murine striatal neurons using immuno-EM (chapter 3.2.1), I decided to look at the localisation of this protein in the R6/2 striatal nuclei. Using pre-embedding immunogold electron microscopy it was possible to see that Hsc70 did not localise to the periphery of the nucleolus in the R6/2 transgenic mice. Instead Hsc70 colocalised with the NII (figure 3.19).

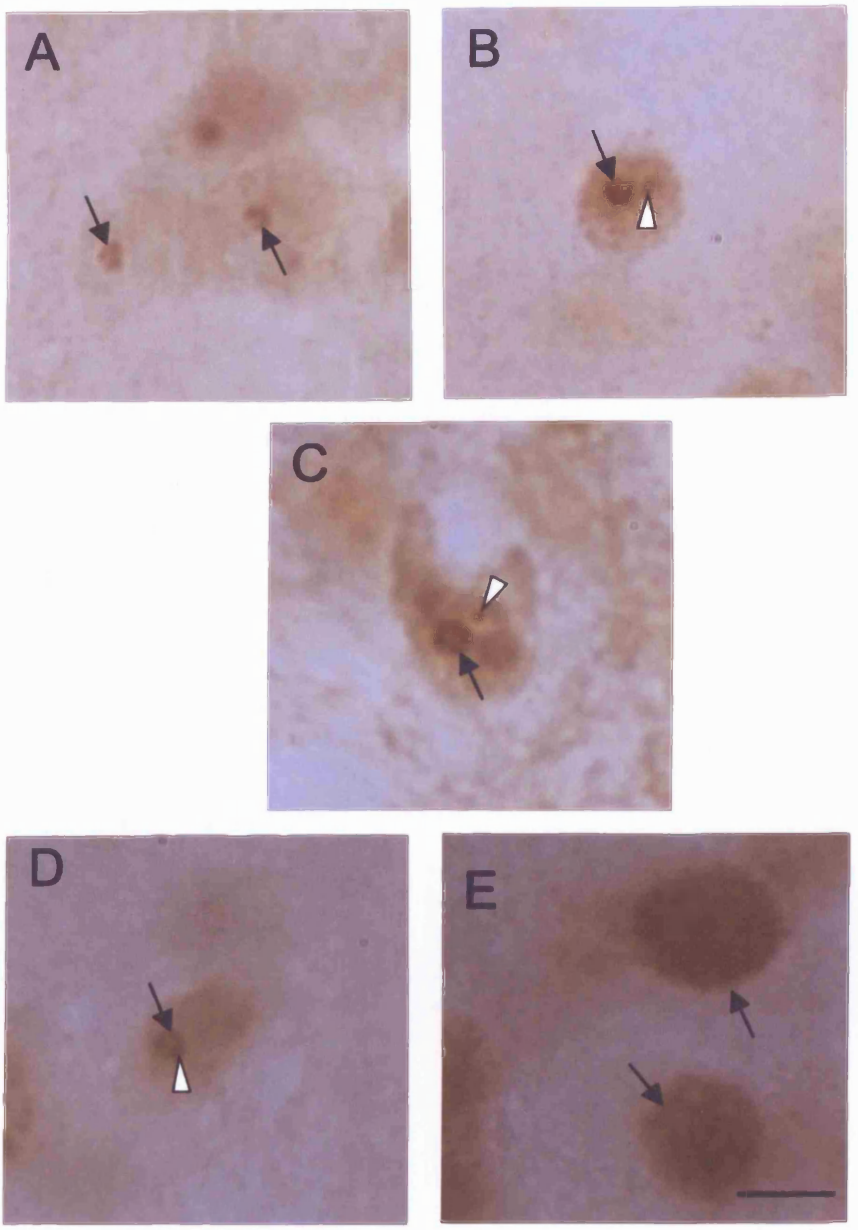

Figure 3.18
Molecular Composition of Nucleoli from R6/2 Striatal Neurons
Photomicrographs showing immunoreactivity for a variety of nucleolar proteins in striatal neurons from 10-week-old R6/2 mouse. The fibrillarin (A), C23 (B), Nopp140 (C), Topo II (D) and RNA polymerase I (E) immunoreactive nucleoli are indicated with arrows. Fibrillarin immunoreactivity (A) using Abcam antibody shows intense nucleolar staining (black arrows). C23 (B) immunoreactivity reveals nucleolar staining as spherical nuclear foci (black arrow). Nucleoplasmic staining can also be seen together with a free CB (white arrowhead). Nopp140 (C) immunoreactivity shows a pale nucleoplasmic stain together with nucleolar staining (black arrow). The nucleolar staining appears as a spherical structure that has a pale centre and a more intense peripheral ring. It is also possible to distinguish free CB (white arrowhead). Topo II (D) immunoreactivity shows a pale nucleoplasmic stain together with nucleolar staining (black arrow). The nucleolar staining appears as a spherical structure that has a pale centre and a more intense peripheral ring. It is also possible to distinguish nucleolar-associated CB (white arrowhead). RNA polymerase I (E) immunoreactivity reveals heterogeneous nucleoplasmic staining.
Scale bar = 10 μm

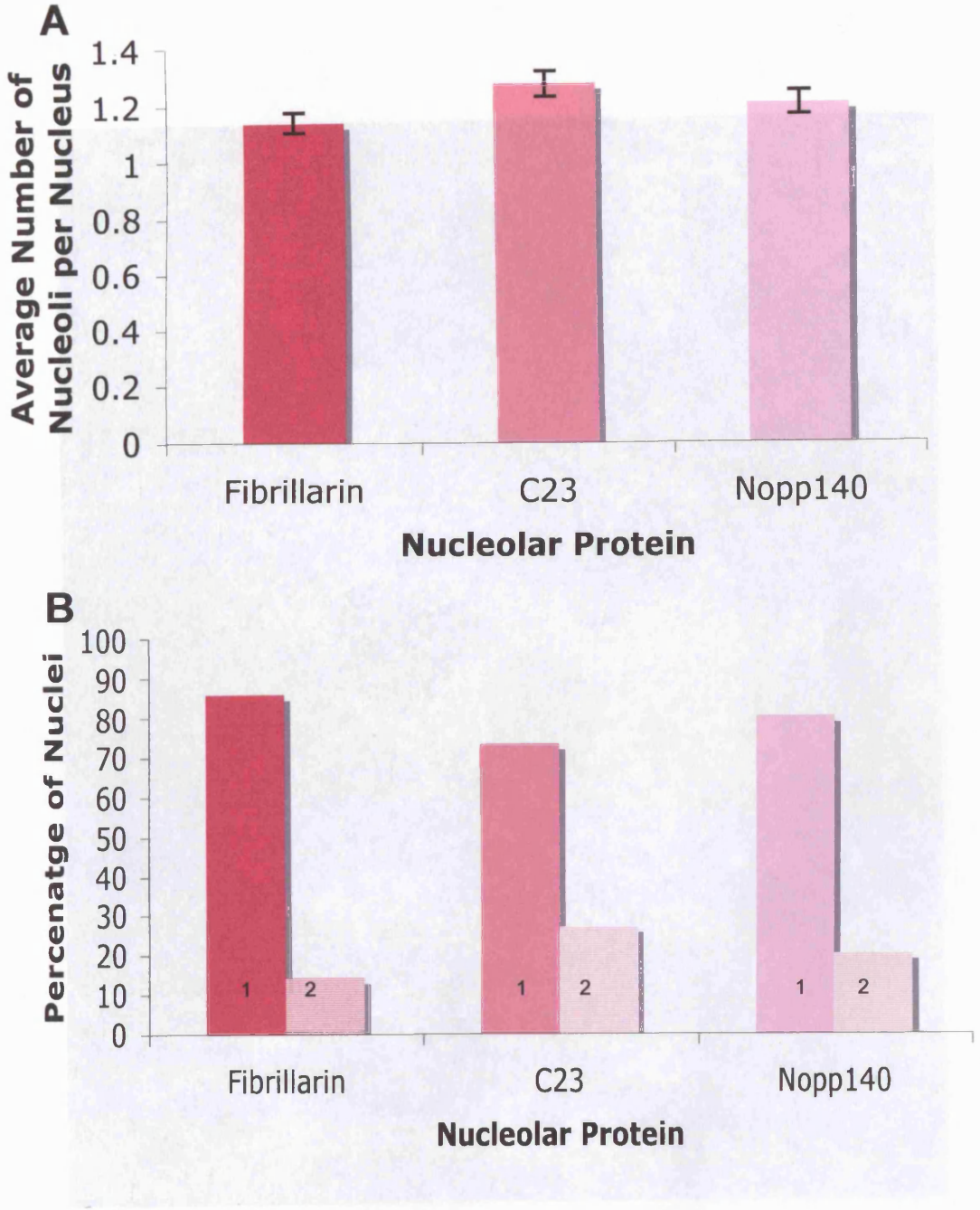

Graph 3.7

Analysis of the Molecular Composition of Nucleoli in R6/2 Striatal Nuclei

(A) A histogram showing the average number of nucleoli per nuclei when analysed with antibodies to three different nucleolar proteins in 10 week old R6/2 transgenic mouse. Error bars are standard errors of mean.

(B) A histogram showing the percentage of nuclei that contained either one or two nucleoli when quantified with antibodies to three different nucleolar proteins in 10 week old R6/2 transgenic mouse. Most nuclei when analysed with any of the three proteins have only one nucleolus.

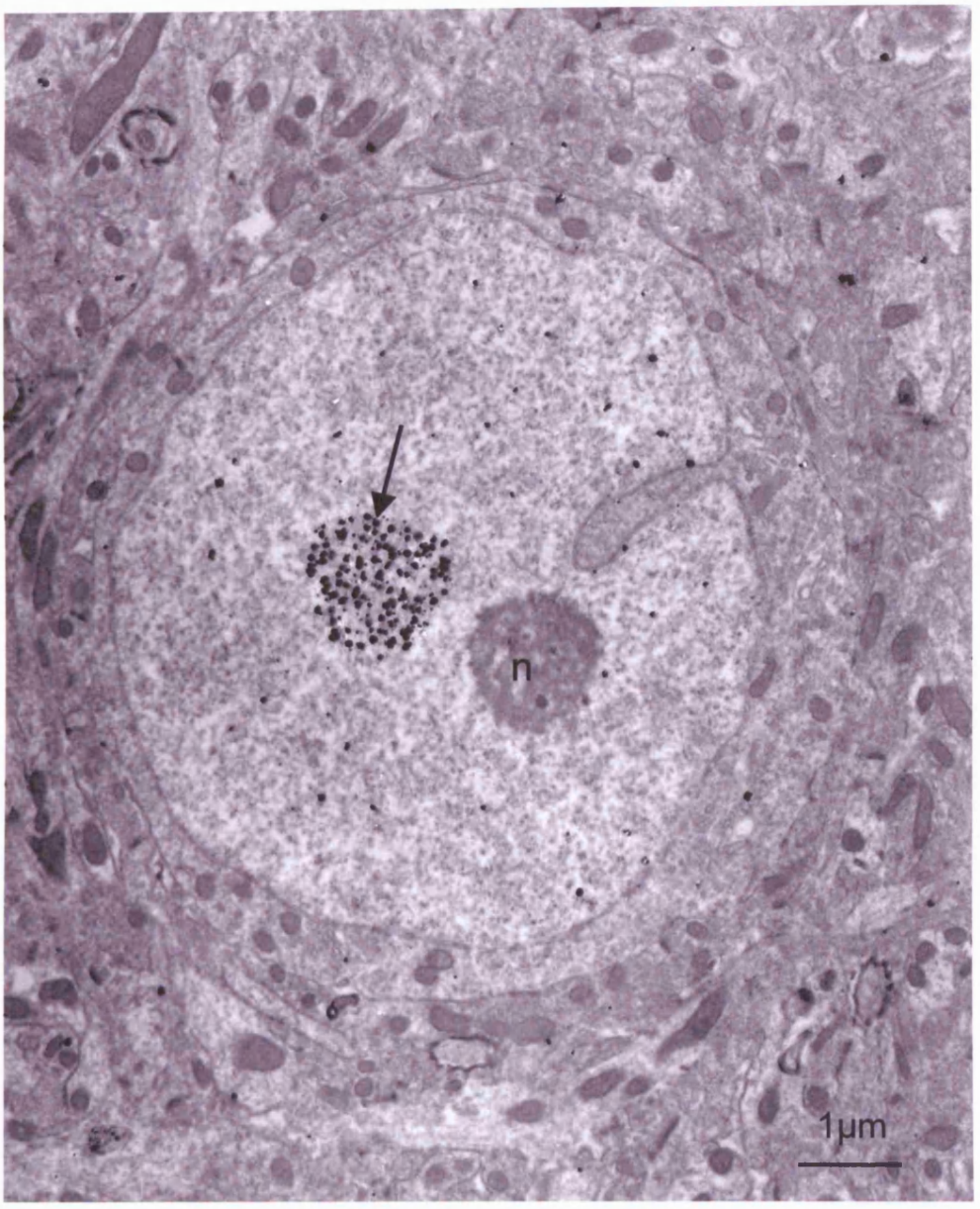

Figure 3.19
Distribution of Hsc70 in R6/2 Striatal Neurons
Electron micrograph of Hsc70 immunoreactivity in striatal neurons from a 10-week-old R6/2 transgenic mouse. Pre-embedding immuno-gold reveals that Hsc70 is localised NII (black arrow) and not the nucleolus (n).

3.4.2 Molecular Composition of R6/2 Neuronal Cajal Body

Immunocytochemical studies were carried out, using antibodies to the same Cajal body proteins in R6/2 mouse striatum that were used to analyse the wild type mouse striatum, at different ages to see if any changes in distribution were seen due to HD. To determine the average number of CBs stained positively for a given antibody, the number of CBs seen within 100 nuclei were counted. These counts were carried out at 4, 10 and 12 weeks of age in the R6/2 mouse (table 3.3).

Cajal body protein	4 weeks of age	10 weeks of age	12 weeks of age
p80 coilin	2.54+/-0.09	1.16+/-0.05	1.13+/-0.04
U2" snRNP	0.91+/-0.04	0.85+/-0.04	0.84+/-0.04
SMN	0.99+/-0.04	0.96+/-0.04	0.96+/-0.04
Gemin2	0.87+/-0.04	0.78+/-0.04	0.94+/-0.05

Table 3.3
A table showing the average number of CBs per nucleus in R6/2 neurons for a number of different CB proteins at different ages.

At 4 weeks of age the antibody against p80 coilin revealed a diffuse nucleoplasmic staining pattern with 1 to 4 CBs, of different sizes, labelled and the average number of CBs per nucleus was 2.54+/-0.09. At 10 and 12 weeks of age, there was a decrease in the number of CBs seen to contain p80 coilin. The nucleoplasmic stain was still seen but generally only one large CB was present (figure 3.20A). The average number of CBs fell to 1.16+/-0.05 for 10 weeks of age and 1.13+/-0.04 for 12 weeks of age.

An antibody against U2" snRNP (small nuclear ribonucleoprotein particles) revealed generally one CB per nucleus (figure 3.20E) and this staining pattern that did not change over the time period studied (0.91+/-0.03, 0.85+/-0.04, 0.84+/-0.04 at 4, 10, 12 weeks of age respectively). SMN, the survival of motor neuron protein, was seen in CBs as well as having a cytoplasmic and diffuse nuclear distribution (figure 3.20B). The mean number of CBs containing SMN

did not significantly change over the time period with the averages being 0.99+/-0.04, 0.96+/-0.04 and 0.96+/-0.04 for 4, 10 and 12 weeks respectively. Gemin2 and Gemin4 showed a very similar distribution as SMN: localised to CBs, the cytoplasm and the nucleoplasm (figure 3.20C-D). For Gemin2 there was no significant change in the average number of CBs from 4 to 12 weeks (0.87+/-0.04, 0.78+/-0.04, 0.94+/-0.05 at 4, 10, 12 weeks of age respectively). Graph 3.8A shows that in the R6/2 transgenic mouse at 10 weeks of age, all Cajal body proteins were generally only found to reveal one CB per nucleus.

Antibodies against other proteins that have been previously shown to localise in CBs were also used to see where they were distributed in murine striatal nuclei. Cleavage and polyadenylation specificity factor (CPSF) is involved in mRNA polyadenylation and splicing of single-intron pre-mRNAs. It has been previously reported in CBs or gems (Hofmann *et al.*, 2002). Profilin is involved in the regulation of actin polymerisation and suggested to be found in CBs (Giesemann *et al.*, 1999; Skare *et al.*, 2003). Poly(A) polymerase (PAP) is involved in the polyadenylation of 3' prime ends of mRNA (Schul *et al.*, 1996). Ewing's sarcoma (EWS) is a RNA binding protein and has been shown to interact with SMN (Young *et al.*, 2003). SmB is one of the core proteins that are found in all major snRNPs, which form the major component of the spliceosome. Gemin3 forms part of the SMN complex (Campbell *et al.*, 2000). Immunoreactivity for all of these proteins did not show any labelling of Cajal bodies in the R6/2 transgenic mouse striatum apart from Gemin3 which was seen to infrequently localise to CBs (data not shown).

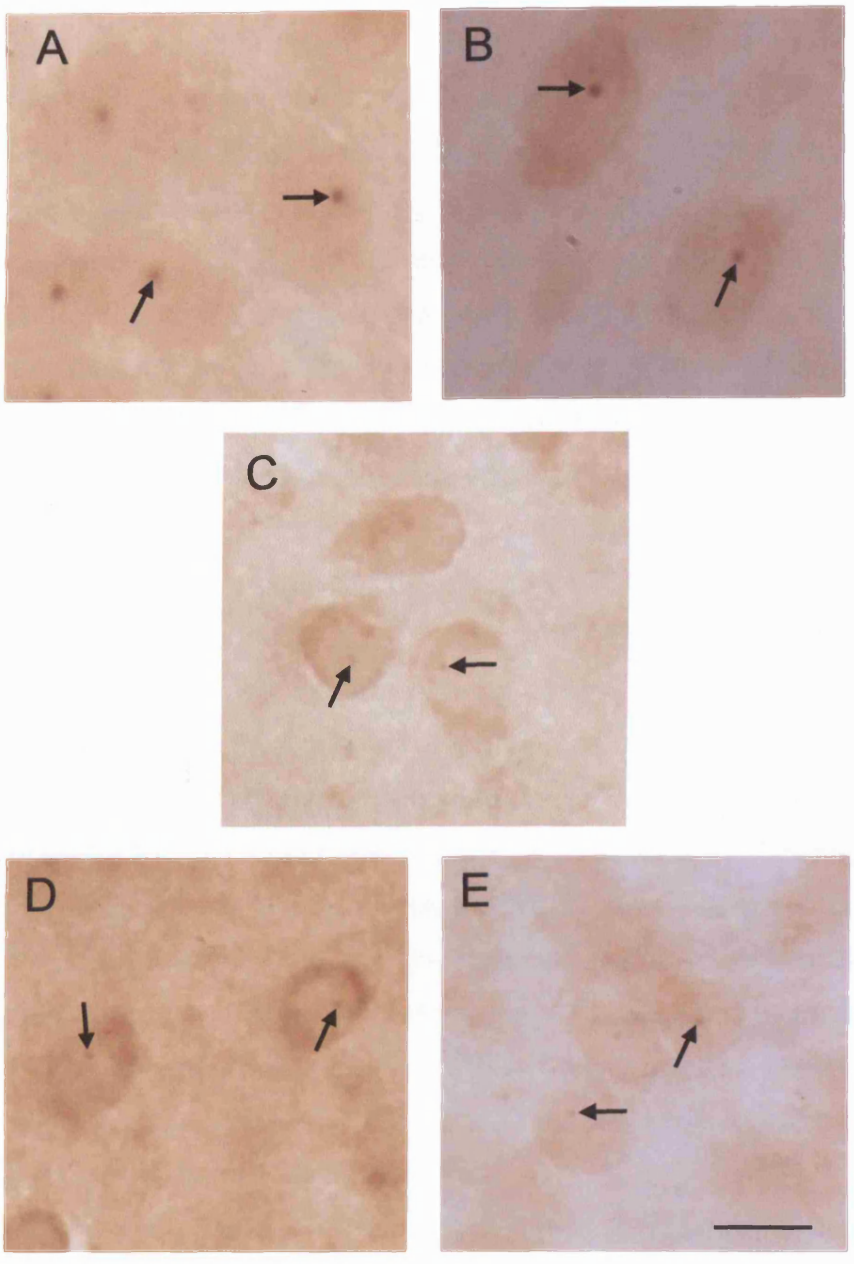

Figure 3.20
Light Microscopy Immunostaining of Cajal Bodies from R6/2 Striatal Nuclei
Photomicrographs showing immunoreactivity for a variety of Cajal body proteins in striatal neurons of 10-week-old R6/2 mice. The p80 coilin (A), SMN (B), Gemin2 (C), Gemin4 (D) and U2 snRNP (E) immunoreactive CBs are indicated by black arrows and a diffuse nucleoplasmic stain can also be seen. Immunoreactivity for all CB proteins reveal only one CB per nucleus. Scale bar = 10 μm.

The results from the light microscopy study showed that the Cajal body proteins studied did localise to CBs in the R6/2 striatal neurons but no information about which type of CB (nucleolar-associated, free or NII-associated) contained which CB protein could be ascertained. Pre-embedding immuno-electron microscopy with DAB was carried out on 10-week-old R6/2 mice using antibodies for some of the CB proteins. Although staining was achieved (figure 3.21A-B), the same problems that were met in the normal study occurred: when using the TEM only one CB was seen in most of the 70 nm ultrathin sections and from the light microscopy study it is clear that some antibodies stain more than one CB. Immuno-electron microscopy could therefore not help to reveal all possible types of CB containing each of the CB proteins in one nucleus.

Confocal microscopy was undertaken to identify different nuclear proteins within different nuclear domains. By using DAPI to reveal the nucleus together with a CB protein antibody and an antibody against huntingtin (htt) to show the NII, it was possible to see one large CB containing either p80 coilin or U2" snRNP (figure 3.21C-D) that was associated with the NII. However, it was still not possible to see where the nucleolus was in relation to the CB and the NII.

Pyronin Y is known to label RNA and therefore is a good substance to identify the nucleolus as it has a high RNA content. Pyronin Y can be seen in the red channel of the confocal microscope so it can be used in conjunction with the fluorescent secondary antibody FITC. I performed a Z-series scan on striatal nuclei from 10-week-old R6/2 mouse that had been labelled with Pyronin Y and either p80 coilin or SMN antibodies.

I analysed 100 reconstructed nuclei that contained CBs that were immunoreactive for either p80 coilin or SMN (figure 3.22). The 204.9 p80 coilin antibody coupled with a FITC secondary antibody showed that R6/2 striatal nuclei generally contained between 1 or 2 CBs per nucleus (table 3.4) and infrequently nuclei with 3 or 4 CBs were seen. The average number of CBs per nucleus was 1.53+/-0.07 (graph 3.8B) and 60% of nuclei contained only one CB (table 3.4). When p80 coilin antibody was replaced with the SMN antibody on most occasions only one CB was seen per nucleus (table 3.4). 93% of nuclei contained only one SMN positive CB and the average number of CBs per nucleus was 1.07+/-0.03 (graph 3.8B).

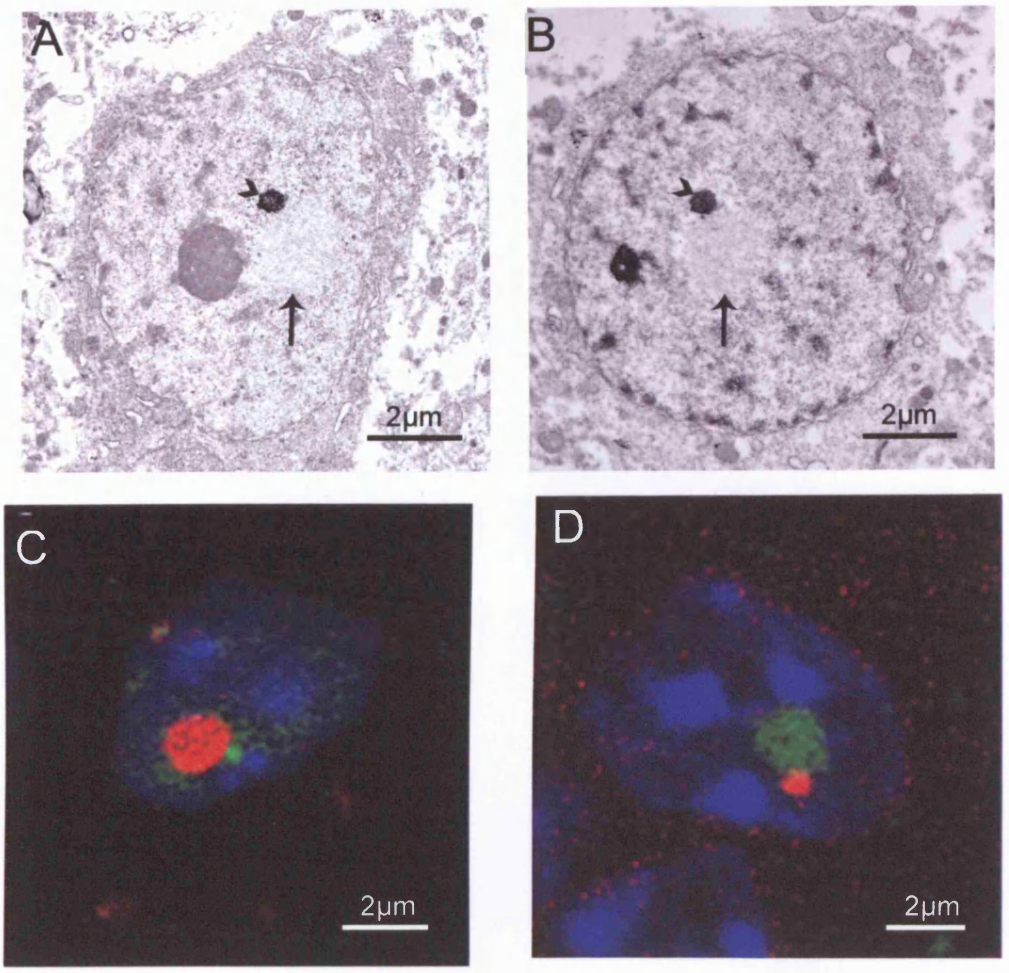

Figure 3.21

Molecular Composition of Cajal Bodies R6/2 Striatal Nuclei

Immuno-Electron Microscopy of Cajal bodies in 10-week-old R6/2 transgenic mouse.

A discrete deposition of DAB reaction product labels a CB with antibodies to p80 coilin (A) and U2" snRNP (B) (black arrowheads). A single stained nuclear foci is seen with both antibodies. NII can also be seen (black arrows).

Confocal Microscopy Immunofluorescence of Cajal bodies in 10-week-old R6/2 transgenic mouse

Triple labelling indirect immunofluorescence using antibodies to U2" snRNP (C) and SMN (D) together with an antibody to huntingtin (htt) to reveal the NII and DAPI to show the nucleus.

(C) U2" snRNP immunofluorescence (green) with htt immunofluorescence (red) and DAPI (blue). The SMN protein is localised in a CB (green) that is associated with a NII (red).

(D) SMN immunofluorescence (red) in conjunction htt immunofluorescence (green) and DAPI (blue) shows a NII-associated CB (red) that contains the protein SMN and a NII (green).

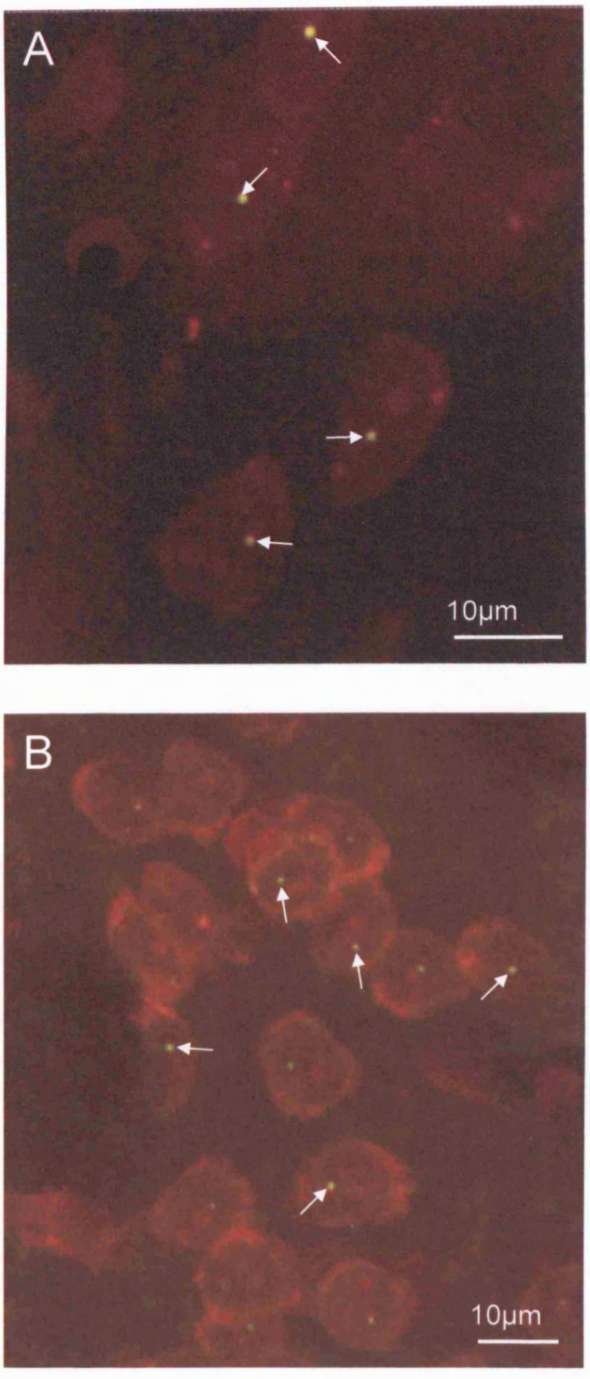

Figure 3.22
Localisation of Cajal Bodies from R6/2 Striatal Nuclei
Confocal Microscopy Immunofluorescence of Cajal bodies in 10-week-old R6/2 transgenic mouse
(A) p80 coilin immunofluorescence (yellow) in conjunction with pyronin Y staining (red) shows the distribution and different localisations of CBs in a Z-series stack. In most visible nuclei it is possible to see one prominent free CB (small white arrows) that is not associated with nucleolus. The nucleolus can be seen as a spherical accumulation of pyronin Y staining in the nucleus.
(B) SMN immunofluorescence (green) in conjunction pyronin Y staining (red) shows the distribution and different localisations of CBs in a Z-series stack. Most nuclei show one CB that is free in the nucleoplasm (white arrows).

Number of Cajal bodies	Percentage of Nuclei (%)	
	p80 coilin	SMN
1	60	97
2	29	7
3	10	0
4	1	0

Table 3.4
A table showing the percentage of R6/2 nuclei that contained 1,2,3 or 4 CBs containing either p80 coilin or SMN. Chi-Square test for independence (X^2_s= 31.56; p<0.001).

The localisation of the p80 coilin or SMN positive CBs in the reconstructed nuclei was also analysed. Of the total number of p80 coilin positive CBs, 56% were seen to be nucleolar-associated and 44% were free in the nucleoplasm (graph 3.8C). 48% of the CBs identified using the SMN antibody were nucleolar-associated and 52% were free in the nucleoplasm (graph 3.8C). The immunofluorescence using either p80 coilin or SMN antibody showed that some nuclei in the R6/2 striatum contained both nucleolar-associated and free CBs. For p80 coilin-positive CBs, this occurred in 28% of the total number of nuclei analysed, but for SMN-positive CBs, it was only seen in 2% of nuclei.

To see if the percentage of free CBs seen to contain either p80 coilin or SMN were actually NII-associated CBs, triple labelling immunofluorescence was carried out. Pyronin Y was used together with a huntingtin (htt) antibody coupled with a FITC secondary antibody and a p80 coilin antibody coupled with a Cy5 secondary antibody (figure 3.23). The Cy5 secondary antibody bleached very rapidly and only 10 nuclei could be reconstructed. 7 of the nuclei contained NII-associated CBs that were p80 coilin positive and 3 nuclei contained CBs that were associated with the nucleolus.

To confirm that p80 coilin and SMN proteins were found in the same CBs, in the R6/2 transgenic mouse striatum, triple labelling immunofluorescence was carried out using DAPI, to reveal the nucleus together with p80 coilin antibody coupled with a TRITC secondary antibody and SMN antibody coupled with a FITC secondary antibody (figure 3.24). It was possible to see that the CB proteins colocalised in the same CB.

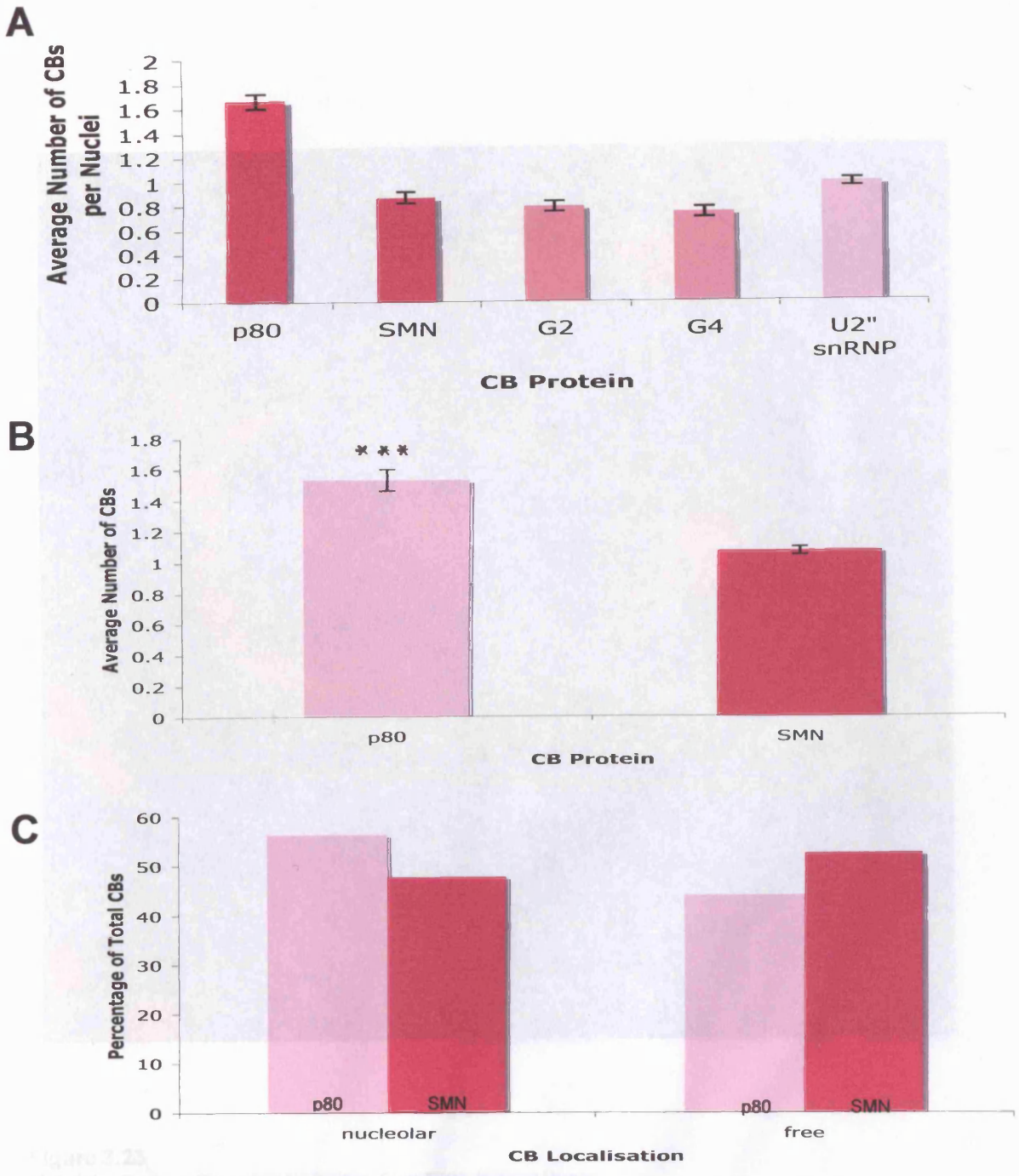

Graph 3.8

Analysis of the Molecular Composition of Cajal Bodies in R6/2 Striatal Nuclei

(A) A histogram showing the average number of CBs per nuclei when analysed with antibodies to different CB proteins using a light microscope in 10-week-old R6/2 transgenic mouse. Apart from p80 coilin, all other CB proteins only reveal one CB per nucleus on average. Oneway ANOVA ($F = 68.53$; $p<0.001$). Error bars are standard errors of mean.

(B) A histogram showing the average number of CBs per nuclei when analysed with antibodies to either p80 coilin or SMN using a confocal microscope in 10 week old R6/2 transgenic mouse. A Z series was performed and entire nuclei reconstructed and CBs counted. p80 coilin appears to be present in more CBs compared to SMN. Student's unpaired *t*-test ($t = 6.04$; ***$p<0.001$). Error bars are standard errors of mean.

(C) A histogram showing the percentage of CBs that are either free or nucleolar-associated seen using either antibodies to p80 coilin or SMN in 10-week-old R6/2 transgenic mouse.

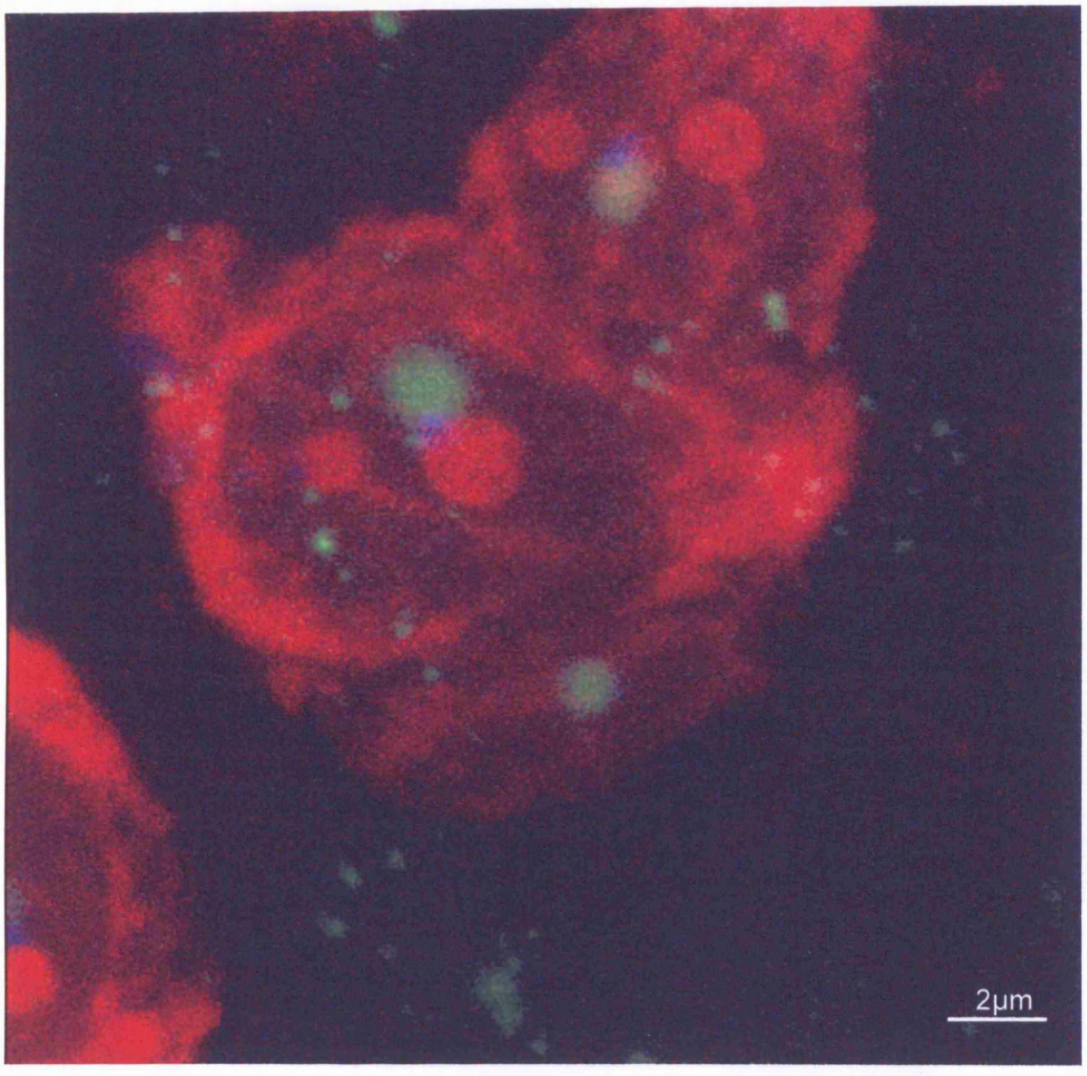

Figure 3.23
Molecular Composition of Cajal Bodies from R6/2 Striatal Nuclei
Confocal Microscopy Immunofluorescence of Cajal bodies
Triple labelling indirect immunofluorescence using antibodies to p80 coilin (blue), huntingtin (green) and pyronin Y staining (red). From the Z-series stack it is possible to see that a CB (blue) is associated with the NII (green). The CB is also in very close proximity to the nucleolus (red).

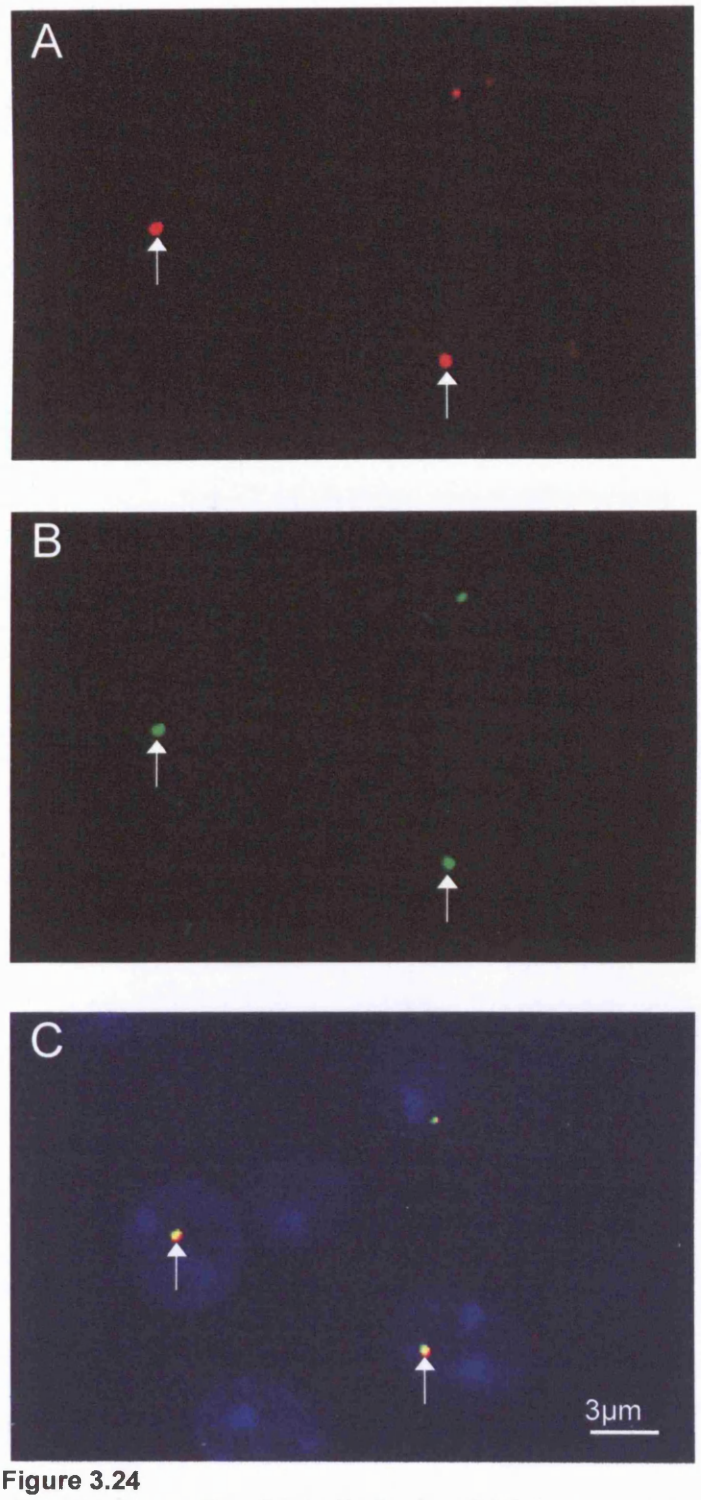

Figure 3.24
Molecular Composition of Cajal Bodies from R6/2 Striatal Nuclei
Confocal Microscopy Immunofluorescence of Cajal bodies
Triple labelling indirect immunofluorescence using antibodies to p80 coilin (A) and SMN (B) together with DAPI to show the nucleus (blue). The immunofluorescence for both proteins reveals one nuclear foci (white arrows) and when they are overlaid (C) it is possible to see that p80 coilin and SMN colocalise (yellow) in the same nuclear foci which is a CB (white arrow) but the colocalisation is not complete as some red is visible.

The localisation of Gemin3 was also analysed using confocal microscopy. When Gemin3 was used in conjunction was pyronin Y and a Z-series scan performed, immunofluorescence revealed that Gemin3 localised to nucleolar-associated CBs and not nucleoplasmic CBs (figure 3.25).

From my earlier analysis of the molecular composition of the R6/2 neuronal nucleolus, it was seen that some nucleolar proteins not only localised to the nucleolus but could also be seen in CBs, both nucleolar-associated and free. I performed double labelling immunofluorescence to see if the nucleolar protein positive CBs at either localisation (nucleolar or free) colocalised with the p80 coilin positive CBs. p80 coilin immunofluorescence revealed CBs (figure 3.26A) that were either nucleolar-associated or free in the nucleoplasm while the immunofluorescence for fibrillarin showed one large nuclear foci, which corresponded to the nucleolus, and smaller nuclear foci (figure 3.26B). When these images were viewed together it was clear that the smaller foci seen with the fibrillarin immunofluorescence were also labelled with the p80 coilin immunofluorescence (figure 3.26C). The smaller foci corresponded to CBs, which could be free or nucleolar-associated. Therefore, the free p80 coilin positive CBs also contain fibrillarin.

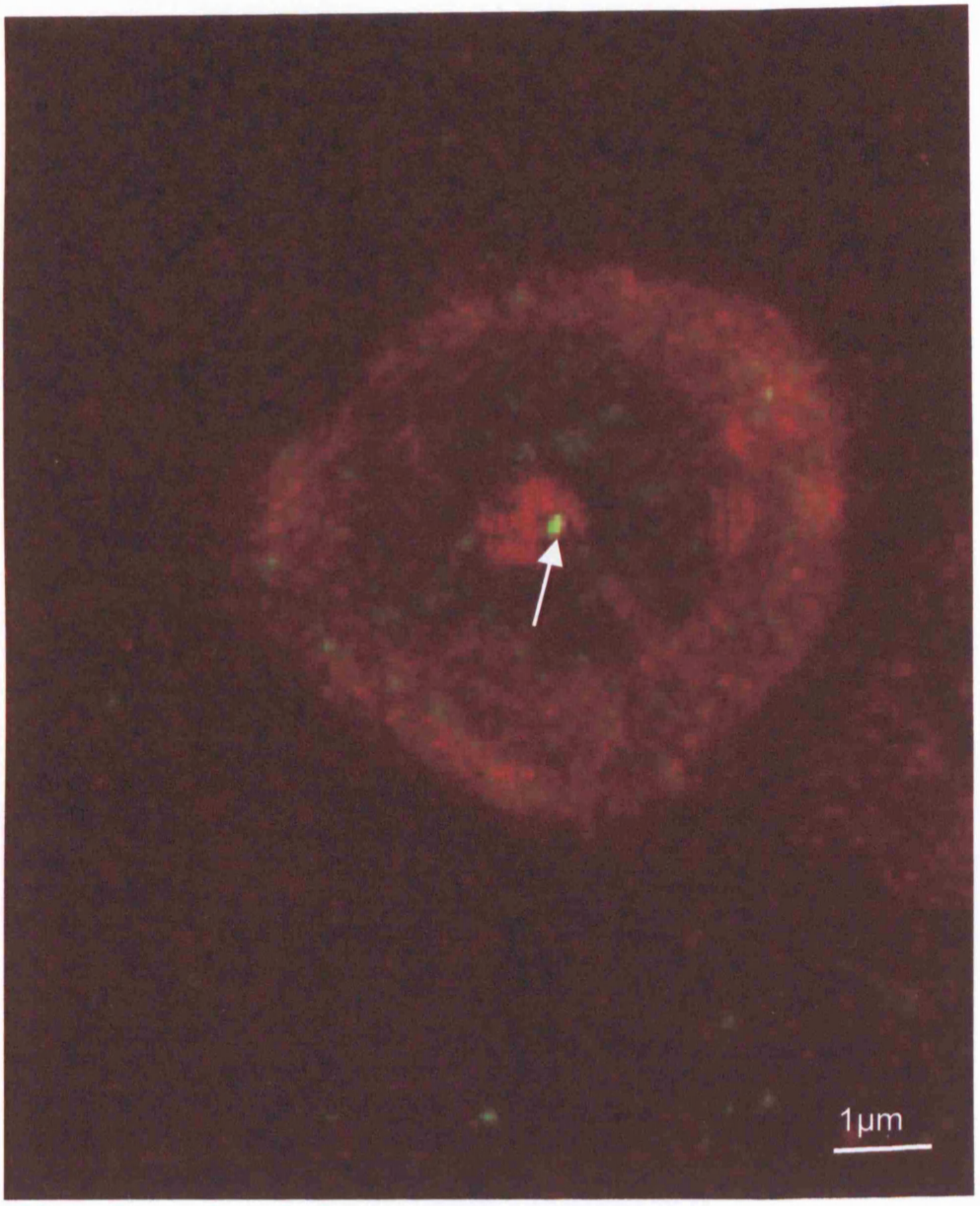

Figure 3.25
Molecular Composition of Cajal Bodies from R6/2 Striatal Nuclei
Confocal Microscopy Immunofluorescence of Cajal bodies
Gemin3 immunofluorescence (green) in conjunction with pyronin Y staining (red). in this nucleus it is possible to see one prominent nucleolar-associated CB (white arrow). The nucleolus can be seen as a spherical accumulation of pyronin Y staining in the nucleus.

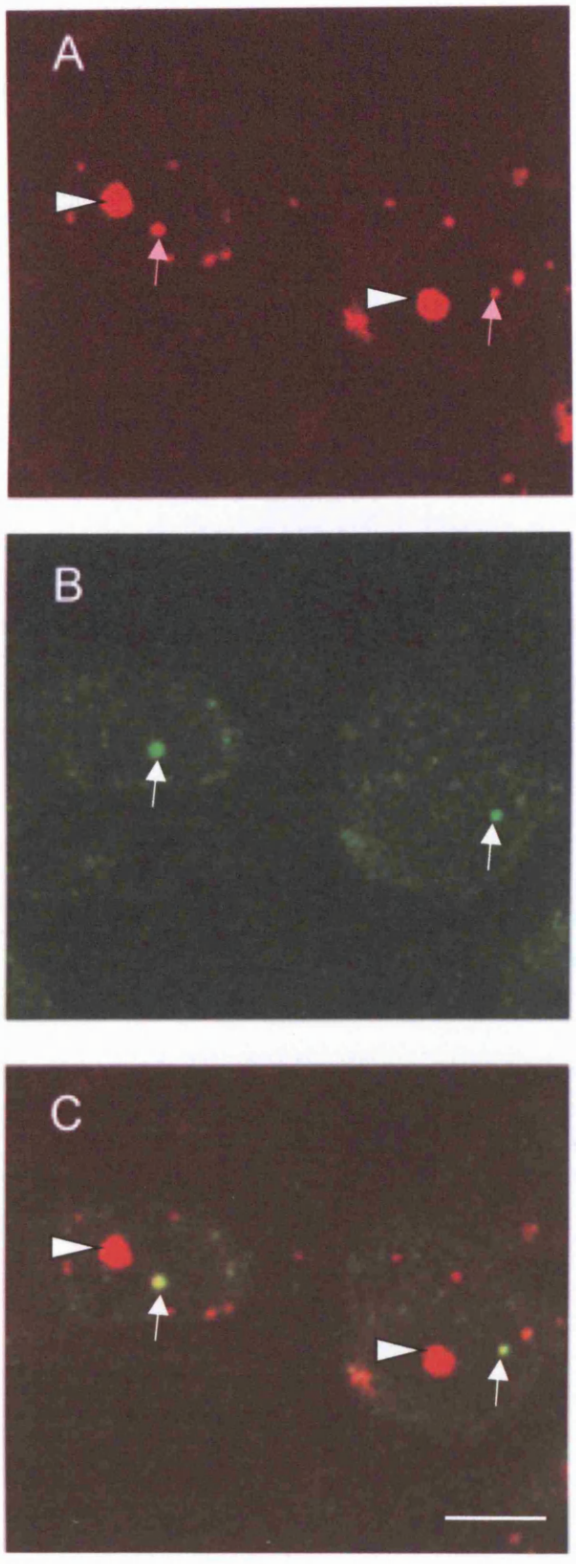

Figure 3.26
Confocal Microscopy Immunofluorescence of Cajal Bodies R6/2 Striatal Nuclei
Double labelling indirect immunofluorescence using antibodies to fibrillarin (A) and p80 coilin (B). (A) Fibrillarin immunofluorescence reveals that the protein is found in nucleoli (white arrowheads) and nuclear foci (pink arrows).
(B) p80 coilin immunofluorescence shows the protein to be in one discrete CB (white arrows).
(C) When both proteins are viewed together it is possible to see that fibrillarin and p80 coilin colocalise in a free CB (white arrows). No colocalisation of the two proteins is seen in the nucleolus (white arrowhead). Scale bar = 5μm

3.4.3 Molecular Composition of R6/2 Neuronal Speckles

I have analysed the molecular composition of speckles in striatal neurons of the R6/2 transgenic mouse. Many proteins that are involved in pre-messenger RNA splicing accumulate in speckles. Immunocytochemistry using the monoclonal antibody against splicing factor SC35 did not show the usual 'speckled' pattern of staining, instead, a diffuse nucleoplasmic pattern was seen (figure 3.27A). When the staining pattern of 2 other proteins involved in pre-mRNA splicing, HYPA and HYPC, were examined, they revealed infrequent speckle staining with many nuclei only exhibiting a nucleoplasmic pattern (figure 3.27B). An antibody specific for 2,2,7-trimethylguanosine (m3G/TMG), which forms part of a complex with snRNPs, shows TMG to have a speckled pattern occupying a portion of the nucleoplasm excluding the nucleolus (figure 3.27C). The speckled distribution consists of numerous irregularly shaped nuclear foci that are suggested to be interconnected.

The paraspeckle is a recently identified nuclear domain that is closely related to the speckle (Fox *et al.*, 2002) and Paraspeckle Protein 1 (PSP1) is a protein that has been shown to localise to paraspeckles. To see if R6/2 striatal nuclei have paraspeckles, double labelling immunofluorescence was performed using an antibody to PSP1 and an antibody against a protein that is localised to speckles, TMG (figure 3.28). Immunofluorescence for both antibodies showed a nuclear distribution but when the images were overlaid only a small area of co-localisation was seen and therefore striatal neuronal nuclei do contain paraspeckles.

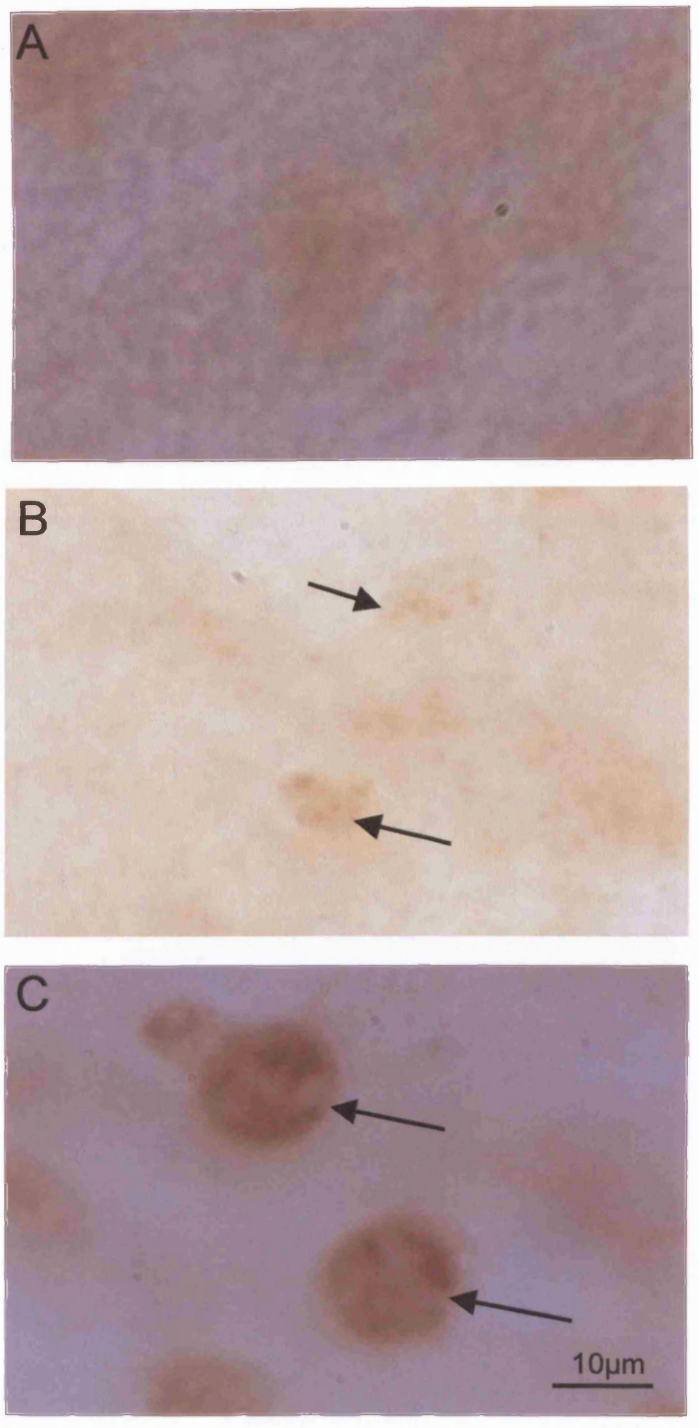

Figure 3.27
Light Microscopy Immunostaining of Speckles from R6/2 Striatal Nuclei
Photomicrographs showing immunoreactivity for a variety of speckle proteins in striatal neurons from 10-week-old R6/2 transgenic mice.
(A) SC35 protein immunoreactivity does not show the "speckled' pattern of nuclear staining.
(B) HYPA protein immunoreactivity shows infrequent nuclei that have the characteristic 'speckled' distribution pattern (black arrows).
(C) TMG protein localises in a speckled nuclear pattern and also diffusely distributed throughout the nucleoplasm (black arrows).

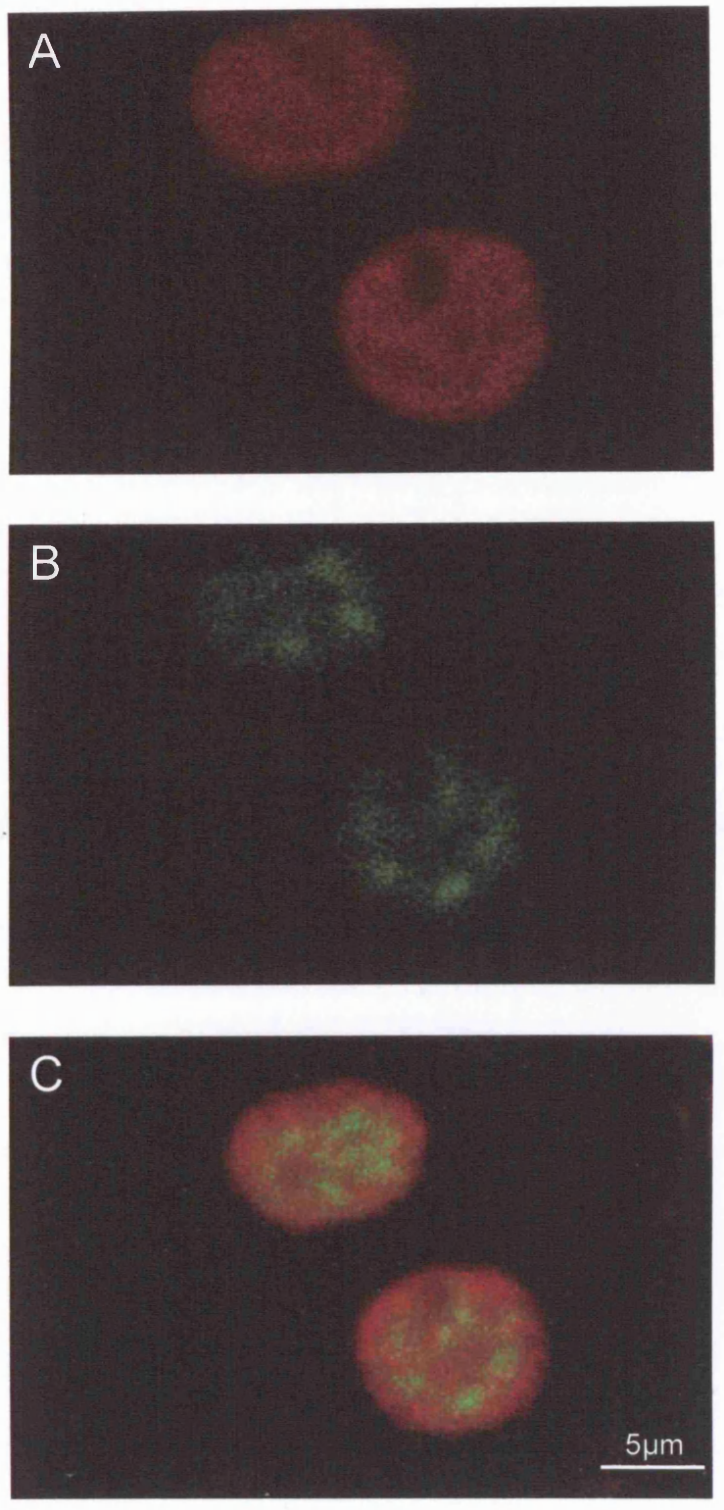

Figure 3.28
Molecular Composition of Speckles from R6/2 Striatal Nuclei
Confocal Microscopy Immunofluorescence of speckles and paraspeckles.
Double labelling indirect immunofluorescence using antibodies to PSP1 (A) and TMG (B). PSP1 immunofluorescence shows the protein to have a punctate nucleoplasmic distribution. TMG immunofluorescence reveals the protein to have a 'speckled' nuclear pattern. When both proteins are viewed together (C) only small areas of colocalisation can be seen (yellow) and these appear to be at the edges of the TMG staining.

3.4.4 Molecular Composition of R6/2 Neuronal NII

Many studies have shown that an increasing number of proteins have been identified that colocalise with the NII (chapter 1.6.6). This study has not concentrated on the molecular composition of the NII but has seen that Hsc70 colocalises with the NII. It has also been possible to demonstrate that NIIs do not contain RNA. This is due to the results from the confocal studies that used pyronin Y and an antibody against huntingtin. The immunofluorescence for huntingtin did not colocalise with the immunofluorescence for pyronin Y and therefore showed the nucleolus (pyronin Y) and the NII (huntingtin) where separate structures (figure 3.23). The fact that the NII did not stain for pyronin Y suggests that it contains no RNA.

3.5 Ultrastructure of p80 coilin KO Neuronal Nucleus

In 20-week-old p80 coilin knock-out mice nuclei of striatal neurons have a round to oval shape and have a normal, dispersed distribution of chromatin with the occasional body of condensed chromatin.

3.5.1 Ultrastructure of p80 coilin KO Neuronal Nucleolus

To study the effects of the deletion of the Cajal body protein p80 coilin on nucleolar morphology I have analysed nucleoli of the striatal neurons in 20-week-old p80 coilin knock-out mice. Nuclei containing nucleoli were randomly sampled.

From my analysis of p80 coilin KO striatal neurons, it is possible to determine that most cells are mononucleolated (94%) and occasionally binucleolated (6%). No nuclei contained more than 2 nucleoli. The mean number of nucleoli per cell is 1.06+/-0.02.

It is possible to divide the p80 coilin KO nucleoli into the same nucleolar classes that were described previously (chapter 3.1.1): closed-reticulate structure (CRS) and open-reticulate structure (ORS).

The CRS was seen in 41% of the cells that were examined (graph 3.9A),

and the morphology reveals small fibrillar centres (FCs) surrounded by a dense material that consists of an entanglement of the dense fibrillar component (DFC) with the granular component (GC). These nucleoli are spherical and have an average diameter of 0.92+/-0.04 μm (graph 3.9B).

The CRS nucleoli can have a perinucleolar cap (PNC) and it is an electron dense structure that lies adjacent to the nucleolus. It seems to be composed of matter that is similar in appearance to the FCs. It has an irregular shape and can be smaller or larger than the nucleolus itself. Perichromatin granules (PGs) and perichromatin fibrils (PFs) are also seen at the nucleolar periphery.

The ORS was seen in 59% of nuclei that were examined (graph 3.9A) and a very disordered ultrastructure can be seen in this class of nucleolus (figure 3.29A). The FCs of the ORS nucleoli can be very large and can take up a significant portion of the nucleolar volume. Smaller FCs are also seen and all FCs are frequently located at the periphery of the nucleolus and not engulfed by the dense material that constitutes the rest of the ORS nucleolus. The dense material seems to be composed of the DFC and the GC entangled together. The ORS nucleoli are not as spherical as the CRS nucleoli and the average diameter is 0.78+/-0.02 μm (graph 3.9B).

ORS nucleoli can also have perinucleolar caps (PNC), PGs and PFs at the nucleolar periphery.

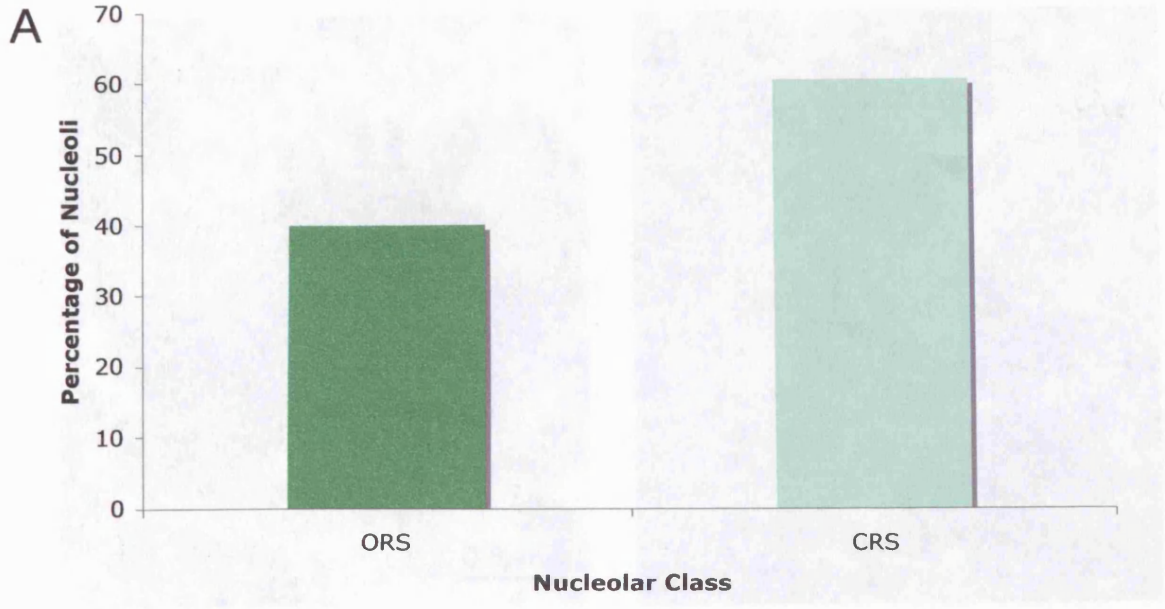

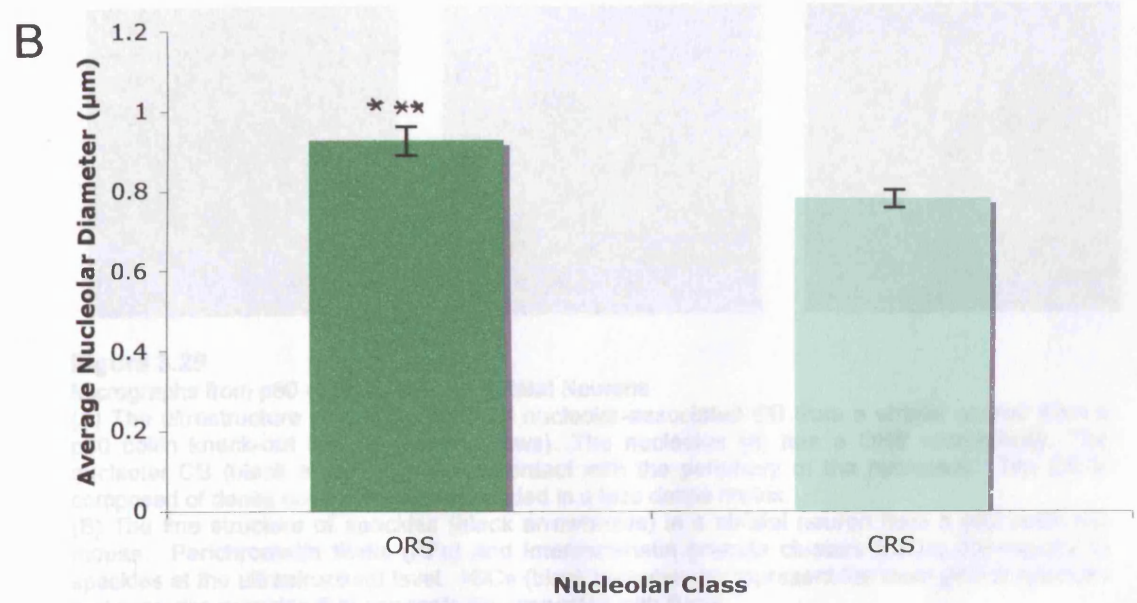

Graph 3.9

Analysis of the Class and Diameters of Nucleoli in p80 coilin KO Striatal Nuclei

(A) A histogram showing the percentages of nucleoli that show an open-reticulate structure (ORS) or a closed-reticulate structure (CRS) in 20-week-old mice. . A 95% confidence interval that the probability of ORS is between 49% and 68% and for CRS is between 32% and 51%.

(B) A histogram showing the average diameters of ORS or CRS nucleoli in 20-week-old mice. It is possible to see that ORS nucleoli have a larger average diameter than the CRS nucleoli. Student's unpaired *t*-test (t = 3.64; ***p<0.001). Error bars are standard errors of mean.

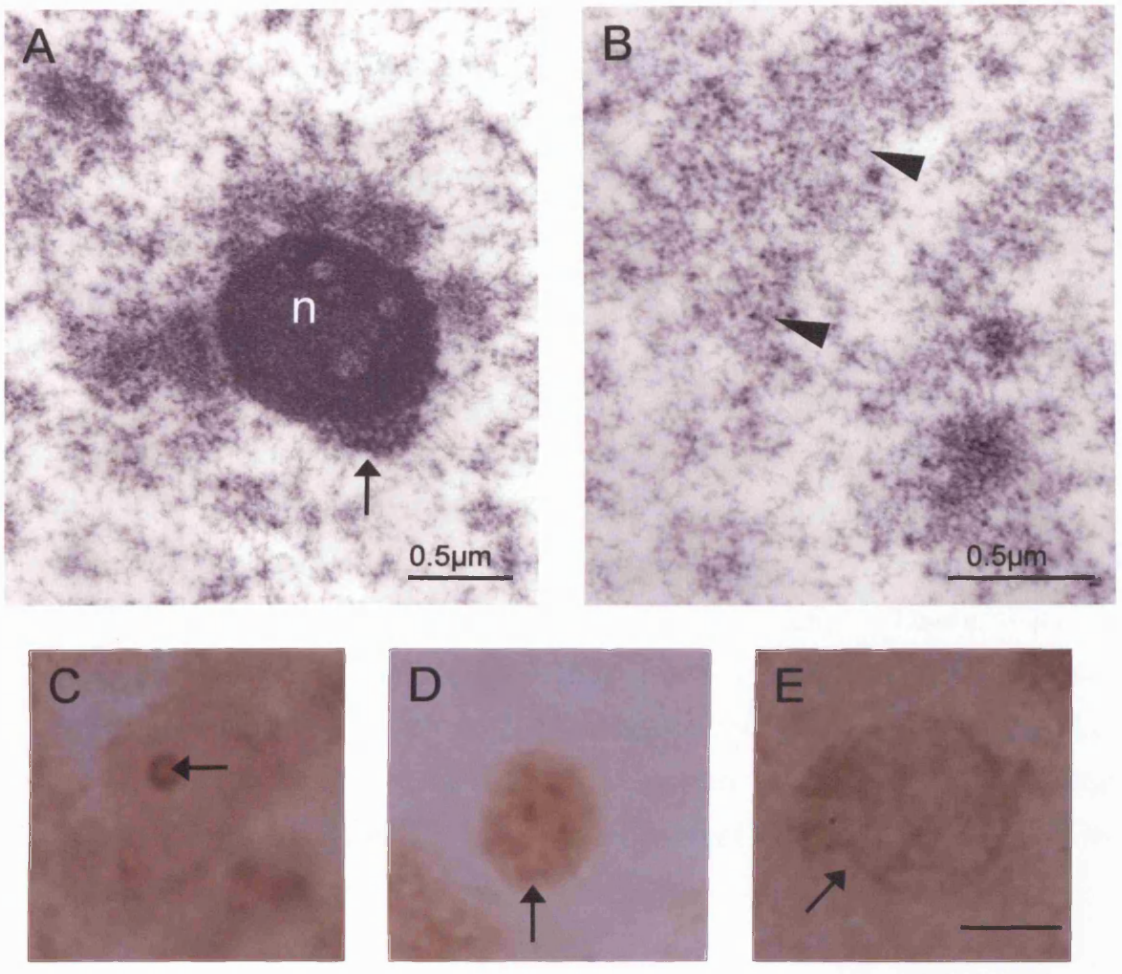

Figure 3.29
Micrographs from p80 coilin Knock-out Striatal Neurons
(A) The ultrastructure of a nucleolus and nucleolar-associated CB from a striatal neuron from a p80 coilin knock-out mouse (black arrows). The nucleolus (n) has a ORS morphology. The nucleolar CB (black arrow)is in direct contact with the periphery of the nucleolus. The CB is composed of dense coiled threads embedded in a less dense matrix.
(B) The fine structure of speckles (black arrowheads) in a striatal neuron from a p80 coilin KO mouse. Perichromatin fibrils (PFs) and interchromatin granule clusters (IGCs) correspond to speckles at the ultrastructural level. IGCs (black arrowheads) represent the main part of speckles and comprise granules that appear to be connected with fibres
Light Microscopy Immunostaining of Nuclear Domains from p80 coilin KO Striatal Neurons.(C) Photomicrograph showing fibrillarin using 17C12 antibody. Intense nucleolar staining is visible (black arrows) with diffuse nucleoplasmic stain as well
(D) Photomicrograph showing immunoreactivity for the Cajal body protein U2" snRNP. Nucleoplasmic staining can be seem together with a 'speckled' pattern of immunoreactivity but no CB staining.
(E) Photomicrograph showing immunoreactivity for the Cajal body protein Gemin2. A diffuse nucleoplasmic and cytoplasmic stain can be seen (black arrow) but no CB staining.
(C-E) Scale bar = 10 µm

3.5.2 Ultrastructure of p80 coilin KO Neuronal Cajal Bodies

As part of the study on the effects of the deletion of Cajal body protein, p80 coilin, on the neuronal nuclear ultrastructure, I decided to examine the morphology and distribution of Cajal bodies in p80 coilin knock-out mice at 20 weeks of age. At the ultrastructural level, only 17% of striatal neurons examined contained a distinct CB and the basic morphology of the CBs in p80 coilin KO nuclei was similar to that seen in the normal murine neuronal nuclei. The CBs were round to oval in shape and were composed of coiled strands of fibrillar material surrounded by a low density amorphous matrix. Tiny fibrils radiating from the periphery of the CB into the nucleoplasm could also be seen.

Most CBs occurred in association with the nucleolus (89%) and very few were free in the nucleoplasm (11%) (graph 3.10A). There were no morphological differences between the CBs in either localisation (figure 3.29A). The average diameters of the nucleolar-associated and nucleoplasmic CBs were 0.19+/-0.02 and 0.18+/-0.01 (graph 3.10B). The nucleolar-associated CBs were seen to be in direct contact with the periphery of the nucleolus.

3.5.3 Ultrastructure of p80 coilin KO Neuronal Speckles

I have analysed the morphology of speckles in 20-week-old p80 coilin knock-out mice. Speckles at the ultrastructural level are composed of interchromatin granule clusters (IGCs) and perichromatin fibrils (PFs). As IGCs have a non-uniform shape a morphological quantification of the speckles in the p80 coilin KO mouse was not possible. However, it was possible to distinguish the numerous granules that constitute the speckles (figure 3.29B).

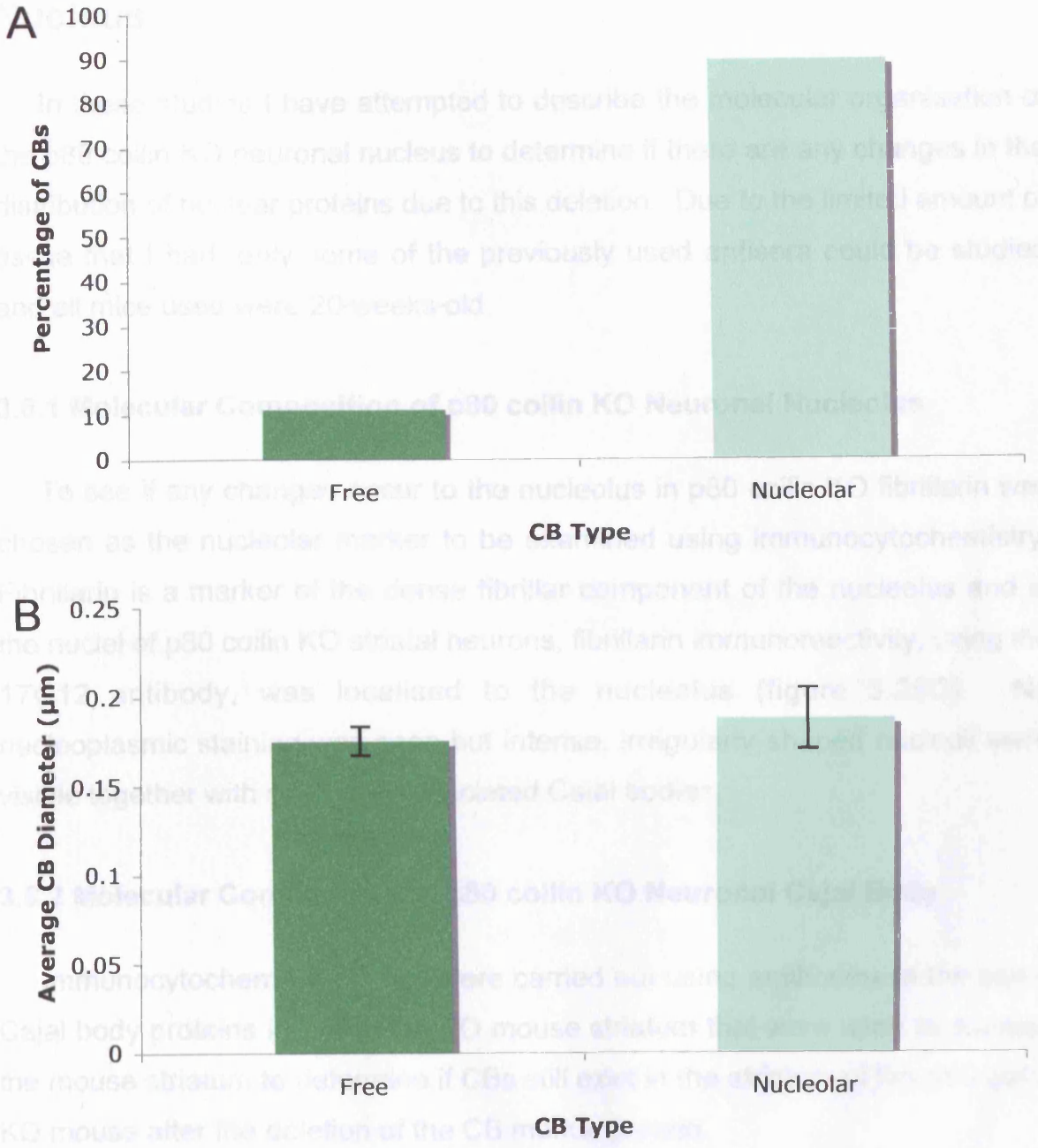

Graph 3.10

Analysis of Cajal Bodies in p80 coilin KO Striatal Nuclei

(A) A histogram showing the percentages of CBs that are either free in the nucleoplasm or nucleolar-associated and found at the periphery of the nucleolus in 20-week-old mice. It is possible to see that most of the CBs in the striatal neurons are nucleolar-associated CBs. A 95% confidence interval that the probability of nucleolar CBs is between 81% and 94% and for free CBs is between 6% and 19%.

(B) A histogram showing the average diameters of free or nucleolar-associated CBs in 20-week-old mice. Nucleolar-associated CBs appear to have a slightly larger average diameter compared to those of the free CBs. Error bars are standard errors of mean.

3.6 Molecular Composition of p80 coilin KO Neuronal Nucleus

In these studies I have attempted to describe the molecular organisation of the p80 coilin KO neuronal nucleus to determine if there are any changes in the distribution of nuclear proteins due to this deletion. Due to the limited amount of tissue that I had, only some of the previously used antisera could be studied and all mice used were 20-weeks-old.

3.6.1 Molecular Composition of p80 coilin KO Neuronal Nucleolus

To see if any changes occur to the nucleolus in p80 coilin KO fibrillarin was chosen as the nucleolar marker to be examined using immunocytochemistry. Fibrillarin is a marker of the dense fibrillar component of the nucleolus and in the nuclei of p80 coilin KO striatal neurons, fibrillarin immunoreactivity, using the 17C12 antibody, was localised to the nucleolus (figure 3.29C). No nucleoplasmic staining was seen but intense, irregularly shaped nucleoli were visible together with nucleolar-associated Cajal bodies.

3.6.2 Molecular Composition of p80 coilin KO Neuronal Cajal Body

Immunocytochemical studies were carried out using antibodies to the same Cajal body proteins in p80 coilin KO mouse striatum that were used to analyse the mouse striatum to determine if CBs still exist in the striatum of the p80 coilin KO mouse after the deletion of the CB marker protein.

p80 coilin is a nucleoplasmic-shuttling phosphoprotein that is known as the molecular marker of CBs and immunocytochemistry using the 204/10 p80 coilin antibody (a gift from A.I Lamond, Dundee, UK) revealed no staining at all.

Immunoreactivity for SMN, the survival of motor neuron protein, together with Gemin2 and Gemin4 showed a cytoplasmic and diffuse nuclear distribution (figure 3.29E) but no CB staining. An antibody against U2" snRNP (small nuclear ribonucleoprotein particles) revealed a 'speckled' staining pattern with no CB immunoreactivity (figure 3.29D).

Discussion & Conclusion

CHAPTER 4

Discussion

4.1 The Ultrastructural Organisation of the Nucleus

It has been well established that the mammalian nucleus is a highly organised structure with many compartments that are involved in gene transcription and RNA processing (Lamond and Earnshaw, 1998; Dundr and Misteli, 2001). Numerous studies on nuclear organisation have used cultured cells to gain an understanding of the structural and molecular organisation of these domains and their spatial relationships (chapter 1). Few research groups have looked at the organisation of neuronal nuclei that, unlike cultured cells, are fully differentiated interphase cells of extreme longevity and, therefore, are cells in which the cell cycle plays merely an initial role in influencing the architecture of the nucleus.

One Spanish research group (Lafarga *et al.,* 1994) has spent many years analysing the organisation/structure of one type of neuron within the supraoptic nuclei (SON) (Berciano *et al.,* 2001), but no studies, that I am aware of to date, have investigated the organisation of the nucleus of medium spiny neurons that are the principle cell type within the striatum. This thesis has attempted to determine the ultrastructural and molecular characterisation of the nucleus of a typical murine striatal neuron and compare these findings with nuclei of the same type of cells in a transgenic mouse model of a neurodegenerative disease in which the medium spiny neurons are the main site of pathology; Huntington's disease (HD) (chapter 1.6). In HD, the sequestration of nuclear factors into NIIs (chapter 1.6.6) and the analysis of altered mRNA levels in R6/2 mice (Luthi-Cater *et al.,* 2000) have led to the hypothesis that transcription is down-regulated and part of the pathological mechanism of the disease (Cha, 2000). Transcription can be easily inhibited in cultured cells using a variety of drugs (chapter 1.4) and many studies have documented the relocalisation of numerous nuclear factors in transcriptionally arrested cells as well as distinct morphological changes. I have used the findings from these studies to create a guide to show the altered localisations of nuclear proteins after transcription has been inhibited. Any relocalisations of proteins seen in the R6/2 nuclei have

then been compared to this guide to see if there are any similarities.

The findings will also be compared to those obtained in a knockout mouse that lacks the Cajal body specific marker protein, p80 coilin (chapter 1.4.3). These findings will provide an insight into the organisation of striatal nuclei *in vivo* and highlight any alterations that occur in a neurodegenerative disease, or, following the deletion of a nuclear protein. The observations illustrate the organisation and behaviour of nuclear subdomains in striatal neurons under different pathological situations.

4.1.1The Ultrastructural Organisation of the Nucleolus

Although it has been shown that the nucleolus of any mammalian cell has a very heterogeneous morphology even within the same cell type, it is still believed that a very distinct overall structure can be distinguished and that this reflects the metabolic activity of that given cell at that given time (Shaw and Jordan, 1995). Many mammalian nucleoli are composed of three ultrastructurally distinct regions; fibrillar centres (FC), the dense fibrillar component (DCF) and the granular component (GC) (chapter 1.1.2 and figure 3.1). One of the first noticeable differences between nucleoli within striatal neurons and many other nucleoli from other mammalian cell types was that the striatal nucleoli had only two easily distinguishable regions. The FCs appear as small, pale areas of the nucleolus that are mostly engulfed by an entanglement of the DFC and the GC which can be seen as a darker, electron dense material. This arrangement of the DFC and GC has been noted before in neurons (Peters *et al.,* 1991). This observation is quite surprising as it is suggested that there is a gradual transition from FCs through the DFC to the GC. The earliest transcriptional events occur at the border between the FCs and the DFC (Carmo-Fonseca *et al.,* 2000) and the pre-rRNA transcripts then move through the DFC into the GC, being processed as they proceed. The finding that the DFC and the GC do not exist as two separate regions in the striatal nucleoli could suggest that all processing of rRNA occurs at the same time. All post-translational modifications must take place in the same area of the nucleolus, even the late processing events, that are reported to occur in the GC (Scheer and Hock, 1999). A similar situation is seen with RNA polymerase II driven

transcription where pre-mRNA splicing takes place at the same time and location as transcription of the nascent pre-mRNA transcripts (Neugebauer and Roth, 1997). It is suggested that co-transcriptional pre-mRNA processing is the result of the fast kinetics of processing compared to the lengthy synthesis of complete pre-mRNA transcripts (Neugebauer, 2002). This may also be true for rRNA transcription and processing in striatal nucleoli. The importance of co-transcriptional splicing is yet to be fully understood but it may play a role in the regulation and efficiency of RNA synthesis for both mRNA and rRNA.

The analysis of the nucleoli in murine striatal neurons demonstrated that most nuclei contained only one nucleolus and that these nucleoli may be subdivided into subclasses each with distinct morphological features. The closed-reticulate structure (CRS) was seen in 44% of nuclei and the main feature was the presence of very small FCs that were numerous and surrounded by an entanglement of the DFC and the GC (figure 3.2A). Lafarga *et al.* (1991) observed nucleoli of similar morphology after the osmotically induced activation of SON neurons in the rat. The presence of many small FCs is thought to indicate that the nucleolus is highly active with increased rRNA transcription. The small FCs give a greater surface to area volume ratio allowing the nucleolus to produce more rRNA. Evidence has been provided that the reduction in the fibrillar centre size is due to splitting of pre-existing FCs into smaller ones, resulting in an associated increase in their number (Ochs and Smetana, 1989). A study using a formic acid silver nitrate staining method showed the precise localisation of FCs, which appear as black dots. Nucleoli from activated cells demonstrated a greater number of small FCs (Derenzini and Ploton, 1991). The area occupied by the silver-stained FCs within the nucleolus is suggested to relate to the total nucleolar volume and the level of ribosome biogenesis.

The open-reticulate structure (ORS) seen in 56% of the nucleoli examined exhibits very prominent FCs that are large and are not always surrounded by the mass of tangled DFC and GC (figure 3.2B). Occasionally the FCs were seen to be in direct contact with the interchromatin space/nucleoplasm. The ORS nucleolar morphology appears to be characteristic of a nucleolus that has lower levels of protein synthesis compared to the activity of the CRS nucleolus (Lafarga *et al.*, 1998). The large FCs may represent fewer rDNA transcription

centres when the demand for ribosomes is not as high as in other nuclei.

This nucleolar morphology has been reported in granule cells of the rat cerebellum (Lafarga *et al.*, 1998). Most granule cells have low levels of protein synthesis and have large FCs surrounded by the DFC and the GC. The formation of few, large FCs have also been seen in cycloheximide treated SON neurons (Lafarga *et al.*, 1994). The FCs were also seen to be incompletely surrounded by the DFC resulting in their direct contact with the nucleoplasm. It has also been shown that when secretion of vasopressin has been completely suppressed by water load in SON neurons, the size of individual FCs was seen to double (Andersen and Keiding, 1990). An increase in the size of FCs has also been seen fibroblasts treated with Actinomycin D (Jordan and McGovern, 1981). These findings support the idea that there is a negative correlation between the size of FCs and the transcriptional activity of the nucleolus.

The average diameters of the CRS and ORS nucleoli were 0.83+/-0.03 μm and 0.90+/-0.03 μm, respectively, and were not significantly different. The slightly larger size of the ORS nucleoli could be explained by the presence of the larger FCs. One study on pig embryo kidney cells (PK cells) has shown that the total volume of FCs does not change with the activation or inactivation of ribosomal genes (Zatsepina *et al.*, 1988). It is instead the fragmentation or fusion of existing, individual FCs that is observed and therefore the total volume of FCs does not increase or decrease. It has also been shown that osmotic stimulation of SON neurons results in a significant increase in the nucleolar size (Lafarga *et al.*, 1991) and SON neurons with high secretory activity have large nucleoli (Andersen, 1990).

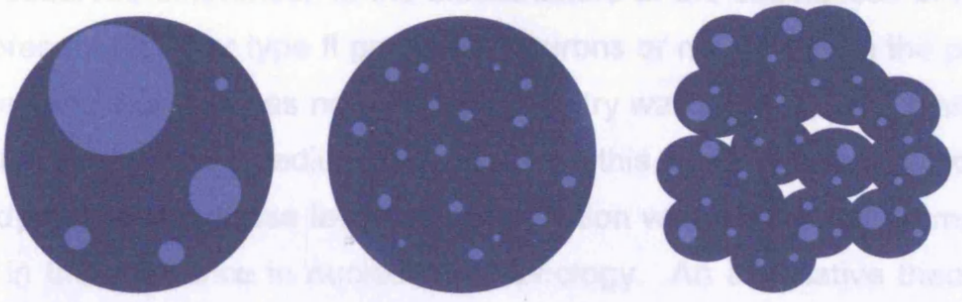

Figure 4.1
Schematic diagrams showing the different nucleolar classes: ORS (A), CRS (B) and SS (C). The ORS nucleoli have few, large FCs (pale blue) whereas the CRS nucleoli have numerous, small FCs (pale blue). In all classes of nucleoli, the remaining part of the nucleolus is composed of the entanglement of the DFC and the GC (dark blue). The SS nucleoli appear to be segregating into microspheres.

One reason for the difference in nucleolar morphology seen in the medium spiny neurons within the murine striatum may be due to the fact there are two different types of projection neurons within this population of neurons. Type I projection neurons mostly project to the substantia nigra pars reticulata (SNPr) and globus pallidus internal segment (GPi)/ entopeduncular nucleus (EP) and produce the neuropeptides, substance P and dynorphin as well as GABA (Bolam *et al.,* 1983). These projection neurons express predominantly D1 dopamine receptors (Gerfen *et al.,* 1990). Type II projection neurons, on the other hand, project to the SNPr and GPi/EP via the globus pallidus external segment (GPe) and subthalamic nucleus (STN) respectively (Gerfen *et al.,* 1992). These projection neurons secrete the neuropeptide enkephalin as well as GABA, and predominantly express D2 dopamine receptors (Gerfen *et al.,* 1990).

However, another level of organisation exists in the striatum. Neurochemical heterogeneity exists in regions of the striatum and has been described as 'patch and matrix'. Regions of striatal neurons that are rich in u-opiate, receive input from the amygdala and parts of the cortex and synapse upon dopaminergic neurons of the substantia nigra pars compacta (SNPc) are termed 'patches' (Pert, 1976). Whereas, the 'matrix' region consists of neurons rich in acetylcholinesterase, somatostatin and calbindin, receive input from the thalamus and other parts of the cortex and synapse upon the output nuclei (GPi/SNPr) (Graybiel and Ragsdale, 1978; Gerfen, 1985). However, the patches only account for fifteen percent of striatal cells (Johnston *et al.,* 1990) and therefore a ratio of 15% patch to 85% matrix would be expected.

The observed differences in the ultrastructure of the subclasses of nucleoli may represent type I or type II projection neurons or neurons from the patch or matrix regions, however, as no immunochemistry was carried out to distinguish either subpopulation of medium spiny neurons this cannot be answered within this study. However, these levels of organisation within the striatum may play no role in the difference in nucleolar morphology. An alternative theory may explain the difference; it may simply be that different neurons at different times have a different rRNA transcriptional activity within the same populations of neurons. If it was possible to analyse the same neuron, hours or days later, a different morphology may be seen but it just so happens that any that given

time approximately half the neuron nuclei have CRS nucleoli and half have ORS nucleoli.

Both of these subclasses of nucleoli were seen in R6/2 transgenic mice and p80 coilin knockout mice. In the R6/2 nuclei, a higher percentage of ORS nucleoli were seen than CRS nucleoli, which was similar to that seen in the wild-type striatal nuclei (graph 4.1). In the p80 coilin knockout nuclei, however, a higher percentage of CRS nucleoli were seen (graph 4.1). The only difference seen in the ultrastructure of nucleoli from the three different mice was found within the nuclei of the R6/2 striatal neurons. The nucleoli seen in the R6/2 striatum exhibited a third structural subclass: the segregating structure (SS). The SS nucleoli have a morphology that is very different from either the ORS nucleoli or the CRS nucleoli because these nucleoli appear to be fragmenting into microspheres, and no longer maintain a spherical shape in the nucleus (figure 3.15). Nucleoli in this subclass have a greater diameter than both the ORS nucleoli and the CRS nucleoli seen in the R6/2 nuclei. In the SS nucleoli, it is still possible to distinguish individual FCs surrounded by the darker, more electron dense material that constitutes the rest of the nucleolus, but intranucleolar vacuoles can also be seen. However, no nucleoli were seen in the R6/2 neurons that were completely segregated into the three distinct components that is the nucleolar ultrastructure that is reported to be characteristic of a completely inactive or transcriptionally arrested nucleoli (Shaw and Jordan, 1995). During the initial phase of osmotic stress when transcription is decreased, SON neurons undergo similar nucleolar reorganisation: the segregation of different regions and the formation of vacuoles that often contain microspheres (Lafarga *et al.,* 1991).

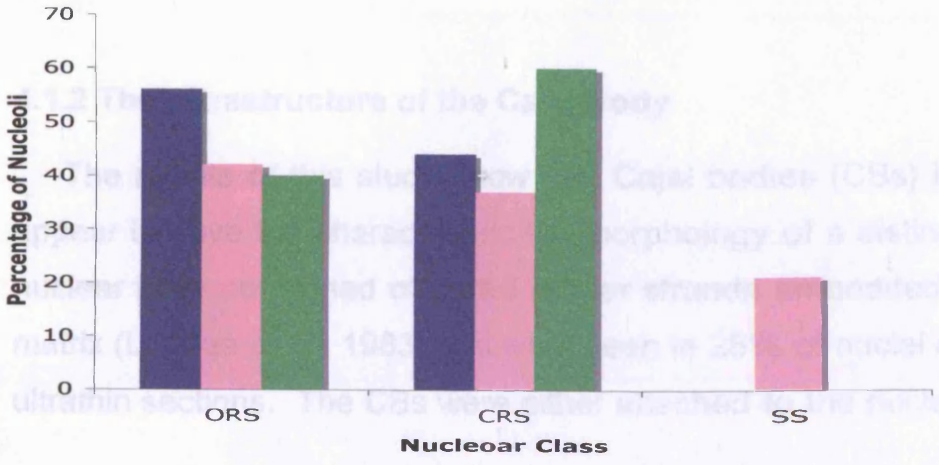

Graph 4.1
A graph showing the percentages of nucleoli in each class (ORS, CRS and SS) for wild-type (blue), R6/2 nuclei (pink) and p80 KO nuclei (green). Chi-Square test for independence (X^2_s= 45.75; p<0.001).

The findings of this ultrastructural study may therefore suggest a reduction in nucleolar transcription rate but not complete transcriptional arrest in the SS nucleoli. This theory is also supported by the fact that the SS nucleoli, seen in the R6/2 neurons, do not share the same morphological characteristics of the segregated nucleoli observed in a study of partial deletion of rRNA genes in *Xenopus* (Miller and Gonzales, 1976). The nucleoli of these oocytes become very compact and segregate completely into fibrillar and granular regions. The formation of microspheres and vacuoles within nucleoli has been documented in cycloheximide treated SON neurons (Lafarga *et al.,* 1994). Cycloheximide treatment inhibits protein and rRNA synthesis and this study revealed a decrease in the size of nucleoli after drug treatment. These results show that protein synthesis and rRNA synthesis is required for the maintenance of nucleolar morphology, but how the formation of microspheres occurs is not fully understood.

Any morphological changes seen in the ultrastructure of the nucleolus are likely to reflect a change or problem with rRNA transcription and synthesis. Reorganisation of nucleolar components clearly reflects a substantial alteration of the transcription activity of ribosomal genes. The reorganisation seen in the SS nucleoli of the R6/2 striatal nuclei may therefore represent a disruption in rRNA transcription or synthesis. Roizin *et al.* (1979) also observed changes in nucleolar morphology when tissue from HD patient biopsies was examined. The altered appearance of the nucleoli was suggested to reflect defective protein synthesis via the nucleolus-ribosomal system. The results from this study do not support a model of HD where transcription of rRNA is completely arrested but it may possibly be decreased with disruption to protein synthesis as well.

4.1.2 The Ultrastructure of the Cajal Body

The results of this study show that Cajal bodies (CBs) in striatal neurons appear to have the characteristic CB morphology of a distinct electron dense, nuclear body composed of coiled fibrillar strands embedded in an amorphous matrix (Lafarga *et al.,* 1983) and were seen in 28% of nuclei examined in 70 nm ultrathin sections. The CBs were either attached to the nucleolus or free in the

nucleoplasm, but CBs at either localisation showed the same morphology. A far greater number of nucleolar-associated Cajal bodies were seen compared to nucleoplasmic CBs (graph 4.2) and the nucleolar CBs had slightly smaller diameters than the free CBs. This greater number of nucleolar-CBs is possibly to be expected in neurons as Cajal did name CBs as 'accessory bodies of Cajal' due to their close association with the nucleolus. However, in different neuronal types, different frequencies of nucleolar versus free CBs can be seen. For example, in hamster facial motor neurons most CBs are associated with the nucleolus, but in pyramidal neurons of the hamster cerebral cortex nucleoplasmic CBs are most frequently seen (Kinderman and LaVelle, 1976). In the murine striatal nuclei no structures that resemble gems were seen adjacent to either nucleolar or nucleoplasmic CBs.

From the ultrastructural study it was not possible to assess the average number of CBs per cell because the ultrathin sections that were examined under the TEM were very thin (70 nm) and the average diameter of a striatal neuronal nucleus is about 10 μm and so all CBs within one nucleus could not be visualised in one section. It was possible to demonstrate that most CBs in the murine striatal nuclei are associated with the nucleolus and serial section reconstructions that have been carried out on a few striatal nuclei, in conjunction with M.Turmaine, confirm this finding (data not shown). It is the larger, free CBs that are reported to be associated with specific gene loci in the nuclei of HeLa cells (Platani *et al.*, 2000). If this is true for all cell types, it is therefore possible to conclude that only a small percentage of CBs (21%) in the striatal nuclei are associated with specific genes at any one time.

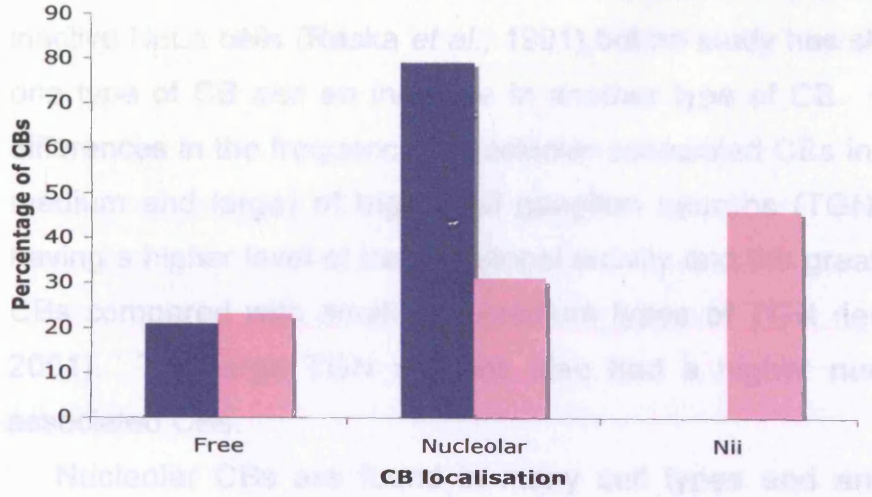

Graph 4.2
A graph showing the percentages of CBs found at the three different localisations (free, nucleolar-associated or NII-associated) in wild-type nuclei (blue) and R6/2 nuclei (pink). Chi-Square test for independence (X^2_s= 67.04; p<0.001).

Morphologically similar CBs were seen in both the striatal nuclei from R6/2 and p80 coilin KO mice. In R6/2 transgenic mice there were more, slightly smaller, nucleolar-associated Cajal bodies compared to the larger, free CBs (graph 4.2). However, in the R6/2 nuclei, CBs were also seen at a different/novel localisation. It is well documented that neuronal intranuclear inclusions (NIIs) are present in striatal nuclei of HD transgenic mice and human HD post-mortem brains (chapter 1.6.5) as well as in other polyglutamine diseases and can be seen as a pale, spherical inclusion in the nucleus of R6/2 striatal neurons (Davies *et al.,* 1997 and chapter 3.3.4). When, in this work, the different localisations of CBs were analysed in the striatum of R6/2 mice nearly half the CBs were seen to be associated with the NII (graph 4.2). This is not the first reported observation of NII-associated CBs as Yamada *et al.* (2001) demonstrated the same association in DRPLA and MJD human brains as well as DRPLA transgenic mouse brains. As with the findings in this study, the CB and NII were seen either in direct contact with each other or connected to each other via fibres (figure 3.16).

In the R6/2 nuclei, only 28% of nuclei examined had a visible CB but of those examined 46% of the CBs were seen juxtaposed to the NII. There was a significant reduction in the percentage of nucleolar-associated CBs but the percentage of CBs that were nucleoplasmic was similar to that seen in the wild-type striatum (graph 4.2). As a similar percentage of nuclei contained CBs in the R6/2 and the wild type neurons, the R6/2 striatal neurons appear to have lost nucleolar-associated CBs and gained NII-associated CBs that have a significantly larger diameter compared to the CBs at the two other localisations.

A reduction in the total number of CBs has been reported in transcriptionally inactive HeLa cells (Raska *et al.,* 1991),but no study has shown a decrease in one type of CB and an increase in another type of CB. One study showed differences in the frequency of nucleolar-associated CBs in three types (small, medium and large) of trigeminal ganglion neurons (TGN), with large types having a higher level of transcriptional activity and the greatest number of total CBs compared with small and medium types of TGN neurons (Pena *et al.,* 2001). The large TGN neurons also had a higher number of nucleolar-associated CBs.

Nucleolar CBs are found in many cell types and are seen as a direct

continuity between CB and nucleolar periphery (chapter 1.2.9). This structural relationship is believed to support the view that CBs can assemble at the nucleolar surface in a transcription-dependent manner (Pena *et al.*, 2001). It is suggested that the higher number of nucleolar-associated CBs seen in the large TGN neurons could facilitate the targeting to the nucleolus of basic constituents of the pre-rRNA processing machinery in neurons with high cytoplasmic needs for ribosome biogenesis and therefore the decrease in nucleolar CBs seen in the R6/2 nuclei could represent a reduction in the need for ribosomes.

When HeLa cells are treated with the protein synthesis inhibitor, cycloheximide, there are reported morphological changes to CBs (Lafarga *et al.*, 1994 and chapter 1.4.2) and CBs are found within the nucleolus when HeLa cells are treated with okadaic acid, a serine-threonine protein phosphatase inhibitor (Lyon *et al.*, 1997 and chapter 1.4.2). Another study showed a positive correlation between transcriptional activity and the number of CBs within nuclei (Pena *et al.*, 2001 and chapter 1.2.14), but none of these studies show a loss of one type of CBs or an increase in CB diameter.

The consequence of the loss of nucleolar-CBs and the gain of NII-associated CB is not known. What affect this novel association between the NII and the CB has on other nuclear subdomains remains to be discovered and whether the association is as a result of changes in other subdomains is yet to be determined.

In the p80 coilin knockout striatal neurons, CBs were somewhat smaller than those examined in the wild-type striatal neurons and were less frequent with only 17% of nuclei containing a CB. Also, 98% of the CBs in the p80 coilin KO nuclei were nucleolar-associated which was greater than the79% seen in wild-type nuclei. This suggests that the lack of p80 coilin leads to smaller CBs that are more frequently associated with the nucleolus. Is this directly or indirectly due to the deletion of p80 coilin? There appeared to be no structural differences between the CBs in the p80 coilin KO and the wild-type neurons despite the fact that the marker protein for Cajal bodies, p80 coilin, is not present.

4.1.3 The Ultrastructure of Speckles

Nuclear speckles are involved in the maturation, trafficking and recycling of pre-mRNA splicing factors and at the ultrastructural level are composed of two distinct regions (Dundr and Misteli, 2001 and chapter 1.3.1). The findings of this study reveal that interchromatin granule clusters (IGCs) in the nuclei of murine striatal neurons have the characteristic morphology that is reported in other cells types (Mintz *et al.,* 1999). The IGCs are comprised of closely packed granules, 20-25 nm in diameter, which are seen in clusters that vary in size.

The second component of speckles at the ultrastructural level is perichromatin fibrils (PFs). The PFs originate from the edge of IGCs and are distributed throughout the nucleoplasm (Spector, 1983). In murine striatal nuclei, fine fibres can be seen emerging from the IGCs as well as the nucleolus. These PFs are reported to be the nascent transcripts as they have been shown to label with [^{3}H]uridine (Fakan, 1994), but the IGCs are not sites of pre-mRNA splicing. Splicing takes place co-transcriptionally at the periphery of the IGCs, which are suggested to supply splicing factors to transcription sites.

Due to the diverse structure and varied size of IGCs and PFs, it was not possible to obtain a meaningful quantification of speckles from the 70 nm ultrathin sections as speckles occupy so much of the nuclear volume. The only solution would have been to carry out a serial section through a complete nucleus to give a three-dimensional image of these complicated structures. It was only possible to demonstrate their fine ultrastructure and confirm that it is possible to distinguish IGCs and PFs in the nucleoplasm without the use of immunolabelling.

The same situation occurred when examining the morphology of speckles in R6/2 striatum and p80 coilin KO striatum. Nuclei from both mice contained IGCs and PFs that showed the same characteristic morphology. However, the IGCs seen in the R6/2 nuclei did seem more distinct than those seen in the wild-type mouse and possibly larger. Large IGCs have been reported in SON neurons that have been treated with the protein and rRNA synthesis inhibitor, cycloheximide (Lafarga *et al.,* 1994) and in cells where transcription has been arrested (Lafarga *et al.,* 1998). In transcriptionally inactive cells it is possible to see enlarged clusters of IGCs that are very prominent and these resemble the

large, spherical IGCs seen when splicing is inhibited using oligonucleotides or specific antibodies (O'Keefe *et al.,* 1994).

However, the IGCs seen in R6/2 nuclei are not spherical and do not resemble the enlarge clusters seen after cycloheximide treatment. The fact that the IGCs in the R6/2 nuclei are slightly more distinct may indicate a slight down regulation in transcription or rRNA and protein synthesis but not a complete arrest of any of these processes.

4.1.4 The Ultrastructure of NIIs

The presence of NIIs in R6/2 striatal nuclei has been documented before (Davies *et al.,* 1997 and chapter 1.6.5), as well as in this study. The findings of this study confirm the ultrastructural appearance of NIIs within striatal nuclei to be a pale, granular inclusion that resembles no other structure in the nucleus (figure 3.16C). NIIs have now been seen in all polyglutamine diseases (chapter 1.7.1) and similar inclusions have been reported in some of the non-coding repeat expansion disorders (chapter 1.7.2), but it is still unclear as to the role they play in the pathology of these two groups of diseases.

Inclusions have also been seen to form in the nucleus when protein synthesis is inhibited with cycloheximide (chapter 1.4.5). In dehydrated rat SON neurons, nuclear aggregates have been seen that are morphologically pale, granular structures (Lafarga *et al.,* 1993). It is suggested that the formation of the inclusion reflects a dysfunction of the nucleolus as rRNA synthesis is also inhibited by cycloheximide. However, the molecular composition of these inclusions was not investigated and it remains unclear as to why dysfunction in the nucleolus would lead to the formation of an inclusion. The formation of inclusions has also been reported in liver cells that were treated with Actinomycin D to inhibit transcription (Reynolds *et al.,* 1964 and chapter 1.4.5). These aggregates were not easily distinguishable and have not been reported in any of the other studies that involve transcriptional inhibition.

What cellular process leads to the formation of these nuclear inclusions (in neurodegenerative diseases and in experiments where drug treatment is used to alter various metabolic activities) remains a mystery, but the NII is still a distinct feature of them all.

4.1.5 Conclusions for the Ultrastructural Analysis

From the ultrastructural analysis of the three nuclear subdomains in murine striatal nuclei, it is possible to conclude the following:

1. Not all striatal nucleoli exhibit the same nucleolar morphology.
2. Most striatal Cajal bodies are nucleolar-associated
3. Free CBs are infrequently present in striatal nuclei. They are slightly larger than nucleolar-associated CBs and it is suggested that these CBs are associated with specific gene loci.
4. Speckles can be seen in the striatal nuclei without immunolabelling.

From the ultrastructural study on three subdomains in the R6/2 nuclei, it could be suggested that there may be a slight downregulation in transcription, ribosome biogenesis or protein synthesis. It must be noted that although these conclusions give an insight into the organisation of the nucleus, they do not give a complete understanding of the architecture of the neuronal nucleus as only a very thin section is being analysed at any one time. For example, from the ultrastructural study, the only 28% of nuclei contained CBs. To try and discover a more three-dimensional image of the striatal nucleus and the relationships of the three subdomains being analysed, other techniques must be used and the results combined.

4.2 The Molecular Composition of the Nucleus

To try and understand how the ultrastructural organisation of the nucleus reflects the functional organisation, the molecular characterisation of many nuclear subdomains has led to the localisation of many nuclear processes to specific nuclear structures (Lamond and Earnshaw, 1998). Numerous experiments have now highlighted the dynamic nature of nuclear proteins (Misteli *et al.*, 1997; Platani *et al.*, 2000; Misteli, 2001) and how alterations in nuclear localisations of certain proteins can reflect a change in metabolic activity (Carmo-Fonseca *et al.*, 1992; Lafarga *et al.*, 1994; Bregman *et al.*, 1995; Zeng *et al.*, 1997; Sleeman *et al.*, 1998; Pena *et al.*, 2001).

This study will look at the molecular composition of the three nuclear domains (nucleolus, Cajal body and speckles) studied ultrastructurally and try to build a detailed three-dimensional image of the murine striatal nucleus. This will then be compared to the R6/2 transgenic mouse and the p80 KO mouse to see if any molecular alterations can be seen. As HD is suggested to have transcriptional dysregulation (chapter 1.6.7-9), any changes reported in the R6/2 mouse will be compared to the alterations seen when transcription is inhibited with Actinomycin D to ascertain if any similarities can be identified.

4.2.1 The Molecular Composition of the Nucleolus

The list of known molecular components of the nucleolus has increased rapidly since the development of mass-spectrometry-based organellar proteomics (Andersen *et al.,* 2002). In 2002, Andersen *et al.* identified 271 proteins that localised to the nucleolus and this number has since risen to 489 proteins that can be seen to localise to nucleoli after cells are treated with different metabolic inhibitors (Andersen *et al.,* 2005). To investigate the molecular composition of nucleoli in striatal neurons, immunocytochemical analyses were performed using a number of antibodies against several nucleolar proteins. Nucleolar proteins that are reported to localise to each of the three distinct regions of the typical mammalian nucleolus were examined (chapter 1.1.4 and figure 3.1).

When examined by light microscopy (using x 100 oil immersion objectives), the immunoreactivity for fibrillarin, GAR1 and Nopp140 revealed a similar staining pattern: a solid, spherical structure in the nucleus with nucleolar-associated Cajal bodies (CBs) frequently labelled as well as occasional nucleoplasmic CBs (figure 3.6B-D). No nucleoplasmic staining could be seen for fibrillarin and GAR1 but it was present for Nopp140. The immunoreactivity for C23 showed a different staining pattern: a circular ring around the nucleolar periphery, with a high level of nucleoplasmic staining and no visible CBs (figure 3.6E). Topoisomerase II revealed a similar staining pattern but it also included staining of nucleolar-associated CBs. Antibodies against B23 unfortunately did not reveal a staining pattern for this nucleolar protein despite many different fixation protocols being tried. An antibody against upstream binding factor

(UBF) revealed occasional small, irregularly shaped nuclear foci that frequently appeared in groups (figure 3.6A). Immunoreactivity for a subunit of RNA polymerase I was mainly nucleoplasmic with occasional small, nuclear foci (figure 3.6F). A quantitative analysis of the nucleolar immunoreactivity in this study supported the results form the ultrastructural investigation that most striatal nuclei contained on average only one nucleolus (graph 3.3).

The findings of this work demonstrate that nucleoli within nuclei of murine striatal neurons are immunoreactive for several of the most studied nucleolar components. The immunoreactive foci seen for the fibrillar centre (FC) marker protein, UBF, appeared to be smaller than those seen for the other nucleolar proteins. From the ultrastructural analysis of striatal nucleoli, this study has shown that FCs can vary in size from either tiny foci seen in closed-reticulate structure (CRS) nucleoli that can only just be distinguished or larger, more prominent regions seen in the open-reticulate structure (ORS) nucleoli. The staining pattern seen for anti-UBF does correlate with these morphological findings and the larger, grouped foci seen probably represent the FCs of ORS nucleoli. Although UBF has been reported to localise within the DFC as well (Shaw and Jordan, 1995), the staining pattern for anti-UBF does not support this in murine striatal nuclei. RNA polymerase I is also proposed to be a marker for FCs, but the results seen in this study do not confirm this for striatal nucleoli as a more heterogeneous nucleoplasmic staining pattern was seen for anti-RNA polymerase I when compared to the staining for UBF.

Fibrillarin, GAR1 and Nopp140 are all reported to be markers for the dense fibrillar component (DFC) of nucleoli whereas B23 and C23 are suggested to be markers for the granular component (GC) (Shaw and Jordan, 1995). The findings of this work do support the idea that C23 is not found in the same region as fibrillarin and GAR1 because the staining pattern for the respective antibodies were different.

The distribution of fibrillarin was also analysed at the ultrastructural level using immuno-electron microscopy (figure 3.7A-B). Fibrillarin immunoreactivity showed a heterogeneous staining pattern within the nucleolus that excluded FCs. When the localisation of fibrillarin was examined using immunofluorescence and a *Z*-series scan was performed that allowed the three dimensional reconstruction of the entire nucleus, it was possible to see that the

spherical structure seen at light microscopy was not a solid sphere (figure 3.12). The immunofluorescence for fibrillarin actually had a heterogeneous distribution within the nucleolus itself. When a single section was analysed, it was possible to see that the entire nucleolus did not contain immunofluorescence for fibrillarin and patches devoid of immunofluorescence were seen. The areas with no immunofluorescence are likely to correspond to the FCs.

The distribution of fibrillarin using either immuno-electron microscopy or confocal microscopy revealed a heterogeneous localisation of this nucleolar protein within the nucleolus. The immunofluorescence results, together with the immuno-electron microscopy results, clearly showed that FCs are devoid of fibrillarin. The immuno-EM data also showed that fibrillarin has an irregular localisation over the remaining region of the nucleolus. The ultrastructural analysis in this study suggested that the DFC and GC of striatal nucleoli were arranged in an entanglement around the FCs as neither region could be clearly identified. The immuno-EM for fibrillarin support this view as the immunoreactivity is not seen in distinct areas surrounding the FCs that is the characteristic distribution of DFCs in many mammalian nucleoli.

However, a difference in the pattern of immunoreactivity was seen for protein markers of the DFC (fibrillarin, GAR1 and Nopp140) compared to the pattern of immunoreactivity seen for protein markers of the GC (C23). This could mean that even though the DFC and the GC could not be easily distinguished using EM, on a molecular level, the two nucleolar regions are distinct. Double labelling immunofluorescence experiments would have shown if different nucleolar proteins, that appear to have a different staining pattern at light microscopy, do actually localise to different nucleolar regions. Unfortunately, the fixation protocols used to achieve immunoreactivity for many of the nucleolar protein antibodies at light microscopy did not work for confocal microscopy, or, the two antibodies for the two nucleolar protein that were to be compared needed different fixation protocols to work and so could not be visualised on the same section (table 2.1). Similar fixation problems arose when trying to use immuno-electron microscopy to study the ultrastructural localisation of many of the nucleolar proteins.

The fact that antibodies against B23 did not reveal any staining pattern does not necessarily mean that this nucleolar protein is absent from striatal nucleoli

as the lack of immunoreactivity may have resulted from the inability of the antibody to recognize the murine B23 epitope.

When the localisation of Hsc70 was analysed using immuno-EM, it was seen to localise to the periphery of the nucleolus in striatal nuclei (figure 3.7C-D). Hsc70 is one of the hsp/hsc70 family of heat shock proteins that are involved in many cellular processes (Moon *et al.*, 2001). These functions include the folding of newly synthesised proteins and the targeting of proteins to their correct localisation within the cell (Moon *et al.*, 2001). One study in HeLa cells showed that Hsc70 associated with the nucleolus but only after heat shock (Welch and Mizzen, 1988). However, the presence of Hsc70 in nucleoli of control 9L RBT (rat brain tumor) cells has been demonstrated (Wang *et al.*, 1998), but the role played by Hsc70 in the nucleolus is unclear.

The localisation of the same nucleolar proteins were analysed in R6/2 transgenic mice striatal nucleoli. A quantitative analysis also showed that most R6/2 striatal nuclei contained only one nucleolus supporting the ultrastructural findings (graph 3.7). The immunoreactivity for fibrillarin, C23, RNA polymerase I and topoisomerase II were all similar to that seen in the wild-type nucleoli (figure 3.18). Nopp140, however, revealed a less intense staining of the nucleolus and a more intense staining of CBs. Immunoreactivity for fibrillarin, Nopp140 and C23 definitely revealed nucleoplasmic CBs whereas topoisomerase did not. Hsc70 was no longer seen at the nucleolar periphery and was seen to colocalise with the NII (figure 3.19).

A study that investigated the effect of different metabolic inhibitors on the distribution of nucleolar proteins showed that the localisations of C23 and B23 were altered when Actinomycin D was used to inhibit the RNA polymerases in breast cancer cells (Perlaky *et al.*, 1997). Both nucleolar proteins no longer localised to the nucleolus but showed a nucleoplasmic distribution. The presence of C23 in nucleoli of R6/2 striatal nucleoli could therefore suggest that these neurons are transcriptionally active. After treatment with Actinomycin D rat primary cerebellum cultures also showed that fibrillarin redistributes when the activities of all the RNA polymerases are inhibited (Raska *et al.*, 1990). Immunoreactivity for fibrillarin revealed cap-like structures at the edge of the nucleolus that colocalised with the CB marker protein, p80 coilin. The localisation of fibrillarin in the R6/2 striatal nucleoli was similar to that seen in

the wild-type striatal nucleoli and can therefore possibly be used as indicator that transcription has not been affected in the R6/2 nuclei.

Nopp140 is suggested to have several functions in the nucleolus and moves between the cytoplasm and the nucleolus as well as moving between the nucleolus and CBs (Snaar *et al.*, 2000). The more prominent staining of CBs with anti-Nopp140 in this study suggests that there may be a change in distribution of Nopp140 in the nucleolus (a decrease) or CBs (an increase).

In R6/2 striatal nuclei, a redistribution of Hsc70 was also seen as it no longer localised to the nucleolar periphery and, instead, was seen to accumulate in the NII. A study by Jana *et al.* (2000) has shown that Hsc70, as well as other chaperones, can bind to polyglutamine proteins and that Hsc70 colocalised with the NII in mouse neuro2a cell lines expressing truncated N-terminal huntingtin with expanded polyglutamines. This colocalisation was also seen in R6/2 mice but as the colocalisation was only seen in some of the nuclear inclusions. It is therefore suggested that the chaperones are not involved in the aggregation of the mutant protein because if this were true all aggregates (nuclear or dendritic) would contain these chaperones (Jana *et al.*, 2000). The consequence of Hsc70 being lost from the nucleolar periphery in the R6/2 nuclei may cause incorrect targeting of other nuclear proteins.

The findings of this study show that there is not a major difference in the molecular composition of the R6/2 striatal nucleolus compared to that of the wild-type striatal nucleolus, and that, only one of the chosen nucleolar proteins revealed a slight redistribution together with the loss of Hsc70. This suggests that, despite the fact that 21% of nucleoli in R6/2 nuclei show an alteration in their ultrastructure, the segregating structure (SS), the nucleolar proteins studied are still recognized by the antibodies and localised to nucleoli in a similar pattern that seen in the wild-type nucleoli. The SS nucleoli seen in R6/2 nuclei have alterations at the morphological level but not at the molecular level.

The ultrastructural analysis of the R6/2 nucleoli and the observation of the SS nucleolar morphology has lead to the conclusion that these nucleoli may reflect a disruption in rRNA transcription and/or protein synthesis as the morphological changes resemble those seen in cycloheximide treated SON neurons (Lafarga *et al.*, 1994). Few studies have analysed the distribution of nucleolar proteins in cycloheximide treated cells but the studies that have

demonstrate that two nucleolar proteins, DNA helicase II (RNA helicase A) and topoisomerase I, are not shown to redistribute after drug treatment (Buckwalter *et al.*, 1996; Zhang *et al.*, 1999). It could therefore be predicted that the inhibition of protein synthesis and disruption of rRNA transcription does not cause a re-distribution of nucleolar components like those seen when cells are treated with inhibitors of all RNA polymerases, like Actinomycin D (chapter 1.4.1). If this is correct, then the findings of this study that demonstrate that a proportion of nucleoli in R6/2 nuclei may have an altered ultrastructure but not a change in the localisation of nucleolar proteins would be expected.

Only the distribution of fibrillarin was analysed in the p80 coilin knockout mice and the immunoreactivity seen with anti-fibrillarin antibodies revealed a similar staining pattern to that seen in the wild-type striatal nuclei: a prominent spherical structure with nucleolar-associated CBs. The findings of this study show that the lack of p80 coilin does not affect the distribution of the nucleolar protein, fibrillarin.

4.2.2 The Molecular Composition of the Cajal Bodies

Like the nucleolus, protocols have now been developed that allow the isolation of Cajal bodies (CBs) and the possible identification of molecular constituents of the isolated nuclear organelle using mass-spectrometry-based proteomics (Lam *et al.*, 2002). Despite the identification of many nuclear components that localise to CBs (Matera, 1999 and chapter 1.2.5), p80 coilin is still regarded as the molecular marker protein and is widely used to detect CBs. In this study, antibodies to p80 coilin together with a number of other nuclear proteins that are found within CBs were used to analyse the molecular composition of murine striatal CBs.

Immunoreactivity for p80 coilin, survival of motor neuron protein (SMN), Gemin2-4, U2" snRNP, poly(A) polymerase (PAP) and Ewing's sarcoma (EWS) all revealed bright nuclear foci when viewed under high power light microscopy (figure 3.20). When the average number of CBs identified per nucleus was compared for p80 coilin and U2" snRNP, this study discovered that more p80 coilin-positive CBs were present in murine striatal nuclei than U2"snRNP-positive CBs (graph 3.4A). From the light microscopy study, on average only

one CB was seen to contain snRNP per nucleus whereas, p80 coilin-containing CBs varied in number from one to four per nucleus. These results did not change from 4 to 12 weeks of age.

Similar results to those seen for U2" snRNP were obtained when the average number of CBs containing SMN, Gemin2 and Gemin4 were analysed. These results suggest that most striatal nuclei do have CBs and this differs from the 28% of nuclei seen to contain CBs in the ultrastructural part of this study. The results also highlight the fact that not all CBs have the same molecular composition. Gemin4 has been reported to localise in the nucleolus of HeLa cells (Charroux *et al.*, 2000), but this was not seen in this study.

The results from the light microscopy study only revealed the presence of a particular protein in CBs and the average number of CBs that contained that protein. The light microscopy study did not show the localisation (nucleolar-associated or nucleoplasmic) of the different CBs that were positively stained for the different proteins. Immuno-electron microscopy was carried out on murine striatal neurons to analyse the different localisations of different CB proteins. However, as only a 70 nm section was being examined and, therefore, on average, only one immunoreactive CB was visible, it was difficult to create a complete understanding of the organisation and distribution of all the CBs in an entire nucleus. Double labelling confocal microscopy was used to solve this problem as experiments could be carried out using secondary antibodies conjugated to FITC, which can be seen in the green channel, and pyronin Y stain that can be seen in the red channel and labels RNA, therefore revealing the nucleolus. A Z-series scan could be performed and this would allow the entire nucleus of a neuron to be reconstructed.

When the average number of CBs was counted for either p80 coilin or SMN immunofluorescence similar results were obtained to those seen in the light microscopy study, with p80 coilin being localised to more CBs compared to SMN (graph 4.3). Anti-SMN was mainly found to label only one CB per nucleus but infrequently labelled two CBs. Anti-p80 coilin, on the other hand, revealed a more varied number of CBs per nucleus with nearly half the nuclei examined containing two CBs. Occasionally nuclei were seen to contain three or four p80 coilin-containing CBs.

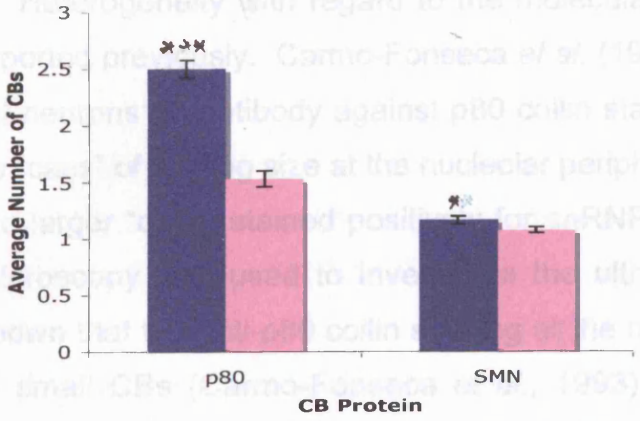

Graph 4.3
A graph showing the average number of CBs per nucleus that contained either p80 coilin or SMN in wild-type nuclei (blue) or R6/2 nuclei (pink). For p80 coilin, Student's unpaired *t*-test (t = 9.25; ***p<0.001). For SMN, Student's unpaired *t*-test (t = 2.00; *p<0.05). Error bars are standard errors of mean.

As the nucleolus could be easily identified due to the pyronin Y staining, the exact localisation of the CBs, immunofluorescence for either SMN or p80 coilin, could be recorded. CBs containing SMN were seen to be only nucleolar-associated while p80 coilin containing CBs were seen to be both nucleolar-associated and free in the nucleoplasm (graph 4.4A-B). The SMN-positive CBs were all of similar size whereas the p80 coilin-positive CBs varied in size. The findings of this study therefore show that not all CBs in striatal nuclei are the same size or have the same protein composition.

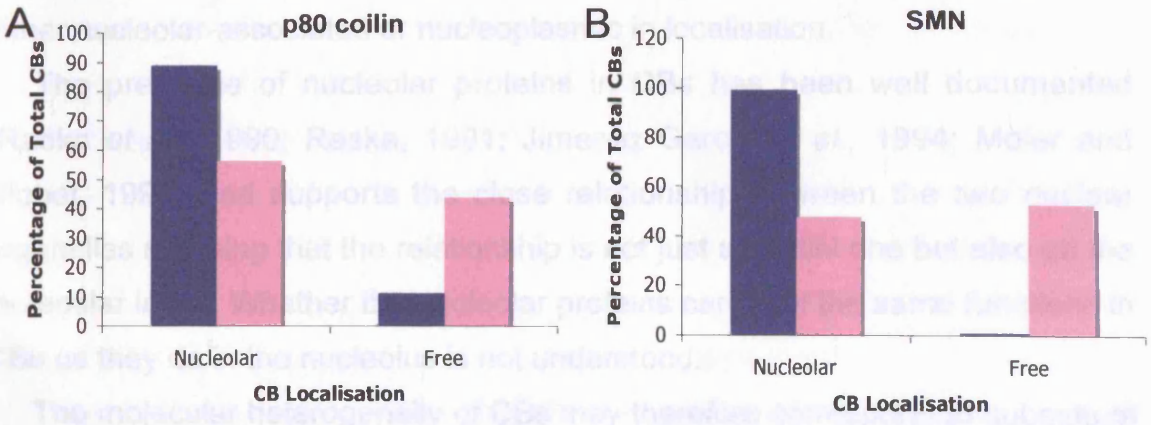

Graph 4.4
Graphs showing the percentage of the total number of CBs that were either nucleolar-associated or free in wild-type mice (blue) or R6/2 mice (pink). Graph A shows the results for CBs containing p80 coilin and graph B shows the results for SMN-containing CBs. For Graph A, Chi-Square test for independence (X^2_s= 12.56; p<0.01). For Graph B, Chi-Square test for independence (X^2_s= 4.03; p<0.05).

Heterogeneity with regard to the molecular composition of CBs has been reported previously. Carmo-Fonseca *et al.* (1993) demonstrated that in primary rat neurons an antibody against p80 coilin stained nucleoplasmic CBs as well as "caps" of varying size at the nucleolar periphery. The study showed that only the larger "caps" stained positively for snRNPs. When immuno-gold electron microscopy was used to investigate the ultrastructure of the "caps", it was shown that the anti-p80 coilin staining at the nucleolar periphery corresponded to small CBs (Carmo-Fonseca *et al.,* 1993). It was suggested that these structures were partially assembled CBs that were either assembling or disassembling at the periphery of the nucleolus. Another study on mammalian endothelial cells revealed that nuclei from these cells contained more p80 coilin-positive CBs when compared to the RNA-binding protein pig pen/TLS-positive CBs or fibrillarin-positive CBs (Alliegro and Alliegro, 1998). This suggests that CBs might have different functions depending on their molecular composition.

From the light microscopy study of nucleolar proteins it can be seen that in murine striatal nuclei, nucleolar-associated CBs and nucleoplasmic CBs contain the nucleolar proteins fibrillarin, GAR1 and Nopp140. Topoisomerase II is also found to localise within nucleolar-associated CBs but not free. From the double labelling confocal microscopy experiments it was possible to see that fibrillarin was found to colocalise with nearly all the p80 coilin-positive CBs that were either nucleolar-associated or nucleoplasmic in localisation.

The presence of nucleolar proteins in CBs has been well documented (Raska *et al.,* 1990; Raska, 1991; Jimenez-Garcia *et al.,* 1994; Meier and Blobel, 1994) and supports the close relationship between the two nuclear organelles meaning that the relationship is not just a spatial one but also on the molecular level. Whether the nucleolar proteins carry out the same functions in CBs as they do in the nucleolus is not understood.

The molecular heterogeneity of CBs may therefore correspond to subsets of CBs that somehow exclude particular molecules, the mechanism for which is not known. The subsets of CBs could either represent functionally distinct subpopulations of CBs or reflect different stages in the assembly or disassembly of CBs.

Double labelling confocal microscopy in this study also demonstrated that p80 coilin and SMN localised to the same nuclear foci, ruling out the possibility

that striatal nuclei contain gems (chapter 1.2.10). This finding is supported by results from a study that investigated the distribution of CBs versus gems in different tissue types (Young *et al.*, 2000). In rabbit, pig and human brain cells independent gems were not observed and the CBs seen were large in size and frequently positioned adjacent to the nucleolus. The same study also reported CB heterogeneity, as 10% of CBs seen were p80 coilin positive but lacked SMN protein.

The results of this study, on ultrastructural and molecular characterisation of the Cajal body, have also shown that depending on which technique is used to analyses CBs, different average numbers per nucleus are seen. For example, from the ultrastructural study, the average number of CBs per nucleus was only 0.28, whereas, at the light microscopy level, the average number of CBs ranged from 0.88 to 2.4 per nucleus. This number rose further, when a Z-series scan was performed and an entire nucleus was reconstructed, to 2.53 CBs per nucleus. These findings demonstrate that to gain a complete understanding of the neuronal nucleus, a number of different techniques must be used.

When the localisation of the same CB proteins were analysed in R6/2 mice striatal nuclei, a number of differences were seen. The first difference observed was a decrease in the average number of CBs containing p80 coilin. At 4 weeks of age, the average number of p80 coilin-positive CBs per nucleus in the R6/2 striatal nuclei was similar to that seen in the wild-type nuclei. However, at 10 weeks of age, the average number of CBs had decreased significantly in the R6/2 nuclei. Surprisingly, the average number of CBs seen to contain the other CB proteins (SMN, Gemin2, Gemin4 and U2" snRNP) did not show any significant differences from the wild-type values over the same time period studied. Even though the p80 coilin-positive CBs decreased in number compared to the average numbers of the wild-type nuclei, there was still a difference between the average numbers of p80 coilin and SMN containing CBs in the R6/2 nuclei. There was a greater average number of p80 coilin-positive CBs compared to SMN-positive CBs.

No immunoreactive CBs were seen in the R6/2 striatal nuclei when antibodies against PAP and EWS were used. Both of these nuclear proteins were seen to localise occasionally in CBs in wild-type striatal nuclei. EWS is an RNA binding protein and it interacts with SMN (Young *et al.*, 2003) and PAP is

involved in the polyadenylation of 3' prime ends of mRNA. The lack of PAP or EWS from CBs in R6/2 nuclei could reflect alterations in protein-protein interactions as a result of the increased CAG repeat in huntingtin (htt). For example, PAP is required for both cleavage of mRNA and polyadenylation (Schul *et al.,* 1996). 14-3-3 is a protein that has been shown to bind to the C-terminal of PAP and this interaction is dependent upon phosphorylation (Kim *et al.,* 2003). The binding of the two proteins affects the localisation and polyadenylation activity of PAP. This interaction is suggested to play a role in the regulation of gene expression (Kim *et al.,* 2003).

14-3-3 has also been shown to interact with ataxin-1, the protein involved in SCA1 (chapter 1.7.1) (Chen *et al.,* 2003) and this interaction increases with increased CAG repeat size in ataxin-1. It could therefore be suggested that 14-3-3 might interact with mutant htt in a similar way and this could, in turn, affect the interaction of 14-3-3 and PAP, altering the localisation of this protein.

When a Z-series scan and a complete nuclear reconstruction was performed on the R6/2 striatal nuclei using the confocal microscope, similar results were obtained to those of the light microscopy study for SMN, with the average number of CBs seen with anti-SMN did not greatly differ from the wild-type nuclei (graph 4.3). However, anti-p80 coilin revealed a significant decrease in the average number of CBs in the R6/2 nuclei compared to that seen in the wild-type nuclei (graph 4.3). The number of p80 coilin-positive CBs seen in the R6/2 nuclei, like the wild type nuclei, varied from one CB to four CBs and the size of CBs also varied.

However, a higher percentage of nuclei contained just one CB in the R6/2 striatal nuclei (60%) compared to the wild-type nuclei (35%) and the frequency of two, three or four CBs in the R6/2 nuclei was also seen to decrease. When the number of SMN-positive CBs was analysed, no significant difference was seen from the wild-type results with the majority of R6/2 nuclei containing only one large SMN-positive CB.

On analysing the distribution of either the p80 coilin or SMN-containing CBs, with regard to their spatial relationship with the nucleolus, it was seen that a greater percentage of CBs, immunoreactive for either p80 coilin or SMN, were nucleoplasmic CB and not associated with the nucleolus (graph 4.4A-B). This result was most striking for SMN-containing CBs. In the wild-type striatal nuclei,

99% of SMN-positive CBs were nucleolar-associated whereas, in the R6/2 nuclei, only 47% of SMN-positive CBs were seen to be associated with the nucleolus. There was also a decrease in the percentage of nucleolar-associated p80 coilin-positive CBs in the R6/2 nuclei. In the wild-type nuclei, approximately 89% of p80 coilin-containing CBs were nucleolar-associated whereas, in the R6/2 nuclei, only approximately 56% of p80 coilin-positive CBs were associated with the nucleolus.

A decrease in the number of p80 coilin-positive CBs has been reported in rat SON neurons during the initial phase of osmotic stress when transcription is inhibited (Lafarga *et al.,* 1998). However, even though Lafarga *et al.* (1998) demonstrated a decrease in the overall number of CBs per nucleus when transcription is arrested, the CBs that were still seen were associated with the nucleolus. These nucleolar CBs were also shown to contain U2" snRNP and when analysed via EM, were described as precursors to CBs. It is suggested that new CBs are constantly forming at the nucleolar periphery and if transcription is inhibited, the pathway of CB maturation is slowed down and consequently more nucleolar-CBs are seen.

The results seen in this study are therefore not consistent with those seen when transcription is inhibited despite there being a decrease in the number of p80 coilin-positive CBs. This is because there was also a decrease in the number of nucleolar-associated CBs in the R6/2 nuclei. The variation in the number of CBs may possibly be related to a change in the requirements of pre-mRNA splicing factors (as snRNP biogenesis is related to the function of CBs) and ribosome synthesis in the R6/2 striatal neurons. Changes in cell size have been reported to influence the number of CBs per nucleus (Pena *et al.,* 2001) and it is reported that there is cell body shrinkage in the R6/2 striatum (A.Raza, personal communications). This decrease in cell size could therefore result in a decrease in the number of CBs.

In R6/2 nuclei, Gemin3 was seen to localise to nuclear foci that resemble the small CBs seen to contain p80 coilin and associate with the nucleolus. When double labelling confocal microscopy was carried out using an antibody against Gemin3 and pyronin Y, it was seen that the small foci were indeed associated with the nucleolus and not free in the nucleoplasm. This finding is surprising as Gemin3 forms part of the SMN complex that is involved in the assembly and re-

import of snRNPs into the nucleus. SMN, Gemin2 and Gemin4 are all seen to colocalise in the NII-associated CB in the R6/2 nuclei together with U2" snRNP. It has been shown that Gemin4 interacts indirectly with SMN to form part of the macromolecular complex via Gemin3. It is therefore intriguing that Gemin4 localises with the other components of the SMN complex without Gemin3.

It has been shown that increased expression of snRNPs is sufficient to cause the formation of CBs in cells that usually lack CBs (Sleeman *et al.,* 2001) and, in SMA, a possible defect in U snRNP assembly and re-assembly may lead to the reduction in the number of gems (Lefebvre *et al.,* 1997 and chapter 1.2.6). The decrease in the number of CBs in the R6/2 nuclei might therefore be related to an impairment or decrease in the biogenesis or expression level of snRNPs. This could be due to the mislocalisation of Gemin3 and the incomplete assembly of a functioning SMN complex, affecting the biogenesis of snRNPs and causing a decrease in the number of CBs. However, even though a decrease in SMN-containing gems was seen in SMA, a decrease in p80 coilin-positive CBs was not reported. The results of this study show no significant difference in the average number of SMN-positive CBs per nucleus for the wild-type neurons and the R6/2 neurons. This suggests that whatever the altered cellular pathway is that contributes to SMA, a different pathway is disrupted in HD.

It has been suggested that an increase in CBs associated with the nucleolus could facilitate the targeting to the nucleolus of components involved in processing of pre-rRNA e.g. fibrillarin, Nopp140 or GAR1, in neurons that have high demands for ribosomes. Therefore, if the inverse is true, the consequence of the decrease in nucleolar CBs seen in the R6/2 nuclei could represent an incorrect targeting of nucleolar proteins away from the nucleolus. The results of this could lead to a disruption of pre-rRNA processing and ribosome biogenesis in the R6/2 nuclei.

From the light microscopy experiments using a number of antibodies against nucleolar proteins, it was possible to see that several nucleolar proteins are also found in CBs in R6/2 striatal nuclei. Fibrillarin, Nopp140 and topoisomerase II were all seen to localise in nucleolar-associated CBs as well as the nucleolus. Fibrillarin and Nopp140 were also seen in nucleoplasmic CBs as well as C23. Double labelling confocal microscopy experiments revealed that fibrillarin

colocalise with p80 coilin in most CBs seen in the R6/2 striatal nuclei whether they were nucleolar-associated or nucleoplasmic.

When the ultrastructural localisation of anti-p80 coilin immunoreactivity was investigated in the R6/2 striatal nuclei, p80 coilin-positive CBs were not only seen at the nucleolar periphery or free in the nucleoplasm but also in a novel localisation: associated with the neuronal intranuclear inclusion (NII) (figure 3.21A). Immunoreactive CBs were seen juxtaposed to the pale, granular inclusion in R6/2 nuclei. The NII-associated CBs were also seen to be immunoreactive for U2" snRNP antibodies (figure 3.21B). When triple labelling immunofluorescence was carried out to ascertain if any of the free CBs, seen with either p80 coilin or SMN immunoreactivity, were in fact NII-associated CBs, this study discovered that 7 out of 10 R6/2 striatal nuclei contained CBs that were associated with NII.

The results from this study can therefore suggest that in the R6/2 nuclei there are two subsets of CBs (figure 4.3). The first subset is a large, prominent nucleoplasmic CB that is the NII-associated CB that contains p80 coilin, SMN, Gemin2, Gemin4, U2" snRNP, fibrillarin, Nopp140 and C23. The second subset is nucleolar-associated and containing p80 coilin, fibrillarin, Nopp140, topoisomerase II, Gemin3 and occasionally SMN. The nucleolar-associated CBs are also seen to vary in size and number per nucleus.

It has been shown that the maturation of snRNPs occurs specifically inside CBs that contain SMN complex (Sleeman *et al.,* 2003) and therefore CBs that lack SMN but contain p80 coilin must be carrying out a different function. It is also proposed that CBs that contain fibrillarin are involved in the biogenesis of nucleolar snoRNPs (Jady *et al.,* 2003). As the NII-associated CB contains both of these proteins it could be suggested that both the biogenesis of snRNPs and snoRNPs could occur in these CBs. Platani *et al.* (2000) also showed that different subsets of CBs exist on a motility level. With small CBs moving faster and over greater distances when compared to larger CBs that appeared to have a more restricted area of movement. It is suggested the latter subset of CBs contains the CBs that have been shown to associate with specific gene loci (snRNA genes and histone genes) (Platani *et al.,* 2000 and chapter 1.4.2). This raises the possibility that the NII-CB could be associated with specific genes.

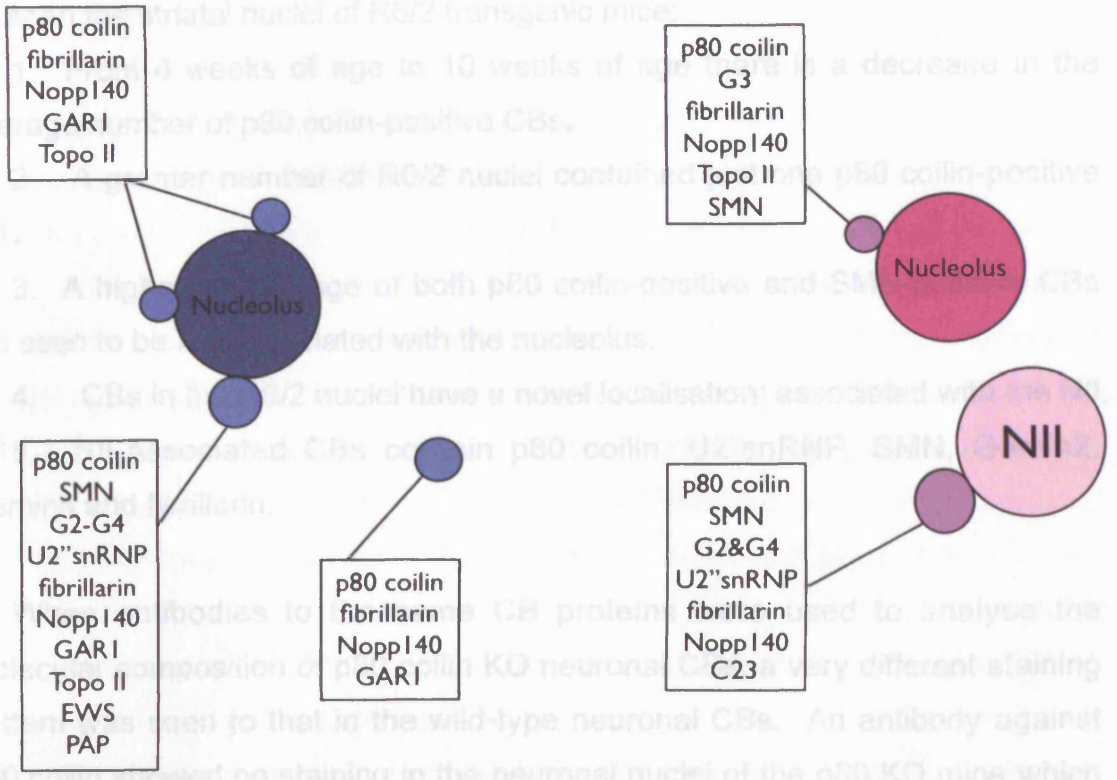

Figure 4.2
A diagram showing the different compositions of different CBs within wild-type (Blue) and R6/2 striatal nuclei (pink).

The association of the NII with the CB could suggest that the CB has moved from its original site, possibly adjacent to the nucleolus, to a new location, juxtaposed to the NII. How this occurred is important, as these two nuclear domains have both been shown to be associated with specific gene loci (chapter 1.1.2 and chapter 1.2.12). There are four models that can explain the new location of the CB in the R6/2 nuclei. The first sees the CB moving from its original site at the periphery of the nucleolus to the NII. The result of which could be loss of association between the CB and the nucleolus. The second model proposes that the NII forms adjacent to the CB and excludes the nucleolus. The consequence of this could be that the nucleolus is then no longer over its normal gene loci. The third and fourth models propose de novo synthesis of a CB adjacent to the NII or synthesis of the NII adjacent to a free

CB. Further investigations will be needed to try and unravel this question.

In summary of the findings of this study a number of alterations to CBs can be seen the striatal nuclei of R6/2 transgenic mice:

1. From 4 weeks of age to 10 weeks of age there is a decrease in the average number of p80 coilin-positive CBs.
2. A greater number of R6/2 nuclei contained just one p80 coilin-positive CB.
3. A higher percentage of both p80 coilin-positive and SMN-positive CBs are seen to be not associated with the nucleolus.
4. CBs in the R6/2 nuclei have a novel localisation: associated with the NII.
5. NII-associated CBs contain p80 coilin, U2"snRNP, SMN, Gemin2, Gemin4 and fibrillarin.

When antibodies to the same CB proteins were used to analyse the molecular composition of p80 coilin KO neuronal CBs, a very different staining pattern was seen to that in the wild-type neuronal CBs. An antibody against p80 coilin showed no staining in the neuronal nuclei of the p80 KO mice which was possibly to be expected as these mice lack 85% of the p80 coilin gene and have been shown to not express no p80 coilin protein (Tucker *et al.*, 2001 and chapter 1.4.3). Antibodies against SMN, Gemin2 and Gemin4 revealed diffuse staining of the nucleoplasm and cytoplasm but did not localise to CBs. In the p80 coilin KO nuclei, U2" snRNP demonstrated a speckled staining pattern and did not obviously localise to any CBs (figure 3.28D). The only nuclear protein seen to localise to the nucleolar-associated CBs in the p80 coilin KO nuclei was fibrillarin. These results are similar to those seen by Tucker *et al.* (2001).

A more recent study on p80 coilin KO mouse embryonic fibroblasts (MEFs) has shown that two types of residual CBs can be identified in these cells (Jady *et al.*, 2003). The first residual CBs seen in the p80 coilin KO nuclei contained fibrillarin, Nopp140 and U3 snoRNA and lacked SMN and snRNPs. The second type of residual CB was shown to accumulate small-Cajal-body-specific RNAs (scaRNAs) and Sm RNAs (snRNAs with a Sm protein binding motif) but not fibrillarin, U3 snoRNA or SMN (Jady *et al.*, 2003). It is suggested that these two types of CBs are either involved in the biogenesis of nucleolar snoRNPs or spliceosomal snRNPs. It is also proposed that p80 coilin plays a role in uniting

the two processes in one structure as in wild-type MEF cells fibrillarin, U3 snoRNA, U2" snRNA, Nopp140 and SMN are all found to colocalise with each other (Tucker *et al.*, 2001; Jady *et al.*, 2003). It also demonstrates that without p80 coilin SMN does not colocalise to either type of residual CB.

Although two types of residual CBs were not seen in the p80 coilin KO nuclei, nucleolar-associated residual CBs were identified that contained fibrillarin and, from the ultrastructural study, these CBs have a similar morphology to that seen in the wild-type striatal nuclei (figure 3.29A). This shows that p80 coilin is not needed to target fibrillarin to nucleolar-associated CBs and that CBs can form at the nucleolar periphery in the absence of the marker protein. This suggests that p80 coilin does not play a structural role in the assembly of CBs or the ultrastructural organisation.

p80 coilin may play a role in the recruiting of SMN and other SMN complex proteins to CBs as without p80 coilin none of the proteins in the SMN complex are seen in the residual CBs. However, the fact that SMN and its associated proteins do not localise together in CBs in the p80 coilin KO nuclei does not appear to affect splicing. This can be seen when the ultrastructure of speckles is analysed in the p80 coilin KO nuclei. It has been shown that when splicing is inhibited in HeLa cells (O'Keefe *et al.*, 1994), speckles, or interchromatin granule clusters (IGCs) become enlarged and more rounded when examined using the electron microscope. The morphology of IGCs in the p80 coilin KO nuclei are similar to that seen in the wild-type nuclei with IGCs not revealing a rounded and enlarged ultrastructure (figure 3.29B). The function of the SMN complex localising with other proteins in CBs may lead to more efficient processing, but is not vital for splicing to occur.

4.2.3 The Molecular Composition of the Speckles

Many pre-mRNA splicing factors have been shown to localise to speckles and, as with the nucleolus and Cajal body, attempts have been made to identify the complete protein composition of speckles using proteomic analysis of an enriched IGC fraction purified from mouse liver cells (Saitoh *et al.*, 2004). 136 proteins have been identified so far and the functions of which are not only related to splicing (chapter 1.3.4).

In this study, only a few of the many proteins that have been shown to localise to speckles and be involved in pre-mRNA splicing have been examined. Antibodies against SC35, HYPA, HYPC and 2,2,7-trimethylguanosine (m3G/TMG) all revealed a punctate nuclear localisation excluding the nucleolus that resembles the characteristic speckled staining pattern (figure 3.13).

In HeLa cells, an antibody to Paraspeckle Protein 1 (PSP1) has been shown to localise to a novel domain termed the paraspeckle that has a close relationship to speckles (Fox et al, 2002). In murine striatal nuclei this antibody revealed a nucleoplasmic staining pattern. When double labelling immunofluorescence was performed using an antibody to PSP1 and an antibody against a protein that is localised to speckles, TMG, both antibodies showed a nuclear distribution, but when the images were overlaid only a small area of co-localisation was seen (figure 3.14). This finding demonstrates that murine striatal neuronal nuclei, PSP1 is not localised to speckles. The staining pattern seen for PSP1 did not resemble the punctate pattern seen by Fox *et al.* (2002) in HeLa cells but does suggest that paraspeckles are a separate nuclear domain from speckles. Other proteins have been shown to localise in paraspeckles and they include PSP2 and p54/nrb. PSP1 has no known function whereas p54/nrb is a multifunctional protein that is implicated in transcriptional regulation, splicing, and apoptosis. PSP2 has been identified as a "co-activator activator" (Fox *et al.,* 2002). Therefore, the paraspeckle is implicated in transcriptional control.

The distribution of the same proteins was examined in R6/2 striatal nuclei and for some proteins a difference was seen. Immunocytochemistry using the monoclonal antibody against splicing factor SC35 did not show the usual 'speckled' pattern of staining, instead, a diffuse nucleoplasmic pattern was seen and antibodies against HYPA and HYPC revealed infrequent speckle staining with many nuclei only exhibiting a nucleoplasmic staining pattern (figure 3.27). Immunoreactivity for TMG, however, did reveal the characteristic speckled staining pattern that excludes the nucleolus.

It has been shown that huntingtin (htt) interacts with HYPA and HYPC, both of which are WW domain proteins, and, these interactions are increased as the polyglutamine repeat increases (Faber *et al.* 1998). HYPA and HYPC are known to be involved in pre-mRNA splicing (Passani *et al.* 2000). The findings

of this study that in many R6/2 nuclei, HYPA and HYPC are not so frequently localised to speckles, but are in fact found to have a mostly nucleoplasmic distribution could suggest that mutant htt not only affects the interactions of the HYP proteins, but the increase in polyglutamine length may also affect the subnuclear distribution of these proteins. A study by Kegel *et al.* (2001) revealed that full length wild-type htt localised to speckles in a transcription independent manner and therefore, the redistribution of htt to the NII may result in the incorrect targeting of other proteins away from speckles. The change in distribution of the HYP proteins and SC35 could suggest that altered mRNA processing and processing may play a role in HD pathogenesis.

Alternatively, the redistribution of SC35 and the HYP proteins may be caused by a disruption to a different cellular pathway. It has been shown that the overexpression of specific kinases, Clk/STY and DYRK1A, both cause the disassembly of speckles and interchromatin granule clusters (IGCs) (Colwill *et al.,* 1996; Sacco-Bubulya and Spector, 2002; Alvarez *et al.,* 2003). These results support the idea that the phosphorylation of SR protein splicing factors leads to their release from speckles and their recruitment to transcription sites (chapter 1.3.8). However, the study by Sacco-Bubulya and Spector (2002) also revealed that all speckle proteins examined redistributed to the nucleoplasm after the overexpression of Clk/STY and electron microscopy showed that speckles/IGCs were no longer found in treated cells and the IGCs had completely disassembled. This is not conclusive with the results of this study for two reasons. Firstly, not all speckle proteins redistributed as TMG still revealed a speckled staining pattern, and secondly, at the ultrastructural level, IGCs could still be distinguished in the R6/2 nuclei.

Okadaic acid treatment, which inhibits serine-threonine protein phosphatases, also causes a redistribution of splicing factors. Misteli *et al.* (1997) revealed that splicing factor, ASF/SF2, shows a more diffuse, nucleoplasmic staining pattern after treatment with okadaic acid. A similar staining pattern is also seen when HeLa cells are treated by heat shock, causing most of RNA polymerase II transcription to be inhibited and an induction of 'heat shock' genes (Carmo-Fonseca *et al.,* 1992). A similar distribution of splicing factors was seen during the late recovery phase of neuronal stress response in rat SON neurons (Lafarga *et al.,* 1998) when there

is an increase in the transcription of neurohormones. IGCs of the SON neurons were seen to be very small. These findings have led to the theory that actively transcribing cells are seen to have predominantly dispersed splicing factors throughout the nucleoplasm.

When all RNA polymerase transcription is inhibited in HeLa cells using Actinomycin D or α-amanitin, speckles are seen to decrease in number and become larger in size (Misteli *et al.,* 1997). A similar distribution of splicing factors is seen when cells are treated with the protein and rRNA synthesis inhibitor, cycloheximide. Therefore the nucleoplasmic redistribution of splicing factors seen in the R6/2 striatal nuclei in this work, could suggests that these nuclei are transcriptionally very active and protein synthesis is not affected.

When the localisation of the paraspeckle protein, Paraspeckle Protein 1 (PSP1) was examined in R6/2 striatal nuclei using double labelling immunofluorescence a similar staining pattern was seen to that in wild-type nuclei (figure 3.28). It was possible to see that the R6/2 nuclei did contain paraspeckles as a separate domain from speckles as the immunofluorescence for PSP1 only colocalised in small areas at the periphery of speckles. PSP1 has been shown to relocalise to nucleolar cap structures after transcription is arrested in HeLa cells (Fox *et al.,* 2002) and as this relocalisation of PSP1 is not seen in the R6/2 nuclei, this supports the idea that the transcription is not inhibited in these nuclei.

4.3 Conclusions

The findings of this study have demonstrated that by analysing the ultrastructure of nuclei in murine striatal neurons in conjunction with the distribution of specific nuclear proteins, an understanding of the metabolic activity of a given neuron can be ascertained. The ultrastructure and molecular composition of the three subdomains examined have previously been shown to alter in response to changes in metabolic activity (chapter 1.4) and these changes have been well documented.

The findings of this study show that subdomains within neuronal nuclei have specific spatial and molecular relationships with each other that despite the fact

that they are similar to those reported in cultured cells, there are characteristics that reveal an organisation that is specific for striatal nuclei.

This detailed analysis of murine striatal nuclei has created a three dimensional guide. This has then been used to directly compare the nuclear organisation within the same type of neuron but in a mouse model of Huntington's disease: a disease that already has documented nuclear changes (chapter 1.6.5). In comparing the wild-type organisation to the organisation of the R6/2 nuclei, a number of differences, ultrastructurally and molecularly, have been seen. This has given some insights into the mechanisms underlying the pathology of HD.

A suggested mechanism of pathology in HD involves the regulation of transcription (chapter 1.6.7). This is because research has shown that htt may play a role in transcription: it has been shown that htt, both wild-type and mutant, interacts with a number of factors involved in transcription (chapter 1.6.3) and that microarray analysis has shown some transcriptional pathways are altered in HD (Luthi-Carter *et al.,* 2000 and chapter 1.6.8). The current view of transcriptional dysregulation in HD, more often than not, proposes a downregulation of transcription due to either sequestration of transcription factors into NIIs or gene chip analysis that shows a downregulation in the expression of some genes but an increase in other genes. Altered protein-protein interactions are also implicated in transcriptional dysregulation as it has been shown that mutant htt disrupts normal binding between some transcription factors.

Actinomycin D has been widely used to inhibit transcription in cultured cells and many of these studies have described the altered localisations of many nuclear proteins. I have produced a diagrammatic representation of these changes (figure 4.3) and have used this as a guide to show the relocalisation of nuclear proteins when transcription is inhibited. The belief being that if transcription is inhibited or downregulated in HD, a similar redistribution of nuclear proteins would be seen. However, the results from this study do not support the idea of transcriptional downregulation in HD due to a number of findings that have also been summarised in a diagram (figure 4.4).

4.3.1 The Nucleolus

The changes seen in R6/2 nucleoli did not resemble the alterations documented in cells were transcription had been inhibited (Reynolds *et al.*, 1964). Ultrastructurally only 21% of nucleoli showed a different morphology to those seen in the wild-type nuclei and this ultrastructure bared a resemblance to that reported in cells that had been treated with a protein synthesis inhibitor and not an inhibitor of transcription (Lafarga *et al.*, 1994). This finding was also supported by the molecular study of the R6/2 nucleoli as nucleolar proteins were seen to localise to the nucleolus in a similar pattern seen in the wild-type neurons. It has been shown that in cells treated with transcriptional inhibitors, nucleolar proteins showed altered distribution patterns (chapter 1.4.1 and figure 4.3).

4.3.2 The Cajal Body

A more dramatic difference was seen when the Cajal body was investigated in the R6/2 nuclei. Ultrastructurally there was no difference between the morphology of CBs in the wild-type nuclei and those in the R6/2 nuclei, regardless of their localisation. However, CBs were seen in a novel localisation juxtaposed to the NII. When the molecular composition of the CBs was examined, the results showed that there was a decrease in the average number of p80 coilin-positive CBs in the R6/2 nuclei but not a decrease in the average number of CBs that contain other CB proteins e.g. SMN and U2" snRNP. When transcription is inhibited in cultured cells, it has been demonstrated that there is a decrease in the overall number of CBs and p80 coilin is seen to redistribute to small nucleolar-associated CBs and snRNPs are localised only to speckles (chapter 1.4.2).

The decrease in number of p80 coilin-positive CBs could reflect a decrease in cell size. The relocation of the CB to the periphery of the NII could affect the targeting of nucleolar proteins and in turn affect rRNA processing. In R6/2 there are 2 subsets of CBs (figure 4.2) –

1. Nucleolar-associated CB containing p80 coilin, fibrillarin, Nopp140, topoisomerase II, Gemin3 and infrequently SMN that vary in number and size.

2. NII-associated CB that contains p80 coilin, SMN, Gemin2, Gemin4, U2" snRNP, fibrillarin, Nopp140 and C23, and, that only one is present per nucleus and all have similar size.

4.3.3 Speckles

The ultrastructural and molecular analysis of speckles in the R6/2 nuclei also produced results that did not resemble those seen in cells treated with drugs that inhibited transcription (Misteli *et al.,* 1997). The loss of splicing factors from speckles in the R6/2 nuclei has previously been reported in transcriptionally very active cells.

The results of this study do suggest that in HD there is a more dramatic nuclear rearrangement than was first reported (Davies *et al.,* 1997) and that this affects three important subdomains: the nucleolus, the Cajal body and the speckles. How the reorganisation of the architecture of the striatal nucleus in this model of HD is caused is yet to be understood but future studies may help us gain a better insight.

Excellent.

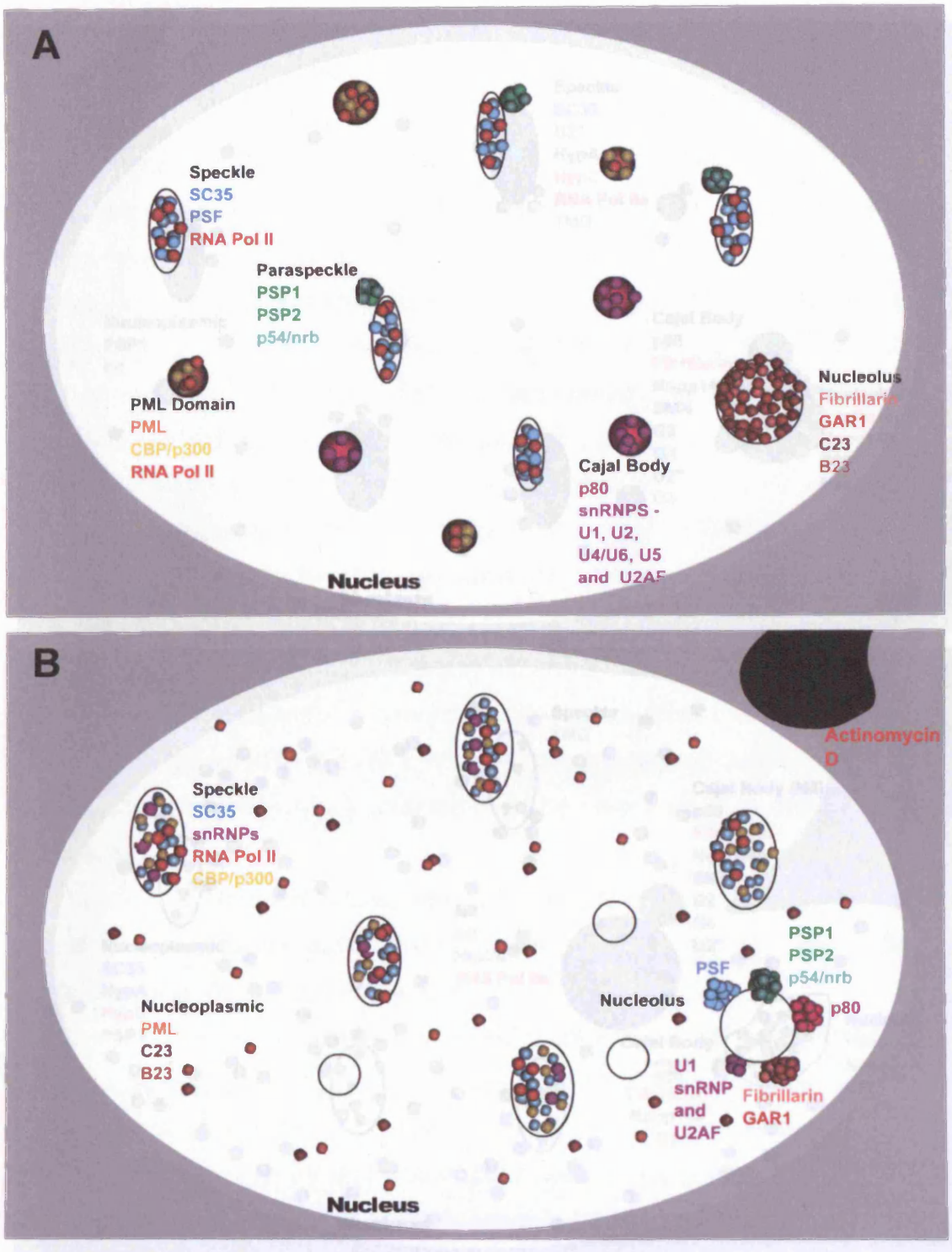

Figure 4.3
A schematic diagram showing the distribution of nuclear proteins in a cultured cell nucleus (A) and the redistribution of the same nuclear proteins after treatment with the transcription inhibitor, Actinomycin D (B). A Quicktime movie of this relocalisation is included in Appendix I.

Excellent.

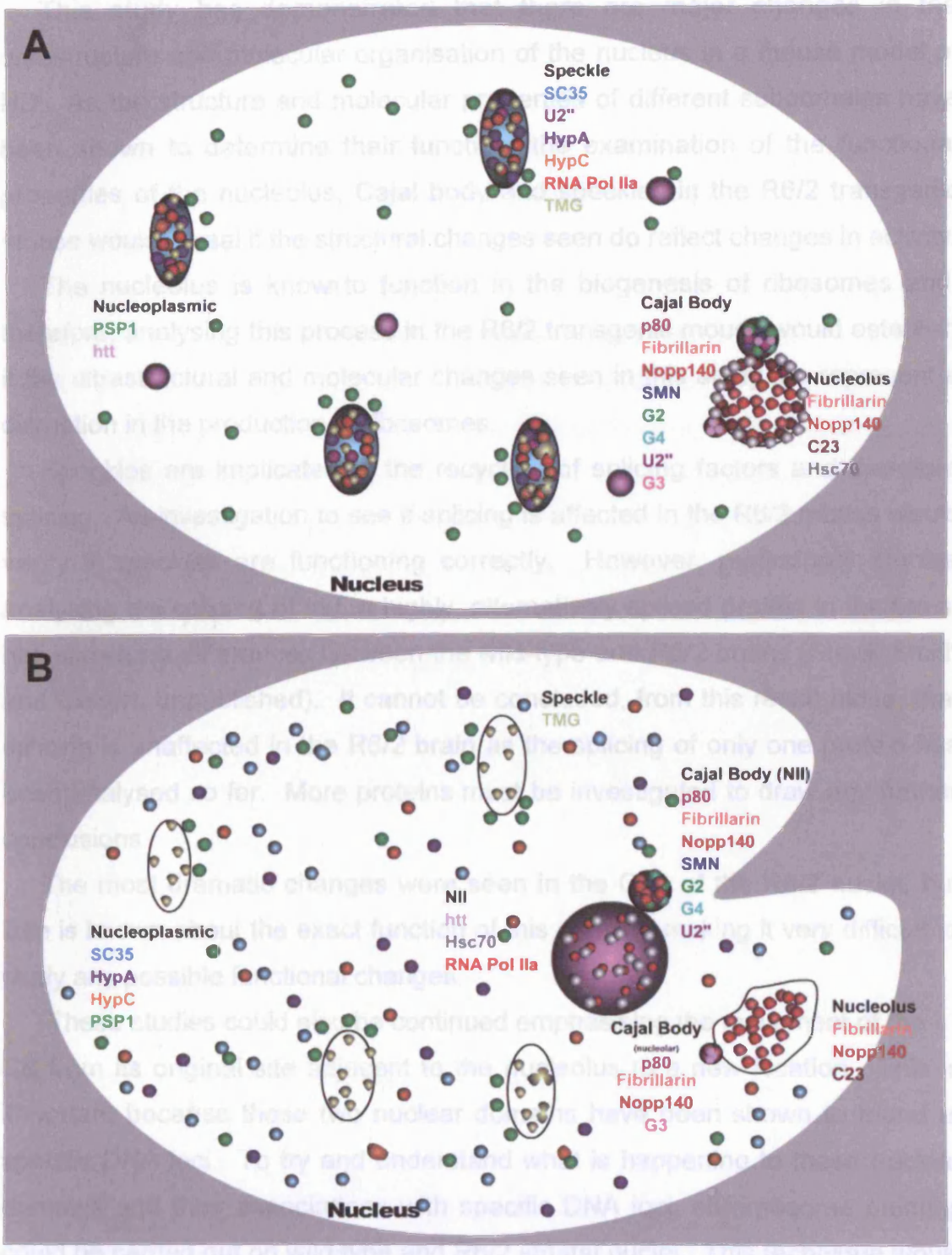

Figure 4.4
A schematic diagram showing the distribution of nuclear proteins in a striatal nucleus (A) and the redistribution of the same nuclear proteins in a 10 week old R6/2 transgenic mouse (B) that is a model of HD. A Quicktime movie of this relocalisation is included in Appendix I

4.4 Future Studies

This study has demonstrated that there are major changes in the ultrastructure and molecular organisation of the nucleus in a mouse model of HD. As the structure and molecular properties of different subdomains have been shown to determine their function, the examination of the functional properties of the nucleolus, Cajal body and speckles in the R6/2 transgenic mouse would reveal if the structural changes seen do reflect changes in activity.

The nucleolus is known to function in the biogenesis of ribosomes and, therefore, analysing this process in the R6/2 transgenic mouse would establish if the ultrastructural and molecular changes seen in this study, do represent a disruption in the production of ribosomes.

Speckles are implicated in the recycling of splicing factors and therefore splicing. An investigation to see if splicing is affected in the R6/2 mouse would verify if speckles are functioning correctly. However, preliminary studies analysing the splicing of tau, a highly, alternatively spliced protein in the brain, has shown no differences between the wild-type and R6/2 brains (Slavik-Smith and Godert, unpublished). It cannot be concluded, from this result alone, that splicing is unaffected in the R6/2 brain as the splicing of only one protein has been analysed so far. More proteins must be investigated to draw any further conclusions.

The most dramatic changes were seen in the CBs of the R6/2 nuclei, but little is known about the exact function of this domain, making it very difficult to study any possible functional changes.

These studies could also be continued emphasising the movement of the CB from its original site adjacent to the nucleolus to a new location. This is important because these two nuclear domains have been shown to found at specific DNA loci. To try and understand what is happening to these nuclear domains and their associations with specific DNA loci, chromosome painting could be carried out on wild-type and R6/2 striatal nuclei. This technique would permit the identification of different gene loci or individual chromosomes using biotinylated DNA probes. After hybridisation, the loci can then be detected with fluorescent avidin conjugates and the relationship between the domain and the loci can be examined (Cremer *et al.*, 1988).

In addition to these experiments it will be important to continue with the molecular characterisation of the nucleolus, Cajal body and speckles in the R6/2 striatal nuclei. In 2002, a proteomic analysis of the nucleolus was carried out (Andersen *et al.*, 2002) and since then the isolation and proteomic analysis of CBs and speckles have also been achieved. It would be interesting to try and repeat these proteomic experiments for striatal nuclei from wild-type mice and compare the molecular composition of each domain with the same domain from the R6/2 striatal nuclei and the NII.

Analysing transcription in wild-type and R6/2 neurons would be another process to examine. Actual sites of transcription can be visualised using Bromo-UTP uptake experiments (Cmarko *et al.*, 1999) or by the distribution of different transcription factors in the nucleus (Grande *et al.*, 1997). It would also be interesting to see what happens when transcription is inhibited in a mouse neuron by treatment with either Actinomycin D, α-amanitin or DRB.

Hopefully these lines of investigation will help explain part of the pathogenic mechanism in Huntington's disease. It will also give valuable insights into the dynamic nature of the neuronal nucleus.

References

CHAPTER 5

References

Abbott, J., Marzluff, W. F. and Gall, J. G. (1999). The stem-loop binding protein (SLBP1) is present in coiled bodies of the Xenopus germinal vesicle. *Mol Biol Cell* **10**, 487-99.

Alliegro, M. C. and Alliegro, M. A. (1998). Protein heterogeneity in the coiled body compartment. *Exp Cell Res* **239**, 60-8.

Almeida, F., Saffrich, R., Ansorge, W. and Carmo-Fonseca, M. (1998). Microinjection of anti-coilin antibodies affects the structure of coiled bodies. *J Cell Biol* **142**, 899-912.

Alvarez, M., Estivill, X. and de la Luna, S. (2003). DYRK1A accumulates in splicing speckles through a novel targeting signal and induces speckle disassembly. *J Cell Sci* **116**, 3099-107.

Ambrose, C. M., Duyao, M. P., Barnes, G., Bates, G. P., Lin, C. S., Srinidhi, J., Baxendale, S., Hummerich, H., Lehrach, H., Altherr, M. et al. (1994). Structure and expression of the Huntington's disease gene: evidence against simple inactivation due to an expanded CAG repeat. *Somat Cell Mol Genet* **20**, 27-38.

Andersen, L. and Keiding, N. (1990). Size of the fibrillar centres of the nucleoli in the supraoptic nucleus of the rat taking the Swiss cheese effect into account. *Acta Anat (Basel)* **138**, 348-51.

Andersen, L. (1990). Number, volume and size distribution of nucleoli in rat neurosecretory cells with suppressed and stimulated secretion. *Acta Anat (Basel)* **137**, 311-5.

Andersen, J. S., Lyon, C. E., Fox, A. H., Leung, A. K., Lam, Y. W., Steen, H., Mann, M. and Lamond, A. I. (2002). Directed proteomic analysis of the human nucleolus. *Curr Biol* **12**, 1-11.

Andersen, J. S., Lam, Y. W., Leung, A. K., Ong, S. E., Lyon, C. E., Lamond, A. I. and Mann, M. (2005). Nucleolar proteome dynamics. *Nature* **433**, 77-83.

Andrade, L. E., Chan, E. K., Raska, I., Peebles, C. L., Roos, G. and Tan, E. M. (1991). Human autoantibody to a novel protein of the nuclear coiled body: immunological characterization and cDNA cloning of p80-coilin. *J Exp Med* **173**, 1407-19.

Andrade, L. E., Tan, E. M. and Chan, E. K. (1993). Immunocytochemical analysis of the coiled body in the cell cycle and during cell proliferation. *Proc Natl Acad Sci U S A* **90**, 1947-51.

Andrew, S. E., Goldberg, Y. P., Kremer, B., Telenius, H., Theilmann, J., Adam, S., Starr, E., Squitieri, F., Lin, B., Kalchman, M. A. et al. (1993). The relationship between trinucleotide (CAG) repeat length and clinical features of Huntington's disease. *Nat Genet* **4**, 398-403.

Baccon, J., Pellizzoni, L., Rappsilber, J., Mann, M. and Dreyfuss, G. (2002). Identification and characterization of Gemin7, a novel component of the survival of motor neuron complex. *J Biol Chem* **277**, 31957-62.

Bates, G. P., Mangiarini, L., Mahal, A. and Davies, S. W. (1997). Transgenic models of Huntington's disease. *Hum Mol Genet* **6**, 1633-7.

Bates, G. P., Mangiarini, L., Wanker, E. E. and Davies, S. W. (1998). Polyglutamine expansion and Huntington's disease. *Biochem Soc Trans* **26**, 471-5.

Bauer, D. W., Murphy, C., Wu, Z., Wu, C. H. and Gall, J. G. (1994). In vitro assembly of coiled bodies in Xenopus egg extract. *Mol Biol Cell* **5**, 633-44.

Bauer, D. W. and Gall, J. G. (1997). Coiled bodies without coilin. *Mol Biol Cell* **8**, 73-82.

Baxendale, S., MacDonald, M. E., Mott, R., Francis, F., Lin, C., Kirby, S. F., James, M., Zehetner, G., Hummerich, H., Valdes, J. et al. (1993). A cosmid contig and high resolution restriction map of the 2 megabase region containing the Huntington's disease gene. *Nat Genet* **4**, 181-6.

Becher, M. W., Kotzuk, J. A., Sharp, A. H., Davies, S. W., Bates, G. P., Price, D. L. and Ross, C. A. (1998). Intranuclear neuronal inclusions in Huntington's disease and dentatorubral and pallidoluysian atrophy: correlation between the density of inclusions and IT15 CAG triplet repeat length. *Neurobiol Dis* **4**, 387-97.

Bellini, M. and Gall, J. G. (1998). Coilin can form a complex with the U7 small nuclear ribonucleoprotein. *Mol Biol Cell* **9**, 2987-3001.

Berciano, M. T., Villagra, N. T., Pena, E., Navascues, J., Casafont, I. and Lafarga, M. (2002). Structural and functional compartmentalization of the cell nucleus in supraoptic neurons. *Microsc Res Tech* **56**, 132-42.

Bergin, A., Kim, G., Price, D. L., Sisodia, S. S., Lee, M. K. and Rabin, B. A. (1997). Identification and characterization of a mouse homologue of the spinal muscular atrophy-determining gene, survival motor neuron. *Gene* **204**, 47-53.

Bessert, D. A., Gutridge, K. L., Dunbar, J. C. and Carlock, L. R. (1995). The identification of a functional nuclear localization signal in the Huntington disease protein. *Brain Res Mol Brain Res* **33**, 165-73.

Beven, A. F., Simpson, G. G., Brown, J. W. and Shaw, P. J. (1995). The organization of spliceosomal components in the nuclei of higher plants. *J Cell Sci* **108 (Pt 2)**, 509-18.

Biggiogera, M., Malatesta, M., Abolhassani-Dadras, S., Amalric, F., Rothblum, L. I. and Fakan, S. (2001). Revealing the unseen: the organizer region of the nucleolus. *J Cell Sci* **114**, 3199-205.

Bohmann, K., Ferreira, J. A. and Lamond, A. I. (1995a). Mutational analysis of p80 coilin indicates a functional interaction between coiled bodies and the nucleolus. *J Cell Biol* **131**, 817-31.

Bohmann, K., Ferreira, J., Santama, N., Weis, K. and Lamond, A. I. (1995b). Molecular analysis of the coiled body. *J Cell Sci Suppl* **19**, 107-13.

Bolam, J. P., Somogyi, P., Takagi, H., Fodor, I. and Smith, A. D. (1983). Localization of substance P-like immunoreactivity in neurons and nerve terminals in the neostriatum of the rat: a correlated light and electron microscopic study. *J Neurocytol* **12**, 325-44.

Boutell, J. M., Thomas, P., Neal, J. W., Weston, V. J., Duce, J., Harper, P. S. and Jones, A. L. (1999). Aberrant interactions of transcriptional repressor proteins with the Huntington's disease gene product, huntingtin. *Hum Mol Genet* **8**, 1647-55.

Brasch, K. and Ochs, R. L. (1992). Nuclear bodies (NBs): a newly "rediscovered" organelle. *Exp Cell Res* **202**, 211-23.

Bregman, D. B., Du, L., van der Zee, S. and Warren, S. L. (1995). Transcription-dependent redistribution of the large subunit of RNA polymerase II to discrete nuclear domains. *J Cell Biol* **129**, 287-98.

Brinkman, R. R., Mezei, M. M., Theilmann, J., Almqvist, E. and Hayden, M. R. (1997). The likelihood of being affected with Huntington disease by a particular age, for a specific CAG size. *Am J Hum Genet* **60**, 1202-10.

Buckwalter, C. A., Lin, A. H., Tanizawa, A., Pommier, Y. G., Cheng, Y. C. and Kaufmann, S. H. (1996). RNA synthesis inhibitors alter the subnuclear distribution of DNA topoisomerase I. *Cancer Res* **56**, 1674-81.

Burghes, A. H., Ingraham, S. E., Kote-Jarai, Z., Rosenfeld, S., Herta, N., Nadkarni, N., DiDonato, C. J., Carpten, J., Hurko, O., Florence, J. et al. (1994). Linkage mapping of the spinal muscular atrophy gene. *Hum Genet* **93**, 305-12.

Caceres, J. F., Misteli, T., Screaton, G. R., Spector, D. L. and Krainer, A. R. (1997). Role of the modular domains of SR proteins in subnuclear localization and alternative splicing specificity. *J Cell Biol* **138**, 225-38.

Campbell, L., Hunter, K. M., Mohaghegh, P., Tinsley, J. M., Brasch, M. A. and Davies, K. E. (2000). Direct interaction of Smn with dp103, a putative RNA helicase: a role for Smn in transcription regulation? *Hum Mol Genet* **9**, 1093-100.

Campuzano, V., Montermini, L., Molto, M. D., Pianese, L., Cossee, M., Cavalcanti, F., Monros, E., Rodius, F., Duclos, F., Monticelli, A. et al. (1996). Friedreich's ataxia: autosomal recessive disease caused by an intronic GAA triplet repeat expansion. *Science* **271**, 1423-7.

Cancel, G., Duyckaerts, C., Holmberg, M., Zander, C., Yvert, G., Lebre, A. S., Ruberg, M., Faucheux, B., Agid, Y., Hirsch, E. et al. (2000). Distribution of ataxin-7 in normal human brain and retina. *Brain* **123 Pt 12**, 2519-30.

Carmo-Fonseca, M., Pepperkok, R., Sproat, B. S., Ansorge, W., Swanson, M. S. and Lamond, A. I. (1991a). In vivo detection of snRNP-rich organelles in the nuclei of mammalian cells. *Embo J* **10**, 1863-73.

Carmo-Fonseca, M., Tollervey, D., Pepperkok, R., Barabino, S. M., Merdes, A., Brunner, C., Zamore, P. D., Green, M. R., Hurt, E. and Lamond, A. I. (1991b). Mammalian nuclei contain foci which are highly enriched in components of the pre-mRNA splicing machinery. *Embo J* **10**, 195-206.

Carmo-Fonseca, M., Pepperkok, R., Carvalho, M. T. and Lamond, A. I. (1992). Transcription-dependent colocalization of the U1, U2, U4/U6, and U5 snRNPs in coiled bodies. *J Cell Biol* **117**, 1-14.

Carmo-Fonseca, M., Ferreira, J. and Lamond, A. I. (1993). Assembly of snRNP-containing coiled bodies is regulated in interphase and mitosis--evidence that the coiled body is a kinetic nuclear structure. *J Cell Biol* **120**, 841-52.

Carmo-Fonseca, M., Mendes-Soares, L. and Campos, I. (2000). To be or not to be in the nucleolus. *Nat Cell Biol* **2**, E107-12.

Carter, K. C., Taneja, K. L. and Lawrence, J. B. (1991). Discrete nuclear domains of poly(A) RNA and their relationship to the functional organization of the nucleus. *J Cell Biol* **115**, 1191-202.

Carvalho, T., Almeida, F., Calapez, A., Lafarga, M., Berciano, M. T. and Carmo-Fonseca, M. (1999). The spinal muscular atrophy disease gene product, SMN: A link between snRNP biogenesis and the Cajal (coiled) body. *J Cell Biol* **147**, 715-28.

Casanova, E., Alonso-Llamazares, A., Zamanillo, D., Garate, C., Calvo, P. and Chinchetru, M. A. (1996). Identification of a long huntingtin mRNA transcript in mouse brain. *Brain Res* **743**, 320-3.

Ceman, S., Brown, V. and Warren, S. T. (1999). Isolation of an FMRP-associated messenger ribonucleoprotein particle and identification of nucleolin and the fragile X-related proteins as components of the complex. *Mol Cell Biol* **19**, 7925-32.

Cha, J. H. (2000). Transcriptional dysregulation in Huntington's disease. *Trends Neurosci* **23**, 387-92.

Chai, Y., Koppenhafer, S. L., Shoesmith, S. J., Perez, M. K. and Paulson, H. L. (1999). Evidence for proteasome involvement in polyglutamine disease: localization to nuclear inclusions in SCA3/MJD and suppression of polyglutamine aggregation in vitro. *Hum Mol Genet* **8**, 673-82.

Chai, Y., Wu, L., Griffin, J. D. and Paulson, H. L. (2001). The role of protein composition in specifying nuclear inclusion formation in polyglutamine disease. *J Biol Chem* **276**, 44889-97.

Chakarova, C. F., Hims, M. M., Bolz, H., Abu-Safieh, L., Patel, R. J., Papaioannou, M. G., Inglehearn, C. F., Keen, T. J., Willis, C., Moore, A. T. et al. (2002). Mutations in HPRP3, a third member of pre-mRNA splicing factor genes, implicated in autosomal dominant retinitis pigmentosa. *Hum Mol Genet* **11**, 87-92.

Chan, E. K., Takano, S., Andrade, L. E., Hamel, J. C. and Matera, A. G. (1994). Structure, expression and chromosomal localization of human p80-coilin gene. *Nucleic Acids Res* **22**, 4462-9.

Chan, E. Y., Luthi-Carter, R., Strand, A., Solano, S. M., Hanson, S. A., DeJohn, M. M., Kooperberg, C., Chase, K. O., DiFiglia, M., Young, A. B. et al. (2002). Increased huntingtin protein length reduces the number of polyglutamine-induced gene expression changes in mouse models of Huntington's disease. *Hum Mol Genet* **11**, 1939-51.

Charroux, B., Pellizzoni, L., Perkinson, R. A., Shevchenko, A., Mann, M. and Dreyfuss, G. (1999). Gemin3: A novel DEAD box protein that interacts with SMN, the spinal muscular atrophy gene product, and is a component of gems. *J Cell Biol* **147**, 1181-94.

Charroux, B., Pellizzoni, L., Perkinson, R. A., Yong, J., Shevchenko, A., Mann, M. and Dreyfuss, G. (2000). Gemin4. A novel component of the SMN complex that is found in both gems and nucleoli. *J Cell Biol* **148**, 1177-86.

Chen, H. K., Fernandez-Funez, P., Acevedo, S. F., Lam, Y. C., Kaytor, M. D., Fernandez, M. H., Aitken, A., Skoulakis, E. M., Orr, H. T., Botas, J. et al. (2003). Interaction of Akt-phosphorylated ataxin-1 with 14-3-3 mediates neurodegeneration in spinocerebellar ataxia type 1. *Cell* **113**, 457-68.

Cmarko, D., Verschure, P. J., Martin, T. E., Dahmus, M. E., Krause, S., Fu, X. D., van Driel, R. and Fakan, S. (1999). Ultrastructural analysis of transcription and splicing in the cell nucleus after bromo-UTP microinjection. *Mol Biol Cell* **10**, 211-23.

Cmarko, D., Verschure, P. J., Rothblum, L. I., Hernandez-Verdun, D., Amalric, F., van Driel, R. and Fakan, S. (2000). Ultrastructural analysis of nucleolar transcription in cells microinjected with 5-bromo-UTP. *Histochem Cell Biol* **113**, 181-7.

Colwill, K., Pawson, T., Andrews, B., Prasad, J., Manley, J. L., Bell, J. C. and Duncan, P. I. (1996). The Clk/Sty protein kinase phosphorylates SR splicing factors and regulates their intranuclear distribution. *Embo J* **15**, 265-75.

Coovert, D. D., Le, T. T., McAndrew, P. E., Strasswimmer, J., Crawford, T. O., Mendell, J. R., Coulson, S. E., Androphy, E. J., Prior, T. W. and Burghes, A. H. (1997). The survival motor neuron protein in spinal muscular atrophy. *Hum Mol Genet* **6**, 1205-14.

Cremer, T., Lichter, P., Borden, J., Ward, D. C. and Manuelidis, L. (1988). Detection of chromosome aberrations in metaphase and interphase tumor cells by in situ hybridization using chromosome-specific library probes. *Hum Genet* **80**, 235-46.

Cummings, C. J. and Zoghbi, H. Y. (2000). Fourteen and counting: unraveling trinucleotide repeat diseases. *Hum Mol Genet* **9**, 909-16.

David, G., Abbas, N., Stevanin, G., Durr, A., Yvert, G., Cancel, G., Weber, C., Imbert, G., Saudou, F., Antoniou, E. et al. (1997). Cloning of the SCA7 gene reveals a highly unstable CAG repeat expansion. *Nat Genet* **17**, 65-70.

Davies, J., Yamagata, H., Shelbourne, P., Buxton, J., Ogihara, T., Nokelainen, P., Nakagawa, M., Williamson, R., Johnson, K. and Miki, T. (1992). Comparison of the myotonic dystrophy associated CTG repeat in European and Japanese populations. *J Med Genet* **29**, 766-9.

Davies, S. W., Turmaine, M., Cozens, B. A., DiFiglia, M., Sharp, A. H., Ross, C. A., Scherzinger, E., Wanker, E. E., Mangiarini, L. and Bates, G. P. (1997). Formation of neuronal intranuclear inclusions underlies the neurological dysfunction in mice transgenic for the HD mutation. *Cell* **90**, 537-48.

Davies, S. W., Sathasivam, K., Hobbs, C., Doherty, P., Mangiarini, L., Scherzinger, E., Wanker, E. E. and Bates, G. P. (1999). Detection of polyglutamine aggregation in mouse models. *Methods Enzymol* **309**, 687-701.

De Rooij, K. E., Dorsman, J. C., Smoor, M. A., Den Dunnen, J. T. and Van Ommen, G. J. (1996). Subcellular localization of the Huntington's disease gene product in cell lines by immunofluorescence and biochemical subcellular fractionation. *Hum Mol Genet* **5**, 1093-9.

Derenzini, M. and Ploton, D. (1991). Interphase nucleolar organizer regions in cancer cells. *Int Rev Exp Pathol* **32**, 149-92.

Derenzini, M., Trere, D., Pession, A., Govoni, M., Sirri, V. and Chieco, P. (2000). Nucleolar size indicates the rapidity of cell proliferation in cancer tissues. *J Pathol* **191**, 181-6.

DiFiglia, M., Sapp, E., Chase, K., Schwarz, C., Meloni, A., Young, C., Martin, E., Vonsattel, J. P., Carraway, R., Reeves, S. A. et al. (1995). Huntingtin is a cytoplasmic protein associated with vesicles in human and rat brain neurons. *Neuron* **14**, 1075-81.

DiFiglia, M., Sapp, E., Chase, K. O., Davies, S. W., Bates, G. P., Vonsattel, J. P. and Aronin, N. (1997). Aggregation of huntingtin in neuronal intranuclear inclusions and dystrophic neurites in brain. *Science* **277**, 1990-3.

Dubowitz, V. (1995). Chaos in the classification of SMA: a possible resolution. *Neuromuscul Disord* **5**, 3-5.

Dunah, A. W., Jeong, H., Griffin, A., Kim, Y. M., Standaert, D. G., Hersch, S. M., Mouradian, M. M., Young, A. B., Tanese, N. and Krainc, D. (2002). Sp1 and TAFII130 transcriptional activity disrupted in early Huntington's disease. *Science* **296**, 2238-43.

Dundr, M. and Misteli, T. (2001). Functional architecture in the cell nucleus. *Biochem J* **356**, 297-310.

Dundr, M. and Misteli, T. (2002). Nucleolomics: an inventory of the nucleolus. *Mol Cell* **9**, 5-7.

Duyao, M. P., Auerbach, A. B., Ryan, A., Persichetti, F., Barnes, G. T., McNeil, S. M., Ge, P., Vonsattel, J. P., Gusella, J. F., Joyner, A. L. et al. (1995). Inactivation of the mouse Huntington's disease gene homolog Hdh. *Science* **269**, 407-10.

Dye, B. T. and Patton, J. G. (2001). An RNA recognition motif (RRM) is required for the localization of PTB-associated splicing factor (PSF) to subnuclear speckles. *Exp Cell Res* **263**, 131-44.

Eilbracht, J. and Schmidt-Zachmann, M. S. (2001). Identification of a sequence element directing a protein to nuclear speckles. *Proc Natl Acad Sci U S A* **98**, 3849-54.

Eils, R., Gerlich, D., Tvarusko, W., Spector, D. L. and Misteli, T. (2000). Quantitative imaging of pre-mRNA splicing factors in living cells. *Mol Biol Cell* **11**, 413-8.

Faber, P. W., Barnes, G. T., Srinidhi, J., Chen, J., Gusella, J. F. and MacDonald, M. E. (1998). Huntingtin interacts with a family of WW domain proteins. *Hum Mol Genet* **7**, 1463-74.

Fakan, S. and Bernhard, W. (1971). Localisation of rapidly and slowly labelled nuclear RNA as visualized by high resolution autoradiography. *Exp Cell Res* **67**, 129-41.

Fakan, S., Leser, G. and Martin, T. E. (1984). Ultrastructural distribution of nuclear ribonucleoproteins as visualized by immunocytochemistry on thin sections. *J Cell Biol* **98**, 358-63.

Fakan, S. (1994). Perichromatin fibrils are in situ forms of nascent transcripts. *Trends Cell Biol* **4**, 86-90.

Fardaei, M., Rogers, M. T., Thorpe, H. M., Larkin, K., Hamshere, M. G., Harper, P. S. and Brook, J. D. (2002). Three proteins, MBNL, MBLL and MBXL, co-localize in vivo with nuclear foci of expanded-repeat transcripts in DM1 and DM2 cells. *Hum Mol Genet* **11**, 805-14.

Ferreira, J. A., Carmo-Fonseca, M. and Lamond, A. I. (1994). Differential interaction of splicing snRNPs with coiled bodies and interchromatin granules during mitosis and assembly of daughter cell nuclei. *J Cell Biol* **126**, 11-23.

Fischer, U., Liu, Q. and Dreyfuss, G. (1997). The SMN-SIP1 complex has an essential role in spliceosomal snRNP biogenesis. *Cell* **90**, 1023-9.

Fox, A. H., Lam, Y. W., Leung, A. K., Lyon, C. E., Andersen, J., Mann, M. and Lamond, A. I. (2002). Paraspeckles: a novel nuclear domain. *Curr Biol* **12**, 13-25.

Frey, M. R. and Matera, A. G. (1995). Coiled bodies contain U7 small nuclear RNA and associate with specific DNA sequences in interphase human cells. *Proc Natl Acad Sci U S A* **92**, 5915-9.

Frey, M. R. and Matera, A. G. (2001). RNA-mediated interaction of Cajal bodies and U2 snRNA genes. *J Cell Biol* **154**, 499-509.

Friesen, W. J. and Dreyfuss, G. (2000). Specific sequences of the Sm and Sm-like (Lsm) proteins mediate their interaction with the spinal muscular atrophy disease gene product (SMN). *J Biol Chem* **275**, 26370-5.

Frugier, T., Tiziano, F. D., Cifuentes-Diaz, C., Miniou, P., Roblot, N., Dierich, A., Le Meur, M. and Melki, J. (2000). Nuclear targeting defect of SMN lacking the C-terminus in a mouse model of spinal muscular atrophy. *Hum Mol Genet* **9**, 849-58.

Fu, X. D. and Maniatis, T. (1990). Factor required for mammalian spliceosome assembly is localized to discrete regions in the nucleus. *Nature* **343**, 437-41.

Fu, Y. H., Kuhl, D. P., Pizzuti, A., Pieretti, M., Sutcliffe, J. S., Richards, S., Verkerk, A. J., Holden, J. J., Fenwick, R. G., Jr., Warren, S. T. et al. (1991). Variation of the CGG repeat at the fragile X site results in genetic instability: resolution of the Sherman paradox. *Cell* **67**, 1047-58.

Gall, J. G. (1954). Observations on the nuclear membrane with the electron microscope. *Exp Cell Res* **7**, 197-200.

Gall, J. G., Stephenson, E. C., Erba, H. P., Diaz, M. O. and Barsacchi-Pilone, G. (1981). Histone genes are located at the sphere loci of newt lampbrush chromosomes. *Chromosoma* **84**, 159-71.

Gall, J. G., Tsvetkov, A., Wu, Z. and Murphy, C. (1995). Is the sphere organelle/coiled body a universal nuclear component? *Dev Genet* **16**, 25-35.

Gall, J. and Murphy, C. (1998). Pictures in cell biology. Lampbrush chromosomes from sperm chromatin. *Trends Cell Biol* **8**, 207.

Gall, J. G., Bellini, M., Wu, Z. and Murphy, C. (1999). Assembly of the nuclear transcription and processing machinery: Cajal bodies (coiled bodies) and transcriptosomes. *Mol Biol Cell* **10**, 4385-402.

Gall, J. G. (2000). Cajal bodies: the first 100 years. *Annu Rev Cell Dev Biol* **16**, 273-300.

Gall, J. G. (2001). A role for Cajal bodies in assembly of the nuclear transcription machinery. *FEBS Lett* **498**, 164-7.

Gall, J. G. (2003). The centennial of the Cajal body. *Nat Rev Mol Cell Biol* **4**, 975-80.

Gerbi, S. A., Borovjagin, A. V. and Lange, T. S. (2003). The nucleolus: a site of ribonucleoprotein maturation. *Curr Opin Cell Biol* **15**, 318-25.

Gerfen, C. R. (1985). The neostriatal mosaic. I. Compartmental organization of projections from the striatum to the substantia nigra in the rat. *J Comp Neurol* **236**, 454-76.

Gerfen, C. R., Engber, T. M., Mahan, L. C., Susel, Z., Chase, T. N., Monsma, F. J., Jr. and Sibley, D. R. (1990). D1 and D2 dopamine receptor-regulated gene expression of striatonigral and striatopallidal neurons. *Science* **250**, 1429-32.

Gerfen, C. R. (1992). The neostriatal mosaic: multiple levels of compartmental organization. *Trends Neurosci* **15**, 133-9.

Ghetti, A., Pinol-Roma, S., Michael, W. M., Morandi, C. and Dreyfuss, G. (1992). hnRNP I, the polypyrimidine tract-binding protein: distinct nuclear localization and association with hnRNAs. *Nucleic Acids Res* **20**, 3671-8.

Ghosh, S. (1976). The nucleolar structure. *Int Rev Cytol* **44**, 1-28.

Giesemann, T., Rathke-Hartlieb, S., Rothkegel, M., Bartsch, J. W., Buchmeier, S., Jockusch, B. M. and Jockusch, H. (1999). A role for polyproline motifs in the spinal muscular atrophy protein SMN. Profilins bind to and colocalize with smn in nuclear gems. *J Biol Chem* **274**, 37908-14.

Girard, J. P., Bagni, C., Caizergues-Ferrer, M., Amalric, F. and Lapeyre, B. (1994). Identification of a segment of the small nucleolar ribonucleoprotein-associated protein GAR1 that is sufficient for nucleolar accumulation. *J Biol Chem* **269**, 18499-506.

Goessens, G. (1984). Nucleolar structure. *Int Rev Cytol* **87**, 107-58.

Gokal, P. K., Cavanaugh, A. H. and Thompson, E. A., Jr. (1986). The effects of cycloheximide upon transcription of rRNA, 5 S RNA, and tRNA genes. *J Biol Chem* **261**, 2536-41.

Gonda, K., Fowler, J., Katoku-Kikyo, N., Haroldson, J., Wudel, J. and Kikyo, N. (2003). Reversible disassembly of somatic nucleoli by the germ cell proteins FRGY2a and FRGY2b. *Nat Cell Biol* **5**, 205-10.

Gottfried, M., Lavine, L. and Roessmann, U. (1981). Neuropathological findings in Wolf-Hirschhorn (4p-) syndrome. *Acta Neuropathol (Berl)* **55**, 163-5.

Gourfinkel-An, I., Cancel, G., Duyckaerts, C., Faucheux, B., Hauw, J. J., Trottier, Y., Brice, A., Agid, Y. and Hirsch, E. C. (1998). Neuronal distribution of intranuclear inclusions in Huntington's disease with adult onset. *Neuroreport* **9**, 1823-6.

Grande, M. A., van der Kraan, I., de Jong, L. and van Driel, R. (1997). Nuclear distribution of transcription factors in relation to sites of transcription and RNA polymerase II. *J Cell Sci* **110 (Pt 15)**, 1781-91.

Granick, D. (1975). Nucleolar necklaces in chick embryo fibroblast cells. I. Formation of necklaces by dichlororibobenzimidazole and other adenosine analogues that decrease RNA synthesis and degrade preribosomes. *J Cell Biol* **65**, 398-417.

Graveley, B. R. (2000). Sorting out the complexity of SR protein functions. *Rna* **6**, 1197-211.

Graybiel, A. M. and Ragsdale, C. W., Jr. (1978). Histochemically distinct compartments in the striatum of human, monkeys, and cat demonstrated by acetylthiocholinesterase staining. *Proc Natl Acad Sci U S A* **75**, 5723-6.

Greco, C. M., Hagerman, R. J., Tassone, F., Chudley, A. E., Del Bigio, M. R., Jacquemont, S., Leehey, M. and Hagerman, P. J. (2002). Neuronal intranuclear inclusions in a new cerebellar tremor/ataxia syndrome among fragile X carriers. *Brain* **125**, 1760-71.

Gubitz, A. K., Mourelatos, Z., Abel, L., Rappsilber, J., Mann, M. and Dreyfuss, G. (2002). Gemin5, a novel WD repeat protein component of the SMN complex that binds Sm proteins. *J Biol Chem* **277**, 5631-6.

Gui, J. F., Lane, W. S. and Fu, X. D. (1994). A serine kinase regulates intracellular localization of splicing factors in the cell cycle. *Nature* **369**, 678-82.

Gusella, J. F., MacDonald, M. E., Ambrose, C. M. and Duyao, M. P. (1993). Molecular genetics of Huntington's disease. *Arch Neurol* **50**, 1157-63.

Gusella, J. F. and MacDonald, M. E. (2000). Molecular genetics: unmasking polyglutamine triggers in neurodegenerative disease. *Nat Rev Neurosci* **1**, 109-15.

Hagerman, R. J. and Hagerman, P. J. (2002). The fragile X premutation: into the phenotypic fold. *Curr Opin Genet Dev* **12**, 278-83.

Hardin, J. H., Spicer, S. S. and Greene, W. B. (1969). The paranucleolar structure, accessory body of Cajal, sex chromatin, and related structures in nuclei of rat trigeminal neurons: a cytochemical and ultrastructural study. *Anat Rec* **164**, 403-31.

Harjes, P. and Wanker, E. E. (2003). The hunt for huntingtin function: interaction partners tell many different stories. *Trends Biochem Sci* **28**, 425-33.

Harper, P.S. (1996). *Huntington's Diseas.e.* WB Saunders Company, London.

Hayashi, Y., Kakita, A., Yamada, M., Egawa, S., Oyanagi, S., Naito, H., Tsuji, S. and Takahashi, H. (1998). Hereditary dentatorubral-pallidoluysian atrophy: ubiquitinated filamentous inclusions in the cerebellar dentate nucleus neurons. *Acta Neuropathol (Berl)* **95**, 479-82.

Hebert, M. D. and Matera, A. G. (2000). Self-association of coilin reveals a common theme in nuclear body localization. *Mol Biol Cell* **11**, 4159-71.

Hebert, M. D., Szymczyk, P. W., Shpargel, K. B. and Matera, A. G. (2001). Coilin forms the bridge between Cajal bodies and SMN, the spinal muscular atrophy protein. *Genes Dev* **15**, 2720-9.

Hernandez-Verdun, D., Roussel, P. and Gebrane-Younes, J. (2002). Emerging concepts of nucleolar assembly. *J Cell Sci* **115**, 2265-70.

Hickey, M. A. and Chesselet, M. F. (2003). The use of transgenic and knock-in mice to study Huntington's disease. *Cytogenet Genome Res* **100**, 276-86.

Hilditch-Maguire, P., Trettel, F., Passani, L. A., Auerbach, A., Persichetti, F. and MacDonald, M. E. (2000). Huntingtin: an iron-regulated protein essential for normal nuclear and perinuclear organelles. *Hum Mol Genet* **9**, 2789-97.

Hirose, Y., Tacke, R. and Manley, J. L. (1999). Phosphorylated RNA polymerase II stimulates pre-mRNA splicing. *Genes Dev* **13**, 1234-9.

Ho, T. H., Charlet, B. N., Poulos, M. G., Singh, G., Swanson, M. S. and Cooper, T. A. (2004). Muscleblind proteins regulate alternative splicing. *Embo J* **23**, 3103-12.

Hockly, E., Richon, V. M., Woodman, B., Smith, D. L., Zhou, X., Rosa, E., Sathasivam, K., Ghazi-Noori, S., Mahal, A., Lowden, P. A. et al. (2003). Suberoylanilide hydroxamic acid, a histone deacetylase inhibitor, ameliorates motor deficits in a mouse model of Huntington's disease. *Proc Natl Acad Sci U S A* **100**, 2041-6.

Hodges, M., Tissot, C., Howe, K., Grimwade, D. and Freemont, P. S. (1998). Structure, organization, and dynamics of promyelocytic leukemia protein nuclear bodies. *Am J Hum Genet* **63**, 297-304.

Hofmann, I., Schnolzer, M., Kaufmann, I. and Franke, W. W. (2002). Symplekin, a constitutive protein of karyo- and cytoplasmic particles involved in mRNA biogenesis in Xenopus laevis oocytes. *Mol Biol Cell* **13**, 1665-76.

Holbert, S., Dedeoglu, A., Humbert, S., Saudou, F., Ferrante, R. J. and Neri, C. (2003). Cdc42-interacting protein 4 binds to huntingtin: neuropathologic and biological evidence for a role in Huntington's disease. *Proc Natl Acad Sci U S A* **100**, 2712-7.

Holmberg, M., Duyckaerts, C., Durr, A., Cancel, G., Gourfinkel-An, I., Damier, P., Faucheux, B., Trottier, Y., Hirsch, E. C., Agid, Y. et al. (1998). Spinocerebellar ataxia type 7 (SCA7): a neurodegenerative disorder with neuronal intranuclear inclusions. *Hum Mol Genet* **7**, 913-8.

Holmes, S. E., Hearn, E. O., Ross, C. A. and Margolis, R. L. (2001). SCA12: an unusual mutation leads to an unusual spinocerebellar ataxia. *Brain Res Bull* **56**, 397-403.

Hoogeveen, A. T., Willemsen, R., Meyer, N., de Rooij, K. E., Roos, R. A., van Ommen, G. J. and Galjaard, H. (1993). Characterization and localization of the Huntington disease gene product. *Hum Mol Genet* **2**, 2069-73.

Hoogeveen, A. T., Willemsen, R. and Oostra, B. A. (2002). Fragile X syndrome, the Fragile X related proteins, and animal models. *Microsc Res Tech* **57**, 148-55.

Hozak, P., Cook, P. R., Schofer, C., Mosgoller, W. and Wachtler, F. (1994). Site of transcription of ribosomal RNA and intranucleolar structure in HeLa cells. *J Cell Sci* **107 (Pt 2)**, 639-48.

Huang, S. and Spector, D. L. (1992). U1 and U2 small nuclear RNAs are present in nuclear speckles. *Proc Natl Acad Sci U S A* **89**, 305-8.

Huang, S. and Spector, D. L. (1996). Dynamic organization of pre-mRNA splicing factors. *J Cell Biochem* **62**, 191-7.

Huang, S., Deerinck, T. J., Ellisman, M. H. and Spector, D. L. (1997). The dynamic organization of the perinucleolar compartment in the cell nucleus. *J Cell Biol* **137**, 965-74.

Huang, S., Deerinck, T. J., Ellisman, M. H. and Spector, D. L. (1998a). The per-inucleolar compartment and transcription. *J Cell Biol* **143**, 35-47.

Huang, C. C., Faber, P. W., Persichetti, F., Mittal, V., Vonsattel, J. P., MacDonald, M. E. and Gusella, J. F. (1998b). Amyloid formation by mutant huntingtin: threshold, progressivity and recruitment of normal polyglutamine proteins. *Somat Cell Mol Genet* **24**, 217-33.

Huang, S. (2002). Building an efficient factory: where is pre-rRNA synthesized in the nucleolus? *J Cell Biol* **157**, 739-41.

The Huntington's Disease Collaborative Research Group, (1993). A novel gene containing a trinucleotide repeat that is expanded and unstable on Huntington's disease chromosomes. *Cell* **72**, 971-83.

Huynh, D. P., Del Bigio, M. R., Ho, D. H. and Pulst, S. M. (1999). Expression of ataxin-2 in brains from normal individuals and patients with Alzheimer's disease and spinocerebellar ataxia 2. *Ann Neurol* **45**, 232-41.

Isaac, C., Yang, Y. and Meier, U. T. (1998). Nopp140 functions as a molecular link between the nucleolus and the coiled bodies. *J Cell Biol* **142**, 319-29.

Ishikawa, K., Fujigasaki, H., Saegusa, H., Ohwada, K., Fujita, T., Iwamoto, H., Komatsuzaki, Y., Toru, S., Toriyama, H., Watanabe, M. et al. (1999). Abundant expression and cytoplasmic aggregations of [alpha]1A voltage-dependent calcium channel protein associated with neurodegeneration in spinocerebellar ataxia type 6. *Hum Mol Genet* **8**, 1185-93.

Ishikawa, K., Owada, K., Ishida, K., Fujigasaki, H., Shun Li, M., Tsunemi, T., Ohkoshi, N., Toru, S., Mizutani, T., Hayashi, M. et al. (2001). Cytoplasmic and nuclear polyglutamine aggregates in SCA6 Purkinje cells. *Neurology* **56**, 1753-6.

Jacobs, E. Y., Frey, M. R., Wu, W., Ingledue, T. C., Gebuhr, T. C., Gao, L., Marzluff, W. F. and Matera, A. G. (1999). Coiled bodies preferentially associate with U4, U11, and U12 small nuclear RNA genes in interphase HeLa cells but not with U6 and U7 genes. *Mol Biol Cell* **10**, 1653-63.

Jady, B. E., Darzacq, X., Tucker, K. E., Matera, A. G., Bertrand, E. and Kiss, T. (2003). Modification of Sm small nuclear RNAs occurs in the nucleoplasmic Cajal body following import from the cytoplasm. *Embo J* **22**, 1878-88.

Jana, N. R., Tanaka, M., Wang, G. and Nukina, N. (2000). Polyglutamine length-dependent interaction of Hsp40 and Hsp70 family chaperones with truncated N-terminal huntingtin: their role in suppression of aggregation and cellular toxicity. *Hum Mol Genet* **9**, 2009-18.

Jarrous, N., Wolenski, J. S., Wesolowski, D., Lee, C. and Altman, S. (1999). Localization in the nucleolus and coiled bodies of protein subunits of the ribonucleoprotein ribonuclease P. *J Cell Biol* **146**, 559-72.

Jimenez-Garcia, L. F. and Spector, D. L. (1993). In vivo evidence that transcription and splicing are coordinated by a recruiting mechanism. *Cell* **73**, 47-59.

Jimenez-Garcia, L. F., Segura-Valdez, M. L., Ochs, R. L., Rothblum, L. I., Hannan, R. and Spector, D. L. (1994). Nucleologenesis: U3 snRNA-containing prenucleolar bodies move to sites of active pre-rRNA transcription after mitosis. *Mol Biol Cell* **5**, 955-66.

Jin, P. and Warren, S. T. (2000). Understanding the molecular basis of fragile X syndrome. *Hum Mol Genet* **9**, 901-8.

Jin, P., Zarnescu, D. C., Zhang, F., Pearson, C. E., Lucchesi, J. C., Moses, K. and Warren, S. T. (2003). RNA-mediated neurodegeneration caused by the fragile X premutation rCGG repeats in Drosophila. *Neuron* **39**, 739-47.

Johnson, C., Primorac, D., McKinstry, M., McNeil, J., Rowe, D. and Lawrence, J. B. (2000). Tracking COL1A1 RNA in osteogenesis imperfecta. splice-defective transcripts initiate transport from the gene but are retained within the SC35 domain. *J Cell Biol* **150**, 417-32.

Johnston, J. G., Gerfen, C. R., Haber, S. N. and van der Kooy, D. (1990). Mechanisms of striatal pattern formation: conservation of mammalian compartmentalization. *Brain Res Dev Brain Res* **57**, 93-102.

Jolly, C., Vourc'h, C., Robert-Nicoud, M. and Morimoto, R. I. (1999). Intron-independent association of splicing factors with active genes. *J Cell Biol* **145**, 1133-43.

Jones, A. L. (1999). The localization and interactions of huntingtin. *Philos Trans R Soc Lond B Biol Sci* **354**, 1021-7.

Jones, K. W., Gorzynski, K., Hales, C. M., Fischer, U., Badbanchi, F., Terns, R. M. and Terns, M. P. (2001). Direct interaction of the spinal muscular atrophy disease protein SMN with the small nucleolar RNA-associated protein fibrillarin. *J Biol Chem* **276**, 38645-51.

Jong, Y. J., Chang, J. G., Lin, S. P., Yang, T. Y., Wang, J. C., Chang, C. P., Lee, C. C., Li, H., Hsieh-Li, H. M. and Tsai, C. H. (2000). Analysis of the mRNA transcripts of the survival motor neuron (SMN) gene in the tissue of an SMA fetus and the peripheral blood mononuclear cells of normals, carriers and SMA patients. *J Neurol Sci* **173**, 147-53.

Jordan, E. G. and McGovern, J. H. (1981). The quantitative relationship of the fibrillar centres and other nucleolar components to changes in growth conditions, serum deprivation and low doses of actinomycin D in cultured diploid human fibroblasts (strain MRC-5). *J Cell Sci* **52**, 373-89.

Jordan, P., Cunha, C. and Carmo-Fonseca, M. (1997). The cdk7-cyclin H-MAT1 complex associated with TFIIH is localized in coiled bodies. *Mol Biol Cell* **8**, 1207-17.

Kaytor, M. D., Duvick, L. A., Skinner, P. J., Koob, M. D., Ranum, L. P. and Orr, H. T. (1999). Nuclear localization of the spinocerebellar ataxia type 7 protein, ataxin-7. *Hum Mol Genet* **8**, 1657-64.

Kegel, K. B., Kim, M., Sapp, E., McIntyre, C., Castano, J. G., Aronin, N. and Di-Figlia, M. (2000). Huntingtin expression stimulates endosomal-lysosomal activity, endosome tubulation, and autophagy. *J Neurosci* **20**, 7268-78.

Kemp, J. M. and Powell, T. P. (1971). The synaptic organization of the caudate nucleus. *Philos Trans R Soc Lond B Biol Sci* **262**, 403-12.

Kennedy, L. and Shelbourne, P. F. (2000). Dramatic mutation instability in HD mouse striatum: does polyglutamine load contribute to cell-specific vulnerability in Huntington's disease? *Hum Mol Genet* **9**, 2539-44.

Kenneson, A., Zhang, F., Hagedorn, C. H. and Warren, S. T. (2001). Reduced FMRP and increased FMR1 transcription is proportionally associated with CGG repeat number in intermediate-length and premutation carriers. *Hum Mol Genet* **10**, 1449-54.

Kim, E., Du, L., Bregman, D. B. and Warren, S. L. (1997). Splicing factors associate with hyperphosphorylated RNA polymerase II in the absence of pre-mRNA. *J Cell Biol* **136**, 19-28.

Kim, Y. J., Noguchi, S., Hayashi, Y. K., Tsukahara, T., Shimizu, T. and Arahata, K. (2001). The product of an oculopharyngeal muscular dystrophy gene, poly(A)-binding protein 2, interacts with SKIP and stimulates muscle-specific gene expression. *Hum Mol Genet* **10**, 1129-39.

Kim, S., Nollen, E. A., Kitagawa, K., Bindokas, V. P. and Morimoto, R. I. (2002). Polyglutamine protein aggregates are dynamic. *Nat Cell Biol* **4**, 826-31.

Kim, S. K. and Srivastava, M. (2003). Stability of Nucleolin protein as the basis for the differential expression of Nucleolin mRNA and protein during serum starvation. *DNA Cell Biol* **22**, 171-8.

Kinderman, N. B. and LaVelle, A. (1976). A nucleolus-associated coiled body. *J Neurocytol* **5**, 545-50.

Klement, I. A., Skinner, P. J., Kaytor, M. D., Yi, H., Hersch, S. M., Clark, H. B., Zoghbi, H. Y. and Orr, H. T. (1998). Ataxin-1 nuclear localization and aggregation: role in polyglutamine-induced disease in SCA1 transgenic mice. *Cell* **95**, 41-53.

Knight, S. J., Flannery, A. V., Hirst, M. C., Campbell, L., Christodoulou, Z., Phelps, S. R., Pointon, J., Middleton-Price, H. R., Barnicoat, A., Pembrey, M. E. et al. (1993). Trinucleotide repeat amplification and hypermethylation of a CpG island in FRAXE mental retardation. *Cell* **74**, 127-34.

Knight, S. P., Richardson, M. M., Osmand, A. P., Stakkestad, A. and Potter, N. T. (1997). Expression and distribution of the dentatorubral-pallidoluysian atrophy gene product (atrophin-1/drplap) in neuronal and non-neuronal tissues. *J Neurol Sci* **146**, 19-26.

Koberna, K., Malinsky, J., Pliss, A., Masata, M., Vecerova, J., Fialova, M., Bednar, J. and Raska, I. (2002). Ribosomal genes in focus: new transcripts label the dense fibrillar components and form clusters indicative of "Christmas trees" in situ. *J Cell Biol* **157**, 743-8.

Koob, M. D., Moseley, M. L., Schut, L. J., Benzow, K. A., Bird, T. D., Day, J. W. and Ranum, L. P. (1999). An untranslated CTG expansion causes a novel form of spinocerebellar ataxia (SCA8). *Nat Genet* **21**, 379-84.

Koyano, S., Uchihara, T., Fujigasaki, H., Nakamura, A., Yagishita, S. and Iwabuchi, K. (1999). Neuronal intranuclear inclusions in spinocerebellar ataxia type 2: triple-labeling immunofluorescent study. *Neurosci Lett* **273**, 117-20.

Krause, A., Sigrist, C. J., Dehning, I., Sommer, H. and Broughton, W. J. (1994). Accumulation of transcripts encoding a lipid transfer-like protein during deformation of nodulation-competent Vigna unguiculata root hairs. *Mol Plant Microbe Interact* **7**, 411-8.

Kremer, B., Goldberg, P., Andrew, S. E., Theilmann, J., Telenius, H., Zeisler, J., Squitieri, F., Lin, B., Bassett, A., Almqvist, E. et al. (1994). A worldwide study of the Huntington's disease mutation. The sensitivity and specificity of measuring CAG repeats. *N Engl J Med* **330**, 1401-6.

La Spada, A. R., Wilson, E. M., Lubahn, D. B., Harding, A. E. and Fischbeck, K. H. (1991). Androgen receptor gene mutations in X-linked spinal and bulbar muscular atrophy. *Nature* **352**, 77-9.

Lafarga, M., Hervas, J. P., Santa-Cruz, M. C., Villegas, J. and Crespo, D. (1983). The "accessory body" of Cajal in the neuronal nucleus. A light and electron microscopic approach. *Anat Embryol (Berl)* **166**, 19-30.

Lafarga, M., Andres, M. A., Berciano, M. T. and Maquiera, E. (1991). Organization of nucleoli and nuclear bodies in osmotically stimulated supraoptic neurons of the rat. *J Comp Neurol* **308**, 329-39.

Lafarga, M., Martinez-Guijarro, F. J., Berciano, M. T., Blasco-Ibanez, J. M., An-

dres, M. A., Mellstrom, B., Lopez-Garcia, C. and Naranjo, J. R. (1993). Nuclear Fos domains in transcriptionally activated supraoptic nucleus neurons. *Neuroscience* **57**, 353-64.

Lafarga, M., Berciano, M. T., Andres, M. A. and Testillano, P. S. (1994). Effects of cycloheximide on the structural organization of the nucleolus and the coiled body in normal and stimulated supraoptic neurons of the rat. *J Neurocytol* **23**, 500-13.

Lafarga, M., Berciano, M. T., Garcia-Segura, L. M., Andres, M. A. and Carmo-Fonseca, M. (1998). Acute osmotic/stress stimuli induce a transient decrease of transcriptional activity in the neurosecretory neurons of supraoptic nuclei. *J Neurocytol* **27**, 205-17.

Lam, Y. W., Lyon, C. E. and Lamond, A. I. (2002). Large-scale isolation of Cajal bodies from HeLa cells. *Mol Biol Cell* **13**, 2461-73.

Lamond, A. I. and Carmo-Fonseca, M. (1993). The coiled body. *Trends Cell Biol* **3**, 198-204.

Lamond, A. I. and Earnshaw, W. C. (1998). Structure and function in the nucleus. *Science* **280**, 547-53.

Landwehrmeyer, G. B., McNeil, S. M., Dure, L. S. t., Ge, P., Aizawa, H., Huang, Q., Ambrose, C. M., Duyao, M. P., Bird, E. D., Bonilla, E. et al. (1995). Huntington's disease gene: regional and cellular expression in brain of normal and affected individuals. *Ann Neurol* **37**, 218-30.

Lefebvre, S., Burglen, L., Reboullet, S., Clermont, O., Burlet, P., Viollet, L., Benichou, B., Cruaud, C., Millasseau, P., Zeviani, M. et al. (1995). Identification and characterization of a spinal muscular atrophy-determining gene. *Cell* **80**, 155-65.

Lefebvre, S., Burlet, P., Liu, Q., Bertrandy, S., Clermont, O., Munnich, A., Dreyfuss, G. and Melki, J. (1997). Correlation between severity and SMN protein level in spinal muscular atrophy. *Nat Genet* **16**, 265-9.

Lefebvre, S., Burglen, L., Frezal, J., Munnich, A. and Melki, J. (1998). The role of the SMN gene in proximal spinal muscular atrophy. *Hum Mol Genet* **7**, 1531-6.

Li, H. and Bingham, P. M. (1991). Arginine/serine-rich domains of the su(wa) and tra RNA processing regulators target proteins to a subnuclear compartment implicated in splicing. *Cell* **67**, 335-42.

Li, M., Miwa, S., Kobayashi, Y., Merry, D. E., Yamamoto, M., Tanaka, F., Doyu, M., Hashizume, Y., Fischbeck, K. H. and Sobue, G. (1998). Nuclear inclusions of the androgen receptor protein in spinal and bulbar muscular atrophy. *Ann Neurol* **44**, 249-54.

Li, F., Macfarlan, T., Pittman, R. N. and Chakravarti, D. (2002a). Ataxin-3 is a histone-binding protein with two independent transcriptional corepressor activities. *J Biol Chem* **277**, 45004-12.

Li, S. H., Cheng, A. L., Zhou, H., Lam, S., Rao, M., Li, H. and Li, X. J. (2002b). Interaction of Huntington disease protein with transcriptional activator Sp1. *Mol Cell Biol* **22**, 1277-87.

Lin, B., Rommens, J. M., Graham, R. K., Kalchman, M., MacDonald, H., Nasir, J., Delaney, A., Goldberg, Y. P. and Hayden, M. R. (1993). Differential 3' polyadenylation of the Huntington disease gene results in two mRNA species with variable tissue expression. *Hum Mol Genet* **2**, 1541-5.

Lin, B., Nasir, J., MacDonald, H., Hutchinson, G., Graham, R. K., Rommens, J. M. and Hayden, M. R. (1994). Sequence of the murine Huntington disease gene: evidence for conservation, alternate splicing and polymorphism in a triplet (CCG) repeat [corrected]. *Hum Mol Genet* **3**, 85-92.

Lin, B., Nasir, J., Kalchman, M. A., McDonald, H., Zeisler, J., Goldberg, Y. P. and Hayden, M. R. (1995). Structural analysis of the 5' region of mouse and human Huntington disease genes reveals conservation of putative promoter region and di- and trinucleotide polymorphisms. *Genomics* **25**, 707-15.

Liquori, C. L., Ikeda, Y., Weatherspoon, M., Ricker, K., Schoser, B. G., Dalton, J. C., Day, J. W. and Ranum, L. P. (2003). Myotonic dystrophy type 2: human founder haplotype and evolutionary conservation of the repeat tract. *Am J Hum Genet* **73**, 849-62.

Liu, Q. and Dreyfuss, G. (1996). A novel nuclear structure containing the survival of motor neurons protein. *Embo J* **15**, 3555-65.

Liu, Q., Fischer, U., Wang, F. and Dreyfuss, G. (1997). The spinal muscular atrophy disease gene product, SMN, and its associated protein SIP1 are in a complex with spliceosomal snRNP proteins. *Cell* **90**, 1013-21.

Lorson, C. L., Hahnen, E., Androphy, E. J. and Wirth, B. (1999). A single nucleotide in the SMN gene regulates splicing and is responsible for spinal muscular atrophy. *Proc Natl Acad Sci U S A* **96**, 6307-11.

Lui, H., Wang, H., Delong, C., Fowke, L. C., Crosby, W. L. and Fobert, P. R. (2000). The Arabidopsis Cdc2a-interacting protein ICK2 is structurally related to ICK1 and is a potent inhibitor of cyclin-dependent kinase activity in vitro. *Plant J* **21**, 379-85.

Luthi-Carter, R., Strand, A., Peters, N. L., Solano, S. M., Hollingsworth, Z. R., Menon, A. S., Frey, A. S., Spektor, B. S., Penney, E. B., Schilling, G. et al. (2000). Decreased expression of striatal signaling genes in a mouse model of Huntington's disease. *Hum Mol Genet* **9**, 1259-71.

Luthi-Carter, R., Strand, A. D., Hanson, S. A., Kooperberg, C., Schilling, G., La Spada, A. R., Merry, D. E., Young, A. B., Ross, C. A., Borchelt, D. R. et al. (2002a). Polyglutamine and transcription: gene expression changes shared by DRPLA and Huntington's disease mouse models reveal context-independent effects. *Hum Mol Genet* **11**, 1927-37.

Luthi-Carter, R., Hanson, S. A., Strand, A. D., Bergstrom, D. A., Chun, W., Peters,

N. L., Woods, A. M., Chan, E. Y., Kooperberg, C., Krainc, D. et al. (2002b). Dysregulation of gene expression in the R6/2 model of polyglutamine disease: parallel changes in muscle and brain. *Hum Mol Genet* **11**, 1911-26.

Lyon, C. E., Bohmann, K., Sleeman, J. and Lamond, A. I. (1997). Inhibition of protein dephosphorylation results in the accumulation of splicing snRNPs and coiled bodies within the nucleolus. *Exp Cell Res* **230**, 84-93.

Mais, C. and Scheer, U. (2001). Molecular architecture of the amplified nucleoli of Xenopus oocytes. *J Cell Sci* **114**, 709-18.

Mangiarini, L., Sathasivam, K., Seller, M., Cozens, B., Harper, A., Hetherington, C., Lawton, M., Trottier, Y., Lehrach, H., Davies, S. W. et al. (1996). Exon 1 of the HD gene with an expanded CAG repeat is sufficient to cause a progressive neurological phenotype in transgenic mice. *Cell* **87**, 493-506.

Marciniak, R. A., Lombard, D. B., Johnson, F. B. and Guarente, L. (1998). Nucleolar localization of the Werner syndrome protein in human cells. *Proc Natl Acad Sci U S A* **95**, 6887-92.

Marsh, K. L., Dixon, J. and Dixon, M. J. (1998). Mutations in the Treacher Collins syndrome gene lead to mislocalization of the nucleolar protein treacle. *Hum Mol Genet* **7**, 1795-800.

Matera, A. G. and Ward, D. C. (1993). Nucleoplasmic organization of small nuclear ribonucleoproteins in cultured human cells. *J Cell Biol* **121**, 715-27.

Matera, A. G., Frey, M. R., Margelot, K. and Wolin, S. L. (1995). A perinucleolar compartment contains several RNA polymerase III transcripts as well as the polypyrimidine tract-binding protein, hnRNP I. *J Cell Biol* **129**, 1181-93.

Matera, A. G. and Frey, M. R. (1998). Coiled bodies and gems: Janus or gemini? *Am J Hum Genet* **63**, 317-21.

Matera, A. G. (1999). Nuclear bodies: multifaceted subdomains of the interchromatin space. *Trends Cell Biol* **9**, 302-9.

Matera, A. G. and Hebert, M. D. (2001). The survival motor neurons protein uses its ZPR for nuclear localization. *Nat Cell Biol* **3**, E93-5.

McCampbell, A., Taylor, J. P., Taye, A. A., Robitschek, J., Li, M., Walcott, J., Merry, D., Chai, Y., Paulson, H., Sobue, G. et al. (2000). CREB-binding protein sequestration by expanded polyglutamine. *Hum Mol Genet* **9**, 2197-202.

McCampbell, A. and Fischbeck, K. H. (2001). Polyglutamine and CBP: fatal attraction? *Nat Med* **7**, 528-30.

McCampbell, A., Taye, A. A., Whitty, L., Penney, E., Steffan, J. S. and Fischbeck, K. H. (2001). Histone deacetylase inhibitors reduce polyglutamine toxicity. *Proc Natl Acad Sci U S A* **98**, 15179-84.

McKie, A. B., McHale, J. C., Keen, T. J., Tarttelin, E. E., Goliath, R., van Lith-Verhoeven, J. J., Greenberg, J., Ramesar, R. S., Hoyng, C. B., Cremers, F. P. et al. (2001). Mutations in the pre-mRNA splicing factor gene PRPC8 in autosomal dominant retinitis pigmentosa (RP13). *Hum Mol Genet* **10**, 1555-62.

Meier, U. T. and Blobel, G. (1992). Nopp140 shuttles on tracks between nucleolus and cytoplasm. *Cell* **70**, 127-38.

Meier, U. T. and Blobel, G. (1994). NAP57, a mammalian nucleolar protein with a putative homolog in yeast and bacteria. *J Cell Biol* **127**, 1505-14.

Meister, G., Buhler, D., Laggerbauer, B., Zobawa, M., Lottspeich, F. and Fischer, U. (2000). Characterization of a nuclear 20S complex containing the survival of motor neurons (SMN) protein and a specific subset of spliceosomal Sm proteins. *Hum Mol Genet* **9**, 1977-86.

Meister, G., Eggert, C. and Fischer, U. (2002). SMN-mediated assembly of RNPs: a complex story. *Trends Cell Biol* **12**, 472-8.

Melcak, I., Cermanova, S., Jirsova, K., Koberna, K., Malinsky, J. and Raska, I. (2000). Nuclear pre-mRNA compartmentalization: trafficking of released transcripts to splicing factor reservoirs. *Mol Biol Cell* **11**, 497-510.

Melese, T. and Xue, Z. (1995). The nucleolus: an organelle formed by the act of building a ribosome. *Curr Opin Cell Biol* **7**, 319-24.

Melki, J., Sheth, P., Abdelhak, S., Burlet, P., Bachelot, M. F., Lathrop, M. G., Frezal, J. and Munnich, A. (1990). Mapping of acute (type I) spinal muscular atrophy to chromosome 5q12-q14. The French Spinal Muscular Atrophy Investigators. *Lancet* **336**, 271-3.

Menalled, L. B. and Chesselet, M. F. (2002). Mouse models of Huntington's disease. *Trends Pharmacol Sci* **23**, 32-9.

Miller, L. and Gonzales, F. (1976). The relationship of ribosomal RNA synthesis to the formation of segregated nucleoli and nucleolus-like bodies. *J Cell Biol* **71**, 939-49.

Mintz, P. J., Patterson, S. D., Neuwald, A. F., Spahr, C. S. and Spector, D. L. (1999). Purification and biochemical characterization of interchromatin granule clusters. *Embo J* **18**, 4308-20.

Misteli, T. and Spector, D. L. (1996). Serine/threonine phosphatase 1 modulates the subnuclear distribution of pre-mRNA splicing factors. *Mol Biol Cell* **7**, 1559-72.

Misteli, T. and Spector, D. L. (1997). Applications of the green fluorescent protein in cell biology and biotechnology. *Nat Biotechnol* **15**, 961-4.

Misteli, T., Caceres, J. F. and Spector, D. L. (1997). The dynamics of a pre-mRNA splicing factor in living cells. *Nature* **387**, 523-7.

Misteli, T. and Spector, D. L. (1998). The cellular organization of gene expression. *Curr Opin Cell Biol* **10**, 323-31.

Misteli, T. (1999). RNA splicing: What has phosphorylation got to do with it? *Curr Biol* **9**, R198-200.

Misteli, T. and Spector, D. L. (1999). RNA polymerase II targets pre-mRNA splicing factors to transcription sites in vivo. *Mol Cell* **3**, 697-705.

Misteli, T. (2000). Cell biology of transcription and pre-mRNA splicing: nuclear architecture meets nuclear function. *J Cell Sci* **113 (Pt 11)**, 1841-9.

Misteli, T. (2001). Protein dynamics: implications for nuclear architecture and gene expression. *Science* **291**, 843-7.

Misteli, T. (2003). A nucleolar disappearing act in somatic cloning. *Nat Cell Biol* **5**, 183-4.

Mizzen, L. A. and Welch, W. J. (1988). Characterization of the thermotolerant cell. I. Effects on protein synthesis activity and the regulation of heat-shock protein 70 expression. *J Cell Biol* **106**, 1105-16.

Mohaghegh, P. and Hickson, I. D. (2001). DNA helicase deficiencies associated with cancer predisposition and premature ageing disorders. *Hum Mol Genet* **10**, 741-6.

Monani, U. R., Sendtner, M., Coovert, D. D., Parsons, D. W., Andreassi, C., Le, T. T., Jablonka, S., Schrank, B., Rossol, W., Prior, T. W. et al. (2000). The human centromeric survival motor neuron gene (SMN2) rescues embryonic lethality in Smn(-/-) mice and results in a mouse with spinal muscular atrophy. *Hum Mol Genet* **9**, 333-9.

Monneron, A. and Bernhard, W. (1969). Fine structural organization of the interphase nucleus in some mammalian cells. *J Ultrastruct Res* **27**, 266-88.

Moon, I. S., Park, I. S., Schenker, L. T., Kennedy, M. B., Moon, J. I. and Jin, I. (2001). Presence of both constitutive and inducible forms of heat shock protein 70 in the cerebral cortex and hippocampal synapses. *Cereb Cortex* **11**, 238-48.

Moreno-Diaz de la Espina, S., Fernandez-Gomez, M. E. and Risueno, M. C. (1979). Occurrence of nucleolar material in the cytoplasm of plant cells. *Cell Biol Int Rep* **3**, 215-25.

Morgan, G. T., Doyle, O., Murphy, C. and Gall, J. G. (2000). RNA polymerase II in Çajal bodies of amphibian oocytes. *J Struct Biol* **129**, 258-68.

Mosemiller, A. K., Dalton, J. C., Day, J. W. and Ranum, L. P. (2003). Molecular genetics of spinocerebellar ataxia type 8 (SCA8). *Cytogenet Genome Res* **100**, 175-83.

Mosgoeller, W., Kastner, P., Fang-Kircher, S., Kitzmueller, E., Hoeger, H., Seither, P., Labudova, O., Lubec, G. and Lubec, B. (2000). Brain RNA polymerase and nucleolar structure in perinatal asphyxia of the rat. *Exp Neurol* **161**, 174-82.

Mourelatos, Z., Abel, L., Yong, J., Kataoka, N. and Dreyfuss, G. (2001). SMN interacts with a novel family of hnRNP and spliceosomal proteins. *Embo J* **20**, 5443-52.

Mutsuddi, M., Marshall, C. M., Benzow, K. A., Koob, M. D. and Rebay, I. (2004). The spinocerebellar ataxia 8 noncoding RNA causes neurodegeneration and associates with staufen in Drosophila. *Curr Biol* **14**, 302-8.

Nakamura, K., Jeong, S. Y., Uchihara, T., Anno, M., Nagashima, K., Nagashima, T., Ikeda, S., Tsuji, S. and Kanazawa, I. (2001). SCA17, a novel autosomal dominant cerebellar ataxia caused by an expanded polyglutamine in TATA-binding protein. *Hum Mol Genet* **10**, 1441-8.

Napierala, M., Michalowski, D., de Mezer, M. and Krzyzosiak, W. J. (2005). Facile FMR1 mRNA structure regulation by interruptions in CGG repeats. *Nucleic Acids Res* **33**, 451-63.

Narayanan, A., Speckmann, W., Terns, R. and Terns, M. P. (1999). Role of the box C/D motif in localization of small nucleolar RNAs to coiled bodies and nucleoli. *Mol Biol Cell* **10**, 2131-47.

Nasir, J., Floresco, S. B., O'Kusky, J. R., Diewert, V. M., Richman, J. M., Zeisler, J., Borowski, A., Marth, J. D., Phillips, A. G. and Hayden, M. R. (1995). Targeted disruption of the Huntington's disease gene results in embryonic lethality and behavioral and morphological changes in heterozygotes. *Cell* **81**, 811-23.

Nemes, J. P., Benzow, K. A., Moseley, M. L., Ranum, L. P. and Koob, M. D. (2000). The SCA8 transcript is an antisense RNA to a brain-specific transcript encoding a novel actin-binding protein (KLHL1). *Hum Mol Genet* **9**, 1543-51.

Neugebauer, K. M. and Roth, M. B. (1997). Distribution of pre-mRNA splicing factors at sites of RNA polymerase II transcription. *Genes Dev* **11**, 1148-59.

Neugebauer, K. M. (2002). On the importance of being co-transcriptional. *J Cell Sci* **115**, 3865-71.

Nucifora, F. C., Jr., Sasaki, M., Peters, M. F., Huang, H., Cooper, J. K., Yamada, M., Takahashi, H., Tsuji, S., Troncoso, J., Dawson, V. L. et al. (2001). Interference by huntingtin and atrophin-1 with cbp-mediated transcription leading to cellular toxicity. *Science* **291**, 2423-8.

O'Keefe, R. T., Mayeda, A., Sadowski, C. L., Krainer, A. R. and Spector, D. L. (1994). Disruption of pre-mRNA splicing in vivo results in reorganization of splicing factors. *J Cell Biol* **124**, 249-60.

Oakes, M., Aris, J. P., Brockenbrough, J. S., Wai, H., Vu, L. and Nomura, M. (1998). Mutational analysis of the structure and localization of the nucleolus in the yeast Saccharomyces cerevisiae. *J Cell Biol* **143**, 23-34.

Ochs, R. L. and Smetana, K. (1989). Fibrillar center distribution in nucleoli of PHA-stimulated human lymphocytes. *Exp Cell Res* **184**, 552-7.

Ochs, R. L., Stein, T. W., Jr. and Tan, E. M. (1994). Coiled bodies in the nucleolus of breast cancer cells. *J Cell Sci* **107 (Pt 2)**, 385-99.

Okazawa, H., Rich, T., Chang, A., Lin, X., Waragai, M., Kajikawa, M., Enokido, Y., Komuro, A., Kato, S., Shibata, M. et al. (2002). Interaction between mutant ataxin-1 and PQBP-1 affects transcription and cell death. *Neuron* **34**, 701-13.

Olson, M. O., Dundr, M. and Szebeni, A. (2000). The nucleolus: an old factory with unexpected capabilities. *Trends Cell Biol* **10**, 189-96.

Ordway, J. M., Tallaksen-Greene, S., Gutekunst, C. A., Bernstein, E. M., Cearley, J. A., Wiener, H. W., Dure, L. S. t., Lindsey, R., Hersch, S. M., Jope, R. S. et al. (1997). Ectopically expressed CAG repeats cause intranuclear inclusions and a progressive late onset neurological phenotype in the mouse. *Cell* **91**, 753-63.

Passani, L. A., Bedford, M. T., Faber, P. W., McGinnis, K. M., Sharp, A. H., Gusella, J. F., Vonsattel, J. P. and MacDonald, M. E. (2000). Huntingtin's WW domain partners in Huntington's disease post-mortem brain fulfill genetic criteria for direct involvement in Huntington's disease pathogenesis. *Hum Mol Genet* **9**, 2175-82.

Paulson, H. L., Perez, M. K., Trottier, Y., Trojanowski, J. Q., Subramony, S. H., Das, S. S., Vig, P., Mandel, J. L., Fischbeck, K. H. and Pittman, R. N. (1997). Intranuclear inclusions of expanded polyglutamine protein in spinocerebellar ataxia type 3. *Neuron* **19**, 333-44.

Pederson, T. (1998). The plurifunctional nucleolus. *Nucleic Acids Res* **26**, 3871-6.

Pellizzoni, L., Kataoka, N., Charroux, B. and Dreyfuss, G. (1998). A novel function for SMN, the spinal muscular atrophy disease gene product, in pre-mRNA splicing. *Cell* **95**, 615-24.

Pellizzoni, L., Charroux, B. and Dreyfuss, G. (1999). SMN mutants of spinal muscular atrophy patients are defective in binding to snRNP proteins. *Proc Natl Acad Sci U S A* **96**, 11167-72.

Pellizzoni, L., Baccon, J., Charroux, B. and Dreyfuss, G. (2001a). The survival of motor neurons (SMN) protein interacts with the snoRNP proteins fibrillarin and GAR1. *Curr Biol* **11**, 1079-88.

Pellizzoni, L., Charroux, B., Rappsilber, J., Mann, M. and Dreyfuss, G. (2001b). A functional interaction between the survival motor neuron complex and RNA polymerase II. *J Cell Biol* **152**, 75-85.

Pellizzoni, L., Baccon, J., Rappsilber, J., Mann, M. and Dreyfuss, G. (2002). Purification of native survival of motor neurons complexes and identification of Gemin6 as a novel component. *J Biol Chem* **277**, 7540-5.

Pena, E., Berciano, M. T., Fernandez, R., Ojeda, J. L. and Lafarga, M. (2001). Neuronal body size correlates with the number of nucleoli and Cajal bodies, and with the organization of the splicing machinery in rat trigeminal ganglion neurons. *J Comp Neurol* **430**, 250-63.

Perlaky, L., Valdez, B. C. and Busch, H. (1997). Effects of cytotoxic drugs on translocation of nucleolar RNA helicase RH-II/Gu. *Exp Cell Res* **235**, 413-20.

Pert, C. B., Kuhar, M. J. and Snyder, S. H. (1976). Opiate receptor: autoradiographic localization in rat brain. *Proc Natl Acad Sci U S A* **73**, 3729-33.

Peters, A., Palay, S.L., & Webster, H., (1991). *The Fine Structure of the Nervous System.* Oxford University Press, Oxford, 59pp.

Phair, R. D. and Misteli, T. (2000). High mobility of proteins in the mammalian cell nucleus. *Nature* **404**, 604-9.

Pilch, B., Allemand, E., Facompre, M., Bailly, C., Riou, J. F., Soret, J. and Tazi, J. (2001). Specific inhibition of serine- and arginine-rich splicing factors phosphorylation, spliceosome assembly, and splicing by the antitumor drug NB-506. *Cancer Res* **61**, 6876-84.

Platani, M., Goldberg, I., Swedlow, J. R. and Lamond, A. I. (2000). In vivo analysis of Cajal body movement, separation, and joining in live human cells. *J Cell Biol* **151**, 1561-74.

Polak, P. E., Simone, F., Kaberlein, J. J., Luo, R. T. and Thirman, M. J. (2003). ELL and EAF1 are Cajal body components that are disrupted in MLL-ELL leukemia. *Mol Biol Cell* **14**, 1517-28.

Pombo, A., Cuello, P., Schul, W., Yoon, J. B., Roeder, R. G., Cook, P. R. and Murphy, S. (1998). Regional and temporal specialization in the nucleus: a transcriptionally-active nuclear domain rich in PTF, Oct1 and PIKA antigens associates with specific chromosomes early in the cell cycle. *Embo J* **17**, 1768-78.

Puvion, E. and Puvion-Dutilleul, F. (1996). Ultrastructure of the nucleus in relation to transcription and splicing: roles of perichromatin fibrils and interchromatin granules. *Exp Cell Res* **229**, 217-25.

Raska, I., Ochs, R. L., Andrade, L. E., Chan, E. K., Burlingame, R., Peebles, C., Gruol, D. and Tan, E. M. (1990). Association between the nucleolus and the coiled body. *J Struct Biol* **104**, 120-7.

Raska, I., Andrade, L. E., Ochs, R. L., Chan, E. K., Chang, C. M., Roos, G. and Tan, E. M. (1991). Immunological and ultrastructural studies of the nuclear coiled body with autoimmune antibodies. *Exp Cell Res* **195**, 27-37.

Raska, I. (2003). Oldies but goldies: searching for Christmas trees within the nucleolar architecture. *Trends Cell Biol* **13**, 517-25.

Raska, I., Koberna, K., Malinsky, J., Fidlerova, H. and Masata, M. (2004). The nucleolus and transcription of ribosomal genes. *Biol Cell* **96**, 579-94.

Rega, S., Stiewe, T., Chang, D. I., Pollmeier, B., Esche, H., Bardenheuer, W., Marquitan, G. and Putzer, B. M. (2001). Identification of the full-length huntingtin- interacting protein p231HBP/HYPB as a DNA-binding factor. *Mol Cell Neurosci* **18**, 68-79.

Reimer, G., Raska, I., Tan, E. M. and Scheer, U. (1987). Human autoantibodies: probes for nucleolus structure and function. *Virchows Arch B Cell Pathol Incl Mol Pathol* **54**, 131-43.

Reynolds, R. C., Montgomery, P. O. and Hughes, B. (1964). Nucleolar "Caps" Produced by Actinomycin D. *Cancer Res* **24**, 1269-77.

Ringel, S. P., Lava, N. S., Treihaft, M. M., Lubs, M. L. and Lubs, H. A. (1978). Late-onset X-linked recessive spinal and bulbar muscular atrophy. *Muscle Nerve* **1**, 297-307.

Roizin, L., Stellar, S. & Liu, J.C., (1979). Neuronal nuclear-cytoplasmic changes in Huntington's chorea: electron microscope investigations. *Advances Neurol* **23** 95-122.

Roth, M. B. (1995). Spheres, coiled bodies and nuclear bodies. *Curr Opin Cell Biol* **7**, 325-8.

Rubinsztein, D. C. (2002). Lessons from animal models of Huntington's disease. *Trends Genet* **18**, 202-9.

Ryu, H., Lee, J., Olofsson, B. A., Mwidau, A., Dedeoglu, A., Escudero, M., Flemington, E., Azizkhan-Clifford, J., Ferrante, R. J. and Ratan, R. R. (2003). Histone deacetylase inhibitors prevent oxidative neuronal death independent of expanded polyglutamine repeats via an Sp1-dependent pathway. *Proc Natl Acad Sci U S A* **100**, 4281-6.

Sacco-Bubulya, P. and Spector, D. L. (2002). Disassembly of interchromatin granule clusters alters the coordination of transcription and pre-mRNA splicing. *J Cell Biol* **156**, 425-36.

Saitoh, N., Spahr, C. S., Patterson, S. D., Bubulya, P., Neuwald, A. F. and Spector, D. L. (2004). Proteomic analysis of interchromatin granule clusters. *Mol Biol Cell* **15**, 3876-90.

Sapp, E., Schwarz, C., Chase, K., Bhide, P. G., Young, A. B., Penney, J., Vonsattel, J. P., Aronin, N. and DiFiglia, M. (1997). Huntingtin localization in brains of normal and Huntington's disease patients. *Ann Neurol* **42**, 604-12.

Sathasivam, K., Hobbs, C., Mangiarini, L., Mahal, A., Turmaine, M., Doherty, P., Davies, S. W. and Bates, G. P. (1999). Transgenic models of Huntington's disease. *Philos Trans R Soc Lond B Biol Sci* **354**, 963-9.

Saudou, F., Finkbeiner, S., Devys, D. and Greenberg, M. E. (1998). Huntingtin acts in the nucleus to induce apoptosis but death does not correlate with the formation of intranuclear inclusions. *Cell* **95**, 55-66.

Savkur, R. S., Philips, A. V. and Cooper, T. A. (2001). Aberrant regulation of insulin receptor alternative splicing is associated with insulin resistance in myotonic dystrophy. *Nat Genet* **29**, 40-7.

Savkur, R. S., Philips, A. V., Cooper, T. A., Dalton, J. C., Moseley, M. L., Ranum, L. P. and Day, J. W. (2004). Insulin receptor splicing alteration in myotonic dystrophy type 2. *Am J Hum Genet* **74**, 1309-13.

Scheer, U. and Hock, R. (1999). Structure and function of the nucleolus. *Curr Opin Cell Biol* **11**, 385-90.

Schmitt, I., Bachner, D., Megow, D., Henklein, P., Hameister, H., Epplen, J. T. and Riess, O. (1995). Expression of the Huntington disease gene in rodents: cloning the rat homologue and evidence for downregulation in non-neuronal tissues during development. *Hum Mol Genet* **4**, 1173-82.

Schul, W., Groenhout, B., Koberna, K., Takagaki, Y., Jenny, A., Manders, E. M., Raska, I., van Driel, R. and de Jong, L. (1996). The RNA 3' cleavage factors CstF 64 kDa and CPSF 100 kDa are concentrated in nuclear domains closely associated with coiled bodies and newly synthesized RNA. *Embo J* **15**, 2883-92.

Schul, W., de Jong, L. and van Driel, R. (1998a). Nuclear neighbours: the spatial and functional organization of genes and nuclear domains. *J Cell Biochem* **70**, 159-71.

Schul, W., van Driel, R. and de Jong, L. (1998b). Coiled bodies and U2 snRNA genes adjacent to coiled bodies are enriched in factors required for snRNA transcription. *Mol Biol Cell* **9**, 1025-36.

Schul, W., van Driel, R. and de Jong, L. (1998c). A subset of poly(A) polymerase is concentrated at sites of RNA synthesis and is associated with domains enriched in splicing factors and poly(A) RNA. *Exp Cell Res* **238**, 1-12.

Schul, W., Adelaar, B., van Driel, R. and de Jong, L. (1999). Coiled bodies are predisposed to a spatial association with genes that contain snoRNA sequences in their introns. *J Cell Biochem* **75**, 393-403.

Shav-Tal, Y., Cohen, M., Lapter, S., Dye, B., Patton, J. G., Vandekerckhove, J. and Zipori, D. (2001). Nuclear relocalization of the pre-mRNA splicing factor PSF during apoptosis involves hyperphosphorylation, masking of antigenic epitopes, and changes in protein interactions. *Mol Biol Cell* **12**, 2328-40.

Shaw, P. J. and Jordan, E. G. (1995). The nucleolus. *Annu Rev Cell Dev Biol* **11**, 93-121.

Shimohata, T., Onodera, O. and Tsuji, S. (2000a). Interaction of expanded polyglutamine stretches with nuclear transcription factors leads to aberrant transcriptional regulation in polyglutamine diseases. *Neuropathology* **20**, 326-33.

Shimohata, T., Nakajima, T., Yamada, M., Uchida, C., Onodera, O., Naruse, S., Kimura, T., Koide, R., Nozaki, K., Sano, Y. et al. (2000b). Expanded polyglutamine stretches interact with TAFII130, interfering with CREB-dependent transcription. *Nat Genet* **26**, 29-36.

Shopland, L. S., Byron, M., Stein, J. L., Lian, J. B., Stein, G. S. and Lawrence, J. B. (2001). Replication-dependent histone gene expression is related to Cajal body (CB) association but does not require sustained CB contact. *Mol Biol Cell* **12**, 565-76.

Siomi, H., Siomi, M. C., Nussbaum, R. L. and Dreyfuss, G. (1993). The protein product of the fragile X gene, FMR1, has characteristics of an RNA-binding protein. *Cell* **74**, 291-8.

Sirri, V., Hernandez-Verdun, D. and Roussel, P. (2002). Cyclin-dependent kinases govern formation and maintenance of the nucleolus. *J Cell Biol* **156**, 969-81.

Skare, P., Kreivi, J. P., Bergstrom, A. and Karlsson, R. (2003). Profilin I colocalizes with speckles and Cajal bodies: a possible role in pre-mRNA splicing. *Exp Cell Res* **286**, 12-21.

Skinner, P. J., Koshy, B. T., Cummings, C. J., Klement, I. A., Helin, K., Servadio, A., Zoghbi, H. Y. and Orr, H. T. (1997). Ataxin-1 with an expanded glutamine tract alters nuclear matrix-associated structures. *Nature* **389**, 971-4.

Sleeman, J., Lyon, C. E., Platani, M., Kreivi, J. P. and Lamond, A. I. (1998). Dynamic interactions between splicing snRNPs, coiled bodies and nucleoli revealed using snRNP protein fusions to the green fluorescent protein. *Exp Cell Res* **243**, 290-304.

Sleeman, J. E. and Lamond, A. I. (1999). Newly assembled snRNPs associate with coiled bodies before speckles, suggesting a nuclear snRNP maturation pathway. *Curr Biol* **9**, 1065-74.

Sleeman, J. E., Ajuh, P. and Lamond, A. I. (2001). snRNP protein expression enhances the formation of Cajal bodies containing p80-coilin and SMN. *J Cell Sci* **114**, 4407-19.

Sleeman, J. E., Trinkle-Mulcahy, L., Prescott, A. R., Ogg, S. C. and Lamond, A. I. (2003). Cajal body proteins SMN and Coilin show differential dynamic behaviour in vivo. *J Cell Sci* **116**, 2039-50.

Smith, K. P., Moen, P. T., Wydner, K. L., Coleman, J. R. and Lawrence, J. B. (1999). Processing of endogenous pre-mRNAs in association with SC-35 domains is gene specific. *J Cell Biol* **144**, 617-29.

Smith, K. P. and Lawrence, J. B. (2000). Interactions of U2 gene loci and their nuclear transcripts with Cajal (coiled) bodies: evidence for PreU2 within Cajal bodies. *Mol Biol Cell* **11**, 2987-98.

Snaar, S., Wiesmeijer, K., Jochemsen, A. G., Tanke, H. J. and Dirks, R. W. (2000). Mutational analysis of fibrillarin and its mobility in living human cells. *J Cell Biol* **151**, 653-62.

Spector, D. L., Schrier, W. H. and Busch, H. (1983). Immunoelectron microscopic localization of snRNPs. *Biol Cell* **49**, 1-10.

Spector, D. L., Fu, X. D. and Maniatis, T. (1991). Associations between distinct pre-mRNA splicing components and the cell nucleus. *Embo J* **10**, 3467-81.

Spector, D. L. (1993). Nuclear organization of pre-mRNA processing. *Curr Opin Cell Biol* **5**, 442-7.

Spector, D. L. (2003). The dynamics of chromosome organization and gene regulation. *Annu Rev Biochem* **72**, 573-608.

Steffan, J. S., Kazantsev, A., Spasic-Boskovic, O., Greenwald, M., Zhu, Y. Z., Gohler, H., Wanker, E. E., Bates, G. P., Housman, D. E. and Thompson, L. M. (2000). The Huntington's disease protein interacts with p53 and CREB-binding protein and represses transcription. *Proc Natl Acad Sci U S A* **97**, 6763-8.

Steffan, J. S., Bodai, L., Pallos, J., Poelman, M., McCampbell, A., Apostol, B. L., Kazantsev, A., Schmidt, E., Zhu, Y. Z., Greenwald, M. et al. (2001). Histone deacetylase inhibitors arrest polyglutamine-dependent neurodegeneration in Drosophila. *Nature* **413**, 739-43.

Stenoien, D. L., Cummings, C. J., Adams, H. P., Mancini, M. G., Patel, K., DeMartino, G. N., Marcelli, M., Weigel, N. L. and Mancini, M. A. (1999). Polyglutamine-expanded androgen receptors form aggregates that sequester heat shock proteins, proteasome components and SRC-1, and are suppressed by the HDJ-2 chaperone. *Hum Mol Genet* **8**, 731-41.

Stenoien, D. L., Mielke, M. and Mancini, M. A. (2002). Intranuclear ataxin1 inclusions contain both fast- and slow-exchanging components. *Nat Cell Biol* **4**, 806-10.

Stine, O. C., Pleasant, N., Franz, M. L., Abbott, M. H., Folstein, S. E. and Ross, C. A. (1993). Correlation between the onset age of Huntington's disease and length of the trinucleotide repeat in IT-15. *Hum Mol Genet* **2**, 1547-9.

Strong, T. V., Tagle, D. A., Valdes, J. M., Elmer, L. W., Boehm, K., Swaroop, M., Kaatz, K. W., Collins, F. S. and Albin, R. L. (1993). Widespread expression of the human and rat Huntington's disease gene in brain and nonneural tissues. *Nat Genet* **5**, 259-65.

Suhr, S. T., Senut, M. C., Whitelegge, J. P., Faull, K. F., Cuizon, D. B. and Gage, F. H. (2001). Identities of sequestered proteins in aggregates from cells with induced polyglutamine expression. *J Cell Biol* **153**, 283-94.

Swift, H. (1959). Studies on nuclear fine structure. *Brookhaven Symp Biol* **12**, 134-52.

Tait, D., Riccio, M., Sittler, A., Scherzinger, E., Santi, S., Ognibene, A., Maraldi, N. M., Lehrach, H. and Wanker, E. E. (1998). Ataxin-3 is transported into the nucleus and associates with the nuclear matrix. *Hum Mol Genet* **7**, 991-7.

Tao, T. and Tartakoff, A. M. (2001). Nuclear relocation of normal huntingtin. *Traffic* **2**, 385-94.

Telenius, H., Kremer, H. P., Theilmann, J., Andrew, S. E., Almqvist, E., Anvret, M., Greenberg, C., Greenberg, J., Lucotte, G., Squitieri, F. et al. (1993). Molecular analysis of juvenile Huntington disease: the major influence on (CAG)n repeat length is the sex of the affected parent. *Hum Mol Genet* **2**, 1535-40.

Terns, M. P. and Terns, R. M. (2001). Macromolecular complexes: SMN--the master assembler. *Curr Biol* **11**, R862-4.

Trinczek, B., Robert-Nicoud, M. and Schwoch, G. (1993). In situ localization of cAMP-dependent protein kinases in nuclear and chromosomal substructures: relation to transcriptional activity. *Eur J Cell Biol* **60**, 196-202.

Tschochner, H. and Hurt, E. (2003). Pre-ribosomes on the road from the nucleolus to the cytoplasm. *Trends Cell Biol* **13**, 255-63.

Tucker, K. E., Massello, L. K., Gao, L., Barber, T. J., Hebert, M. D., Chan, E. K. and Matera, A. G. (2000). Structure and characterization of the murine p80 coilin gene, Coil. *J Struct Biol* **129**, 269-77.

Tucker, K. E., Berciano, M. T., Jacobs, E. Y., LePage, D. F., Shpargel, K. B., Rossire, J. J., Chan, E. K., Lafarga, M., Conlon, R. A. and Matera, A. G. (2001). Residual Cajal bodies in coilin knockout mice fail to recruit Sm snRNPs and SMN, the spinal muscular atrophy gene product. *J Cell Biol* **154**, 293-307.

Tuma, R. S., Stolk, J. A. and Roth, M. B. (1993). Identification and characterization of a sphere organelle protein. *J Cell Biol* **122**, 767-73.

Utz, P. J., Hottelet, M., van Venrooij, W. J. and Anderson, P. (1998). Association of phosphorylated serine/arginine (SR) splicing factors with the U1-small ribonucleoprotein (snRNP) autoantigen complex accompanies apoptotic cell death. *J Exp Med* **187**, 547-60.

Velier, J., Kim, M., Schwarz, C., Kim, T. W., Sapp, E., Chase, K., Aronin, N. and DiFiglia, M. (1998). Wild-type and mutant huntingtins function in vesicle trafficking in the secretory and endocytic pathways. *Exp Neurol* **152**, 34-40.

Verheggen, C., Le Panse, S., Almouzni, G. and Hernandez-Verdun, D. (1998). Presence of pre-rRNAs before activation of polymerase I transcription in the building process of nucleoli during early development of Xenopus laevis. *J Cell Biol* **142**, 1167-80.

Vithana, E. N., Abu-Safieh, L., Allen, M. J., Carey, A., Papaioannou, M., Chakarova, C., Al-Maghtheh, M., Ebenezer, N. D., Willis, C., Moore, A. T. et al. (2001). A human homolog of yeast pre-mRNA splicing gene, PRP31, underlies autosomal dominant retinitis pigmentosa on chromosome 19q13.4 (RP11). *Mol Cell* **8**, 375-81.

Voss, M. D., Hille, A., Barth, S., Spurk, A., Hennrich, F., Holzer, D., Mueller-Lantzsch, N., Kremmer, E. and Grasser, F. A. (2001). Functional cooperation of Epstein-Barr virus nuclear antigen 2 and the survival motor neuron protein in transactivation of the viral LMP1 promoter. *J Virol* **75**, 11781-90.

Vuillaume, I., Vermersch, P., Destee, A., Petit, H. and Sablonniere, B. (1998). Genetic polymorphisms adjacent to the CAG repeat influence clinical features at onset in Huntington's disease. *J Neurol Neurosurg Psychiatry* **64**, 758-62.

Waelter, S., Boeddrich, A., Lurz, R., Scherzinger, E., Lueder, G., Lehrach, H. and Wanker, E. E. (2001). Accumulation of mutant huntingtin fragments in aggresome-like inclusion bodies as a result of insufficient protein degradation. *Mol Biol Cell* **12**, 1393-407.

Wang, T. T., Chiang, A. S., Chu, J. J., Cheng, T. J., Chen, T. M. and Lai, Y. K. (1998). Concomitant alterations in distribution of 70 kDa heat shock proteins, cytoskeleton and organelles in heat shocked 9L cells. *Int J Biochem Cell Biol* **30**, 745-59.

Wang, J. and Dreyfuss, G. (2001). Characterization of functional domains of the SMN protein in vivo. *J Biol Chem* **276**, 45387-93.

Wang, C., Politz, J. C., Pederson, T. and Huang, S. (2003). RNA polymerase III transcripts and the PTB protein are essential for the integrity of the perinucleolar compartment. *Mol Biol Cell* **14**, 2425-35.

Weinstein, L. B. and Steitz, J. A. (1999). Guided tours: from precursor snoRNA to functional snoRNP. *Curr Opin Cell Biol* **11**, 378-84.

Weisenberger, D. and Scheer, U. (1995). A possible mechanism for the inhibition of ribosomal RNA gene transcription during mitosis. *J Cell Biol* **129**, 561-75.

Whitehead, S. E., Jones, K. W., Zhang, X., Cheng, X., Terns, R. M. and Terns, M. P. (2002). Determinants of the interaction of the spinal muscular atrophy disease protein SMN with the dimethylarginine-modified box H/ACA small nucleolar ribonucleoprotein GAR1. *J Biol Chem* **277**, 48087-93.

Willemsen, R., Bontekoe, C., Tamanini, F., Galjaard, H., Hoogeveen, A. and Oostra, B. (1996). Association of FMRP with ribosomal precursor particles in the nucleolus. *Biochem Biophys Res Commun* **225**, 27-33.

Willemsen, R., Hoogeveen-Westerveld, M., Reis, S., Holstege, J., Severijnen, L. A., Nieuwenhuizen, I. M., Schrier, M., van Unen, L., Tassone, F., Hoogeveen, A. T. et al. (2003). The FMR1 CGG repeat mouse displays ubiquitin-positive intranuclear neuronal inclusions; implications for the cerebellar tremor/ataxia syndrome. *Hum Mol Genet* **12**, 949-59.

Wood, J. D., Nucifora, F. C., Jr., Duan, K., Zhang, C., Wang, J., Kim, Y., Schilling, G., Sacchi, N., Liu, J. M. and Ross, C. A. (2000). Atrophin-1, the dentato-rubral and pallido-luysian atrophy gene product, interacts with ETO/MTG8 in the nuclear matrix and represses transcription. *J Cell Biol* **150**, 939-48.

Wu, C. H. and Gall, J. G. (1993). U7 small nuclear RNA in C snurposomes of the Xenopus germinal vesicle. *Proc Natl Acad Sci U S A* **90**, 6257-9.

Wu, Z., Murphy, C. and Gall, J. G. (1994). Human p80-coilin is targeted to sphere organelles in the amphibian germinal vesicle. *Mol Biol Cell* **5**, 1119-27.

Wu, C. H., Murphy, C. and Gall, J. G. (1996). The Sm binding site targets U7 snRNA to coiled bodies (spheres) of amphibian oocytes. *Rna* **2**, 811-23.

Wu, L., Davies, S. L., North, P. S., Goulaouic, H., Riou, J. F., Turley, H., Gatter, K. C. and Hickson, I. D. (2000). The Bloom's syndrome gene product interacts with topoisomerase III. *J Biol Chem* **275**, 9636-44.

Xue, Z. and Melese, T. (1994). Nucleolar proteins that bind NLSs: a role in nuclear import or ribosome biogenesis? *Trends Cell Biol* **4**, 414-7.

Yamada, M., Sato, T., Shimohata, T., Hayashi, S., Igarashi, S., Tsuji, S. and Takahashi, H. (2001). Interaction between neuronal intranuclear inclusions and promyelocytic leukemia protein nuclear and coiled bodies in CAG repeat diseases. *Am J Pathol* **159**, 1785-95.

Yankiwski, V., Marciniak, R. A., Guarente, L. and Neff, N. F. (2000). Nuclear structure in normal and Bloom syndrome cells. *Proc Natl Acad Sci U S A* **97**, 5214-9.

Young, P. J., Le, T. T., thi Man, N., Burghes, A. H. and Morris, G. E. (2000). The relationship between SMN, the spinal muscular atrophy protein, and nuclear coiled bodies in differentiated tissues and cultured cells. *Exp Cell Res* **256**, 365-74.

Young, P. J., Le, T. T., Dunckley, M., Nguyen, T. M., Burghes, A. H. and Morris, G. E. (2001). Nuclear gems and Cajal (coiled) bodies in fetal tissues: nucleolar distribution of the spinal muscular atrophy protein, SMN. *Exp Cell Res* **265**, 252-61.

Young, P. J., Francis, J. W., Lince, D., Coon, K., Androphy, E. J. and Lorson, C. L. (2003). The Ewing's sarcoma protein interacts with the Tudor domain of the survival motor neuron protein. *Brain Res Mol Brain Res* **119**, 37-49.

Yu, Z. X., Li, S. H., Nguyen, H. P. and Li, X. J. (2002). Huntingtin inclusions do not deplete polyglutamine-containing transcription factors in HD mice. *Hum Mol Genet* **11**, 905-14.

Zatsepina, O. V., Chelidze, P. V. and Chentsov, Y. S. (1988). Changes in the number and volume of fibrillar centres with the inactivation of nucleoli at erythropoiesis. *J Cell Sci* **91 (Pt 3)**, 439-48.

Zeng, C., Kim, E., Warren, S. L. and Berget, S. M. (1997). Dynamic relocation of transcription and splicing factors dependent upon transcriptional activity. *Embo J* **16**, 1401-12.

Zhang, S., Herrmann, C. and Grosse, F. (1999). Nucleolar localization of murine nuclear DNA helicase II (RNA helicase A). *J Cell Sci* **112 (Pt 16)**, 2693-703.

Zhuchenko, O., Bailey, J., Bonnen, P., Ashizawa, T., Stockton, D. W., Amos, C., Dobyns, W. B., Subramony, S. H., Zoghbi, H. Y. and Lee, C. C. (1997). Autosomal dominant cerebellar ataxia (SCA6) associated with small polyglutamine expansions in the alpha 1A-voltage-dependent calcium channel. *Nat Genet* **15**, 62-9.

Zini, N., Santi, S., Ognibene, A., Bavelloni, A., Neri, L. M., Valmori, A., Mariani, E., Negri, C., Astaldi-Ricotti, G. C. and Maraldi, N. M. (1994). Discrete localization of different DNA topoisomerases in HeLa and K562 cell nuclei and subnuclear fractions. *Exp Cell Res* **210**, 336-48.

Zuhlke, C., Riess, O., Bockel, B., Lange, H. and Thies, U. (1993). Mitotic stability and meiotic variability of the (CAG)n repeat in the Huntington disease gene. *Hum Mol Genet* **2**, 2063-7.